Progress and Prospects of Ergot Alkaloid Research

Joydeep Mukherjee, Miriam Menge

Institut für Technische Chemie, Universität Hannover, Callinstr. 3, D-30167 Hannover, Germany
E-mail: mukherjee@mbox.iftc.uni-hannover.de

Ergot alkaloids, produced by the plant parasitic fungi *Claviceps purpurea* are important pharmaceuticals. The chemistry, biosynthesis, bioconversions, physiological controls, and biochemistry have been extensively reviewed by earlier authors. We present here the research done on the organic synthesis of the ergot alkaloids during the past two decades. Our aim is to apply this knowledge to the synthesis of novel synthons and thus obtain new molecules by directed biosynthesis. The synthesis of clavine alkaloids, lysergic acid derivatives, the use of tryptophan as the starting material, the chemistry of 1,3,4,5-tetrahydrobenzo[*cd*]indoles, and the structure activity relationships for ergot alkaloids have been discussed. Recent advances in the molecular biology and enzymology of the fungus are also mentioned. Application of oxygen vectors and mathematical modeling in the large scale production of the alkaloids are also discussed. Finally, the review gives an overview of the use of modern analytical methods such as capillary electrophoresis and two-dimensional fluorescence spectroscopy.

Keywords. Ergot, Alkaloid synthesis, Claviceps, Directed biosynthesis, Bioreactors

Advances in Biochemical Engineering/
Biotechnology, Vol. 68
Managing Editor: Th. Scheper

1 Introduction

Today, ergot alkaloids have found widespread clinical use and more than 50 formulations contain natural or semisynthetic ergot alkaloids. They are used in the treatment of uterine atonia, postpartum bleeding, migraine, orthostatic circulatory disturbances, senile cerebral insufficiency, hypertension, hyperprolactinemia, acromegaly, and Parkinsonism. Recently, new therapeutic applications have emerged, e.g., against schizophrenia and for therapeutic usage based on newly discovered antibacterial and cytostatic effects, immunomodulatory and hypolipemic activity. The broad physiological effects of ergot alkaloids are based mostly on their interactions with neurotransmitter receptors on the cells. The presence of "hidden structures" resembling some important neurohumoral mediators (e.g., noradrenaline, serotonin, dopamine) in the molecules of ergot alkaloids could explain their interactions with these receptors [1].

Ergot alkaloids are produced by the filamentous fungi of the genus, *Claviceps* (e.g., *Claviceps purpurea* – Ergot, Mutterkorn). On the industrial scale these alkaloids were produced mostly by parasitic cultivation (field production of the ergot) till the end of the 1970s. Today this uneconomic method has been replaced by submerged fermentation. Even after a century of research on ergot alkaloids the search still continues for new, more potent and more selective ergot alkaloid derivatives.

A number of reviews have been published over the years. Some of the most recent are [2–9]. Much has been said about the chemistry, biosynthesis, physiological controls, and biochemistry of the fungus *Claviceps purpurea*. We present this review focusing on the organic synthesis of ergot alkaloids which has been put aside as impracticable. Nevertheless, its importance lies in the targeted development of new drugs, establishment of pharmacophore moieties, and finally what we believe to be the most interesting – probing the biosynthetic route and the development of synthons which, when added to the growing culture of *Claviceps purpurea*, will yield new alkaloid molecules. This review also gives information about recent progress in molecular biology, fermentation technology, and analytical methods as applied to ergot alkaloid research.

2 Chemistry, Bioconversions, and Directed Biosynthesis

There has been a continued effort towards the search for new ergot alkaloid molecules. In this exploration various approaches have been taken. The first approach is the total chemical synthesis of ergot alkaloids and the synthesis of analogs thereof with improved biological properties. Due to their property of regional selectivity with polyfunctional molecules, biological systems have advantages over many chemical reagents which cannot distinguish between multiple similar functional groups. Bioconversion, thus, is the second approach. Directed biosynthesis represents the third approach in which new ergot alkaloid molecules can be obtained by feeding the *Claviceps* with appropriate precursors. This kind of external regulation holds promise for obtaining new

pharmacologically interesting alkaloid analogs. Our objective in this part of the review is to unify the knowledge gained in these endeavors.

2.1 Chemical Synthesis

2.1.1 *Chemical Structures*

Most of the natural ergot alkaloids possess the tetracyclic ergoline ring system as their characteristic structural feature (Fig. 1).

In the majority of ergot alkaloid molecules, the ring system is methylated on nitrogen N-6 and substituted on C-8. Most ergot alkaloids have a double bond in position C-8, C-9 ($\Delta^{8,9}$-ergolenes, C-5 and C-10 being the asymmetric centers) or in position C-9, C-10 ($\Delta^{9,10}$-ergolenes, C-5 and C-8 being the asymmetric centers). The hydrogen atom on C-5 is always in β-configuration. $\Delta^{8,9}$-Ergolene has the hydrogen atom at C-10 in α-configuration, *trans*- to 5-H. The asymmetric carbon atom at C-8 of $\Delta^{9,10}$-ergolene gives rise to two epimers, ergolenes and isoergolenes [2, 3, 7, 9].

The classification of the ergot alkaloids are based on the type of substituent at C-8 and are divided into four groups:

- Clavine alkaloids
- Simple lysergic acid derivatives
- Ergopeptine alkaloids
- Ergopeptam alkaloids

2.1.1.1 Clavine Alkaloids

The clavines are hydroxy and dehydro derivatives of 6,8-dimethylergolenes and the corresponding ergolines. This group includes the chanoclavines with an open D-ring between N-6 and C-7. Figure 2 shows the structure of chanoclavine I. This group is described in detail in a review [7].

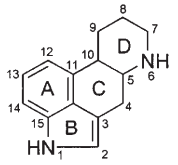

Fig. 1. Ergoline ring system

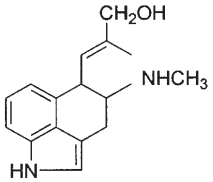

Fig. 2. Chanoclavine I

2.1.1.2
Simple Lysergic Acid Derivatives

The derivatives of lysergic acid are amides in which the amidic moiety is formed by a small peptide or an alkylamide. The derivatives of (+)-lysergic acid with 8β-configuration are pharmacologically active. Nonpeptide amides of lysergic acids isolated from ergot fungi are ergometrine, lysergic acid 2-hydroxyethylamide, lysergic acid amide, and paspalic acid (Fig. 3). Further information is available in [2, 3, 7].

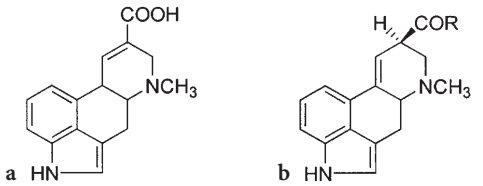

Fig. 3. **a** Paspalic acid. **b** Simple derivatives of lysergic acid: R=OH, lysergic acid; $R=NH_2$, lysergic acid amide; $R=NHCHOHCH_3$, lysergic acid 2-hydroxyethylamide; $R=NHCHCH_3$ CH_2OH, ergometrine

2.1.1.3
Ergopeptines

The ergopeptines, also called cyclol ergot alkaloids (CEA) are composed of two parts, namely lysergic acid and a tripeptide moiety. Figure 4 shows the general structure of the ergopeptines.

Their characteristic feature is the cyclol part which results from the reaction of an α-hydroxy-amino acid adjacent to lysergic acid with a carboxyl group of proline. Amino acid **III** of this tripeptide is L-proline and is common to all the naturally occurring ergopeptines. Their molecular structures have been described by the exchangeability of the L-amino acid **I** and the L-amino acid **II** between alanine, valine, phenylalanine, leucine, isoleucine, homoleucine, and α-aminobutyric acid. The groups of the ergopeptines formed by the combination of these amino acids are ergotamine, ergotoxine, ergoxine, and ergoannines [2, 7].

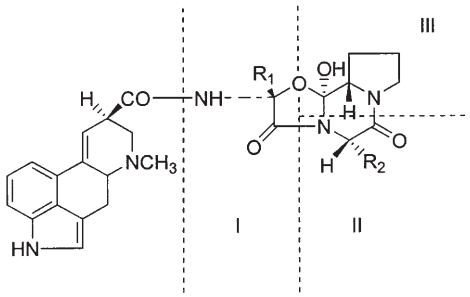

Fig. 4. General structure of ergopeptines. (R_1 = substituent of amino acid **I**; R_2 = substituent of amino acid **II**; amino acid **III** is L-proline)

2.1.1.4
Ergopeptams

Ergopeptams are noncyclol lactam ergot alkaloids (LEA). Their structure is similar to ergopeptines except that the amino acid **III** is D-proline and the tripeptide chain is a noncyclol lactam (Fig. 5). The ergopeptams are further classified as ergotamams, ergoxams, ergotoxams, and ergoannams [2, 7, 9].

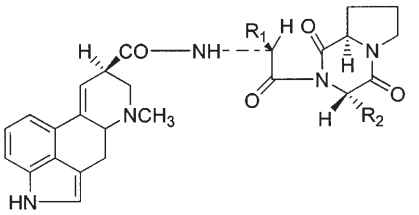

Fig. 5. General structure of ergopeptams. (R_1 = substituent of amino acid **I**; R_2 = substituent of amino acid **II**; amino acid **III** is D-proline)

2.1.2
Synthesis of Clavine Alkaloids and Lysergic Acid Derivatives

The ergoline nucleus has long been a challenging target for total synthesis with attempts dating back to the classic work of Uhle in 1949 and culminating in the synthesis of lysergic acid by Kornfeld and coworkers in 1954. The central intermediate in several successful syntheses, for example Ramage et al. in 1976, Nichols et al. in 1977, and Kornfeld and Bach in 1971, has been Uhle's ketone, either as the protected derivative or its carbonyl transposition (for references see [10, 11]). The total synthesis of ergot alkaloids has received increasing attention in the 1980s and 1990s, is the focus of this section, and is presented in tabular form (Table 1).

Table 1. Overview of the research work done on the chemical synthesis of ergot alkaloids

Target	Strategy/reaction	Reference
(±)-Lysergic acid	Reductive photocyclization of the enamide, derived from a tricyclic ketone followed by ring opening of the resulting dihydrofuran derivative	[12]
Racemic lysergene, agroclavine	Reductive photocyclization of the furylenamide followed by formation of the dihydrofuran ring; final products were formed by ring opening	[13]
(±)-Elymoclavine, (±)-isolysergol	Synthesis according to the synthetic route involving enamide photocyclization	[14]
(±)-Isofumigaclavine B, methyl(±)-lysergate, methyl(±)-isolysergate	Reductive photocyclization of the enamide followed by glycol formation and oxidative cleavage of the dihydrofuran ring	[15]
(±)-Agroclavine, (±)-agroclavine I, (±)-fumigaclavine B, lysergene	Reductive photocyclization of the enamide followed by glycol formation and oxidative cleavage of the dihydrofuran ring	[16]

Table 1 (*continued*)

Target	Strategy/reaction	Reference
(±)-Isofumigaclavine B, (±)-lysergol, (±)-fumigaclavine B, (±)-isolysergol, (±)-elymoclavine, (±)-isolysergene, (±)-agroclavine, (±)-lysergene, methyl(±)-lysergates	Dehydrogenation of indolines to indoles with phenylseleninic anhydride applied to the final steps in the total synthesis of these alkaloids	[17]
(±)-Lysergol, (±)-isolysergol, (±)-elymoclavine	Dehydrogenation of indolines to indoles with benzeneseleninic anhydride	[18]
(±)-Chanoclavine I, (±)-isochanoclavine I	Total synthesis of 6,7-secoergolines based on the fragmentation reaction of 3-amino alcohols	[19]
Agroclavine I	Lewis acid assisted condensation reactions between a constituted 5-methoxy-isoxazolidine and silicon-based nucleophiles	[20]
(±)-Chanoclavine I, (±)-isochanoclavine I	Stereoselective total synthesis by a nitrone-olefin/ cycloaddition	[21]
(±)-6,7-Secoagroclavine, (±)-paliclavine, (±)-costaclavine	Stereoselective total synthesis by a nitrone-olefin/ cycloaddition	[22]
(–)-Chanoclavine I	The key step of the synthesis involves the creation of the C ring by the formation of the C5-C10 bond, catalyzed by chiral palladium(0) complexes	[23]
(±)-Chanoclavine I	Palladium catalyzed intramolecular cyclization (Heck reaction)	[24]
(±)-Norchanoclavine I, (±)-chanoclavine I, (±)-isochanoclavine	Regioselective oxidation of the Z-methyl group of the isoprenyl system with selenium dioxide	[25]
(±)-Agroclavine I, (±)-6-norchanoclavine II, (±)-chanoclavine II	Regioselective oxidation of the Z-methyl group of the isoprenyl system with selenium dioxide	[26]
(±)-Chanoclavine I, (±)-dihydrosetoclavine	Synthesis involves a synthetic method of 4-alkylindoles	[27]
6,7-Secoagroclavine	Synthesis of the versatile intermediate 4-(sulfonyl-methyl)indole from 4-oxo-4,5,6,7-tetrahydroindole for the formal total synthesis	[28]
Chanoclavine I	Intramolecular [3+2] cycloaddition reaction	[29]
(±)-Lysergic acid	Intramolecular Imino-Diels-Alder-Reaction starting from 4-hydroxymethyl-1-tosylindole	[30]
(±)-Claviciptic acid	Combinational use of 4-selective lithiation of 1-(triisopropylsilyl)gramine and fluoride ion induced elimination-addition reaction of 4-[(*E*)-3-hydroxy-3-methyl-1-butenyl]-1-(triisopropylsilyl)gramine	[31]

2.1.3
Use of Tryptophan as the Starting Material

The synthetic access to the ergot alkaloids could have been limited by the selection of the raw materials. Thus, an informal synthesis of lysergine from a more accessible starting material, tryptophan, which is the biosynthetic precursor, was reported [32]. The methyl ester of lysergic acid has been obtained from tryptophan in ten steps [33]. The authors have also reported the first total synthesis of setoclavine from tryptophan [34]. The total syntheses of lysergine, setoclavine, and lysergic acid have been described [11]. Tryptophan, protected as its dihydro, dibenzoyl derivative is dehydrated to the corresponding azlactone, which undergoes stereoselective intramolecular Friedel-Crafts acylation to give a tricyclic ketone intermediate. A spiromethylene lactone is formed by Reformatsky reaction that represents the branching point of the syntheses to different ergot alkaloids. The synthesis of optically active ergot alkaloids from L-tryptophan was possible because of the high selectivity of the reactions.

Enantiomerically pure 4-alkyl substituted derivatives of tryptophan required for the asymmetric syntheses of ergot alkaloids has been obtained [35]. The author used the method [36] to produce 4-alkyl substituted indoles and combined this organometallic reaction with an enantioselective enzymatic transformation. An efficient eight stage synthesis of *N*-benzenesulphonyl-3-(3′-methoxyprop-2′-en-1′-yl)-4-(1′-hydroxy-2′-trimethylsilymethyl-prop-2′-en-1′-yl)-indoles from 4-carbomethoxyindole has been described [37]. The use of these benzylic alcohols for intramolecular cation-olefine cycloadditions yielding either a tetracyclic or a tricyclic product was also demonstrated.

A methodology [38] was presented to obtain 4-substituted intermediates for the synthesis of claviciptic acid via an *N*-protected indole-$Cr(CO)_3$ complex. The addition of a nucleophile to this complex leads to a regioselective introduction of a substituent at C-4 or C-7 on the indole ring. Racemic lysergine and lysergic acid diethylamide (LSD) were synthesized by a cobalt catalyzed cocyclization of 4-ethynyl-3-indoleacetonitriles with alkynes [39]. The total synthesis of optically active claviciptic acids was reported [40], which involves (*S*)-4-bromotryptophan as a key intermediate and occurs via 4-(1′,1′-dimethyl-1′-hydroxy-2-propenyl-3-yl)-tryptophan, the synthetic equivalent of the naturally occurring 4-(γ,γ-dimethylallyl)tryptophan (DMAT), the first pathway-specific intermediate in ergot biosynthesis.

2.1.4
1,3,4,5-Tetrahydrobenzo[cd]indoles

The simplified analogs of ergot alkaloids such as 1,3,4,5-tetrahydrobenzo[*cd*]indoles containing an amino substituent at position 4 possess interesting biological properties like affinity for dopamine or serotonin receptors. Bicyclic and tricyclic ergoline partial structures were synthesized [41] and it was proved that the rigid pyrroethylamine moiety of the ergolines is the portion of the molecule responsible for dopamine agonist activity.

In one synthetic approach, the bicyclic isonitriles were cyclized with strong bases to the corresponding tricyclic compounds [42]. A synthesis of dihydrolysergic acid starting from appropriately substituted 5-nitro-2-tetralones via a tricyclic isonitrile to the indole ring closure as the last step has been described [43].

In another strategy, the tricyclic ring has been formed in a single step from a benzene derivative by tandem radical cyclizations to yield methyl 1-acetyl-2,3,9,10-tetrahydrolysergate as an example [44].

The tricyclic system has also been constructed from an indole via electrophilic substitution reactions at positions 3 and/or 4. Synthesis of tricyclic ergoline synthons from 5-methoxy-1*H*-indole-4-carboxaldehyde has been described [45]. Sodium cyanoborohydride mediated reductive amination provided easy access to 1,3,4,5-tetrahydrobenz[*cd*]indole-4-amines, compounds which show specificity for serotonin and dopamine receptors.

Various 4-substituted indoles were prepared and a synthetic method for 4-nitro-1,3,4,5-tetrahydrobenz[*cd*]-indole derivatives was carried out [46] and also for 4,5-disubstituted 1*H*-1,3,4,5-tetrahydrobenz[*cd*]indole derivatives [47] using intramolecular Michael addition. Furthermore, a method [48] was published describing the successful syntheses of 4-nitro-1,3,4,5-tetrahydrobenz[*cd*]indole and its 1-hydroxy derivative.

It has recently been shown that Vicarious Nucleophilic Substitution (VNS) can be a useful tool for the synthesis of biologically active compounds containing the 1,3,4,5-tetrabenz[*cd*]indole nucleus, such as 6-methoxy-1,3,4,5-tetrahydrobenz[*cd*]indole-4-amine [49].

L-tryptophan has been used as a starting point for partial ergot structures such as 1-benzoyl-4-(amino)-1,2,2a,3,4,5-hexahydrobenz[*cd*]indoles. An optically pure amine, a key intermediate, was prepared via a four-step sequence employing an intramolecular Friedel-Crafts cyclization and a C-5 deoxygenation procedure [50].

2.1.5
Structure Activity Relationships

Structural analogies between the ergoline ring system and the several neurotransmitters (serotonin, dopamine, and noradrenaline) may give rise to the diverse pharmacological properties of the different ergot alkaloids. It has been shown that small changes in the chemical structure of the alkaloids results in marked effects on their biological activity [2, 9].

Different 6-substituted tricyclic partial ergoline analogs which exhibited strong serotonin agonist activity were synthesized [51]. A methoxy group at the 6-position greatly enhances activity and an electron-withdrawing group in the 6-position enhances both activity and stability. Some tricyclic partial ergoline analogs were synthesized [52]. It was observed that the vascular $5HT_2$ receptor interactions for the partial ergolines, compared to amesergide, the parent ergoline, were dramatically reduced. The isopropyl tricyclic ergolines inhibited the pressor response to serotonin like amesergide. The author concluded that the isopropyl moiety on the indole nitrogen is important for vascular $5HT_2$ receptor activity.

Dihydroergotoxine has a clinical use for patients with cerebral and peripheral circulatory disturbances. Bromokryptine and pergolide have been used in the therapy of Parkinson's disease, acromegaly, and hyperprolactinemia. Cianergoline is a potent antihypertensive. Since these ergot-related compounds sometimes show undesirable side effects, a series of ergolines were synthesized [53], hoping to find compounds with potent antihypertensive or dopaminergic activity and with weaker side effects. Different (5*R*,8*R*,10*R*)-6-alkyl-8-ergoline tosylates were prepared and treated with various five-membered heterocycles containing nitrogen atoms to yield new ergolines. It was found that (5*R*,8*R*,10*R*)-8-(1,2,4-triazol-1-ylmethyl)-6-methylergoline exhibited potent dopaminergic activity, about 18-fold greater than bromokryptine mesylate. Extremely potent dopaminergic activity was shown by (5*R*,8*R*,10*R*)-8-(1,2,4-triazol-1-ylmethyl)-6-propylergoline, being about 220 and 1.15 times more active than bromokryptine and pergolide mesylate, respectively. In continuation of this work, a series of (5*R*,8*S*,10*R*)-ergoline derivatives were synthesized [54], following the same synthetic methodology. (5*R*,8*S*,10*R*)-8-(1-Imidazolylmethyl)-6-methylergoline and (5*R*,8*S*,10*R*)-2-bromo-6-methyl-8-(1,2,4-triazol-1-ylmethyl)ergoline exhibited potent antihypertensive activity but without potent dopaminergic activity.

In an attempt to gain insight into the pharmacophore moiety of the ergot alkaloids, aza-transposed ergolines were synthesized [55] with the nitrogen atom in the 9-position by alkylation-amination of a tricyclic enamine in the presence of ethyl α,α,-bis(dibromomethyl)acetate, triethylamine, and methylamine which led to the construction of the azatransposed ergoline.

Syntheses of potent 5-HT agonists were accomplished in several steps from a 6-iodo partial ergoline alkaloid. A new and general methodology critical for the construction of oxazole-containing alkaloids was developed for the synthesis of the 5-HT agonists using a novel palladium(0)- and copper(I)-cocatalyzed cyanation reaction [56].

A new semisynthetic peptide alkaloid, 9,10-α-dihydro-12′-hydroxy-2′-isopropyl-5′α-(*R*-1-methylpropyl)ergotaman-3′,6′,18-trione (DCN 203–922), which contains the unnatural amino acid L-allo-isoleucine, was prepared and was found to have affinity to different monoamine binding sites in the brain [57].

Because the activities of ergot alkaloids are mediated by neurotransmitter receptors, clavine alkaloids also possess antibiotic and cytostatic activities [58, 59]. With the idea that the antineoplastic and antiviral activity of various heterocycles can be enhanced by their *N*-ribosylation, *N*-β-ribosides of agroclavine, elymoclavine, lysergene, lysergol, and 9,10-dihydrolysergol were prepared by $SnCl_4$ catalyzed ribosylation of their trimethylsilyl (TMS) derivatives with 1-*O*-acetyl-2,3,5-tri-*O*-benzoyl-β-D-ribofuranose. None of the new compounds exhibited activity against HIV or other viruses tested [60]. *N*-2-deoxy-D-Ribosides of agroclavine, lysergol, and 9,10-dihydrolysergol were prepared by $SnCl_4$ catalyzed glycosylation of their TMS derivatives with 1-chloro-3,5-di-*O*-toluoyl-2-deoxy-D-ribofuranose. None of the compounds, however, possessed antiviral activity against HIV [61].

2.2 Bioconversions of Ergot Alkaloids

Bioconversions of ergot alkaloids have been excellently reviewed [5]. In his article the author has discussed clavine bioconversions, bioconversions of lysergic acid derivatives, bioconversion as a tool to study the metabolism of ergot alkaloids in mammals, and finally the use of immobilization in ergot alkaloid bioconversion. We will look into developments after this period. Chemical oxidations yield complex and inseparable product mixtures. Oxidative biotransformations can thus be a substitute for the intricate ergot alkaloid molecules. The discovery of elymoclavine-*O*-β-D-fructoside, elymoclavine-*O*-β-D-fructofuranosyl(2-1)-*O*-β-D-fructofuranoside, and chanoclavine fructosides revealed a new group of naturally occurring ergot alkaloids, the ergot alkaloid glycosides. By conversion from their aglycones, the respective fructosides of chanoclavine, lysergol, and dihydrolysergol were obtained [5]. Presence of the fructosyl residue in the molecule, however, does not lead to any interesting biological activities. Incorporation of the β-galactosyl moiety in the ergot alkaloids might create new pharmacologically useful compounds. With this objective, β-galactosides of elymoclavine, chanoclavine, lysergol, 9,10-dihydrolysergol, and ergometrine were prepared using β-galactosidase from *Aspergillus oryzae* [62]. The effect of the galactosides on human lymphocytes was tested for their natural killer (NK) activity against a NK-sensitive target cell. The galactosides of the three compounds had stimulatory effects which appeared to be dose dependent.

Ergot alkaloid *O*-glycosides, ergot alkaloid *N*-glycosides, and biological activity of new ergot alkaloid glycosides have been recently reviewed [1].

Agroclavine and elymoclavine were modified using plant cell cultures exhibiting high peroxidase activity. Setoclavine and isosetoclavine were obtained from the media after transformation of agroclavine on a semipreparative scale. Similar treatment of elymoclavine produced 10-hydroxyelymoclavine [63]. A new spiro-oxa dimer of lysergene was isolated as a product of the biotransformation of lysergene by *Euphorbia calyptrata* suspension cell culture [64]. Structures of oxepino[5,4,3-*c,d*]indole derivatives and 3,4-disubstituted indoles, end products from the biotransformation of chanoclavine by *Euphorbia calyptrata* cell culture, have been elucidated by NMR and mass spectroscopy [65]. The stereoselective oxidation of agroclavine by haloperoxidase from *Streptomyces aureofaciens* was reported [66].

2.3 Directed Biosynthesis

Directed biosynthesis is a possible method for the synthesis of new ergot alkaloid molecules and for probing the biosynthetic pathway by feeding *Claviceps* spp. with natural and unnatural amino acids and synthetic precursors.

In order to test the possible involvement of free tripeptide intermediates L-valyl-(1-^{14}C)-L-valyl-L-proline was synthesized [67], which was fed to cultu-

Table 2. Application of different feeding strategies in the directed biosynthesis of *Claviceps*

Synthon	Incorporation strategy	Target/Objective	Reference
L-Valine, L-leucine, L-isoleucine	Addition to *Claviceps* strain producing ergornine, α- and β-ergokryptine	Higher yields of ergocornine, α-ergokryptine and β-ergokryptine respectively	[2]
L-Valine	Use of lower concentration of synthon and addition at an optimal time (towards the end of the bioprocess)	Change of the ergocornine/ergokryptine ratio 2:1 to the desired ratio 1:1 for better pharmacologic activity	[68]
p-Chlorophenylalanine, *p*-fluorophenylalanine, 5,5,5-trifluoroleucine, β-hydroxyleucine	Use of a phenylalanine auxotrophic ergocristine producing and a leucine auxotrophic ergocornine and ergokryptine producing strain	New alkaloids with the synthons as amino acid **II**	[2]
[1-^{14}C]-Aminobutyric acid	Use of *Claviceps purpurea* strain 231 F1 (producer of ergocornine)	Isolation of ergobine, the missing member of the series in the ergotamine group having α-aminobutyric acid as amino acid **II**	[69]
L-Thiazolidine-4-carboxylic acid	Use of ergosine, ergotamine and ergocristine producing *Claviceps* strains	Sulfur-containing peptide alkaloids	[2]
Norvaline	Use of *Claviceps purpurea* strain 231 F1 (producer of ergocornine)	Incorporation of norvaline in position of amino acid **I** led to the isolation of three unnatural ergopeptine alkaloids – ergorine, ergonorine, and ergonornorine	[70]
Derivative of DMAT: 3-[4-((*E*)-3,4-dihydroxy-3-methyl-1-butenyl)-1H-indol-3-yl]-2-(methylamino)propanoic acid, trideuterated in its methyl group	Use of washed mycelium of *Claviceps* sp. SD58	To probe the possibility of diastereomeric amino acids being intermediates in ergot alkaloid biosynthesis	[71]
2 Derivatives of DMAT: (*E*)-*N*-(methyl-d_3)-4-(3-methyl-1,3-butadienyl)-DL-tryptophan, (*E*)-*N*-(methyl-d_3)-4-(3-hydroxy-3-methyl-1-butenyl)-DL-tryptophan	Use of washed mycelium of *Claviceps* sp. SD58	To study the mode of C ring formation in ergot alkaloid biosynthesis	[72]

res of the ergocorine/ergokryptine producing *Claviceps purpurea* strain, Fb299. The results showed that the radioactivity from L-valyl-(1-^{14}C)-L-valyl-L-proline was incorporated only after breakdown of the precursor into its component amino acids. The results provided a basis for further investigations in this field. Incorporation of natural amino acids by variation of amino acid **I**, **II**, and **III** is reviewed [2]. Table 2 contains a summary of the research work done on the directed biosynthesis of *Claviceps* using different synthons and incorporation strategies.

3 Molecular Biology

The application of molecular biology to ergot alkaloid biosynthesis in *Claviceps purpurea* has been reviewed [3, 6, 8]. In the first review, the authors have discussed genetic recombination, gene amplification, transposition, and fungal cloning vectors, specifying that mitochondrial DNA or mitochondrial plasmids may serve as a basis for development of a eukaryotic cloning system for the fungus. In the second review, mutation, selection, and genetic recombination have been highlighted, especially the development of a transformation system and the widespread homology between mitochondrial plasmids and mitochondrial DNA in *Claviceps purpurea.* The third review focuses on transformation systems and application of newer techniques such as restriction enzyme mediated integration (REMI) for mutagenesis, pulse-field-gel electrophoresis (PFGE) for karyotype analyses, and PCR methods such as random amplified polymorphic DNA (RAPD) for identification/differentiation of *C. purpurea*. The work done by Tudzynski and Arntz to identify the genes which are expressed during alkaloid biosynthesis by differential cDNA screening led to the identification of gene coding for DMAT-synthase as an alkaloid pathway specific gene, (for details see [73]), thus confirming earlier work [74] wherein partial sequence information for the purified enzyme DMAT-synthase was obtained and a degenerate oligonucleotide mixture was used to identify and amplify segments of the gene. The complete gene and near full length cDNA were cloned in a yeast expression vector and sequenced. The reviews of 1990 [3] and 1996 [6] say that the application of modern molecular biology has been limited in this system due to the complex life cycle and long generation periods of the fungus. However, the review from 1997 [8] is very optimistic and the authors feel that application of modern molecular biology will open up interesting new perspectives for the analysis of ergot alkaloid biosynthesis.

In this part of our review we mention further interesting work on the molecular biology of the fungus not covered in the earlier reviews. In addition, very recent work on the enzymology of *Claviceps purpurea* is presented.

The peptide synthetase gene families of *Acremonium coenophialum* and *Claviceps purpurea* were investigated [75]. Hybridization analyses indicated that the four fragments cloned from *Acremonium coenophialum* represented three different peptide synthetase genes, most of which were present in multiple copies in the genome of the fungus. Each of the three clones from *Claviceps purpurea* appeared to be from a different peptide synthetase gene, only one of

which is duplicated. One clone from *Acremonium coenophialum* hybridizes with DNA from *Claviceps purpurea,* making it a good candidate for involvement in ergopeptine production. The authors concluded that ergopeptine-producing fungi have multiple families of peptide synthetase genes.

A comparative analysis of the nucleotide sequences of the structural gene for farnesylpyrophosphate synthase (FPPS), a key enzyme in the isoprenoid biosynthesis, of *Neurospora crassa*, *Gibberella fujikuroi, Sphaceloma manihoticola*, and *Claviceps purpurea* showed the presence of conserved regions [76].

In parallel, recent studies on enzymology of *Claviceps purpurea* have given us an insight to the molecular mechanisms and the information will be of importance to molecular biologists. The elucidation of the mechanism of reaction of dimethylallyltryptophan synthase [77] is worth mentioning. The authors showed that the prenyl-transfer reaction catalyzed by DMAT-synthase is an electrophilic aromatic substitution and is mechanistically similar to the electrophilic alkylation catalyzed by farnesyldiphosphate synthase. The other significant work was the purification of an enzyme activity capable of synthesis of D-lysergyl-L-alanyl-L-phenylalanyl-L-proline lactam, the noncyclol precursor of ergotamine [78]. Amino acid activation and lysergic acid activation domains were identified. Kinetic analysis indicated that under in vivo conditions, D-lysergyl peptide formation is limited by the D-lysergic acid concentration of the cell. The enzyme was also found to be produced constitutively. Studies on substrate specificities of this enzyme, D-lysergyl peptide synthetase (LPS), by the same research group showed that the peptide synthetase domain catalyzing the incorporation of proline appears to be specific for this amino acid [79].

4 Fermentation Technology

The review [2] describes the large-scale production of ergot alkaloids in bioreactors. It contains information of media, operating conditions, and purification processes. Another review [3] extensively describes the fermentative production of the alkaloids including the basis of the selection of carbon and nitrogen sources, the addition of trace elements, antifoam agents, the temperature of cultivation, and aeration requirements. This review also mentions semicontinuous fermentation, scaling up, culture rheology, bioreactor design, and solid state fermentation. The production of ergot alkaloids covering the selection of the carbon and nitrogen sources and environmental factors affecting the fermentative production has also been described [6]. Another recent review [8] covers the large-scale production of ergot alkaloids.

The effect of some stimulants and depressants of alkaloid production, the use of oxygen vectors, recent studies on solid state fermentation, and mathematical modeling, which have not been reviewed earlier, are covered in this section.

The oxidation and cyclization of chanoclavine is dependent on the cultivation conditions. The enzyme, chanoclavine cyclase, reponsible for this biochemical reaction, is a membrane bound enzyme and is thus influenced by membrane-affecting agents. This was studied with *Claviceps purpurea* mutant

strain 59 [80] by addition of clomiphene which decreases the contents of sterol in yeast and algae and increases the percentage of shorter saturated and monoene fatty acids. Clomiphene increased both oxidation and cyclization. Nystatin, which damages the membrane structure by binding to ergosterol, increases the membrane rigidity, and causes its permeabilization, was found to increase oxidation and decrease cyclization. The cultivation temperature was also strongly correlated to the oxidation and cyclization. The ancestral strain of strains 59, 129, and 35, producing mainly tetracyclic clavines, changed only the quantity, not the quality, of the clavines produced after addition of clomiphene [81]. The effect of triadimefon, a triazole inhibitor of ergosterol biosynthesis, was tested with *Claviceps purpurea* strain 59. The culture growth decreased and specific clavine production increased [82].

The effect of soybean peptones as stimulants of clavine alkaloid production has also been studied [83]. Soybean peptones type III (Sigma) were found to be excellent nutrients in the production media of the fungus *C. fusiformis* and gave higher alkaloid yields than meat peptones. Chromatography on Sephadex G-25 was used to resolve soybean peptone type III (Sigma) into seven fractions which exhibited different effects on the biosynthesis of clavine ergot alkaloids. One fraction proved to be the best nutrient for the fungus [84]. The effect of peptones from Difco Bacto and Torlak P-2 was also reported [85]. They found that low molecular weight fractions from Torlak P-2 had the strongest promoting effect on clavine production.

It was reported [86] that addition of some surfactants of polyglycol structure and Tweens to the submerged cultures of a highly productive strain of *C. paspali* caused a change in the intensity of alkaloid synthesis. Pluronik (polyethoxy-polypropoxypolymer) added in the range of 0.25 – 0.75 % enhanced the alkaloid production. Not only was the amount of alkaloid formed in the Pluronik supplemented media double the amount formed in the control without this antifoam, but the maximal yield was also reached earlier by 1 – 2 days as compared to the control. The effect of vitamins on the fermentative production ergot alkaloids was studied [87]. Biotin, folic acid, and riboflavin enhanced the production while pyridoxine inhibited the production.

The ergot alkaloid elaboration by the fungus is highly dependent on the level of dissolved oxygen in the medium. It has been shown that the final conidial concentration in batch fermentation depends on the end of the vegetative phase which occurs when glucose is exhausted. The vegetative cells are then converted into conidia. This process can be regulated by oxygen input [88]. In another study [89] it has been shown that, for optimal fungal development and alkaloid production, a balance between the uptake of oxygen from the liquid and gaseous phase has to be established by a defined ratio between aeration and agitation. Recently there has been efforts made to increase the transfer of oxygen to the cells by the use of hydrocarbons in the fermentation media [90]. In our laboratory we are trying to improve the oxygen transfer by the use of other oxygen vectors such as hydrogen peroxide and perfluorocarbons.

Use of solid state fermentation for the production of ergot alkaloids is an attractive proposition. It was reported that the production of total ergot alkaloids by *Claviceps fusiformis* in solid state fermentation was 3.9 times

higher compared to that in submerged fermentation [91]. Although there was no increase in the total alkaloid content for *Claviceps purpurea*, the content of ergonovine and ergotamine was higher, which is important from the commercial point of view. Further work [92] with *Claviceps purpurea* 1029c involving impregnation of the inert solid support, sugar cane pith bagasse, with 16 different combinations of the liquid nutrient medium such as rye meal or sucrose as the carbon source, ammonium sulphate, urea, and ammonium oxalate as the nitrogen source(s), other nutrients, namely potassium dihydrogen phosphate, magnesium sulphate, calcium nitrate, citric acid, and the amino acids valine, proline, tryptophan, and Tween 80 showed that there was a significant change in the alkaloid spectra and the authors suggested the possibility of achieving tailor-made spectra of ergot alkaloids, economically. Use of different solid substrates also resulted in major changes in the spectra of alkaloids produced. Ergonovine amounted to 93% of the total alkaloid in wheat grain medium while lysergic acid derivatives and ergonovine comprised 66% and 32% of the total alkaloids in rye grain medium, respectively [93].

The use of mathematical models in this system is a further advancement in the field of research on the production of ergot alkaloids. The first model [94] described a growth model for an ergotamine producing *Claviceps purpurea* in submerged culture. In developing the model, the basic principles of the growth and the morphological properties of the fungus were considered. The association between cell morphology, culture age, and ergot alkaloid production has been well established, assuming that the growth occurs in a three-step manner. The first involves the assimilation and the growth of the cells, the second cell division, and the third transformation of the mature cells to a state where they have no ability to divide but can produce the alkaloids and then gradually die. As the limiting substrate for the first and second steps, inorganic phosphate was presumed in the condition of the carbon source, sucrose being in excess. Another mathematical model [95] for the batch cultivation of *Claviceps purpurea* 129, producing clavine alkaloids, was formulated. The effect of extracellular and intracellular phosphate on the growth of the cells and production of clavine alkaloid under experimental conditions without carbon and nitrogen limitation was the objective of their study. The method of nonlinear regression was used to predict the optimal strategy of the phosphate addition in the batch culture at different time intervals of addition. In another study, kinetic parameters of production of clavine alkaloids were evaluated in two *Claviceps purpurea* strains [96]. Addition of glucose into the fermentation medium altered the zero order kinetics of production to activation-inhibition kinetics. The activation-inhibition kinetics of agroclavine and elymoclavine indicated the possibility of developing an integrated fermentation and separation unit in a closed loop, the cultivation of *Claviceps purpurea* being possible at the physiological maximum of specific alkaloid production rates. A new mathematical model was developed for the production of lysergic acid by *Claviceps paspali* [97]. The authors described an on-line modeling and control of a fed-batch fermentation process using a set of off-line identified models and their respective optimal control curves. Their concept was tested through simulation using experimental data from large scale fermentations and had given en-

couraging results. The most recent model for ergot alkaloid production during batch fermentation of *Claviceps purpurea* based on microbial life as the main characteristic for microbial development during fermentation process was proposed [98]. The aging process of the microorganism is represented by life function, defined in microbial life space which is a measure of space in which the observer follows the development of a biosystem through physiological and morphological changes of a microorganism. As a consequence of such an approach, the relativistic theory is recognized. Growth and alkaloid synthesis data from an industrial fermentation were tested to validate the developed model.

Metabolic flux analysis has not yet been applied to this system. It has been suggested that an extension of the principles of metabolic control theory would make it possible to identify rational optimal strategies for improvement of ergot alkaloid formation [4].

It has also been suggested that the redox state of the cellular cytoplasm is critical for the activity of coordinated enzymic events and thus for the elaboration of ergot alkaloids.

5 Analytical Methods

A very detailed review of the HPLC methods has been carried out [7]. The author has described the stationary phase, the mobile phase, flow rate, and detector system used by researchers since 1973. We would like to describe the other analytical methods such as the capillary electrophoresis, flow injection analysis and two-dimensional fluorescence spectroscopy which have found applications in ergot alkaloid research.

Using capillary zone electrophoresis (CZE), the resolution of ergot alkaloid enantiomers and epimers was obtained [99]. Complete separation of racemic mixtures in their enantiomers was obtained by using γ-cyclodextrin as a chiral additive in the background electrolyte. An easy and sensitive high performance capillary zone electrophoresis (HPCZE) method for the determination of ergovaline in the endophyte-infected fescue seed was reported [100]. With this method, detection and quantification of ergovaline at low micrograms per kilogram of the seeds were possible. The simultaneous assay of caffeine and ergotamine in the pharmaceutical dosage tablet formulations by capillary electrophoresis was reported [101]. The qualitative and quantitative determination of ergonovine, ergonovinine, ergocorninine, ergocornine, ergokryptine, ergosine, ergocristine, ergocristinine, and ergotamine by using capillary electrophoresis (CE) was developed [102]. Using a laser-induced fluorescence detection, the limit of detection of these alkaloids can be improved 30-fold compared to UV detection.

A micellar electrokinetic capillary chromatographic (MECC) method to separate 17 dihydroergotoxines, aci-alkaloids, and oxidation products has been described [103]. The authors used novel cationic dimeric (Gemini) surfactants such as 1,3-bis(dodecyl-*N,N*-dimethyl ammonium)-2-propanol and 1,3-bis(tetradecyl-*N,N*-dimethyl ammonium)-2-propanol for the separation in less than 8 min.

Ergot alkaloids themselves can act as chiral selectors. The publication [104] compares the stereoselectivities of several ergot alkaloids added to the background electrolyte towards some racemic hydroxy organic acids. The 1-allyl derivative of (5*R*,8*S*,10*R*)-terguride (allyl-TER) proved to be the best chiral selector. The differential pulse voltametric behavior of ergot alkaloids was studied [105] in respect of the effects of pH and composition of media and an automated FIA system with amperometric detection has been used to develop a selective and sensitive method for the routine quantitative assay of the alkaloids. In another study, the oxidative electrode reaction of lysergic acid-type ergot alkaloids was described [106] which provides a theoretical and experimental basis for liquid chromatographic or flow-injection determination with amperometric detection of the alkaloids.

Shelby's research group has worked on the development of assay systems to determine ergot alkaloid poisoning by immunological methods. As an example, ergovaline in tall fescue was detected by a specific monoclonal antibody which was produced by conjugation of ergovaline and bovine serum albumin. This antibody was specific for ergot peptide alkaloids with an isopropyl group at the C(5′) position of the peptide moiety [107].

A recent development has been the use of two-dimensional fluorescence spectroscopy as a new method for on-line monitoring of bioprocesses [108]. As ergot alkaloids fluoresce, the formation of the product during cultivation can be observed by two-dimensional fluorescence spectroscopy. Substraction spectra offered on-line real time information about the productivity during the cultivation. It was possible to follow the biomass concentration on-line by monitoring the culture fluorescence intensity in the region of riboflavine and its derivatives. This is a powerful application of this new sensor since the on-line determination of biomass is extremely complicated for this fungus.

6 Conclusions

Rapid developments in biotechnology in the last 20 years necessitates the re-engineering of our strategies for the achievement of better ergot alkaloids, both qualitatively and quantitatively. Combinatorial chemistry can tell us which derivative, be it of tryptophan or lysergic acid, incorporated in the final molecule would interact with the receptors to give better clinical effects with lesser side reactions. Today we have advanced software programs which can combinatorially create thousands of distinct molecules, one atom or functional group at a time, with real-time assessment of the steric and chemical complementarity of the nascent molecule to the three-dimensional structure of the receptor site. Notwithstanding the complexity of fungal genetics, the knowledge of the amino acid and nucleotide sequences of the alkaloid biosynthesis specific enzymes would give us the chance to modify the active sites by altering the amino acids in such a way that the engineered active site shows better binding characteristics with new synthons. The application of mathematical models and metabolic flux analysis would give a rational approach to the large scale production of ergot alkaloids. Although newer techniques such as capillary electro-

phoresis, FIA analysis, and two-dimensional fluorescence spectroscopy have been used for the analysis of ergot alkaloids, other modern methods such as pyrolysis mass spectrometry and molecular imprinting chromatographic analysis could find potential applications.

Acknowledgements. The authors are thankful to the Deutsche Forschungsgemeinschaft for financial support.

References

1. Kren V (1997) Top Curr Chem 186 : 45
2. Kobel H, Sanglier J-J (1986) Ergot alkaloids In: Rehm H-J, Reed G (eds) Biotechnology, vol 4. VCH, Weinheim, p 569
3. Rehacek Z, Sajdl P (1990) Bioactive molecules, vol 12. Elsevier, Amsterdam
4. Rehacek Z (1991) Folia Microbiol 36 : 323
5. Kren V (1991) Adv Biochem Eng/Biotechnol 44 : 124 – 144
6. Didek-Brumec M, Gaberc-Porekar V, Alacevic M (1996) Crit Rev Biotechnol 16 : 257
7. Flieger M, Wurst M, Shelby R (1997) Folia Microbiol 42 : 3
8. Lohmeyer M, Tudzynski P (1997) Claviceps Alkaloids. In: Anke T (ed) Fungal biotechnology. Chapman and Hall, Weinheim, p 173
9. Gröger D, Floss HG (1998) In: Cordell GA (ed) The alkaloids: chemistry and biology, vol 50. Academic Press, London, p 171
10. Ponticello GS, Baldwin JJ, Lumma PK, McClure DE (1980) J Org Chem 45 : 2436
11. Rebek J Jr, Tai DF, Shue YK (1984) J Am Chem Soc 106 : 1813
12. Kiguchi T, Hashimoto C, Naito T, Ninomiya I (1982) Heterocycles 19 : 2279
13. Kiguchi T, Hashimoto C, Ninomiya I (1984) Heterocycles 22 : 43
14. Ninomiya I, Hashimoto C, Kiguchi T (1984) Heterocycles 22 : 1035
15. Ninomiya I, Hashimoto C, Kiguchi T, Naito T (1985) J Chem Soc Perkin Trans 1 941
16. Ninomiya I, Hashimoto C, Kiguchi T, Naito T (1991) Chem Pharm Bull 39 : 23
17. Ninomiya I, Hashimoto C, Kiguchi T (1985) Tetrahedron Lett 26 : 4187
18. Ninomiya I, Hashimoto C, Kiguchi T, Naito T, Barton DH (1990) J Chem Soc Perkin Trans 1 : 707
19. Ninomiya I, Hashimoto C, Kiguchi T, Naito T (1991) J Chem Soc Perkin Trans 1 : 3275
20. Kozikowski AP, Stein PD (1985) J Am Chem Soc 107 : 2569
21. Oppolzer W, Grayson JI (1980) Helv Chim Acta 63 : 1706
22. Oppolzer W, Grayson JI, Wegmann H, Urrea M (1983) Tetrahedron 39 : 3695
23. Kardos N, Genet J-P (1994) Tetrahedron:Asymetry 5 : 1525
24. Yokoyama Y, Kondo K, Mitsuhashi M, Murakami Y (1996) Tetrahedron Lett 37 : 9309
25. Somei M, Makita Y, Yamada F (1986) Chem Pharm Bull 34 : 948
26. Somei M, Makita Y, Yamada F (1987) Heterocycles 26 : 895
27. Natsume M, Muratake H (1981) Heterocycles 16 : 375
28. Hatanaka N, Ozaki O, Matusumoto M (1986) Tetrahedron Lett 27 : 3169
29. Kozikowski AP, Ishida H (1980) J Am Chem Soc 102 : 4265
30. Oppolzer W, Francotte E, Bättig K (1981) Helv Chim Acta 64 : 478
31. Iwao M, Ishibashi F (1997) Tetrahedron 53 : 51
32. Rebek J, Shue YK (1982) Tetrahedron Lett 23 : 279
33. Rebek J (Jr.), Tai DF (1983) Tetrahedron Lett 24 : 859
34. Rebek J (Jr.), Tai DF (1983) Heterocycles 20 : 583
35. Nettekoven M, Psiorz M, Waldmann H (1995) Tetrahedron Lett 36 : 1425
36. Iwao M (1993) Heterocycles 36 : 29
37. Mann J, Barbey S (1995) Tetrahedron 51 : 12763
38. Semmelhack MF, Knochel P, Singleton T (1993) Tetrahedron Lett 34 : 5051
39. Saa C, Crotts DD, Gishun Hsu G, Vollhardt PC (1994) Synlett 7 : 487

40. Yokoyama Y, Matsumoto T, Murakami Y (1995) J Org Chem 60:1486
41. Bach NJ, Kornfeld EC, Jones ND, Chaney MO, Dorman E, Paschal W, Clemens JA, Smalstig EB (1980) J Med Chem 23:481
42. Haefliger W, Knecht H (1984) Tetrahedron Lett 25:289
43. Haefliger WE (1984) Helv Chim Acta 67:1942
44. Özlü Y, Cladingboel DE, Parsons PJ (1994) Tetrahedron 50:2183
45. Kruse LI, Meyer MD (1984) J Org Chem 49:4761
46. Somei M, Yamada F, Ohnishi H, Makita Y, Kuriki M (1987) Heterocycles 26:2823
47. Galambos G, Csokasi P, Csaba S (Jr.), Czira G, Szantay C (1994) Heterocycles 38:1727
48. Nakagawa K, Akoi N, Mukaiyama H, Somei M (1992) Heterocycles 34:2269
49. Makosza M, Stalewski J, Wojciechowski K, Danikiewicz W (1997) Tetrahedron 53:193
50. Varie DL (1990) Tetrahedron Lett 31:7583
51. Flaugh ME, Mullen DJ, Fuller RW, Mason NR (1988) J Med Chem 31:1746
52. Martinelli MJ, Bloomquist W, Peterson BC, Cohen ML (1993) J Med Chem 36:2671
53. Ohno S, Adachi Y, Koumori M, Mizukoshi K, Nagasaka M, Ichihara K, Kato E (1994) Chem Pharm Bull 42:1463
54. Ohno S, Adachi Y, Koumori M, Mizukoshi K, Nagasaka M, Ichihara K (1994) Chem Pharm Bull 42:2042
55. Stamos IK, Kelley EA, Floss HG, Cassady JM (1995) J Heterocycl Chem 32:1303
56. Anderson BA, Becke LM, Booher RN, Flaugh ME, Harn NK, Kress TJ, Varie DL, Wepsiec JP (1997) J Org Chem 62:8634
57. Giger RKA, Loosli HR, Walkinshaw MD, Clark BJ, Viguoret, JM (1987) Experientia 43:1125
58. Schwarz G, Eich E (1983) Planta Med 47:212
59. Eich E, Becker C, Sieben R, Maidhof A, Müller WEG (1986) J Antibiot 39:804
60. Kren V, Oslovsky P, Havlicek V, Sedmera P, Witvrouw M, DeClercq E (1997) Tetrahedron 53:4503
61. Kren V, Piskala A, Sedmera P, Havlicek, V, Prikrylova V, Witvrouw M, DeClercq E (1997) Nucleosides Nucleotides 16:97
62. Kren V, Sedmera P, Havlicek V, Fiserova A (1992) Tetrahedron Lett 33:7233
63. Scigelova M, Macek T, Minghetti A, Mackova M, Sedmera P, Prikrylova V, Kren V (1995) Biotechnol Lett 17:1213
64. Kren V, Sedmera P (1996) J Nat Prod 59:609
65. Kren V, Sedmera P, Prikrylova V (1996) J Nat Prod 59:484
66. Kren V, Kawulokova L, Sedmera P, Polasek M, Lindhorst TK, van Pee KH (1997) Liebigs Ann/Recueil 2379
67. Floss HG, Tcheng-Lin M, Kobel H, Stadler P (1974) Experientia 30:1369
68. Puc A, Milicic S, Kremser M, Socic H (1987) Appl Microbiol Biotechnol 25:449
69. Crespi Perillino NC, Malyszko J, Ballabio M, Gioia B, Minghetti A (1993) J Nat Prod 56:489
70. Crespi Perellino M, Malyszko J (1992) J Nat Prod 55:424
71. Kozokowski AP, Okita M, Kobayashi M, Floss HG (1988) J Org Chem 53:863
72. Kozokowski AP, Chen C, Wu J-P, Shibuya M, Kim C-G, Floss HG (1993) J Am Chem Soc 115:2482
73. Arntz C, Tudzynski P (1997) Curr Genet 31:357
74. Tsai H-F, Wang H, Gebler JC, Poulter CD, Schardl CL (1995) Biochem Biophys Res Commun 216:119
75. Panacionne DG (1996) Mycol Res 100:429
76. Homann V, Mende K, Arntz C, Ilardi V, Macino G, Morelli G, Böse G, Tudzynski B (1996) Curr Genet 30:232
77. Gebler JC, Woodside AB, Poulter CD (1992) J Am Chem Soc 114:7354
78. Riederer B, Han M, Keller U (1996) J Biol Chem 271:27524
79. Walzel B, Riederer B, Keller U (1997) Chem Biol 4:223
80. Pazoutova S, Flieger M, Rylko V, Kren V, Sajdl P (1987) Current Microbiol 15:97
81. Pazoutova S, Kren V, Rezanka T, Sajdl P (1988) Biochem Biophys Res Commun 152:190

82. Pazoutova S, Kren V, Rezanka T, Amler E, Flieger M, Sadjl P (1989) Pestic Biochem Physiol 34:211
83. Rozman D, Pertot E, Belic I, Komel R (1985) Biotechnol Lett 7:563
84. Rozman D, Pertot E, Belic I, Komel R (1988) Prerambeno-tehnolska i biotehnolaska revija 26:29
85. Rubesa R, Pertot E, Belic I (1987) Vestn Slov Kem Drus 34:53
86. Matosic S, Mehak M, Suskovic J, Golob Z (1994) Acta Bot Croat 53:39
87. Gupta A, Tiwari KP (1989) J Microb Biotechnol 4:54
88. Milicic S, Kremser M, Povsic Z, Socic H (1984) Appl Microbiol Biotechnol 20:356
89. Milicic S, Kremser M, Gaberc-Porekar V, Didek-Brumec-M, Socic H (1989) Appl Microbiol Biotechnol 31:134
90. Gil'manov V, Flieger M, Dymshits V (1996) J Appl Bacteriol 81:678
91. Trejo Hernandez MR, Raimbault M, Roussos S, Lonsanne BK (1992) Lett Appl Microbiol 15:156
92. Trejo Hernandez MR, Lonsanne BK, Raimbault M, Roussos S (1993) Process Biochem 28:23
93. Trejo Hernandez MR, Lonsanne BK, Raimbault M, Roussos S (1993) Chem Mikrobiol Technol Lebensm 15:1
94. Grm B, Mele M, Kremser M (1980) Biotechnol Bioeng 22:255
95. Pazoutova S, Votruba J, Rehacek Z (1981) Biotechnol Bioeng 23:2837
96. Flieger M, Votruba J, KrenV, Pazoutova S, Rylko V, Sajdl P, Rehacek Z (1988) Appl Microbiol Biotechnol 29:181
97. Taralova I, Tzonkov S (1992) IFAC Symp Adv Control Chem Processes 8:279
98. Milicic S, Veluscek J, Kremser M, Socic, H (1993) Biotechnol Bioeng 41:503
99. Fanali S, Flieger M, Steinerova N, Nardi A (1992) Electrophoresis 13:39
100. Ma Y, Meyer KG, Afzal D, Agena EA (1993) J Chromatogr A 652:535
101. Hassan Y, Aboul-Enein, Bakr SA (1997) J Liq Chromatogr Related Technol 20:47
102. Frach K, Blaschke G (1998) J Chromatogr A 808:247
103. Chen K, Locke DC, Maldacker T, Lin J-L, Awasiripong S, Schurrath U (1998) J Chromatogr A 822:281
104. Ingelse BA, Flieger M, Claessens HA, Everaets FM (1996) J Chromatogr A 755:251
105. Inczeffy J, Somodi ZB, Pap-Sziklay Z, Farsang G (1993) J Pharm Biomed Anal 11:191
106. Dankhazi T, Fekette E, Paal K, Farsang G (1993) Anal Chim Acta 282:289
107. Shelby RA, Bridgman RC, Smith FT, Atigada VR (1998) Food Agric Immunol 10:339
108. Marose S, Lindemann C, Scheper T (1998) Biotechnol Prog 14:63

Received June 1999

Antimicrobial Peptides of Lactic Acid Bacteria: Mode of Action, Genetics and Biosynthesis

E. Sablon[1], B. Contreras[2], E. Vandamme[2]

[1] Innogenetics N.V., Industriepark Zwijnaarde 7/4, B-9052 Ghent, Belgium
[2] University of Ghent, Laboratory of Industrial Microbiology and Biocatalysis, Department of Biochemical and Microbial Technology, Coupure links 653, B-9000 Ghent, Belgium
E-mail: erick.vandamme@rug.ac.be

A survey is given of the main classes of bacteriocins, produced by lactic acid bacteria: I. lantibiotics II. small heat-stable non-lanthionine containing membrane-active peptides and III. large heat-labile proteins. First, their mode of action is detailed, with emphasis on pore formation in the cytoplasmatic membrane. Subsequently, the molecular genetics of several classes of bacteriocins are described in detail, with special attention to nisin as the most prominent example of the lantibiotic-class. Of the small non-lanthionine bacteriocin class, the *Lactococcus* lactococcins, and the *Lactobacillus* sakacin A and plantaricin A-bacteriocins are discussed. The principles and mechanisms of immunity and resistance towards bacteriocins are also briefly reported. The biosynthesis of bacteriocins is treated in depth with emphasis on response regulation, post-translational modification, secretion and proteolytic activation of bacteriocin precursors. To conclude, the role of the leader peptides is outlined and a conceptual model for bacteriocin maturation is proposed.

Keywords. Antimicrobial peptides, Bacteriocins, Biosynthesis, Genetics, Immunity, Lactic acid bacteria, Lantibiotics

Advances in Biochemical Engineering/
Biotechnology, Vol. 68
Managing Editor: Th. Scheper

1 Lactic Acid Bacteria and Their Bacteriocins

1.1 Lactic Acid Bacteria

Lactic acid bacteria are Gram-positive, catalase-negative, oxidase negative, non-sporulating microaerophilic bacteria whose main fermentation product from carbohydrates is lactate. The lactic acid bacteria comprise both cocci (e.g. *Lactococcus*, *Leuconostoc*, *Oenococcus*, *Pediococcus*, *Tetragenococcus*, *Streptococcus*, *Enterococcus*) and rods (*Lactobacillus*, *Carnobacterium*, *Bifidobacterium*). Many of these lactic acid bacteria are generally recognized for their contribution to flavor and aroma development and to spoilage retardation [1]. Therefore, the traditional use of these microorganisms in the fermentation of foods and beverages has resulted in their application in many starter cultures currently involved in the fermentation of a wide variety of agricultural raw materials such as milk, meat, fruit, vegetables, cereals, etc. [2–7]. The lactic acid bacterial strains present in these starter cultures contribute to the organoleptic properties and the preservation of the fermented products by in situ production of antimicrobial substances such as lactic acid and acetic acid, hydrogen peroxide, bacteriocins, etc. [8–11]. Because of the general tendency to decrease the use of chemical additives, such natural inhibitors could replace the use of chemical preservatives such as sulfur dioxide, benzoic acid, sorbic acid, nitrate, nitrite, etc. [12]. For this reason, bacteriocins produced by lactic acid bacteria may be very promising as biological food preservatives in future food preservation [13]. Furthermore, certain lactic acid bacteria, especially some lactobacilli and bifidobacteria, are believed to play a beneficial role in the gastro-

intestinal tract [14]. Lactobacilli are also potentially useful as carriers for oral immunization, since orally administered lactobacilli trigger both a mucosal and systemic immune reaction against epitopes associated with these organisms [15, 16].

1.2 Bacteriocins

Bacteriocins are proteinaceous compounds produced by bacteria, both Gram-positive and Gram-negative, and they are active chiefly against closely related bacteria [17]. The discovery of bacteriocins dates back to 1925, when *E. coli* V was shown to produce an antimicrobial compound active against *E. coli* Φ [18]. These antimicrobial substances by *E. coli* were named colicins and 17 different types, based on their adsorption, were later reported [19]. Like the colicins (25–90 kDa, produced by *E. coli* and active against other *Enterobacteriaceae*) and microcins (<10 kDa, produced by *Enterobacteriaceae* and active against other Gram-negative bacteria), the bacteriocins produced by Gram-positive bacteria were defined as proteinaceous compounds that kill only closely related species [17, 20]. Although true for the majority of compounds, it is now evident that bacteriocins produced by lactic acid bacteria display bactericidal activity beyond species that are closely related [21]. Except for the colicins and the microcins, many other bacteriocins produced by non-lactic acid bacteria such as *Bacillus*, *Staphylococcus*, *Streptomyces*, *Streptoverticillium*, etc. have been reported [1, 22, 23].

The first report of the production of a bacteriocin produced by lactic acid bacteria was made in 1928 [24]. The substance was determined as a polypeptide [25] and subsequently named nisin [26, 27]. Since that time the bacteriocin field has expanded exponentially, and now bacteriocins produced by all genera of the lactic acid bacteria have been reported [1, 21].

The majority of bacteriocins from lactic acid bacteria have been characterized according to the early definition of a proteinaceous inhibitor, estimation of their molecular mass, and determination of their inhibition spectrum [1, 21]. Recent developments in the biochemical and molecular biological characterization of many of these compounds have elucidated their genetic organization, structures and mode of action. Despite their heterogeneity, bacteriocins produced by lactic acid bacteria were subdivided into three distinct classes based on these genetic and biochemical resemblances [28].

1.2.1 *Lantibiotics (Class I)*

Lantibiotics are small, membrane-active peptides (<5 kDa) containing the unusual amino acids lanthionine, β-methyl-lanthionine, and the dehydrated residues dehydroalanine and dehydrobutyrine; e.g. nisin, lacticin 481, carnocin U-149, lactocin S, sublancin 168 [29–38]. The intrachain positioning of these polycyclic structures of the lantibiotics has been used to group them into linear (Group IA) or circular (Group IB) lantibiotics [39]. Based on similarities in the

size, net charge and sequence of the leaders, the group IA lantibiotics can be further classified into two main groups, i.e. class IA_I (nisin) and class IA_{II} (lacticin 481). The lactocin S *N*-terminal extension displays no homology with the class IA_I or class IA_{II} leader peptides and may therefore represent a new class [40].

1.2.2
Small, Heat-Stable, Non-Lanthionine Containing, Membrane-Active Peptides (Class II)

These are less than 10 kDa in size and are characterized by a Gly-Gly$^{-2/-1}$ Xaa processing site in the bacteriocin precursor. This site is not restricted to class II bacteriocins, as it is also present in some lantibiotics [41]. The mature bacteriocins are predicted to form amphiphilic helices with varying amounts of hydrophobicity, β-sheet structure, and moderate (100 °C) to high (121 °C) heat stability; e.g. pediocin PA-1, lactococcin A, B, and M, leucocin A, sakacin A (= curvacin A), sakacin P, and lactacin F. Protein engineering of lactococcin B indicated that its cysteine residue was not necessary for activity [28]. Subgroups that can be defined within the class II bacteriocins are:

Class (IIA) Listeria-active peptides. They have a consensus sequence in the *N*-terminus of-T-G-N-G-V-X-C-; represented by pediocin PA-1. Other examples are sakacin A, sakacin P, leucocin A, mesentericin Y105 [42–45].

Class (IIB) Poration complexes consisting of two proteinaceous peptides. These two peptides are necessary for full activity; examples are lactococcin G, lactococcin M, lactacin F and two-component peptide systems found in the operon located in the plantaricin A gene cluster [46–49].

Class (IIC) Small, heat-stable, and non-modified bacteriocins translated with *sec*-dependent leaders. Only two reports have been made up to now; divergicin A and acidocin B [50, 51].

1.2.3
Large Heat-Labile Proteins (Class III)

These are greater than 30 kDa in size; examples are helveticin J, helveticin V, acidophilicin A, lactacins A and B [52–56].

A fourth class, proposed by Klaenhammer [21] is rather questionable. This class comprised the complex bacteriocins, composed of protein plus one or more chemical moieties (lipid, carbohydrate) required for activity; plantaricin S, leuconocin S, lactocin 27, pediocin SJ-1 [57–61]. The existence of this fourth class was supported by the observation that some bacteriocin activities were destroyed by glycolytic and lipolytic enzymes [60]. However, such bacteriocins have not yet been characterized adequately at the biochemical level and the recognition of this class therefore seems to be premature. The class IIC of the Klaenhammer [21] classification has recently been shown not to exist.

2 Mode of Action

The class I bacteriocin nisin and some of the class II bacteriocins have been shown to be membrane-active peptides that destroy the integrity of the cytoplasmic membrane via the formation of membrane channels (Fig. 1). In doing so, they alter the membrane permeability and therefore cause leakage of low molecular mass metabolites or dissipate the proton motive force, thereby inhibiting energy production and biosynthesis of proteins or nucleic acids [1, 62]. Most bacteriocins produced by lactic acid bacteria display a bactericidal effect on the sensitive cells, all or not resulting in cell lysis [63–67]. On the other hand, other bacteriocins, such as lactocin 27 [68], leucocin A [69] and leuconocin S [59] have been reported to act bacteriostatically. However, the designation of lethal versus static effect can be dependent upon aspects of the assay system, including the number of arbitrary units, the buffer or broth, the purity of the inhibitor, and the indicator species and cell density used [1]. The mode of action of numerous bacteriocins has been reported and, therefore, only a few of them, representing the different classes are described in this section.

The class IA_I lantibiotic nisin was shown to form ion-permeable channels in the cytoplasmic membrane of susceptible cells, resulting in an increase in the membrane permeability, disturbing the membrane potential and causing an efflux of ATP, amino acids, and essential ions such as potassium and magnesium. Ultimately, the biosynthesis of macromolecules and energy production are inhibited resulting in cell death. Nisin does not require a membrane receptor but requires an energized membrane for its activity, which appeared to be dependent on the phospholipid composition of the membrane [67].

Lactococcin A can alter the permeability of the *L. lactis* cytoplasmic membrane leading to the loss of proton motive force and leakage of intracellular ions and constituents [65, 70]. LcnA acts in a voltage independent manner on intact cells or membrane vesicles, but not on liposomes suggesting that a specific membrane receptor is required for LcnA recognition and action [65, 70].

Analogously, the antimicrobial activity of Las5 was not dependent on an energized membrane, but required a trypsin-sensitive protein receptor to elicit bactericidal action on protoplasted cells [64, 70].

The voltage independent activity of lactococcin B, similar to thiol-activated toxins, was proposed to be dependent on the reduced state of its unique cysteine residue on position 24 [71]. Recently, it was shown by means of protein engineering that the Cys-24 residue was not necessary for activity of lactococcin B [28]. Lactococcin G is a novel lactococcal class IIB bacteriocin whose activity depends on the action of two peptides [47]. The combination of the α and β peptide dissipated the membrane potential, induced a dramatic decrease in the cellular ATP level, and resulted in a rapid efflux of potassium [72].

The class IIA pediocins PA-1/AcH and JD were reported to exhibit their bactericidal action at the cytoplasmic membrane and to cause a collapse of the pH gradient and proton motive force [66, 73]. Furthermore, a leakage of K^+, UV-adsorbing materials, permeability to ONPG, and in some cases cell lysis, although not attributed to the primary pediocin AcH action were observed [66,

74]. Pediocin PA-1 was shown to dissipate the proton motive force and inhibit the amino acid transport in sensitive cells [75]. Lipoteichoic acid is essential for non-specific pediocin AcH binding, and sensitive cells present a specific receptor that potentiates contact with the membrane [17, 66]. Pediocin PA-1 displays an important *N*-terminal -Y-G-N-G-V-X-C- consensus common with other *anti-Listeria* bacteriocins such as sakacin A (= curvacin A) and P, and leucocin A. This finding suggests an important role of the *N*-terminus in either the recognition and/or activity of the pediocin-like bacteriocins.

The mechanism of action of the class III bacteriocins remains to be elucidated [21].

In general, the secondary structures of membrane-active peptides play a significant role in their biological activity [76]. For several of the membrane active bacteriocins, the presence of amphiphilic α-helices or β-sheets which form a hydrophobic and a hydrophilic face has been predicted [43, 47, 70]. These features suggest that lateral oligomerization of peptide monomers occurs in the membrane according to the so called barrel-stave mechanism with the hydrophobic side facing the membrane and the hydrophilic side forming the pore of the channel (Fig. 1) [21]. In case of a class IIB bacteriocin (lactococcin M, G, plantaricin S, lactacin F), of which the activity depends on the complementation of two molecules, a two-component poration complex is predicted [21, 47, 65, 77].

The need of a receptor, present in the target membranes of bacteriocin susceptible organisms has been extensively studied for microcin 25, produced

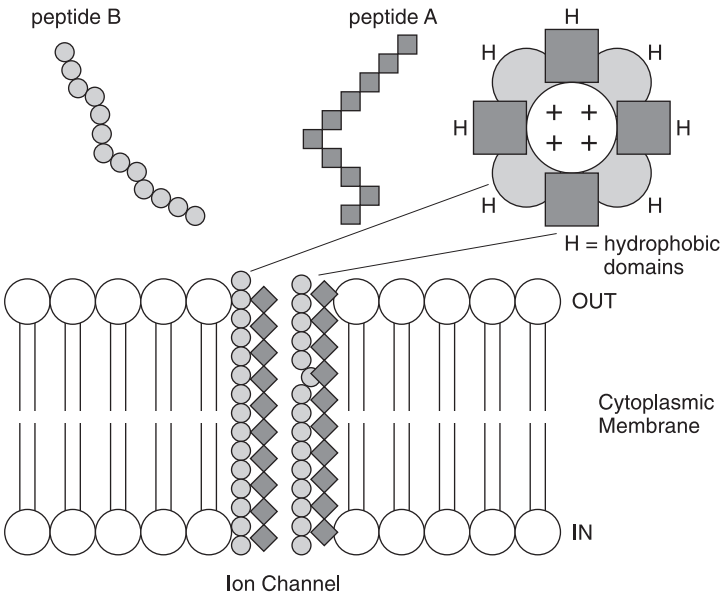

Fig. 1. Barrel-stave poration complexes proposed for class II bacteriocins. Complexes may be formed between one or two amphiphilic peptides which oligomerize and form membrane pores and ion channels [21]

by members of the *Enterobacteriaceae* [78]. Selection of spontaneous mutants for insensitivity to the peptide antibiotic microcin 25 led to the isolation of five categories of mutations, located in the *fhuA*, *exb*, *tonB* and *sbmA* genes [79]. The latter three are all proteins of the cytoplasmic membrane, whereas FhuA is a multifunctional protein of the outer membrane. [78, 79]. The region of FhuA, which is important of microcin 25 interaction has subsequently been mapped [80]. Several of these mutants showed an additional resistance to colicin M, colicin B, and to bacteriophages T1 and Φ80 [79]. These results indicate that microcin 25 interacts with an extracellular domain of the multifunctional receptor FhuA, and is imported through the TonB pathway and the SbmA protein [79].

In conclusion, pore formation in the cytoplasmic membrane seems to be a common mode of action of those LAB bacteriocins for which the mode of action has been determined. Some of the class II bacteriocins (lactococcin A, B, G and lactacin F) require a specific receptor molecule for adsorption, whereas nisin also acts on liposomes and exerts a receptor-independent action. Differences between narrow or wide host-range bacteriocins seem to be correlated with this aspect of a specific receptor, needed for activity. However, which bacteriocin domains confer binding specificities to lipid, protein, or reactive groups remain to be elucidated.

3
Genetics of Bacteriocins Produced by Lactic Acid Bacteria

3.1
Nisin, the Most Prominent Member of the Class IA_I Lantibiotics

The class I bacteriocins, the so-called lantibiotics, contain the posttranslationally modified amino acids lanthionine and methyl-lanthionine and their precursors dehydroalanine and dehydrobutyrine [39, 81, 82]. Nisin is a pentacyclic class IA_I lantibiotic consisting of 34 L-amino acids, including two dehydroalanine residues (positions 5 and 33), a dehydrobutyrine residue (position 2) and five intramolecular thio-ether lanthionine (residues 3–7) and methyl-lanthionine (residues 8–11, 13–19, 23–26, 25–28) bridges (Fig. 2). Two different forms, nisin A and nisin Z were shown to differ in only one amino acid residue [83]. During maturation, a 23-residue leader peptide is cleaved from a 57-residue precursor molecule to result in the mature bactericidal peptide of 34 amino acid residues. Many of these lantibiotics are produced by non-lactic acid bacteria, such as *Staphylococcus*, *Bacillus*, *Streptococcus*, *Actinoplanes*, *Streptomyces*, *Streptoverticillium* [1, 22]. Some of them, for instance subtilin, Pep5, and epidermin have been genetically studied in detail [29, 84–89]. The organization of the genetic determinants is comparable to that of nisin, produced by *Lactococcus lactis* subsp. *lactis* [22, 29, 84, 86–88, 90–93].

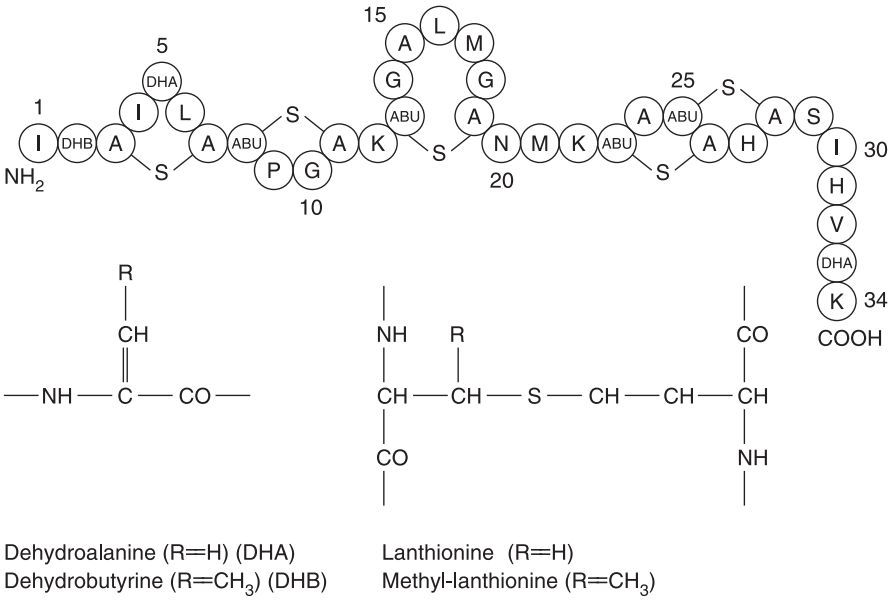

Fig. 2. The primary structure of nisin, a representative of the class IA_I lantibiotics

3.2 Conjugative Transposition of the Sucrose-Nisin Gene Cluster

A genetic linkage between nisin production, nisin immunity and the ability to use sucrose as a carbon source, was corroborated by the observation that these properties were transferred in a conjugation-like process [94]. It appeared that nisin and sucrose genes were clustered on chromosomal elements that were conjugative transposons [32, 37, 95, 96].

The best characterized conjugative sucrose-nisin transposons are the 70-kb *Tn5276* and *Tn5301* [95, 97]. The conjugative transposon *Tn5276* and Tn5301 [95, 97] has been found to display a RecA-independent insertion in at least five different chromosomal sites in derivatives of the *L. lactis* strain MG1363, but a single insertion site was preferred and integration of *Tn5276* occurred in a single orientation [97]. The organization of the *Tn5276* is given in Fig. 3. The insertion sequence *IS1068* at the left end of *Tn5276* was described as an *isoIS904* element because of its similarities with *IS904*, present at the same location in an other sucrose-nisin conjugative element, *Tn5301* [32, 37]. Sucrose-nisin conjugative elements lacking this *IS1068* still showed efficient conjugative transposition [37]. It is more likely that the *xis*/*int* genes found at the right end of *Tn5276* and shown to be required for the recA-independent excision of *Tn5276* ends in *E. coli*, are involved in site-specific insertion of *Tn5276* in *Lactococcus* [37, 98]. The *int* gene could encode a protein of 379 amino acids with homology to various integrases [98]. The *xis* gene encodes a small basic protein that enhances the excision process of *Tn5276* [98]. Similar genes are located at the ends of the conjugative transposons *Tn1545*/*Tn916* [99].

3.3
Genetic Organization of the Sucrose-Nisin Transposon TN5276

The nisin gene cluster *nisABTCIPRKFEG* of approximately 15 kb includes eleven different genes (Fig. 3) [40, 91, 92, 95, 96, 100–103]. Except for *nisK*, all other genes were essential for nisin production or immunity [92, 101, 103, 104]. The structural *nisA* and the *nisI* gene were shown to be both necessary for producer strain immunity [92]. The *nisP* gene encodes a subtilisin-like serine protease [101], whereas the *nisB* and *nisC* genes are very conserved in other lantibiotic operons and therefore very likely to encode proteins involved in the post-translational modification reactions of lantibiotics [40]. *NisT* belongs to the ABC family of exporter proteins, involved in ATP-dependent secretion [105, 106]. The proteins corresponding to the *nisR* and *nisK* genes, display homology to the well-known two-component signal transduction regulator and sensor-kinase proteins [101, 107, 108].

The *nisFEG* gene cluster downstream from *nisABTCIPRK* appeared to be involved in immunity to nisin besides the *nisA* and *nisI* gene products [104]. *NisI-NisF* is homologous to an ABC transporter of *Bacillus subtilis* and the MbcF-MbcE transporter of *E. coli*, which are involved in subtilin and microcin B17 immunity, respectively [104, 109, 110]. *NisG* displays homology with pre-

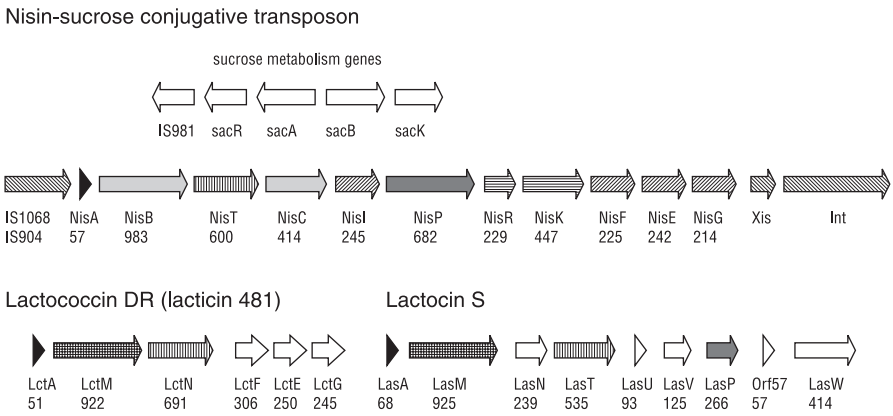

Fig. 3. Representative lantibiotic gene clusters. A representative of the class IA_I leader peptides included in this figure is nisin [40, 92, 103, 104, 107]. A representative of the class IA_{II} lantibiotics included in this figure is lactococcin DR (lacticin 481) [118]. The lactocin S leader does not follow the class IA_I or the class IA_{II} rules and might therefore represent a new maturation pathway [40, 82]. The structural genes are highlighted as black arrowheads. Genes with similar proposed function or substantial sequence similarity are highlighted in the same manner. The number of amino acids encoded by each gene is indicated below the arrowheads, which indicate the direction of transcription. The function of several genes in the lactocin S gene cluster is unknown (*lasN*, *lasU*, *lasV*, *lasW* and *orf57*). The suffix A is used to indicate the structural genes, the suffix T is used for ABC transporters, and the suffixes B, C and M indicate the potential modification enzymes. *NisI* is the nisin immunity protein, MsR and NisK constitute the two-component signal transduction system, and NisFEG forms a heteromer involved in nisin immunity as an ABC exporter

dominantly hydrophobic proteins with three or four potential transmembrane domains, described to play a role in immunity to colicins [111, 112]. Approximately 1 kb downstream from nisG, three more open reading frames with an opposite orientation were observed. The largest protein of 318 amino acids shows similarities with the helix-loop-helix type of DNA binding proteins, and its *N*-terminus of 27 amino acids was identical to the SacR regulatory protein [104]. The two further open reading frames showed homology to the lactococcal insertion element, IS981 [104].

Based on DNA homology, five different promoter regions were identified in the nisin gene cluster in front of *nisB*, *nisT*, *nisC*, *nisR* and *nisF* and two potential transcription terminators downstream from *nisB* and *nisK* [100, 104, 113, 114]. The promoter preceding *nisA* and the promoter upstream from *nisR* [103] both display characteristics of positively regulated promoters [114]. The intergenic region between *nisA* and *nisB* contains an inverted repeat that could act as a transcription terminator [91], transcription attenuator [103], or a signal for internal processing between the *nisA*/Z and *nisB* gene [115]. Recent studies showed that the *nisZBTCIPRKFEG* gene cluster consists of at least two operons resulting in a *nisZBTCIPRK* and a *nisFEG* transcript [115, 116]. The *nisZBTCIPRK* transcript is processed downstream from the structural *nisZ* gene [115]. Both promoters were inducible by raising of extracellular nisin concentrations, suggesting that nisin biosynthesis and immunity were autoregulated [115].

The *sac* genes, encoded by the *Tn5276* conjugative transposon in the opposite orientation of the nisin gene cluster are involved in sucrose metabolism and organized in two divergent operons with a back-to-back configuration [97]. Both operons are controlled by a sucrose-inducible promoter [97] and result in a rightward transcript, containing the *sacBK* (sucrose-specific PTS enzyme II and a putative fructose kinase) genes and a leftward transcript, containing the *sacAR* (sucrose-6-phosphate hydrolase and a putative regulator) genes [103].

3.4 The Class IA_{II} Lantibiotics Lactococcin DR and Lactocin S

Besides nisin, three other lantibiotics produced by LAB, namely lactococcin DR (= lacticin 481) [30, 117–119], lactocin S [31, 33, 82] and carnocin U-I49 [35, 36, 120] have been reported, but only the first two were genetically studied in more detail (Fig. 3) [82, 118–121]. Both lactocin S and lactococcin DR are members of the class IA_{II} lantibiotics. Lantibiotics of this class have a divergent leader peptide compared with the class IA_I lantibiotics represented by nisin, but also their genetical organization differs significantly from that of the class IA_I lantibiotics [40, 82].

Downstream from the structural lacticin 481 (= lactococcin DR) gene, *lctA* (= *lcnDR1*), *lctM* (= *lcnDR2*) encoded a protein of 922 amino acids [82, 118]. A 925-residue protein (LasM) with striking homology to LctM, was encoded downstream from the structural lactocin S gene [82], and cylM, a 993-amino acid residue protein was shown for the non-lactic acid bacteria lantibiotic, cytolysin [122]. This protein family is typical for the class IA_{II} lantibiotics, and

no homologues were found yet in any other bacteriocin operon [40]. The *C*-terminus of LctM was shown to display striking homology with NisC, proposed as a post-translational modification enzyme for nisin [118, 123]. Both the lactococcin DR and the lactocin S operons contain coding information for an ABC transporter protein (LctT (= LcnDR3), LasT) [82, 118]. For lactocin S, the structural *lasP* gene encodes a proteinase of 266 amino acid residues [82]. The lactocin S gene cluster contains several other genes (*lasN*, *U*, *V*, *W* and *orf57*) without putative function or homologous counterparts in other bacteriocin operons [82].A similar cluster was recently identified for lacticin 481 [119]. The proteins encoded by IctF, IctE and IctG were proposed to form an ABC transporter and should play some role in the immunity against lacticin 481.

3.5
Class II Non-Lantibiotic Bacteriocins

3.5.1
Introduction

The class II non-lantibiotic bacteriocins consist of a large heterologous group produced by different species of the lactic acid bacteria [21]. Despite this heterogeneity, all class II bacteriocins display a very conserved *N*-terminal leader peptide and a characteristic double-glycine-type ($Gly^{-2}Gly^{-1}Xaa$) proteolytic processing site [21]. The conserved mechanism of secretion and processing suggested by these findings is reflected in the organization of the operon structures encoding these bacteriocins (Fig. 4). The genetic determinants involved in the production of several class II bacteriocins have been genetically studied in detail (Fig. 4): lactacin F produced by *Lactobacillus johnsonii* [48, 124], lactococcin G, and the lactococcin A, B and M gene cluster of *Lactococcus lactis* [125–128], leucocin *A-UAL* produced by *Leuconostoc gelidum* [42, 129] and mesentericin Y105 produced by *Leuconostoc mesenteroides* [124], the identical bacteriocins pediocin PA-1.0 and pediocin AcH produced by *Pediococcus acidilactici* [130–132], sakacin A produced by *L. sake* [133] and plantaricin A, produced by *L. plantarum* [49, 134] (Fig. 4).

3.5.2
The Lactococcal Bacteriocins, Lactococcin A, B and M

The lactococcin A, B, and M operon cluster on the 60-kb conjugal plasmid p9B4–6, was the first class II bacteriocin genetic determinant to be analyzed. Two fragments, conferring bacteriocin production and immunity, were cloned [46, 135]. The lactococcin A operon encoded one bacteriocin (LcnA) and an immunity protein (LciA), and expressed a high antagonistic activity against *L. lactis* indicator strains.

In the lactococcin M operon, two bacteriocins (LcnM and LcnN) and one immunity protein (*LciM*) were found, displaying a low antagonistic activity against *L. lactis* indicator strains [46, 135]. In the lactococcin M operon, disruption of both *lcnM* and *lcnN* resulted in a non-producer phenotype. Therefore,

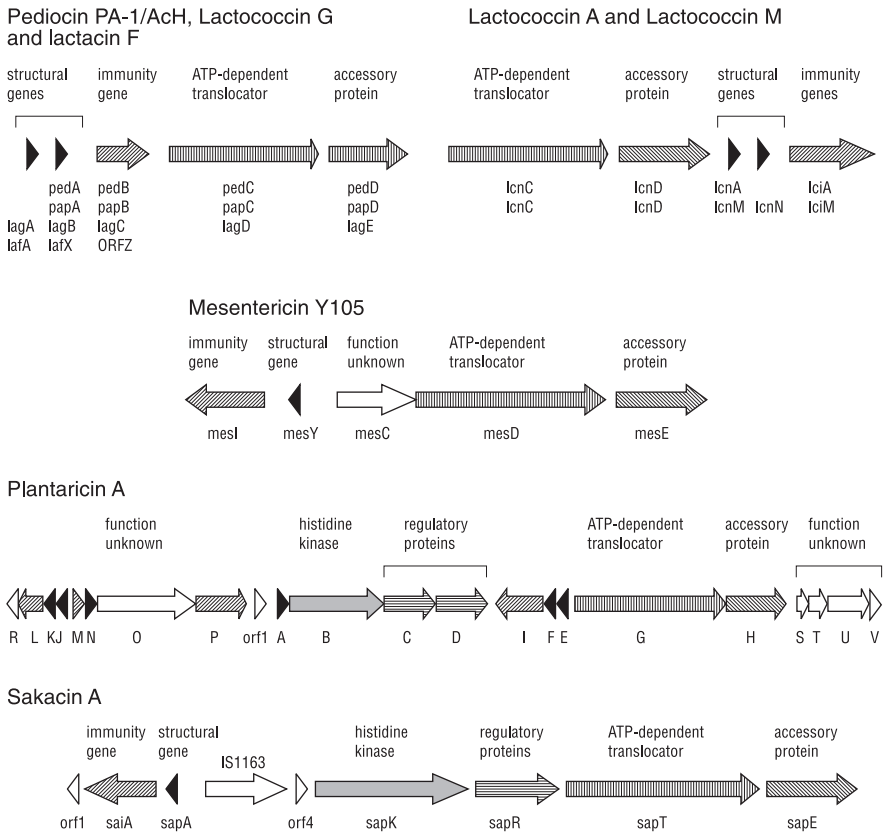

Fig. 4. Representative class II non-lantibiotic bacteriocin operons. The class II non-lantibiotic bacteriocins include lactococcin A, B, M and G [46, 125, 126, 128, 135, 136], lactacin F [77], pediocin PA-1 and AcH [62, 130, 131], mesentericin Y105 [124], sakacin A [133] and plantaricin A [49, 134]. The structural genes are high1ighted as black arrowheads. Genes with similar proposed function or substantial sequence similarity are highlighted in the same manner. The arrowheads indicate the direction of transcription. The function of MesC, and SapOSTUV of the mesentericin Y150 and plantaricin A operons is unknown

two gene products are required for activity, and lactococcin M was classified as a class IIB bacteriocin according to the classification of Nes et al. [128] (1995). Cloning and sequence analysis of the region downstream from lactococcin A identified a third lactococcin operon, designated as *LcnB* and its immunity protein *LciB* [136]. Site-directed mutagenesis showed that *LciA* and *LciM* were essential for producer strain immunity but did not cross-protect against the other bacteriocins [46]. Lactococcin A, produced by *L. lactis* subsp. *cremoris* LMG2130 was independently purified and sequenced [125]. The structural gene was mapped to a 55-kb conjugal plasmid of the producer strain and DNA sequencing revealed that this lactococcin was identical to the high activity lactococcin *A*, cloned and sequenced by van Belkum et al. [135].

Completion of the current genetic view of the lactococcin system was provided by Stoddard et al. [126]. The production of a bacteriocin of *L. lactis* subsp. *lactis* biovar *diacetylactis* WM4 was linked to a 131-kb plasmid *pNP2* [137]. DNA sequence of a 5.6-kb AvaII fragment of *pNP2* revealed two large open reading frames upstream from the *lcnA* and *lciA* genes, designated as *lcnD* (716 amino acids) and *lcnC* (474 amino acids) [126]. *Tn5* insertional mutagenesis of both *lcnD* and *lcnC* disrupted lactococcin *A* production without affecting immunity [126]. LcnC displayed highest homology with the HlyB-like family of ATP-dependent membrane translocators (Stoddard et al., 1992). It contains a highly conserved ATP-binding site and six *N*-terminal hydrophobic domains, which could promote integration in the cytoplasmic membrane. LcnD showed structural similarities to proteins of the HlyD and PrtE secretion systems of *E. coli* [126]. The carboxy-terminal part of LcnD was also encoded by the partial open reading frames upstream from the structural *IcnA* and *IcnM* genes of the 60-kb plasmid p9B4–6 [127]. The three lactococcin operons were preceded by conserved and functional promoter regions. The promoter upstream from *lcnA*, overlapped with a 19-bp inverted repeat. This palindromic sequence with a $\Delta G = -9.9$ kcal/mol could form a hairpin and therefore may resemble an SOS box for binding of the *Escherichia coli* RecA-sensitive *LexA* repressor [125]. However, *lcnA* has not been found to be inducible [125]. Stoddard et al. [126] noted that there were no obvious transcription terminators positioned between lcnC and lcnA, suggesting a possible read through in the *lcnA*/*lciA* operon, and speculated that besides a large transcript covering all four genes, a smaller transcript spanning *lcnA* and *lciA* was produced.

The transporter proteins LcnD and LcnC were shown to be essential for lactococcin A production but not for immunity [126]. Secretion systems based on such ATP-binding exporters have been reported for both Gram-negative and Gram-positive bacteria for export of extracellular proteins whose secretion does not depend on the general signal peptide-dependent export pathway [111, 138]. Such examples for Gram-negative bacteria include the haemolysin and colicin V proteins of *E. coli* [139, 140] cydolysin produced by *Bordetella pertussis* [141], leucotoxin produced by *Pasteurella haemolytica* [142], and metalloproteases B and C of *Erwinia chrysanthemi* [143]. For Gram-positive bacteria, these proteins have been described for ATP-dependent membrane translocation, for instance required for competence in *Streptococcus pneumoniae* [144]. It was therefore likely that a universal export apparatus, involved in class II bacteriocin secretion could consist of these two exporter proteins. Genetic analysis revealed that in the case of the identical *Pediococcus* bacteriocins, pediocin PA-1.0/AcH, the *Lactococcus* bacteriocin lactococcin G, the *Leuconostoc* bacteriocin mesentericin Y105, and the *Lactobacillus* bacteriocins sakacin A and plantaricin A an ATP-dependent ABC exporter apparatus was encoded adjacent to the bacteriocin operon [124, 127, 128, 130–132, 136, 145, 146] (Fig. 4).

3.5.3
The Class IIA Bacteriocins Pediocin PA-1/AcH and Mesentericin Y105

Although the class IIA, anti-listerial bacteriocins pediocin PA-1/AcH and mesentericin Y105, are produced by *Pediococcus* and *Leuconostoc* sp., respectively, they are nevertheless genetically organized in a way almost identical to the lactococcal bacteriocins (Fig. 4) [124, 130, 131]. MesC, a 137-amino acid protein upstream mesD in the mesentericin Y105 gene cluster shows no homology with known protein [124].

3.5.4
The Lactobacillus Bacteriocins Sakacin A and Plantaricin A

Axelsson et al. [147] (1993) shotgun cloned the plasmid fraction of *L. sake* Lb706 directly in a sakacin A non-producing and sensitive variant *L. sake* Lb706-B. One of the two clones, necessary for the restoration of immunity encoded a 430-amino acid residue protein designated as *SakB* [147]. Hybridization and sequence analysis revealed that *sakB* complemented a mutated copy of *sakB* present in *L. sake* Lb706-B. The gene mapped 1.6 kb from the structural sakacin A gene on the 60-kb plasmid. Further investigation showed that SakB was part of a two-component, bacterial signal transduction system, adjacent to the sakacin A operon [133]. SakB was renamed SapK, and showed striking homology to the *Staphylococcus aureus* AgrC histidine protein kinase (HPR). A second member of the two-component signal transduction apparatus, SapR, was encoded downstream from SapK. The SapR protein has homology to AgrA, a member of the response regulator (RR) family [108, 133, 148].

A comparable signal transduction system was found to be encoded in the same operon as the structural plantaricin A gene (*plnA*), and was transcribed as a 3.3 kb *plnABCD* messenger [134]. PlnB, PlnC, and PlnD showed highest homology to their counterparts in the *agr* (accessory gene regulatory) two-component regulatory system of *Staphylococcus aureus* [134, 149, 150]. PlnB showed highest homology to the histidine protein kinase family and is predicted as an integral protein of the cytoplasmic membrane with six transmembrane domains located in its *N*-terminus [134]. *PlnC* and *PlnD* are very homologous and corresponded to the response regulator family protein of the *Staphylococcus aureus agr* locus [134, 149, 150]. Additionally, recent findings suggest that two bacteriocins of the two-peptide type (PlnJ and PlnK of the *plnJKLR* operon and *PlnE* and *PlnF* of the *plnEFI* operon) and a bacteriocin of the one-peptide type (*PlnM* of the *plnM*NOP operon) were located adjacent to the *plnABCD* cluster and could hence be responsible for bacteriocin activity [49]. *PlnI* (257 amino acids), *PlnP* (247 amino acids), and *PlnL* (138 amino acids) encode hydrophobic proteins with three (*PlnL*) and seven (*PlnI* and *PlnP*) transmembrane domains, respectively. In the case of *PlnI* and *PlnL*, these proteins are encoded in the 3′ end immediately downstream from the bacteriocin determinants, following the conserved genetic organization of all two-component bacteriocins described up to now [49, 77, 128, 136]. PlnP however, is separated from the bacteriocin genes by *plnO*, an open reading frame of 399

amino acids [49]. However, based on its striking homology with PlnI, it could also be considered as an immunity protein for PlnN [49]. Upstream from *plnN*, a 66 amino acid protein, PlnM with one putative transmembrane helix was found. Besides PlnP, PlnM could hence be considered as a second valid candidate for PlnN immunity, although located in the 5′ end of the operon. Two proteins, PlnG (ABC transporter) and plnH (accessory protein), shown to constitute an ATP-dependent transport apparatus, were located downstream of the *plnABCD* operon [49]. The homologous counterparts in the sakacin A operon were named SapT and SapE, respectively [133]. The region encoding plantaricin A activity has proven to be a multiple gene locus consisting of not less than 22 different open reading frames in the same or opposite orientation to the previously described *plnABCD* operon [49, 134]. Besides the above described proteins, PlnROSTUV and orf1 display no homology with other protein sequences, and their function in plantaricin A activity has not been elucidated [49].

The sakacin A region was transcribed as two operons: the first one encompassed the structural sakacin A gene *sakA*, and its immunity factor SaiA, and the second covered the *sapK*, *sapR*, *sapT* and *sapE* genes involved in transcription regulation and sakacin A export [133]. Northern blot analysis revealed that the putative SapR/SapK system probably acted as a transcription activator [133]. A 35-bp region, upstream from the putative *sapA* promoter, and a similar sequence upstream from *sapK* were necessary for proper expression and could be possible targets for transcriptional activation [133]. Five promoters (upstream from *plnA*, *plnE*, *plnJ*, *plnM* and *plnG*) and six rho-independent transcription terminators (downstream from the operons *plnABCD*, *plnJKLR*, *plnMNOP*, *plnEFI* and the ORFs *plnF* and *plnN*) have been mapped in the plantaricin A cluster, resulting in a complex expression pattern [49, 134]. The −10 consensus sequences were located 6 to 7 bp upstream from the transcription start site, but the −35 consensus was more difficult to identify [49]. Just upstream from the putative − 35 region, all promoters were seen to harbor two direct repeats spaced by an A + T-rich strand of 12 bp [49].

3.5.5
Class IIB Bacteriocins

Two bacteriocins and an immunity protein, organized in one operon, comparable with the lactococcin M operon, were detected in the case of lactacin F, lactococcin *G*, and in two operons (*plnEFI* and *plnJKLR*) of the plantaricin A gene cluster. All four depend on complementation of two bacteriocin peptides for highest activity and therefore belong to the class IIB bacteriocins [46, 49, 124, 128].

Purification of lactococcin G identified two peptides, α and β, that individually exhibited marginal levels of activity. Upon complementation of the two peptides in a 7α:1β ratio, a seven-fold increase in activity was noted [47]. Allison et al. [48] proved that lactacin F activity and host range were expanded upon the complementation of two heterologously expressed peptides of the lactacin F operon, although initially only one bioactive peptide (LafA) was purified

from the *L. johnsonii* VPI11088 fermentation supernatant using *L. helveticus* NCK338 as an indicator organism [151]. Therefore, the lafA gene product, LafA, is a bacteriocin that kills *L. helveticus* NCK338. Expansion of the host range to include *L. delbrueckii* and *Enterococcus faecalis* occurs only after the interaction of LafA and LafX. The need of complementation of two bacteriocins for optimal activity is reflected in the presence of two bacteriocins encoded in the same operon and, together with lactococcin M [46], lactacin F [77], plantaricin A [49] and lactococcin G [128] they are the only class IIB bacteriocins determined on the genetic level.

Plantaricin A was shown to be dependent on complementation of two almost identical peptides which differed only in one *N*-terminal alanine residue [152]. Therefore, plantaricin A was the first known class IIB bacteriocin not to be encoded by two different adjacent structural bacteriocin genes [134]. When the plantaricin A gene cluster was genetically analyzed only one structural gene encoding plantaricin A was detected [134]. Detailed analysis of the plantaricin A genetic determinants revealed that plantaricin A acts as an inducer peptide of an agr-like signal transduction system and does not possess any bacteriocinogenic activity [49, 134, 145]. Recent findings confirmed that bacteriocin activity is most likely encoded by two two-peptide type and one one-peptide type bacteriocins adjacent to the *plnA*BCD operon [49, 134]. The proteins that constitute the production and maturation machinery of class IIB bacteriocins do not differ significantly from the other class II bacteriocins, as deduced from the lactococcin M and G, and plantaricin A operons [127, 128, 134, 145].

4 Immunity and Resistance Towards Bacteriocins

Three important phenotypes can confer non-sensitivity to bacteriocins: (i) immunity is genetically linked with bacteriocin production and exerts the strongest level of non-sensitivity, (ii) resistance can occur as the appearance of spontaneous mutants following selection on the bacteriocin; and (iii) resistance conferred by a gene that is not genetically linked with bacteriocin production. These three categories of resistance are likely to be similar for any bacteriocin [21].

The genetic determinant for nisin immunity has been defined as *nisI*, the fifth gene encoded in the nisin operon [92, 101, 153]. The entire NisI protein showed no significant similarities to other proteins, but its *N*-terminus strongly resembles that of signal peptide sequences of lipoproteins from Gram-negative *E. coli* and Gram-positive *Bacillus* and *L. lactis* [92, 107, 154]. Bacterial lipoproteins are a group of exported proteins that are anchored to the cellular or outer membrane by lipid moieties. The lipids are covalently linked to the cysteine residue located at the *N*-terminus of the secreted protein [92]. Furthermore, the typical consensus sequence of the cleavage site and the tripartite structure of signal peptides is also found in the *N*-terminus of NisI [92, 107]. NisI therefore is a membrane-bound lipoprotein located on the outside of the cell membrane [92, 107, 155]. Similar results have been described for the only other immunity protein reported thus far for a lantibiotic, i. e. PepI, which

is encoded by the *pep5* operon [85, 156, 157]. The mechanism of immunity conferred by the NisI protein remains very speculative. The lipoprotein NisI could, when attached to the exterior of the cellular membrane by lipid moieties, confer immunity by direct interaction with extracellular nisin or by disturbing the association of nisin aggregates, thus preventing channel formation [107].

For all class II bacteriocins genetically studied until now, a protein conferring immunity to the producer organism was encoded in the 3′ end of the bacteriocin operon, for example lactococcin A [46], lactococcin B [136], lactococcin M [46], lactococcin G [128], pediocin PA-1 and AcH [130, 131], mesentericin Y105 [124], carnobacteriocin B2 and BM1 [158], leucocin UAL-187 [42], plantaricin A [49] and sakacin A [133]. These immunity proteins have a high pI [49]. Furthermore, those associated with two-peptide bacteriocins consist of 110 to 154 amino acids containing several transmembrane domains [65, 77, 128], while those of the one-peptide bacteriocins are generally smaller (51 to 113 residues) and contain few (one or two) or no putative transmembrane helices [65, 130, 133, 136, 158, 159]. Recently, a new class of immunity proteins was reported consisting of 247 to 257 residues spanning the cytoplasmic membrane seven times [49].

Based on these findings, it seems that an important group of the immunity proteins exert their activity at the cytoplasmic membrane, although lciA is the only immunity protein studied in detail. The lactococcin A immunity factor was purified and shown to interact with the cell membrane, whereas the presence of free intracellular lciA is considered as a reservoir of immunity factor protein [161]. LciA may span the membrane once by virtue of an α-amphiphilic helix between residues 29 and 47 [162]. Topological studies showed that the carboxy-terminus of LciA was orientated at the outside of the cytoplasmic membrane [162]. LcnA acts on intact cells or membrane vesicles, but not on liposomes suggesting that a specific membrane receptor is required for LcnA recognition and action [65, 162]. Membrane vesicles are protected from LcnA action if they are derived from cells expressing LcnA immunity. Exposing lactococcin A-sensitive cells to excess of the immunity protein did not affect the LcnA-induced killing of the cells, indicating that the immunity protein does not protect cells by simply binding to lactococcin A, or to externally exposed domains of the cell surface [161]. Comparable results were reported for carnobacteriocin immunity factors [158]. This suggests that LcnA immunity occurs at the cytoplasmic membrane via a mechanism that either blocks a receptor, prevents LcnA channel formation, or inactivates the bacteriocin [62, 65]. The cell localization and mode of action of immunity proteins without apparent potential membrane-spanning helices is not yet known, although membrane association of such proteins can not be excluded. Interestingly, two such proteins MesI and PedB display an almost identical hydrophobicity plot, suggesting a common mode of action.

Recently, three additional open reading frames, *nisF*, *nisE* and *nisG*, were revealed adjacent to *nisK* [104]. A comparable gene cluster, *epiFEG* has been described for the lantibiotic epidermin, produced by *Staphylococcus epidermidis* [163]. The NisE/EpiE and NisG/EpiG proteins are both predominantly hydrophobic with six transmembrane domains [104, 163]. The NisF/EpiF com-

ponent contains two potential ATP-binding consensus sites [104]. The proteins encoded by these operons resemble the *E. coli* MalFGK2 and HisMQP2 transporters [163–165] and the SpaFG and McbFE proteins, which are involved in immunity against subtilin [110] and microcin B17 [109], respectively. The hydrophobicity plot of NisF and NisE together resembles that of the complete SpaF protein [104]. It was therefore proposed that NisF and NisE constitute the transmembrane and ATP-binding domains of an ATP-dependent translocator [104]. Based on homologies with colicin immunity proteins, NisG was predicted to have a similar function in nisin immunity [104]. In the case of epidermin, EpiE and EpiG were, based on mutual homology, both predicted as ABC transporter membrane components with six potential membrane-spanning helices, a common feature of these transporter systems [163]. EpiEGF2 were therefore thought to act as a hetero-tetrameric complex, including EpiG, in comparison with the well-characterized MalFGK2 and HisMQP2 transporters [163–165] but in contradiction with the postulated function for NisG [104]. Immunity conferred by this ABC secretory system could be mediated by active extrusion or by their uptake and intracellular degradation [104, 163].

A gene, *nsr*, conferring resistance against nisin has been isolated from *L. lactis* subsp. *lactis* biovar *diacetylactis* DRC5, which is a nisin-nonproducer [166, 167]. Nsr is a 318-amino acid residue protein with a hydrophobic *N*-terminus, resulting in membrane association. The level of resistance conferred by Nsr was only 10% of the immunity of the nisin producer strain [107]. The nsr gene did not hybridize with genomic DNA of the nisin producer strain *L. lactis* subsp. *lactis* ATCC 11454, demonstrating that the genetic determinants for immunity and resistance are different, as are their expected mechanisms of action [167]. Although nisin resistance has been reported among a variety of Gram-positive bacteria [34], in the only case studied up to now, *B. cereus* produced a nisin reductase that presumably inactivated one or more of the dehydroresidues required for nisin activity [168, 169].

5
Biosynthesis of Bacteriocins Produced by Lactic Acid Bacteria

5.1
Response Regulation

Many of the bacterial metabolic pathways are induced by various extracellular stimuli. Those environmental conditions are sensed and signaled through, by means of signal transduction systems. Many of these systems consist of two components, a sensor, often located in the cytoplasmic membrane and a cytoplasmic response regulator [108, 170–172]. They are therefore generally called two-component systems. The environmental sensor acts as a histidine protein kinase (HPK) and modifies the response regulator (RR) protein, which in turn triggers an adapting response, in most cases by gene regulation. Most histidine protein kinases consist of an *N*-terminal sensory domain and a cytoplasmic *C*-terminal transmitter. The latter contains an autokinase domain and a conserved histidine residue as a site for phosphorylation. Both domains

are linked by membrane-spanning segments [28]. Most response regulator proteins contain an *N*-terminal aspartic residue as a site for phosphorylation and a *C*-terminal output domain involved in mediating an adaptive response [28]. Response regulators bind as dimers to a specific site (mostly direct or inverted repeats) present near the promoter, thereby stimulating or inhibiting binding of the RNA polymerase to the promoter region [173–177]. Interestingly, direct repeats referred to as potential binding sites for response regulator dimers have been reported upstream from the promoters of the different operons involved in the production of several inducible bacteriocin promoters, suggesting a common positive mechanism of regulation for bacteriocin production [49].

Such a regulatory operon, encoding an inducer peptide (plantaricin A), a histidine protein kinase with six transmembrane domains (PlnB) and two regulatory proteins (PlnC and PlnD) has been reported for plantaricin A [49, 134]. Genes for a histidine protein kinase (*nisK*, *sakK*) and a response regulator (*nisR*, *sakR*) were also found in the locus encoding sakacin A, sakacin P, carnobacteriocin A and nisin production [28, 92, 101, 103, 107, 133].

PlnB/SakK, PlnC/SakR and PlnD show highest homology with their counterparts in the *agr* (accessory gene regulatory) system of *Staphylococcus aureus* [134, 149, 150]. The biosynthesis of extracellular proteins which are subject to growth phase-dependent control and play an important role in staphylococcal infection are regulated by the *agr* locus, which consists of two divergent operons [134, 148, 178–180]. The first transcription unit encoded AgrA (RR), AgrC (HPK) and AgrD. An octapeptide processed from AgrD, is involved in activation of the *agr* locus [49, 181]. Activation of the *agr* operon also results in a higher transcription level of *hld*, which in turn is responsible for the *agr*-dependent regulation of the above mentioned extracellular toxins and enzymes [134, 180]. Although initially purified, and characterized as a bacteriocin depending on the complementation of two almost identical peptides, it is now believed that plantaricin A is not a bacteriocin but acts as an *agr*-dependent inducer molecule [47, 49, 134, 145]. Extracellular addition of plantaricin A to a Bac^- mutant restored transcription of the different units invo1ved in bacteriocin production as well as antagonistic activity, indicating a role as induction factor for plantaricin A [49]. In general, these induction factors (IF) involved in bacteriocin production are (i) bacteriocin-like peptides with a double-glycine leader peptide, (ii) their mature form is shorter than a regular bacteriocin and, (iii) the genes encoding IF are located upstream from the histidine kinase gene of the two component system [28]. Small peptides preceding the histidine proteinase kinase, response regulator tandem have also been reported for sakacin A (orf4), sakacin P (orf Y) and carnobacteriocins A, B 1 and BM2 (orf6) [28, 49] (Fig. 5). The role of orf4 in induction of the sakacin P production has already been established [49].

Analogously, it has been shown that NisK and NisP constitute the histidine proteinase kinase and response regulator components of the nisin signal transduction system [92, 101, 107]. NisK is a 447-residue, membrane-integrated protein with two potential *N*-terminal membrane anchors and a cytoplasmic carboxy-terminus [107]. The carboxy-terminus contains a His-238 residue for

Bacteriocin	Peptide sequence
Plantaricin A:	KSSAYSLQMGATAIKQVKKLFKKWGW
Sakacin P:	MAGNSSNFIHKIKQIFTHR
Sakacin A:	TNRNYGKPNKDIGTCIWSGFRHC
Carnobacteriocin A:	SKNSQIGKSTSSISKCVFSFFKKC

Fig. 5. The amino acid sequence of the putative induction factors of class II non-lantibiotic bacteriocins plantaricin A, sakacin A and P and carnobacteriocin A [28]

autophosphorylation and might be the signal-transducing domain with kinase activity [107]. The region between the membrane anchors is hydrophilic and may correspond to the extracellular sensor domain [107]. NisR is a 229-residue protein of the cytoplasm. The *N*-terminus, which forms the part with highest similarity among regulatory proteins contains a very conserved Asp-53 residue where phosphorylation takes place [182, 183]. The exact role of NisK in NisR phosphorylation must still be determined, since inactivation of NisK did not affect nisin production in a plasmid-based complementation system [101]. Mature nisin acts as an inducer of both the *nisA*BTCIKR and nisFEG operon [115]. Extracellular administered nisin complements for the *nisZ*B anti-sense and the *nisT* knock-out mutation, and results in the restoration of transcription of both nisin operons [115]. Nisin induction also resulted in a higher amount of *NisI* gene and an increased level of immunity [115]. The requirement of the structural *nisA* gene for full immunity of the nisin producer had also been recognized by Kuipers et al. [92]. In contradiction to the class II non-lantibiotic inducible bacteriocins, nisin serves a dual function of being a bacteriocin and an induction factor involved in autoregulation [92].

In conclusion, the large similarity among the different systems suggests that a two-component signal transduction mechanism, including a histidine protein kinase and a regulatory protein is a common feature in the regulation of bacteriocin production. The external stimuli triggering the induction or autoinduction system which induces bacteriocin production remain to be elucidated.

5.2 Post-Translational Modifications

The lantibiotics differ extensively from the class II bacteriocins in that they contain post-translationally modified amino acids, as for example dehydrated amino acids and lanthionine residues, forming intramolecular thioether bridges [39, 184]. The chemical modification reactions leading to the typical lanthionines were first proposed by Ingram [185] and are assumed to be catalyzed by specific enzymes encoded in the lantibiotic gene cluster. In the lantibiotic lactocin S, D-alanine residues were discovered, probably by conversion of dehydrated serine residues via a dehydrogenation reaction [82]. In some

lantibiotics produced by non-lactic acid bacteria, such as Pep5, lactocin S and epilancin K7, the *N*-terminal threonine and serine residues are modified into 2-oxy-butyryl, 2-oxy-propionyl and 2-hydroxy-pyruvyl residues, respectively [82, 186, 187]. The *N*-terminal deaminations of dehydroamino acids are considered to occur spontaneously [82]. In the case of epilancin, the 2-oxy-pyruvyl group may be enzymatically reduced to a 2-hydroxy-pyruvyl residue which then would be the very last biosynthetic reaction [82]. In addition, the *C*-terminal cysteine residues of epidermin and the related gallidermin are modified into *S*-[(*Z*)-2-aminovinyl]-D-cysteine [90, 188, 189]. In contrast to earlier reports where *C*-terminal modifications were claimed to occur after lanthionine bridge formation [90], it has recently been shown that the *C*-terminal modification reaction, catalyzed by EpiD, may take place intracellularly as the first step in the post-translational modification of epidermin [184, 189]. This modification reaction and its corresponding enzyme are unique for epidermin and have not been found in any other lantibiotic. Detection of sixfold, fivefold, fourfold, etc. dehydrated pre-Pep5 molecules in the cytoplasmic fraction of the PepS producer showed that (i) dehydration and ring formation are separate steps and (ii) ring formation happens after dehydration [82].

The presence of two genes, nisB and nisC, encoding 993- and 414-residue proteins without significant homology to other known proteins, but conserved in several lantibiotic operons, has made them strong candidates for post-translational modifications in the maturation pathway of lantibiotics [40]. Limited similarity between NisB and *E. coli* IlvA, a threonine dehydratase, was reported and hence a dehydratase function for NisB was suggested [40]. Mutation studies of NisB, NisC, EpiB, EpiC, and SpaB indicated that these proteins were essential for nisin, epidermin and subtilin biosynthesis, respectively [40, 86, 87, 190]. As no precursors have been identified and characterized in these mutants, conclusions about the reaction that is catalyzed by these proteins remain speculative [40]. Secondary-structure predictions and experimental evidence confirmed that NisB and SpaB are both membrane-bound [100].

Some lantibiotic operons, such as lactocin S, lactococcin DR (lacticin 481) or cytolysin contain no homologues of the *nisB* and *nisC* genes [82, 118, 122]. In these operons, the homologous genes *lasM*, *lctM*, and cylM were found [82, 118, 122]. Since CylM and LctM contain a *C*-terminal domain with striking homology to NisC, it could be hypothesized that they combine the function of a dehydratase and the enzymatic reaction leading to lanthionin ring formation [40, 122, 123]. There is a striking correlation between this grouping and the classification of lantibiotics based on their leader sequences [22, 40]. It is therefore tempting to assume that NisB/NisC and its homologues interact with class IA_I leader peptides, whereas an interaction between the larger proteins of the CylM family and the class IA_{II} leader peptides occurs [40]. The post-translational modification reactions of a pre-lantibiotic leads to the formation of an inactive precursor molecule, consisting of the completely matured lantibiotic, still attached to its leader peptide [101, 102]. The *N*-terminal modification of the lantibiotics Pep5, lactocin S and epilancin K7, occurs after proteolytic cleavage of the precursor and is therefore an exception to this rule [82].

5.3
Secretion and Proteolytic Activation of Bacteriocin Precursors

5.3.1
ATP-Dependent Translocation and Processing

The NisP protein product encoded by the *nisP* gene upstream from *nisR* in the nisin gene cluster showed an *N*-terminal signal sequence, a catalytic domain with a high degree of similarity to that of the subtilisin-like serine proteases, and a carboxyterminal membrane anchor [101]. Those features of its primary structure are indicative of secretion followed by membrane anchoring resulting in an extracellularly located catalytic *N*-terminal tail [40, 101]. Precursor nisin devoid of biological activity could be activated by incubation with cell membranes from a *nisP*-expressing strain, while mutation of NisP resulted in the secretion of a fully modified but unprocessed nisin precursor, indicating that the activating NisP protease is membrane located and involved in maturation of nisin [101].

The *nisT* gene encodes a 600-residue protein with strong homology to ABC exporters [92, 100]. These ABC transporters share two main regions of homology, i.e. an ATP-binding motif in the *C*-terminal half and six transmembrane domains located in the *N*-terminal half of the protein [105]. These data indicate that proteolytic cleavage is a process that occurs at the extracellular face of the cytoplasmic membrane following secretion [101]. The counterparts of NisP in the epidermin (EpiP) and cytolysin (CylP) operons contain a signal sequence but lack a membrane-spanning domain, suggesting that they are attached in another way or are not membrane associated [88, 122, 190]. PepP, LasP and ElkP involved in respectively Pep5, lactocin S and epilancin K7 proteolytic processing all lack a signal sequence, and may therefore function intracellularly, which is in agreement with their *N*-terminal modification [40, 186, 187]. The subtilin gene cluster did not contain a peptidase-like protein [87, 89, 110]. However, the subtilin producer *B. subtilis* is known to contain a variety of secreted proteases that could be involved in proteolytic activation [40].

ABC transporters encoded in the same operon or an operon adjacent to the structural bacteriocin gene have been reported for all class II bacteriocins genetically studied in detail [49, 62, 118, 119, 127, 130, 131, 136, 146]. Those proteins are characterized by six transmembrane domains, a carboxy-terminal ATP-binding cassette and an *N*-terminal proteolytic domain, both located in the cytoplasm [146] (Fig. 6.). The energy needed for the translocation process is provided by hydrolysis of ATP [146, 191, 192]. It was remarkably that the ABC transporters involved in the secretion of the lantibiotics nisin, epidermin and subtilin are devoid of a conserved *N*-terminal extension of about 150 amino acids that is only present in the larger transporters and involved in proteolytic processing of the prebacteriocin [146]. Among the larger ABC transporter proteins, two conserved amino acid stretches were shown to be exclusively found in *N*-terminal extensions of bacteriocin transporters and not in exporters of substrates that are not proteolytically processed during transport, such as the haemolysin transporters AppB [193], HlyB [194], LktB [195], and

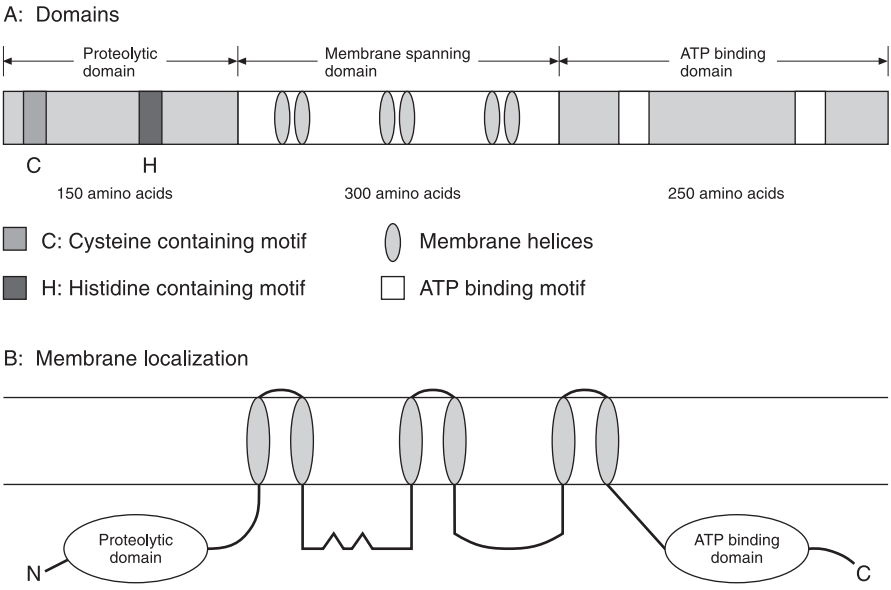

Fig. 6. The organization of the domains of ABC transporters of class II bacteriocins with double-glycine leader peptides and the presumed localization of the domains in relation with the cytoplasmic membrane

CyaB [146, 196–198]. Since it was shown that the 150 *N*-terminal amino acids of the lactococcin G and pediocin PA-1.0 ABC transporters were capable of cleaving the corresponding precursor bacteriocins at the correct consensus processing site, its role for class II leader peptide processing was accepted [132, 146]. Replacement of the cysteine residue on position 13 with an alanine residue resulted in a complete loss of proteolytic activity, demonstrating that this residue is part of the active site 146]. It was therefore concluded that the new class of proteolytic ABC transporters belonged to the cysteine proteases [146]. The absence of this proteolytic domain in ABC transporters of class Al lantibiotics is complemented by an individually encoded subtilisin-like protease in these operons, and thus processing and translocation of the class IA_I lantibiotics depends on the action of two divergent proteins [88, 101, 122, 190].

As mentioned before, NisB, NisC and their homologues are likely to interact with class IA_I leader peptides, whereas an interaction between the large proteins of the CylM family and the class IA_{II} leader peptides was proposed [40]. Leader peptides of the class IA_{II} lantibiotics such as lactococcin DR [118], salivaricin A, streptococcin A-FF22 [199] and cytolysin [122] do not contain the -F-N-L-D-V- box typical for class IA_I lantibiotics [40]. Unexpectedly, these class IA_{II} leader peptides showed considerable similarities with leaders of the class II non-lantibiotic bacteriocins [21, 40, 146]. Furthermore, they also contained a proteolytic processing site, identical or comparable to the double-glycine cleavage site of class II non-lantibiotic peptides [21, 40, 146]. It is therefore likely that the processing and secretion mechanism of the class IA_{II} lantibiotics more

closely resembles that of the non-lantibiotics. In agreement with this model, an ABC transporter including the *N*-terminal proteolytic domain was encoded in the lactococcin DR (LctT) and cytolysin (CylT) operons, indicating that they share a common mechanism of export with the non-lantibiotic, double-glycine type leader peptide bacteriocins [118, 122]. However, in contradiction to the class II non-lantibiotic bacteriocins, downstream from the 714-amino acid residue translocator CylT, a 412 amino acid residue protease is encoded [122]. Functional analysis studies and newly obtained information residing from other class IA_{II} bacteriocin operons will have to resolve this apparently conflicting data.

Recently, a new lantibiotic, lactocin S has been characterized. Its leader peptide is typical for the class IA_{II} lantibiotics but lacks a double-glycine processing site, suggesting an alternative proteolytic cleavage [82, 121]. This hypothesis is reflected in the lactocin S operon which encodes an ABC transporter of 535 amino acids, a protease of 266 residues as well as several open reading frames with unknown functions [82, 121].

5.3.2
Accessory Proteins of the Class II Non-Lantibiotic Bacteriocins

Additionally, all non-lantibiotic class II bacteriocin operons, studied so far, were shown to encode the homologous counterpart of HlyD, the accessory protein of the haemo1ysin A secretion apparatus of *E. coli* [49, 124, 127, 128, 130–133]. These so-called accessory proteins are encoded adjacent to the structural ABC exporter gene and characterized by a unique, *N*-terminal transmembrane domain [49, 124, 127, 128, 130–133]. They are predicted as integral proteins of the cytoplasmic membrane speculated to facilitate signal sequence independent secretion. It has been shown that the biosynthesis of non-lantibiotic bacteriocins requires both the ABC transporter and the accessory factor [105, 126, 133]. These accessory proteins belong to a recently identified, novel class of export proteins designated as the membrane fusion protein (MPF) family [200]. Proteins of the MPF family have been hypothesized to cause local interaction of the bacterial membranes, allowing direct exchange of substrates between the two membranes of the Gram-negative envelope [201]. For some members of the HlyD protein family, including HlyD, evidence has been presented that ten residues of their periplasmic carboxy-terminus mediate association with the outer membrane [202]. Based on these data, the long carboxy-terminal tail of the accessory proteins for the secretion of non-lantibiotic class II bacteriocins of Gram-positive bacteria could hence be expected at the extracellular face of the cytoplasmic membrane since Gram-positive bacteria do not have an outer membrane. The function of such MPF in the cytoplasmic membrane of Gram-positive bacteria, however, is not clear. Counterparts of these accessory proteins in either class IA_I or IA_{II} lantibiotic operons have not yet been reported.

5.3.3
Conclusion

In conclusion, these data indicate striking differences in the processing and secretion mechanism of lantibiotic class IA_I and class IA_{II} and non-lantibiotic class II bacteriocins. Secretion and processing of class IA_I lantibiotics is mediated by two different proteins. Processing occurs extracellularly, except for class IA_I lantibiotics that are *N*-terminally modified prior to export. Class IA_{II} lantibiotics and class II non-lantibiotic bacteriocins are both characterized by an ABC transporter containing a conserved proteolytic processing domain in its *N*-terminal tail. Processing occurs at the cytoplasmic side of the cellular membrane followed by secretion of the mature bacteriocin. Although its function and occurrence in other class IA_{II} lantibiotics remains to be investigated, an additional proteolytic enzyme was detected in the cytolysin operon. The accessory factor protein, also conserved in Gram-negative secretion systems, was characterized as an unique feature of non-lantibiotic class II bacteriocin secretion systems. Based on its divergent leader peptide, containing an ELS box but missing a double-glycine type processing site, an alternative model is expected to emerge for lactocin S.

6
Role of the Leader Peptide

The bacteriocin leader peptides differ from the *N*-terminal signal sequences for export of proteins secreted by the *sec*-dependent pathway in that they lack a hydrophobic membrane-spanning stretch of 10 or more residues as well as the typical proteolytic processing site [82, 120]. Class IA_I leaders are slightly positively or negatively charged and contain conserved residues such as a proline residue at position –2, a serine residue at position –6 and the so-called -F-N-L-D-V-box (Fig. 7 [40]). Site-directed mutagenesis has shown that the very conserved proline residue is not essential for processing, but that a positive charge at position –1 and a small hydrophobic residue at position –4 are essential [102]. Mutation of the phenylalanine, leucine or aspartate residue in the -F-N-L-D-V-box or the serine residue at position –6 prevented biosynthesis of nisin, not even the precursor could be detected [102]. The results so far obtained with site-directed mutagenesis clearly demonstrate the importance of particular residues in the leader peptide for biosynthesis. Meanwhile, there is evidence that processing is the last step in lantibiotic maturation, so that modification reactions are made at the prepeptide stage, and that the precursor molecule is inactive [102]. Therefore, the leader peptide might have an essential role in biosynthesis, either in that it could contain a specific recognition motif which would direct the precursor towards biosynthetic enzymes and/or in that the leader peptide may interact with the propeptide region to stabilize a conformation which is essential for correct modification [39]. In contrast, the class IA_{II} lantibiotics contain a double-glycine type processing site and a leader peptide that matches the consensus of the non-lantibiotic class II bacteriocins [21, 40] (Fig. 7). However, putative modifying enzymes for the class IA_{II}

Class IA_I antibiotics

Precursor	Processing	
MEAVKEKNDL**FNLDV**KVNAKE**S**N-**DS**G-AE**PR**	IASK	epidermin
MEAVKEKNEL**FDLDV**KVNAKE**S**N-**DS**G-AE**PR**	IASK	gallidermin
MKNNKNL**FDLE**IKK--ET**S**Q-**NT**DELE**PQ**	TAGP	pep5
MSKFDD**FDLDV**VK---V**S**KQ**DS**K-IT**PQ**	WKSE	subtilin
MSTKD**FNLD**LVS---V**S**KK**DS**G-AS**PR**	ITSI	nisin A
MSTKD**FNLD**LVS---V**S**KK**DS**G-AS**PR**	ITSI	nisin Z
MNNSL**FDL**NLNK-GVE**T**Q-**KS**D-LE**PQ**	SASV	epilancin K7
FNLDV **S** **DS** **PR**		consensus

Class IA_{II} antibiotics

Precursor	Processing	
VLNKENQENYYSNKLELVGPSFE**ELS**LE**EM**EA**I**Q**GS**	GDVQ	cytolysin L2
MNAMKNSKDILNNAIE**EVS**EK**EL**ME**V**A**GG**	KRGS	salivaricin A
MEKNNEVINSIQ**EVS**LE**EL**DQ**II**G**A**	GKNG	streptococcin FF-22
MENLSVVPSFE**ELS**VE**EM**EA**I**Q**GS**	GDVQ	cytolysin L1
MKEQNSFNLLQ**EVT**ES**EL**DL**IL**G**A**	KGGS	lacticin 481
EVS **EL** **I** **GA**		consensus

Class II non-lantibiotic bacteriocins

Precursor	Processing	
MMNMKPTFSYEQ**LD**NS**AL**EQVV**GG**	KYYG	leucocin A
MKNQLNFNI**VS**DE**EL**SEAN**GG**	KLTF	lactococcin A
MKNQLNFNI**VS**DE**EL**AEVN**GG**	SLQY	lactococcin B
MKNQLNFEI**LS**DE**EL**QGIN**GG**	IRGT	lactococcin M
MKKIEK**LT**EK**EM**ANII**GG**	KYYG	pediocin PA-1
MMMVKE**LS**MT**EL**QTIT**GG**	ARSY	sakacin A
MKQFNY**LS**HK**DL**AVVV**GG**	RNNW	lactacin F
LS **EL** **GG**		consensus

Fig. 7. Alignment of leader peptides of class IA_I and class IA_{II} lantibiotics and class II non-lantibiotic bacteriocins. Lantibiotics with class IA_I leaders include nisin A and nisin Z from different strains of *Lactococcus lactis* [83], subtilin from *Bacillus subtilis* [84], epidermin, gallidermin and Peps from various *Staphylococcus epidermidis* strains [29, 90, 188]. Lantibiotics with class IA_{II} leaders include lacticin 481 (lactococcin DR) from *L. lactis* [211], streptococcin A-FF22 from *Streptococcus* sp. [199], salivaricin A from *Streptococcus salivarius* and cytolysin L1 and L2 from *Enterococcus faecalis* [122]. Bacteriocins of the non-lantibiotic class II type include leucocin A from *Leuconostoc gelidum* [69], lactococcin A, B and M from *L. lactis* [46, 125, 126, 135, 136], pediocin PA-1 from *Pediococcus acidilactici* [130], and sakacin A and lactacin F from *Lactobacillus* sp. [43, 203]

lantibiotics differ significantly from those of the class IA_I lantibiotics [40, 82, 118, 122].

Lactacin F was the first non-lantibiotic bacteriocin characterized in lactic acid bacteria for which both DNA and protein sequences were available [77, 203]. This information demonstrated that lactacin F is translated as a 75-amino acid residue precursor which is posttranslationally processed by cleavage of a

18-residue *N*-terminal leader peptide at a very conserved double-glycine-residue processing site. Site-directed mutagenesis of the lactacin F (LafA) precursor was employed to modify the glycine residues at positions –1 and –2, and the valine (–3 position) and arginine (+1 position) residues [77]. Replacement of glycine at position –1 with valine, or replacement of the glycine residue at position –2 with arginine, or even the polarityneutral amino acid serine eliminated lactacin F expression. Replacement of valine at position –3 with a charged residue (Asp) or arginine at position +1 with another positively charged residue did not disrupt bacteriocin activity [77]. Based on these experiments and sequence alignments, a more conserved pattern for the bacteriocin leader peptide was proposed [77] including (i) two conserved glycines at positions –1, and –2, (ii) hydrophobic residues at positions 4, –7, –12, and –15, (iii) a core of charged amino acids at positions –8 and –10, and (iv) a serine at position –11. Heterologous expression of lactacin F peptides in *Carnobacterium piscicola* LV17, and *Leuconostoc gelidum* resulted in the production of mature, bioactive lactacin F [204, 205].

These results confirm the conservative nature of the processing and secretion apparatus involved in class II non-lantibiotic maturation, as it was capable of recognizing and properly processing heterologously expressed lactacin F [204, 205]. Heterologous expression of the lactococcin A operon in *Pediococcus* and expression of the pediocin PA-1 operon in *Lactococcus lactis* also resulted in fully matured bioactive peptides [206]. Recently, the new bacteriocin divergicin A was shown to be secreted by the *sec*-dependent pathway [51]. The *N*-terminal extension of divergicin A had a -A-S-A-(positions –3 to –1) cleavage site and acts as a signal peptide that accessed the general export system of the cell [51]. Production of divergicin A was demonstrated in heterologous hosts containing the two genes associated with the bacteriocin and immunity [51]. These data indicate that a fully functional bacteriocin molecule can be produced in the absence of the typical leader peptide consensus and the corresponding ABC transporter gene.

Comparison of the leader peptides and the ABC transporter systems of the class IA_{II} lantibiotics and the class II non-lantibiotic bacteriocins suggest that both are processed and secreted in the same manner [21, 40, 146]. A striking feature of the class IA_{II} lantibiotic leader peptides consists of a very conserved glutamate residue at position –13, missing in the class II leaders and resulting in the ELS consensus [40]. The class IA_{II} lantibiotics, in contradiction to the class II non-lantibiotic bacteriocins undergo post-translational modification and their leader peptide would hence not only be involved in proper processing of the precursor, but might fulfill a comparable role in conformational stabilization during post-translational modification, as the class IA_I leader peptides [21, 40, 82].

7 Conceptual Model for Bacteriocin Maturation

A combination of the above described findings could hence result in the following hypothetical model for bacteriocin biosynthesis (Figs. 8 and 9). Firstly,

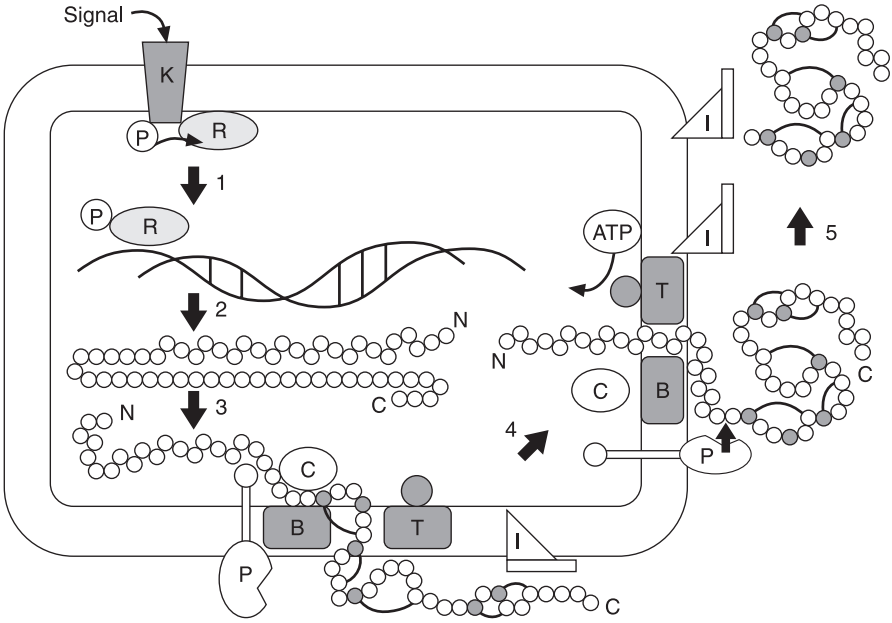

Fig. 8. A conceptual maturation pathway for nisin is given as a 5-step process [40]. A two-component signal transduction system induces transcription (*step 1*). Translation results in an inactive unmodified precursor peptide (*step 2*). The leader peptide is proposed to play a role in targeting of the precursor to a membrane-located modification complex (*step 3*). Dehydration and lanthionine and dehydro-lanthionine formation (*step 4*) is followed by extracellular processing and secretion (*step 5*)

an inducing signal activates, via the two-component signaling pathway, the promoters responsible for the expression of the operons involved in bacteriocin production. In the case of nisin, production and immunity have shown to be autoregulated. Expression of several inducible class II non-lantibiotic bacteriocins (e.g. sakacin A, sakacin P, plantaricin P) is controlled by a bacteriocin-like peptide, processed at a double-glycine consensus sequence site which lacks antagonistic activity. The two-component signal transduction system has not yet been shown for most of the class II non-lantibiotic bacteriocins, which may therefore display a constitutive expression. Transcription results in the concerted production of the proteins constituting the modification and secretion machinery, together with the inactive bacteriocin precursor molecule.

In case of the lantibiotics, this precursor contains free cysteines and no dehydrated residues. The lantibiotic precursor molecule is directed, presumably by virtue of the leader peptide, to a membrane-located complex containing the modifying enzymes NisB (possibly involved in dehydration) and *NisC* (conceivably involved in establishing the thioether bonds). Lantibiotics of the class IA_{II} type (lactococcin DR, cytolysin, lactocin S) lack genes of the nisB and nisC type in their corresponding operons [207]. It is assumed but not yet established that one protein belonging to the so called CylM family mediates a one-step for-

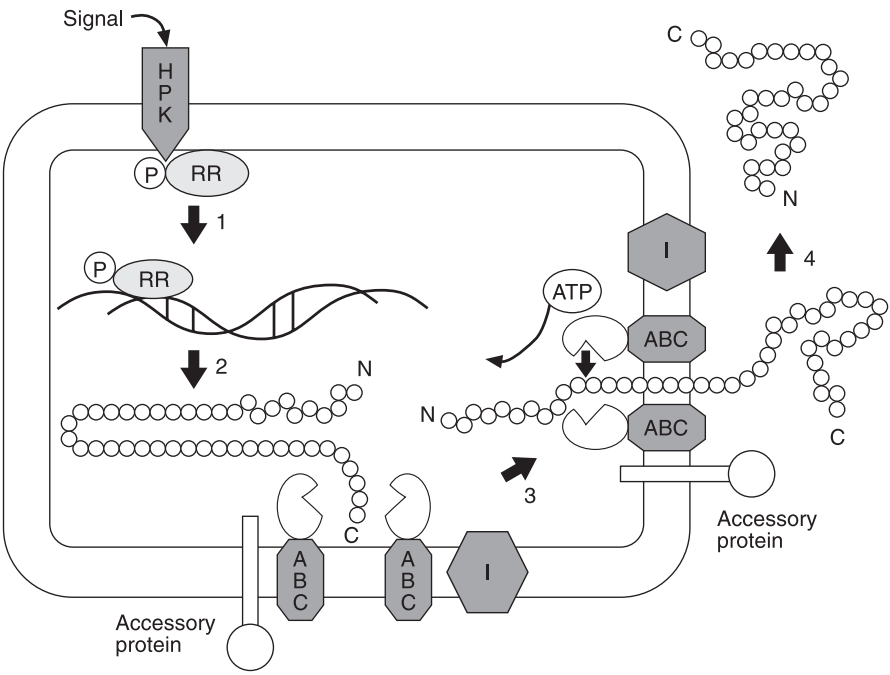

Fig. 9. Maturation pathway of a class II non-lantibiotic bacteriocin presented as a 4-step process. The HPK and RR constitute a protein complex involved in signal transduction of external stimuli (*step 1*), resulting in transcription and translation of the bacteriocin precursor (*step 2*). The inactive precursor peptide is targeted to a membrane anchored ATP dependent translocation complex and processing at the double-glycine consensus site occurs intracellularly (*step 3*) and is followed by secretion (*step 4*). The role of the accessory protein in this mechanism is not yet understood

mation of lanthionine and methyl-lanthionine bridges. This reaction presumably takes place in the cytoplasm of the cell. Bacteriocins of the non-lantibiotic type do not undergo such post-translational reactions. It is generally assumed that the modification reactions leading to lanthionine bridge formation are the first post-translational modification reactions following translation. Dehydration precedes lanthionine ring formation and both occur separated in time.

Conflicting reports have been made about the *C*-terminal modification of epidermin, mediated by the unique enzyme EpiD, but the most recent data suggest that this reaction could be expected as the first enzymatic modification involved in epidermin maturation. The modifications result in the formation of an inactive precursor molecule. At this point, the leader may help to maintain the peptide in an inactive form.

Subsequently, both the modified lantibiotic precursor and the unmodified non-lantibiotic bacteriocin precursor are secreted via an ABC transporter, at the expense of ATP hydrolysis. Processing of the class IA_{II} lantibiotics and the non-lantibiotic bacteriocins is associated with the intracellular *N*-terminal tail of the ABC exporter. Nisin, the representative of the lantibiotic class IA_{I} pre-

cursors is activated by the extracellular protease NisP, which is hooked to the cell membrane by means of a fatty acyl membrane anchor. Processing of *N*-terminally modified lantibiotics (Pep5, epilancin K7, lactocin S) occurs in the cytoplasm, prior to *N*-terminal modification. This latter modification is a spontaneous reaction, except; for the enzymatic reduction of epilancin K7, which would hence be the last step in the modification of this lantibiotic and secretion. The contribution of the leader peptide in this *sec*-independent process is not known, nor is its fate after processing or the polarity of the export process. Secretion results in the release of a bioactive bacteriocin.

While class II non-lantibiotic bacteriocins appear to be secreted by the *sec*-independent universal ABC transporter system, it has recently been shown that some bacteriocins do not possess a double-glycine leader peptide but are, instead, synthesized with a typical *N*-terminal leader peptide of the *sec-type*. So far four such *sec*-dependent bacteriocins have been reported divergicin A [51], acidocin B (50], bacteriocin 31 [208] and enterocin P [209]. Recently, two bacteriocins, enterocin L5OA and L5OB, were found to be secreted without an *N*-terminal leader sequence or signal peptide [210].

References

1. De Vuyst L, Vandamme EJ (eds) (1994) Bacteriocins of Lactic Acid Bacteria: Microbiology, Genetics and Applications. Blackie Academic & Professional, London
2. Rose AH (1982) Fermented Foods. Academic Press, New York
3. Reed G (1983) Food and Feed Production with Microorganisms. Verlag Chemie, Deerfield Beach, Florida
4. Steinkraus KH (1983) Handbook of Indigenous Fermented Foods. Marcel Dekker, New York
5. Wood BJB (1985) Microbiology of Fermented Foods. Elsevier, London
6. Gilliland SE (1986a) Bacterial Starter Cultures for Foods. CRC Press, Boca Raton, Florida
7. Buckenhüskes HJ (1993) Selection criteria for lactic acid bacteria to be used as starter cultures for various food commodities. FEMS Microbiol Rev 12 : 253 – 271
8. Gilliland SE (1986b) Role of starter culture bacteria in food preservation. In: Gilliland SE (ed) Bacterial Starter Cultures for Foods. CRC Press, Boca Raton, Florida, pp 175 – 185
9. Lindgren SE, Dobrogosz WJ (1990) Antagonistic activities of lactic acid bacteria in food and feed fermentations. FEMS Microbiol Rev 12 : 207 – 220
10. Schillinger U (1990) Bacteriocins of lactic acid bacteria. In: Bills DD, Kung SD (eds) Biotechnology and Food Safety. Burrerworth-Heinemann, Boston, pp 55 – 74
11. Vandenbergh PA (1993) Lactic acid bacteria, their metabolic products and interference with microbial growth. FEMS Microbiol Rev 12 : 221 – 237
12. Lloyd AG, Drake JJP (1975) Problems posed by essential food preservatives. Br Med bull. 31 : 214 – 219
13. Lewus CB, Kaiser A, Montville TJ (1991) Inhibition of food-borne bacterial pathogens by bacteriocins from lactic acid bacteria isolated from meat. Appl Environ Microbiol 57 : 1683 – 1688
14. Marteau P, Rambeaud J-C (1993) Potential of using lactic acid bacteria for therapy and immunomodulation in man. FEMS Microbiol Rev 12 : 207 – 220
15. Gerritse K, Posno M, Schellekens M, Boersma WJA, Claassen E (1990) Oral administration of *TNP-Lactobacillus* conjugates in mice: a model for evaluation of mucosal and systemic immune responses and memory formation elicited by transformed lactobacilli. Res Microbiol 141 : 955 – 962

16. Norton PM, Wells JM, Brown HWG, Macpherson AM, Le Page RWF (1997) Protection against tetanus toxin in mice nasally immunized with recombant *Lactobacillus lactis* expressing tetanus toxin fragment C. Vaccine 15 : 616 – 649
17. Tagg JR, Dajani AS, Wannamaker LW (1976) Bacteriocins of Gram-positive bacteria. Bacteriol Rev 40 : 722 – 756
18. Gratia A (1925) Sur un remarquable example d'antagonisme entre souches de colibacille. CR Soc Biol 93 : 1040 – 1041
19. Frédericq P (1948) Actions antibiotiques reciproques chez les *Enterobacteriaceae*. Rev Bel Pathol Med Exp 19 : 1 – 107
20. Jack RW, Tagg JR, Ray B (1995) Bacteriocins of Gram-positive bacteria. Microbiol Rev 59 : 171 – 200
21. Klaenhammer TR (1993) Genetics of bacteriocins produced by lactic acid bacteria. FEMS Microbiol Rev 12 : 39 – 86
22. Jung G, Sahl H-G (1991) Nisin and Novel Lantibiotics, ESCOM Science Publishers BV., Leiden
23. Baba T, Schneewind O (1998) Instruments of microbial warfare: bacteriocin synthesis, toxicity and immunity. Trends Microbiol 6 : 66 – 71
24. Rogers LA (1928) The inhibitory effect of *Streptococcus lactis* on *Lactobacillus bulgaricus*. J Bacteriol 16 : 321 – 325
25. Whitehead HR (1933) A substance inhibiting bacterial growth, produced by certain strains of lactic streptococci. Biochem J 27 : 1793 – 1800
26. Mattick ATR, Hirsch A (1947) Further observations on an inhibitory substance (nisin) from lactic streptococci. Lancet 2 : 5 – 7
27. Hurst A (1981) Nisin. Adv Appl Microbiol 27 : 85 – 123
28. Nes IF, Diep DB, Håvarstein LS, Brurberg MB, Eijsink V, Holo H (1996) Biosynthesis of bacteriocins in lactic acid bacteria. Antonie van Leeuwenhoek
29. Kaletta C, Entian K-D (1989) Nisin, a peptide antibiotic: cloning and sequencing of the *nisA* gene and posttranslational processing of its peptide product. J Bacteriol 171 : 1597 – 1601
30. Piard JC, Delorme F, Giraffa G, Commissaire J, Desmazeaud M (1990) Evidence for a bacteriocin produced by lactococcus *lactis* CNRZ 481. Neth Milk Dairy J 44 : 143 – 158
31. Møfrtveldt CI, Nes IF (1990 Plasmid-associated bacteriocin production by a *Lactobacillus sake* strain. J Gen Microbiol 136 : 1601 – 1607
32. Horn N, Swindell S, Dodd H, Gasson M (1991) Nisin biosynthesis genes are encoded by a novel conjugative transposon. Mol Gen Genet 228 : 129 – 135
33. Møfrtveldt CI, Nissen-Meyer J, Sletten K, Nes IF (1991) Purification and amino acid sequence of lactocin S, a bacteriocin produced by *Lactobacillus sake* L45. Appl Environ Microbiol 57 : 1829 – 1834
34. Harris LJ, Fleming HP, Klaenhammer TR (1992) Developments in nisin research. Food Res Int 25 : 57 – 66
35. Stoffels G, Nes IF, Gudmundsdottir A (1992) Isolation and properties of a bacteriocin-producing *Carnobacterium piscicola* isolated from fish. J Appl Bacteriol 73 : 309 – 316
36. Stoffels G, Nissen-Meyer J, Gudmundsdottir A, Sletten K, Holo H, Nes IF (1992) Purification and characterization of a new bacteriocin isolated from a *Carnobacterium* sp. Appl Environ Microbiol 58 : 1417 – 1422
37. Rauch PJG, Beerthuyzen MM, De Vos WM (1990) Nucleotide sequence of IS904 from *Lactococcus lactis* subsp. *lactis* strain NIZO R5. Nucleic Acids Res 18 : 4253 – 4254
38. Paik SH, Chakicherla A, Hansen JN (1998) Identification and Characterization of the Structural and Transporter Genes for, and the Chemical and Biological Properties of Sublancin 168, a Novel lantibiotic Produced by *Bacillus subtilis* 168. J Biol Chem 273 : 23134 – 23142
39. Jung G (1991) Lantibiotics: a survey. In: Jung G, Sahl H-G (eds) Nisin and Novel Lantibiotics. ESCOM Science, Leiden, pp 1 – 34

40. De Vos WM, Kuipers OP, van der Meer JR, Siezen RJ (1995b) Maturation pathway of nisin and other lantibiotics: post-translational modified antimicrobial peptides exported by Gram-positive bacteria. Mol Microbiol 17 : 427 – 437
41. Havarstein LS, Holo H, Nes IF (1994) The leader peptide of colicin V shares consensus sequences with leader peptides that are common among peptide bacteriocins produced by gram positive bacteria. Microbiology 140 : 2383 – 2389
42. Hastings JW, Sailer M, Johnson K, Rou KK, Vederas JC, Stiles ME (1991) Characterization of leucocin A UAL 187 and cloning of the bacteriocin gene from *Leuconostoc gelidum*. J Bacteriol 173 : 7491 – 7500
43. Holck A, Axelsson L, Birkeland *S*-E, Aukrust T, Blom H (1992) Purification and amino acid sequence of sakacin A, a bacteriocin from *Lactobacillus sake* Lb706. J Gen Microbiol 138 : 2715 – 2720
44. Lozano JCN, Meyer JN, Sletten K, Pelaz C, Nes IF (1992) Purification and amino acid sequence of a bacteriocin produced by Pedicococcus acidilactici. J Gen Microbiol 138 : 1985 – 1990
45. Tichaczek PS, Nissen-Meyer J, Nes IF, Vogel RF, Hammes WP (1992) Characterization of the bacteriocin curvacin A from *Lactobacillus curvatus* LTH 1174 and sakacin P from *L. sake* LTH673. Syst Appl Microbiol 15 : 460 – 468
46. van Belkum MJ, Hayema BJ, Jeeninga RE, Kok J, Venema G (1991a) Organization and nucleotide sequence of two lactococcal bacteriocin operons. Appl Environ Microbiol 57 : 492 – 498
47. Nissen-Meyer J, Holo H, Håvarstein LS, Sletten K, Nes IF (1992) A novel lactococcal bacteriocin whose activity depends on the complementary action of two peptides. J Bacteriol 174 : 5686 – 5692
48. Allison GE, Frémaux C, Klaenhammer TR (1994) Expansion of bacteriocin activity and host range upon complementation of two peptides encoded within the lactacin F operon. J Bacteriol 176 : 2235 – 2241
49. Diep DB, Håvarstein LS, Nes IF (1996) Characterization of the locus responsible for the bacteriocin production in *Lactobacillus plantarum* Cll. J Bacteriol 178 : 4472 – 4483
50. Leer RL, van der Vossen JMBM, van Giezen M, van Noort JM, Pouwels PH (1995) Genetic analysis of acidocin B, a novel bacteriocin produced by *lactobacillus acidophilus*. Microbiology 141 : 1629 – 1635
51. Worobo RW, van Belkum MJ, Sailer M, Roy KL, Vederas JC, Stiles ME (1995) A signal peptide-dependent bacteriocin from *Carnobacterium divergens*. J Bacteriol 177 : 3143 – 3149
52. Metha AM, Patel KA, Dave PJ (1983) Isolation and purification of an inhibitory protein from *Lactobacillus acidophilus* ACT. Microbiology 37 : 37 – 43
53. Joerger MC, Klaenhammer TR (1986) Characterization and purification of helveticin J and evidence for a chromosomally determined, bacteriocin produced by *Lactobacillus helveticus* 481. J Bacteriol 167 : 439 – 446
54. Joerger MC, Klaenhammer TR (1990) Cloning, expression and nucleotide sequence of the *Lactobacillus helveticus* 481 gene encoding the bacteriocin helveticin J JBacteriol 172 : 6339 – 6347
55. Toba T, Yoshioka E, Itoh T (1991) Acidophilucin A, a new heat-labile bacteriocin produced by *Lactobacillus acidophilus* LAPT 1060. Lett Appl Microbiol 12 : 106 – 108
56. Vaughan EE, Daly C, Fitzgerald GF (1992) Identification and characterization of helveticin V-1829, a bacteriocin produced by *Lactobacillus helveticus* 1829. J Appl Bacteriol 73 : 299 – 308
57. Upreti GC, Hinsdill RD (1973) Isolation and characterization of a bacteriocin from a homofermentative *Lactobacillus*. Antimicrob Agents Chemother 4 : 487 – 494
58. Upreti GC, Hinsdill RD (1975a) Isolation and characterization of a bacteriocin from a homofermentative *Lactobacillus*. Antimicrob Agents Chemother 7 : 139 – 145
59. Lewus CB, Sun S, Montville TJ (1992) Production of an amylase-sensitive bacteriocin by an atypical *Leuconostoc paramesenteroides* strain. Appl Environ Microbiol 58 : 143 – 149

60. Jiménez-Díaz R, Rios-Sánchez RM, Desmazeaud M, Ruiz-Barba JL, Piard J-C (1993) Plantaricin S and T, two new bacteriocins produced by *Lactobacillus plantarum* LPCO10 isolated from a green olive fermentation. Appl Environ Microbiol 59 : 1416 – 1424
61. Schved F, Lalazar A, Henis Y, Juven BJ (1993) Purification, partial characterization and plasmid linkage of pediocin SJ-1, a bacteriocin produced by *Pediococcus acidilacitici*. JAppl Bacteriol 74 : 67 – 77
62. Venema K, Venema G, Kok J (1995) Lactococcal bacteriocins: mode of action and immunity. Trends Microbiol 3 : 299 – 304
63. Davey GP (1981) Mode of action of diplococcin, a bacteriocin from *Streptococcus cremoris* 346. NZJ Dairy Sci Technol 16 : 187 – 190
64. Zajdel JK, Ceglowski P, Dobrzanski WT (1985) Mechanism of action of lactostrepcin 5, a bacteriocin produced by *Streptococcus cremoris*. Appl Environ Microbiol 49 : 969 – 974
65. van Belkum MJ, Kok J, Venema G, Holo H, Nes IF, Konings WN and Abee T (1991b) The bacteriocin lactococcin A specifically increases permeability of lactococcal cytoplasmic membranes in a voltage-independent, protein-mediated manner. J Bacteriol 173 : 7934 – 7941
66. Bhunia AK, Johnson MC, Ray B, Kalchayanand N (1991) Mode of action of pediocin AcH from *Pediococcus acidilactici* H on sensitive bacterial strains. J Appl Bacteriol 70 : 25 – 33
67. Sahl H-G (1991) Pore formation in bacterial membranes by cationic lantibiotics. In: Jung G, Sahl H-G (eds) Nisin and Novel Lantibiotics. ESCOM Science, Leiden, pp 347 – 358
68. Upreti GC, Hinsdill RD (1975b) Production and mode of action of lactocin 27 bacteriocin from a homofermentative *Lactobacillus*. Antimicrob Agents Chemother 7 : 139 – 145
69. Hastings JW, Stiles ME (1991) Antibiosis of *Leuconostoc gelidum* isolated from meat. J Appl Bacteriol 70 : 127 – 134
70. Kok J, Holo H, van Belkum MJ, Haandrikman AJ, Nes IF (1993) Non-nisin bacteriocins in lactococci: biochemistry, genetics and mode of action. In: Hoover D, Steenson L (eds) Bacteriocins of Lactic Acid Bacteria. Academic Press, New York, pp 121 – 150
71. Venema K, Abee T, Haandrikman AJ, Leenhouts KJ, Kok J, Konings WN, Venema G (1993) Mode of action of lactococcin B, a thiol-activated bacteriocin from *Lactococcus lactis*. Appl Environ Microbiol 59 : 1041 – 1048
72. Moll G, Ubbink-Kok T, Hildeng-Hauge H, Nissen-Meyer J, Nes IF, Konings WN, Driessen AJM (1996) Lactococcin G is a potassium ion-conducting, two-component bacteriocin. J Bacteriol 178 : 600 – 605
73. Christensen DP, Hutkins RW (1992) Collapse of the proton motive force in *Listeria monocytogenes* caused by a bacteriocin produced by *Pediococcus acidilactici*. Appl Environ Microbiol 58 : 3312 – 3315
74. Ray B, Hoover DG (1993) Pediocins. In: Hoover DG, Steenson LR (eds) Bacteriocins of Lactic Acid Bacteria. Academic Press, New York, pp 181 – 210
75. Chikindas ML, Garcia-Garcera MJ, Driessen AJM, Ledeboer AM, Nissen-Meyer N, Nes IF, Abee T, Konings WN, Venema G (1993) Pediocin PA-1, a bacteriocin from *Pediococcus acidilactici* PAC1.0, forms hydrophylic pores in the cytoplasmic membrane of target cells. Appl Environ Microbiol 59 : 3577 – 3584
76. Kaiser ET (1987) Design of amphiphilic peptides. In: Alan R (ed) Protein Engineering. Liss, New York, pp 193 – 199
77. Frémaux C, Ahn C, Klaenhammer TR (1993) Molecular analysis of the lactacin F operon. Appl Environ Microbiol 59 : 3906 – 3915
78. Salomon RA, Farias RN (1993) The FhuA protein is involved in microcin 25 uptake. J Bacteriol 175 : 7741 – 7742
79. Salomon RA, Farias RN (1995) The peptide antibiotic microcin 25 is imported through the TonB pathway and the SbmA protein. J Bacteriol 177 : 3323 – 3325
80. Moeck GS, Fasly Bazzaz BS, Gras MF, Ravi TS, Ratcliffe MJH, Coulton JW (1994) Genetic insertion and exposure of a reporter epitope in the ferrichrome-iron receptor of *Escherichia coli* K-12. J Bacteriol 176 : 4250 – 4259
81. Gross E, J Morell J (1971) The stucture of nisin. J Am Chem Soc 93 : 4634 – 4635

82. Sahl H-G, Jack RW, Bierbaum G (1995) Biosynthesis and biological activities of lantibiotics with unique post-translational modifications. Eur J Biochem 230 : 827 – 833
83. Mulders JW, Boerrigter LJ, Rollema HS, Siezen RJ, De Vos WM (1991) Identification and characterization of the lantibiotic nisin Z, a natural nisin variant. Eur J Biochem 201 : 581 – 584
84. Banerjee S, Hansen JN (1988) Structure and expression of a gene encoding the precursor of subtilin, a small protein antibiotic. J Biol Chem 263 : 9508 – 9514
85. Reis M, Sahl H-G (1991) Genetic analysis of the producer self-protection mechanism ('immunity') against Pep5. In: Jung G, Sahl H-G (eds) Nisin and Novel Lantibiotics. ESCOM, Leiden, pp 320 – 331
86. Chung YJ, Steen MT, Hansen JN (1992) The subtilin gene of *Bacillus subtilis* ATCC 6633 is encoded in an operon that contains a homologue of the hemolysin B transport protein. J Bacteriol 174 : 1417 – 1422
87. Klein C, Kaletta C, Schnell N, Entian K-D (1992) Analysis of genes involved in the biosynthesis of the lantibiotic subtilin. Appl Environ Microbiol 58 : 132 – 142
88. Schnell N, Engelke G, Augustin J, Rosenstein R, Ungermann V, Götz F, Entian K-D (1992) Analysis of genes involved in the biosynthesis of the lantibiotic epidermin. Eur J Biochem 204 : 57 – 68
89. Klein C, Kaletta C, Entian K-D (1993) Biosynthesis of the lantibiotic subtilin is regulated by a histidine kinase/response regulator system. Appl Environ Microbiol 59 : 296 – 303
90. Schnell N, Entian K-D, Schneider U, Götz F, Zähner H, Kellner R, Jung G (1988) Prepeptide sequence of epidermin, a ribosomally synthesized antibiotic with four sulphide-rings. Nature 333 : 276 – 278
91. Steen MT, Chung YJ, Hansen JN (1991) Characterization of the nisin gene as a part of a polycistronic operon in the chromosome of *Lactococcus lactis* ATCC 11454. Appl Environ Microbiol 57 : 1181 – 1188
92. Kuipers OP, Beerthuyzen MM, Siezen JR, De Vos W (1993) Characterization of the nisin gene cluster *nisABTCIPR* of *Lactococcus lactis*. Requirement of expression of the *nisA* and *nisI* genes for development of nisin immunity. Eur J Biochem 216 : 281 – 291
93. Siezen RJ, Kuipers OP, de Vos WM (1996) Comparison of lantibiotics geneclu sters and encoded proteins. Antonie van Leeuwenhoek 69 : 171 – 184
94. Gasson MJ (1984) Transfer of sucrose fermenting ability, nisin resistance and nisin production in *Streptococcus lactis* 712. FEMS Microbiol Lett 21 : 7 – 10
95. Dodd HM, Horn N, Gasson MJ (1990) Analysis of the genetic determinant for production of the petpide antibiotic nisin. J Gen Microbiol 136 : 555 – 566
96. Rodriguez JM, Dodd HM (1996) Genetic determinants for the biosynthesis of nisin, a bacteriocin produced by *Lactobacillus lactis*. Microbiologia SEM 12 : 61 – 74
97. Rauch PJG, De Vos WM (1992) Characterization of the novel nisin-sucrose conjugative transposon *Tn5276* and its insertion in *Lactococcus lactis*. J Bacteriol 174 : 1280 – 1287
98. Rauch PJG, De Vos WM (1994) Identification and characterization of the genes involved in excision of the *Lactococcus lactis* conjugative transposon *Tn5276*. J Bacteriol 176 : 2165 – 2171
99. Poyart-Salmeron C, Trieu-Cuot P, Carlier C, Courvalin P (1989) Molecular characterization of two proteins involved in the excision of the conjugative transposon *Tn1545*: homologies with other site-specific recombinases. EMBO J 8 : 2425 – 2433
100. Engelke G, Gutowski-Eckel Z, Hammelmann M, Entian K-D (1992) Biosynthesis of the lantibiotic nisin: genomic organization and membrane localization of the NisB protein. Appl Environ Microbiol 58 : 3730 – 3743
101. van der Meer FR, Polman J, Beerthuyzen MM, Siezen RJ, Kuipers OP, De Vos W (1993) Characterization of the *Lactococcus lactis* nisin A operon genes *nisP*, encoding a subtilisin-like serine protease involved in precursor processing and *nisR*, encoding a regulatory protein involved in nisin biosynthesis. J Bacteriol 174 : 2152 – 2159
102. van der Meer FR, Rollema HS, Siezen RJ, Beerthuyzen MM, Kuipers OP, De Vos WM (1994) Influence of amino acid substitutions in the nisin leader peptide on biosynthesis and secretion of nisin by *Lactococcus lactis*. J Biol Chem 269 : 3555 – 3562

103. De Vos WM, Beerthuyzen MM, Luesink EL, Kuipers OP (1995a) Genetics of the nisin operon and the sucrose-nisin conjugative transposon *Tn5276*. In: Ferretti JJ, Gilmore MS, Klaenhammer TR (eds) Genetics of *Streptococci*, *Enterococci* and *Lactococci*. Karger, New York, pp 617–625
104. Siegers K, Entian K-D (1995) Genes involved in immunity to the lantibiotic nisin produced by *Lactococcus lactis* 6F3. Appl Environ Microbiol 61:1081–1089
105. Fath MJ, Kolter R (1993) ABC exporters: bacterial exporters. Microbiol Rev 57:995–1017
106. Qiao M, Saris PE (1996) Evidence for a role of Nis T in transport of the lantibiotic nisin produced by *Lactococcus lactis* N8. FEMS Microbil Lett 144:89–93
107. Engelke G, Gutowski-Eckel Z, Kiesau P, Siegers K, Hammelmann M, Entian K-D (1994) Regulation of nisin biosynthesis and immunity in *Lactococcus lactis* 6F3. Appl Environ Microbiol 60:814–825
108. Stock JB, Ninfa AJ, Stock AM (1989) Protein phosphorylation and regulation of adaptive response in bacteria. Microbiol Rev 53:450–490
109. Garido MC, Herrero M, Kolter R, Moreno F (1988) The export of the DNA replication inhibitor microcin B17 provides immunity for the host cell. EMBO J 7:1853–1862
110. Klein C, Entian K-D (1994) Genes involved in self-protection against the antibiotic subtilin produced by *Bacillus subtilis* ATCC 6633. Appl Environ Microbiol 60:2793–2801
111. Pugsley AP (1988) Protein secretion across the outer membrane of Gram-negative bacteria. In: Das RA, Robins PW (eds) Protein transfer and organelle biogenesis. Academic Press, Orlando, pp 607–652
112. Song HY, Cramer WA (1991) Membrane topography of ColEI gene products: the immunity protein. J Bacteriol 173:2935–2943
113. Immonen T, Ye S, Ra R, Quia M, Paulin L, Saris PEJ (1991) The codon usage of the *nisZ* operon in *Lactococcus lactis* N8 suggests a non-lactococcal origin of the conjugative nisin-sucrose transposon. DNA sequence 5:203–218
114. De Vos WM, Simmons GFM (1994) Gene cloning and expression systems in lactococci. In: Gasson MJ, De Vos WM (eds) Genetics and Biotechnology of Lactic Acid Bacteria. Blackie Academic & Professional, Glasgow, pp 52–97
115. Ra SR, Qiao M, Immonen T, Pujana I, Saris PEJ (1996) Genes responsible for nisin synthesis, regulation and immunity form a regulon of two operons and are induced by nisin in *Lactococcus lactis* N8. Microbiology 142:1281–1288
116. Ra SR, Saris PEJ (1995) Characterization of procaryotic mRNAs by RT-PCR. Biotechniques 18:792–795
117. Piard JC, Muriana PM, Desmazeaud PJ, Klaenhammer TR (1992) Purification and partial characterization of lacticin 481, a lanthionine-containing bacteriocin produced by *Lactococcus lactis* subsp. *lactis* CNRZ 481. Appl Environ Microbiol 58:279–284
118. Rince A, Dufour A, Le Pogam S, Thuault D, Bourgeois CM, Le Pennec JP (1994) Cloning, expression and nucleotide sequence of genes involved in production of lactococcin DR, a bacteriocin from lactococcus *lactis* subsp. lactis. Appl Environ Microbiol 60:1652–1657
119. Rince A, Dufour A, Uguen P, Le Pennec JP, Haras D (1997) Characterization of the lacticin 481 operon: the *Lactococcus lactis* genes IctF, IctE and IctG encode a pupative ABC transporter involved in bacteriocin immunity. Appl Environ Microbiol 63:4252–4260
120. Nes IF, Tagg JR (1996) Novel lantibiotics and their prepeptides. Antonie van Leeuwenhoek 69:89–97
121. Skaugen M, Abildgaard CI, Nes IF (1997) Organization and expression of a gene cluster involved in the biosynthesis of the lantibiotic lactocin S. Mol Gen Genet 253:674–686
122. Gilmore MS, Segarra RA, Booth MC, Bogie CP, Hall LR, Clewell DB (1994) Genetic structure of the *Enterococcus faecalis* plasmid pAD1-encoded cytolytic toxin system and its relationship to lantibiotic determinants. J Bacteriol 176:7335–7344
123. Siezen RJ, De Vos WM, Leunissen JAM, Dijkstra BW (1995) Homology modelling and protein engineering strategy of subtilases, the family of subtilisin-like serine proteinases. Protein Eng 4:719–737

124. Frémaux C, Héchard Y, Cienatiempo Y (1995) Mesentericin Y105 gene cluster in *Leuconostoc* mesenteroides Y105. Microbiology 141:1637–1645
125. Holo H, Nilssen Ø, Nes IF (1991) Lactococcin A, a new bacteriocin from *Lactococcus lactis* subsp. *cremoris*. Isolation and characterization of the protein and its gene. J Bacteriol 173:3879–3887
126. Stoddard GW, Petzel JP, van Belkum MJ, Kok J, McKay LL (1992) Molecular analysis of the lactococcin A gene cluster from *Lactococcus lactis* subsp. *lactis Biovar diacetylactis* WM4. Appl Environ Microbiol 58:1952–1961
127. van Belkum MJ (1994) Lactococcins, bacteriocins of *Lactococcus lactis*. In: De Vuyst L, Vandamme EJ (eds) Bacteriocins of Lactic Acid Bacteria: Microbiology, Genetics and Applications. Blackie Academic & Professional, London, pp 301–318
128. Nes IF, Håvarstein LS, Holo H (1995) Genetics of non-lantibiotic bacteriocins. In: Ferretti JJ, Gilmore MS, Klaenhammer TR (eds) Genetics of *Streptococci*, *Enterococci* and *Lactococci*. Karger, New York, pp 645–651
129. Van Belkum MJ, Stiles ME (1995) Molecular characterization of the genes involved in the production of the bacteriocin leucocin A from *Leuconostoc gelidum*. Appl Environ Microbiol 61:3573–3579
130. Marugg JD, Gonzalez CF, Kunka BS, Ledeboer AM, Pucci MF, Toonen MY, Walker SA, Zoetmulder LCM, Vandenberg PA (1992) Cloning, expression and nucleotide sequence of genes involved in production of pediocin PA-1, a bacteriocin from *Pediococcus acidilactici* PACl.0. Appl Environ Microbiol 58:2360–2367
131. Bukhtiyarova M, Yang R, Ray B (1994) Analysis of the pediocin AcH gene cluster from plasmid pSMB74 and its expression in a pediocin-negative strain. Appl Environ Microbiol 60:3405–3408
132. Venema K, Kok J, Marugg JD, Toonen MY, Ledeboer AM, Venema G, Chikindas L (1995) Functional analysis of the pediocin operon of *Pediococcus acidilactici* PAC 1.0 PedB is the isnmunity protein and PedD is the precursor processing enzyme. Mol Microbiol 17:515–522
133. Axelsson L, Holck A (1995) The genes involved in production of and immunity to sakacin A, a bacteriocin from *Lactobacillus sake* Lb706. J Bacteriol 177:2125–2137
134. Diep DB, Håvarstein LS, Nissen-Meyer J, Nes IF (1994) The gene encoding plantaricin A, a bacteriocin from *Lactobacillus plantarum* C ll, is located on the same transcription unit as an agr-like regulatory system. Appl Environ Microbiol 60:160–166
135. van Belkum MJ, Hayema BJ, Jeeninga RE, Kok J, Venema G (1989) Cloning of two bacteriocin genes from a lactococcal bacteriocin plasmid. Appl Environ Microbiol 55:1187–1191
136a. van Belkum MJ, Kok J, Venema G (1992) Cloning, sequencing and expression in *Escherichia coli* of *IcnB*, a third bacteriocin determinant from the lactococcal bacteriocin plasmid p9B4–6. Appl Environ Microbiol 58:572–577
136b. Delepelaire P, Wandersman C (1990) Protein secretion in Gram-negative bacteria. J Biol Chem 265:17118–17125
137. Harmon KS, McKay LL (1987) Restriction enzyme analysis of lactose and bacteriocin plasmids from *Streptococcus lactis* subsp. *diacetylactis* WM4 and cloning of *BclII* fragments coding for bacteriocin production. Appl Environ Microbiol 53:1171–1174
138. Randall LL, Hardy SJS, Thom JR (1987) Export of protein: a biochemical view. Annu Rev Microbiol 41:507–541
139. Wagner W, Vogel M, Goebel W (1983) Transport of hemolysin across the outer membrane of *Escherichia coli* requires two functions. J Bacteriol 27:1793–1800
140. Gilson L, Mahanty HK, Kolter R (1990) Genetic analysis of an MDR-like export system: the secretion of colicin V. EMBO J 9:3875–3884
141. Delepelaire P, Wandersman C (1990) Protein secretion in Gramnegative bacteria. J Biol Chem 265:17118–17125
142. Strathdee CA, Lo RY (1989) Cloning, nucleotide sequence and characterization of genes encoding the secretion function of the *Pasteurella haemolytica* leukotoxin determinant. J Bacteriol 171:916–928

143. Letoffe S, Delepelaire P, Wandersman C (1990) Protease secretion by *Erwinia chrysanthemi*: the specific secretion functions are analogous to those of *Escherichia coli* A-hemolysin. EMBO J 9:1375–1382
144. Hui FM, Morrison DA (1991) Genetic transformation in *Streptococcus pneumoniae*: nucleotide sequence analysis shows *comA*, a gene required for competence induction, to be a member of the bacterial ATP-dependent transport protein family. J Bacteriol 173:372–381
145. Diep DB, Håvarstein LS, Nes IF (1995) A bacteriocin-like peptide induces bacteriocin synthesis in *Lactobacillus plantarum* Cll. Food Microbiol 60:160–166
146. Håvarstein LS, Diep DB, Nes IF (1995) A family of bacteriocin ABC transporters carry out proteolytic processing of their substrates concomitant with export. Mol Microbiol 16:229–240
147. Axelsson L, Holck A, Birkeland *S*-T, Aukrust T, Blom H (1993) Cloning and nucleotide sequence of a gene from *Lactobacillus sake* Lb706 necessary for sakacin A production and immunity. Appl Environ Microbiol 59:2868–2875
148. Kornblum J, Kreiswirth B, Projan SJ, Ross H, Novick RP (1990) agr: a polycistronic locus regulating exoprotein synthesis in *Staphylococcus aureus*. In: Novick RP (ed) Molecular Biology of the Staphylococci. VCH Publishers, New York, pp 373–402
149. Morfeldt CI, Janzon L, Arvidson S, Löfdahl S (1988) Cloning of a chromosomal locus (*exp*) which regulates the expression of several exoprotein genes in *Staphylococcus aureus*. Mol Gen Genet. 211:1601–1607
150. Peng H, Novick RP, Kreitswirth B, Kornblum J, Schlievert P (1988) Cloning, characterization and sequencing of an accessory gene regulator (*agr*) in *Staphylococcus aureus*. J Bacteriol 170:4365–4372
151. Muriana PM, Klaenhammer TR (1991b) Cloning, phenotypic expression and DNA sequence of the gene for lactacin F, an antimicrobial peptide produced by lactobacillus spp. J Bacteriol 173:1779–1788
152. Nissen-Meyer J, Larsen AG, Sletten K, Daeschel M, Nes IF (1993b) Purification and characterization of plantaricin A, a *Lactobacillus plantarum* bacteriocin whose activity depends on the action of two peptides. J Gen Microbiol 139:1973–1978
153. Saris EJ, Immonen T, Reis M, Sahl H (1996) Immunity of lantibiotics. Antonie van Leeuwenhoeh 69:151–159
154. Immonen Y, Ye S, Ra R, Qiao M, Paulin L, Saris P (1995) The codon usage of the nisin Z operon in *Lactococcus lactis* N8 suggests a non-lactococcal origin of the conjugative nisin-sucrose transposon. Sequence 5:203–218
155. Qiao M, Immonen T, Koponen O, Saris PEJ (1995) The cellular location and effect on nisin immunity of the NisI protein from *Lactococcus lactis* N8 expressed in *Escherichia coli* and *L. lactis*. FEMS Microbiol Lett 131:75–80
156. Reis M, Eschbach-Bludau M, Iglesias-Wind MI, Kupke T, Sahl H-G (1994) Producer immunity towards the lantibiotic Pep5: identification of the immunity gene *pepI* and localization and functional analysis of its gene product. Appl Environ Microbiol 60:2876–2883
157. Meyer C, Beirbaum G, Heidrich C, Reis M, Suling J, Iglesias-Wind MI, Kempter C, Molitor E, Sahl HG (1995) Nucleotide sequence of the lantibiotic Pep 5 biosynthetic gene cluster and functional analysis of PepP and PepC. Evidence for a role in PepC in thioether formation. Eur J Biochem 232:478–489
158. Quadri LEN, Sailer M, Roy KL, Vederas JC, Stiles ME (1994) Chemical and genetic characterization of bacteriocins produced by *Carnobacterium piscicola* LV17B. J Mol Biol 269:12204–12211
159. Tichaczek PS, Vogel RF, Hammes WP (1993) Cloning and sequencing of *curA* encoding curvacin A, the bacteriocin produced by *Lactobacillus curvatus* LTH1174. Arch Microbiol 160:279–283
160. Tichaczek PS, Vogel RF, Hammes WP (1994) Cloning and sequencing of *sakP* encoding sakacinP, the bacteriocin produced by *Lactobacillus sake* LTH673. Microbiology 140:361–367

161. Nissen-Meyer J, Håvarstein LS, Holo H, Sletten K, Nes IF (1993a) Association of the lactococcin A immunity factor with the cell membrane: purification and characterization of the immunity factor. J Gen Microbiol 139:1503–1509
162. Kok J, Venema K, Venema G (1995) Analysis of lactococcin secretion and immunity in *Lactococcus lactis*. In: Ferretti JJ, Gilmore MS, Klaenhammer TR (eds) Genetics of Streptococci, Enterococci and Lactococci. Karger, New York, pp 653–659
163. Peschel A, Götz F (1996) Analysis of the *Staphylococcus epidermidis* genes *epiF*, *-E* and *-G* involved in epidermin immunity. J Bacteriol 178:531–536
164. Kerpolla RE, Shyamala VK, Klebba P, Ferro-Luzzi Ames G (1991) The membrane-bound proteins of periplasmic permeases form a complex. J Biol Chem 266:9857–9865
165. Panagiotidis CH, Reyes M, Sievertsen A, Boos W, Shuman HA (1993) Characterization of the structural requirements for assembly and nucleotide binding of an ATP-binding cassette transporter. J Biol Chem 268:23685–23696
166. Froseth BR, Herman RE, McKay LL (1988) Cloning of nisin resistance determinant and replication origin on 7.6-kilobase EcoRI fragment of pNP40 from *Streptococcus lactis* subsp. *diacetylactis* DRC3. Appl Environ Microbiol 54:2136–2139
167. Froseth BR, McKay LL (1991) Molecular characterization of the nisin resistance region of *Lactococcus lactis* subsp. *lactis* biovar *diacetylactis* DRC3. Appl Environ Microbiol 57:804–811
168. Jarvis B, Farr J (1971) Partial purification, specificity and mechanism of action of the nisin-inactivating enzyme from *Bacillus cereus*. Biochim Biophys Acta 227:232–240
169. Hansen JN (1993) The molecular biology of nisin and its structural analogues. In: Hoover D, Steenson L (eds) Bacteriocins of Lactic Acid Bacteria. Academic Press, New York, pp 93–120
170. Bouret RB, Borkovich KA, Simon MI (1991) Signal transduction pathways involving protein phosphorylation in prokaryotes. Annu Rev Biochem 60:401–441
171. Parkinson JS, Kofoid EC (1992) Communication modules in bacterial signaling proteins. Annu Rev Gen 26:71–112
172. Kleerebezem M, Quadri IE, Kuipers OP, de Vos WM (1997) Quorum sensing by peptide pheromones and two-component signal-transductionsystems in Gram-positive bacteria. Mol Microbiol 24:895–904
173. Huo L, Martin KJ, Schleif R (1988) Alternative loops regulate the arabinose operon in *Escherichia coli*. Proc Natl Acad Sci USA 85:5444–5448
174. Igo MM, Losick R (1986) Regulation of a promoter that is utilized by minor forms of RNA polymerase holoenzyme in *Bacillus subtilis*. J Mol Biol 191:615–624
175. Martin K, Huo L, Schleifer RF (1986) The DNA loop model for *ara* repression: AraC protein occupies the proposed loop sites in vivo and repression-negative mutations lie in these same sites. Proc Natl Acad Sci USA 83:3654–3658
176. Ptashne M (1992) The genetic switch. Cell Press and Blackwell Scientific Publications, Cambridge
177. Cara JH, Schleif RF (1993) Variation of half-site organization and DNA looping by AraC protein. EMBO J 12:35–44
178. Coleman, Bown GS, Stormonth DA (1975) A model for the regulation of bacterial extracellular enzyme and toxin biosynthesis. J Theor Biol 52:143–148
179. Janzon L, Löfdahl S, Arvidson S (1989) Identification and nucleotide sequence of the delta-lysin gene, hld, adjacent to the accessory gene regulator (*agr*) of *Staphylococcus aureus*. Mol Gen Genet 70:337–349
180. Janzon L, Arvidson S (1990) The role of the δ-lysin gene (*hld*) in the regulation of virulence genes by the accessory gene regulator (*agr*) in *Staphylococcus aureus*. EMBO J 9:1391–1399
181. Ji G, Beavis RC, Novick RP (1995) Cell density control of Staphylococcal virulence mediated by an octapeptide pheromone. Proc Natl Acad Sci USA 92:12055–12059
182. Sanders DA, Koshland DE Jr (1988) Receptor interactions through phosphorylation and methylation pathways in bacterial chemotaxis. Proc Natl Acad Sci USA 85:8425–8429

183. Sanders DA, Gillece-Castro BL, Stock AM, Burlington AL, Koshland DE Jr (1989) Identification of the site of phosphorylation of the chemotaxis response regulator protein. J Biol Chem 264 : 21770 – 21778
184. Kupke T, Gotz F (1996) post-translational modifications of lantibiotics. Antonie van Leeuwenhoek 69 : 139 – 150
185. Ingram LC (1970) A ribosomal mechanism for synthesis of peptides related to nisin. Biochim Biophys Acta 224 : 263 – 265
186. Kellner J, Jung G, Josten M, Kaletta C, Entian K-D, Sahl H-G (1989) Pep5, a new lantibiotic: structure elucidation and amino acid sequence of the propeptide. Angew Chem Int Ed Engl 28 : 616 – 619
187. van Kamp M, Horstink LM, van den Hooven HW, Konings RNH, Hilbers CW, Frey A, Sahl H-G, Metzger JW, van de Ven FJM (1995) Sequence analysis by NMR spectroscopy of the peptide lantibiotic epilancin K7 from *Staphylococcus epidermidis* K7. Eur J Biochem 227 : 757 – 771
188. Schnell N, Entian K-D, Götz F, Hörner T, Kellner R, Jung G (1989) Structural gene isolation and prepeptide sequence of gallidermin, a new lanthionine containing antibiotic. FEMS Microbiol Lett 58 : 263 – 268
189. Kupke T, Stevanovic S, Sahl H-G, Götz F (1992) Purification and characterization of EpiD, a flavoprotein involved in the biosynthesis of the lantibiotic epidermin. J Bacteriol 174 : 5354 – 5361
190. Augustin J, Rosenstein R, Wieland B, Schneider U, Schnell N, Engelke G, Entian K-D, Gotz F (1992) Genetic analysis of epidermin biosynthetic genes and epidermin-negative mutants of *Staphylococcus epidermidis*. Eur J Biochem 204 : 1149 – 1154
191. Bishop L, Agbayani R, Ambudkar SV, Maloney PC, Ames GF-L (1989) Reconstitution of a bacterial periplasmic permease in proteoliposomes and demonstration of ATP hydrolysis concomitant with transport. Proc Natl Acad Sci USA 86 : 6953 – 6957
192. Mimmack ML, Gallangher MP, Pearce SR, Hyde SC, Booth IR, Higgins CF (1989) Energy coupling to periplasmic binding protein-dependent transport in vivo. Proc Natl Acad Sci USA 86 : 8257 – 8261
193. Chang YF, Young R, Struck DK (1991) The *Actinobacillus pleuropneumonia* haemolysin determinant: unlinked *appCA* and *appBD* loci flanked by pseudogenes. J Bacteriol 173 : 5151 – 5158
194. Juranka P, Zhang F, Kulpa J, Endicott J, Blight M, Holland IB, Ling V (1992) Characterization of the haemolysin transporter, HlyB, using an epitope insertion. J Biol Chem 267 : 3764 – 3770
195. Guthmiller JM, Kolodrubetz D, Cagle MP, Kraig E (1990) Sequence of the *lktB* gene from *Actinobacillus actinomycetecomitans*. Nucl Acids Res 18 : 5291 – 5293
196. Glaser P, Sakamoto H, Bellalou J, Ullmann A, Danchin A (1988) Secretion of cyclolysin, the calmodulin-sensitive adenylate cyclase-haemolysin bifunctional protein of *Bordetella pertussis*. EMBO J 7 : 3997 – 4004
197. Felmlee T, Pellett S, Lee E-Y, Welch RA (1985) *Escherichia coli* haemolysin is released extracellularly without cleavage of a signal peptide. J Bacteriol 163 : 88 – 93
198. Wandersmann C (1992) Secretion across the bacterial outer membrane. Trends Genet 8 : 317 – 322
199. Ross KF, Ronson CW, Tagg JR (1993) Isolation and characterization of the lantibiotic salivaricin A and its structural gene *salA* from *Streptococcus salivarius* 20P3. Appl Environ Microbiol 59 : 2014 – 2021
200. Dinh T, Paulsen IT, Saier MH (1994) A family of extracytoplasmic proteins that allow transport of large molecules across the outer membranes of Gram-negative bacteria. J Bacteriol 176 : 3825 – 3831
201. Skvirsky RC, Shoba R, Xiaoyu S (1995) Topology analysis of the colicin V export protein CvaA in *Escherichia coli*. J Bacteriol 177 : 6153 – 6159
202. Schulein R, Gentschev I, Mollenkopf H-J, Goebel W (1992) A topological model for the haemolysin translocator protein HlyD. Mol Gen Genet 234 : 155 – 163

203. Muriana PM, Klaenhammer TR (1991a) Purification and partial characterization of lactacin F, a bacteriocin produced by *Lactobacillus acidophilus* 11088. Appl Environ Microbiol 57:114–121
204. Allison GE, Ahn C, Stiles ME, Klaenhammer TR (1995a) Utilization of the leucocin A export system in *Leuconostoc gelidum* for production of a *Lactobacillus* bacteriocin. FEMS Microbiol 131:87–93
205. Allison GE, Worobo RW, Stiles ME, Klaenhammer TR (1995b) Heterologous expression of the lactacin F peptides by *Carnobacterium piscicola* LV17. Appl Environ Microbiol 61:1371–1377
206. Chikindas ML, Venema K, Ledeboer AM, Venema G, Kok J (1995) Expression of lactococcin A and pediocin PA-1 in heterologous hosts. Lett Appl Microbiol 21:183–189
207. Sahl HG, Bierbaum G (1998) Lantibiotics: biosynthesis and biological activities of modified peptides from Gram-positive bacteria. Annu Rev Microbiol 52, 41–79
208. Tomita H, Fujimoto S, Tanimoto K, Ike Y (1996) Cloning and genetic organization of the bacteriocin 31 determinant encoded on the *Enterococcus faecalis* pheromone-responsive conjugative plasmid pY117. J Bacteriol 178:3585–3593
209. Cintas LM, Casaus P, Haverstein LS, Hernandez PE, Nes IF (1997) Biochemical and genetic characterization of enterocin P, a novel *sec*-dependent bacteriocin from *Enterococcus faecium* P13 with a broad antimicrobial spectrum. Appl Environ Microbiol 63:4321–4330
210. Cintas LM, Casaus P, Holo H, Hernandez PE, Nes IF, Havarstein LS (1998) Enterocins L50 A and L50B, two novel bacteriocins from *Enterococcus faecium* L50, are related to staphylococcal hemolysins. J Bacteriol 180:1988–1994
211. Piard J-C, Kuipers OP, Rollema HS, Desmazeaud MJ, De Vos MJ (1993) Structure, organization and expression of the lct gene for lacticin 481, a novel lantibiotic produced by *Lactococcus lactis*. In: La lacticine 481, une nouvelle bacteriocine de type lantibiotique produite par *Lactococcus lactis*: characterization biochemique et genetique, Piard J-C (PhD Thesis): Universite de Caen, France, pp 85–116

Received January 1999

Biochemical Engineering Aspects of Solid State Bioprocessing

David A. Mitchell[1], Marin Berovic[2], Nadia Krieger[3]

[1] Departamento de Solos, Setor de Ciências Agrárias, Universidade Federal do Paraná, Rua dos Funcionários 1540, Juvevê, Curitiba 80035–050, Paraná, Brazil
[2] Department of Chemical and Biochemical Engineering, University of Ljubljana, Hajdrihova 19, Ljubljana, Slovenia
[3] Departamento de Química, Universidade Federal do Paraná, Cx. P. 19081, 81531–990 Curitiba, Paraná, Brazil
E-mail: marin.berovic@ki.si

Despite centuries of use and renewed interest over the last 20 years in solid-state fermentation (SSF) technology, and despite its good potential for a range of products, there are currently relatively few large-scale commercial applications. This situation can be attributed to the complexity of the system: Macroscale and microscale heat and mass transfer limitations are intrinsic to the system, and it is only over the last decade or so that we have begun to understand them. This review presents the current state of understanding of biochemical engineering aspects of SSF processing, including not only the fermentation itself, but also the auxiliary steps of substrate and inoculum preparation and downstream processing and waste disposal.

The fermentation step has received most research attention. Significant advances have been made over the last decade in understanding how the performance of SSF bioreactors can be controlled either by the intraparticle processes of enzyme and oxygen diffusion or by the macroscale heat transfer processes of conduction, convection, and evaporation. Mathematical modeling has played an important role in suggesting how SSF bioreactors should be designed and operated. However, these models have been developed on the basis of laboratory-scale data and there is an urgent need to test these models with data obtained in large-scale bioreactors.

Keywords. Mathematical modeling, Heat transfer, Mass transfer, Upstream processing, Downstream processing

Advances in Biochemical Engineering/
Biotechnology, Vol. 68
Managing Editor: Th. Scheper

List of Abbreviations

a_w	water activity
a_{w0}	optimal water activity for growth
A	fitting constant
B	fitting constant
C	humidity (kg-water kg-dry air^{-1})
DDF	dimensionless design factor
E_{a1}	activation energy (J mol^{-1})
E_{a2}	activation energy (J mol^{-1})
C	concentration (g l^{-1} or mol l^{-1})
C_{pa}	heat capacity of the air (J kg^{-1} °C^{-1})
D	drum diameter (m)
Da_M	modified Damkohler number (dimensionless)
f	slope of a linear approximation to the humidity curve (kg-water kg-air^{-1} °C^{-1})
F_a	air flowrate (m^3 h^{-1})
f	fraction of maximum specific growth rate (dimensionless)
H	bed height (m)
h_A	overall coefficient for heat transfer (J h^{-1} K^{-1})
$K_F a$	biofilm conductance (mol-O_2 h^{-1})
$K_L a$	overall oxygen mass transfer coefficient (mol-O_2 h^{-1})
k	first order decay constant for loss of viability of hyphal tips
k_{do}	frequency factor for death (h^{-1})
k_{md}	constant (h^{-1})
K	saturation constant (g l^{-1} or mol l^{-1})
K_i	substrate inhibition constant (g l^{-1} or mol l^{-1})

L	original particle length (mm)
L	fraction of active hyphal tips surviving entry into deceleration phase (dimensionless)
l_c	length of the residual particle core (mm)
m_A	maintenance coefficient for compound A (g-A h^{-1} g-biomass^{-1})
m_d	specific inactivation rate (h^{-1})
m_{d0}	basal specific inactivation rate (h^{-1})
m_o	maintenance coefficient for oxygen (mol O_2 g-biomass^{-1} h^{-1})
N_C	critical rotational speed (rpm)
OUR	oxygen uptake rate (mol h^{-1})
r	radial extension rate (mm h^{-1})
r_m	radial extension rate at the optimal water activity for growth (mm h^{-1})
R	universal gas constant (J mol^{-1} K^{-1})
R_A	rate of production or consumption of compound A (g g-substrate^{-1} h^{-1} or g h^{-1})
R_q	peak rate of heat generation (J h^{-1})
RH	relative humidity (%)
SLF	submerged liquid fermentation
SSF	solid-state fermentation
t	time (h)
t_a	time of entry into deceleration phase (h)
T	temperature (°C or K)
T_c	time for complete particle degradation (h)
T_{max}	maximum temperature for growth (K)
vvm	volumetric air flow rate (m^3-air m^{-3}-volume min^{-1})
V_Z	superficial velocity of the air (m h^{-1})
X	biomass (either kg-biomass m^{-3} or kg-biomass kg-dry-matter^{-1})
Y	heat yield coefficient (J kg-biomass^{-1}).
Y_{AX}	stoichiometric coefficient relating compound A with growth (g-A g-biomass^{-1})
Y_{XO}	yield coefficient for growth on oxygen (g-biomass mol O_2^{-1})
$\|_Z$	at location Z in space
a	air
aw	water activity
B	bed
d	death
g	growth
G	glucose
IN	inlet air
max	maximum
N	nutrient
O_2	oxygen
OUT	outlet air
pH	pH
S	substrate
SURR	surrounding air
T	temperature

X	biomass
V	variable
W	water
ε	void fraction within the bed (dimensionless)
λ	heat of vaporization of water (J kg^{-1})
μ	specific growth rate (h^{-1})
μ_{max}	maximum specific growth rate (h^{-1})
μ_{To}	frequency factor for growth (h^{-1})
ϱ, ρ	density (kg m^{-3})

1 Definition and Applications

Fermentation processes can be divided generally into submerged and solid-state fermentations. The major difference between these two bioprocesses is the amount of free liquid in the substrate. Solid-state fermentation (SSF) involves the growth of microorganisms on moist solid substrate particles in the absence or near absence of visible liquid water between the particles. Of course microbes need water for growth. In SSF systems they obtain water from the moisture held within the substrate particles. The growth medium within a bioreactor consists of a bed containing many moist solid substrate particles, the water content of which could conceivably range anywhere from 12 wt%, below which biological activity does not occur, up to the maximum water-holding capacity of the solid, which in some cases is as high as 80 wt%, although typical water contents are near the middle of this range [1]. In contrast, the nutrient broth in a typical submerged liquid fermentation (SLF) might contain around 50 g l^{-1} of solutes, and therefore has a water content of 95 wt%, and appears and behaves reasonably similarly to pure water. Figure 1 gives an overview of the most obvious differences between SSF and SLF systems, while Table 1 gives a more detailed comparison [2].

There is not a sharp boundary between SSF and SLF. First, the water content at which liquid water appears between the substrate particles is a function of the absorbency of the material, and this varies amongst the various solid substrates used in SSF processes, such as wood chips, grains, and meals. Second, as one increases the water content of the substrate past the maximum water-holding capacity, the system would first be considered a slurry, and later a suspension of insoluble solids. There is no direct transition from SSF to SLF.

Many SSF processes involve the utilization of polymeric carbon and energy sources, which might be present in the substrate bound within relatively complex structures. They may only become accessible to the microorganism after the degradation or penetration of cell walls, for example. In contrast, most SLF processes involve soluble monomeric nutrients, and even when polymers are used they are usually either soluble or at least well dispersed. As a consequence, in SLF the net amount of carbon and energy substrate accessible will typically decline throughout the fermentation, but may either decline, increase, or remain constant at different stages of growth with solid substrates [3].

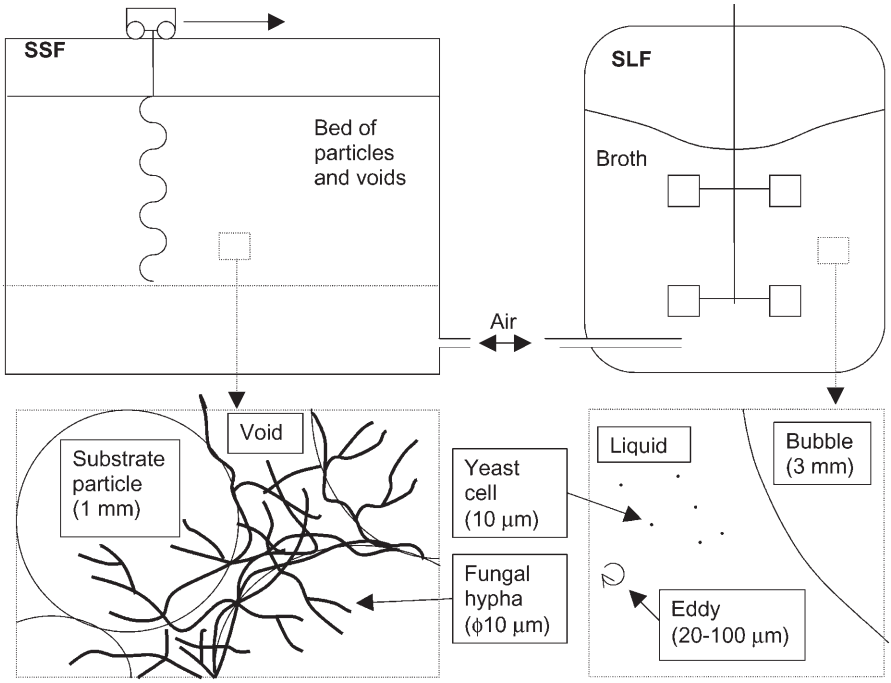

Fig. 1. Comparison of typical solid-state fermentation (SSF) and submerged liquid fermentation (SLF) systems. A stirred-bed SSF bioreactor of the design of Durand and Chereau [2] is compared with a typical stirred SLF bioreactor. For each bioreactor an expanded view of the microscale is also shown, in order to highlight differences between the micro-structure of the two systems. The relative scales make it clear that mixing is possible on much smaller scales in SLF than in SSF, since in SSF mixing cannot take place at scales smaller than the particle size. Note that particle sizes in SSF are commonly larger than 1 mm

Other terms have been used to describe solid-state fermentation and related processes, such as solid-phase fermentation, solid-state cultivation, solid-substrate fermentation, and moist solids fermentation. Also, some workers have used the term solid-state fermentation to describe processes which have significant amounts of free water. Moo-Young et al. [4] proposed use of the more general term solid-substrate fermentation to describe any process in which solid particles of substrate are involved, regardless of the amount of free water. Solid-substrate fermentations therefore include solid-state fermentations and other processes with increasing amounts of water: a solid matrix with an aqueous phase leaching through it, slurries of solid particles, and solids suspended in an aqueous phase.

Solid-state fermentation was documented as long as 1000 years BC in Chinese Confucius classics, where the use of soy sauce was mentioned [1]. This art of food production spread out and influenced many other Asian countries, where it is presently used to produce a variety of foods, beverages, and related products: chiang, sufu, soy sauce, red rice, tempe, ontjom, tape ketan and tape ketella, miso, hamanatto, natto, sake, and nata de pina, among others [5].

Table 1. Comparison of solid-state fermentation and submerged liquid fermentation

Solid state fermentation (SSF)	Submerged liquid fermentation (SLF)
Some products are only produced well under low moisture conditions	A very wide range of products can be produced from a wide range of micro-organisms. Many products are produced best under SLF
The medium is relatively simple (e.g., a grain) and unrefined. It may contain all nutrients necessary for growth, or only require wetting with a mineral solution. Pretreatment can be as simple as cooking or grinding. However, the substrate can be variable	The medium often contains more highly processed ingredients and is therefore more expensive. Unprocessed ingredients may need processing to extract and solubilize the nutrients. With defined media good reproducibility is possible
The low water availability helps to select against growth of contaminants	The water activity is usually very high and many contaminants can grow well
Media are concentrated and smaller bioreactors can be used, leading to higher volumetric productivities, even with lower rates and yields	Media are dilute and therefore occupy larger volumes, leading to lower volumetric productivities
High substrate concentrations can enable high product concentrations	High substrate concentrations can cause rheological problems. Substrate feeding systems may be required
Aeration requires less power since pressures are lower	High air pressures can be required. Gas transfer from the gas to liquid phase is usually limiting
Mixing within particles is impossible and growth can be limited by nutrient diffusion	Vigorous mixing can be used and diffusion of nutrients is usually not limiting
Ability to remove metabolic heat is restricted, leading to overheating problems	High water content and more dilute nature makes temperature control easier
Process control can be difficult due to difficulties in making on-line measurements, and in measuring biomass	Many on-line sensors are available and more are being developed. Additions of substances can be made to control the process
Downstream processing may be simpler since products are more concentrated. Extracts can be contaminated with substrate components	Downstream processing requires removal of large volumes of water and is expensive. Product purification may be easier.
Large volumes of liquid waste are not produced	Large volumes of liquid wastes are produced
Growth kinetics and transport phenomena are relatively poorly characterized.	Much kinetic and transport information is available to guide reactor design and operation.

As a rule, the traditional foods prepared by SSF do not produce an overall enrichment of protein levels in the substrate. In fact, in substrates of higher protein content, such as soya beans, there may be an overall loss of nutrients, although these fermentation processes may enrich specific nutrients, improve digestibility, destroy toxins or reduce toxicity, change the organic nitrogen content, and cause favorable changes in taste [1]. However, with substrates comprised predominantly of starch, an overall enrichment of protein content is possible. Cassava, a low protein staple root crop, can be fermented in SSF to produce a food of higher protein content. This result can be of great value to nations whose people suffer from protein deficiency [6].

The traditional koji process may be considered the archetype of SSF. Koji is a generic Japanese name for starters used in a variety of fermentations; its functional importance lies in its high content of various amylolytic and proteolytic enzymes which can catalyze the degradation of starches and proteins to soluble products capable of subsequent fermentation by yeasts or bacteria. A variety of raw materials are used in the production of kojis but, typically, steamed rice is inoculated with spores of an *Aspergillus oryzae* strain and incubated under carefully controlled conditions of temperature and humidity [7].

The introduction of the koji process to the West is chiefly due to the work of Takamine, which started in 1891 in the USA using wheat bran to make the preparation named Taka-Koji. Takamine introduced the technique of acclimatizing the mold to various antiseptics in order to minimize growth of contaminants during the process. The process was carried out on an industrial scale in rotating drum bioreactors. Large scale trials of the use of Taka-Koji instead of malt in distilleries were carried out in the plant of Hiram Walker & Sons in Ontario Canada in 1913. This was marketed as a digestive aid under the name of Takadiastase [8].

Solid-state fermentation has also been traditionally carried out in the West, such as in the production of blue-veined cheese with *Penicillium roqueforti*, in which the mycelium develops throughout the cheese, and of Camembert and Brie in which molds such as *Penicillium camemberti* and *Penicillium caseicolum* grow on the surface of the cheese [9]. There are also the classical processes of ensiling, an anaerobic SSF process involving the lactic acid fermentation of agricultural products at 25–40% dry matter and ambient temperatures of 25–30 °C, and composting, a thermophilic SSF which involves growth of a succession of microorganisms on agricultural byproducts, starting with mesophiles and followed by thermophilic bacteria, actinomycetes, and fungi [10].

In the last two to three decades there has been a rapid growth of interest in using SSF for the production of various bioproducts such as enzymes, organic acids, ethanol, biogas, antibiotics, surfactants, toxins, bioremediation agents, mushrooms, composts, microbial polysaccharides, biopesticides, protein-enriched fermented foods, pre-digested feeds for ruminants, reduced-toxicity feedstuffs, and variants of traditional fermented foods. Applications of SSF have been reviewed elsewhere [11] and therefore are not discussed here; however, a selection of current research into products and processes involving SSF is given in Table 2 [12–63]. Within these products there are many instances where the product produced in SSF is superior to that produced in SLF. For example,

Table 2. A selection of recent research into applications of SSF

Product or process	Organism	Substrate	Ref
Enzymes			
Glucoamylase	*Aspergillus niger*	Tea waste	[12]
Glucoamylase	*Aspergillus niger*	Rice bran	[13]
Glucoamylase	*Aspergillus sp.*	Wheat bran	[14]
Lipase	*Aspergillus niger*	Gingelly oil cake	[15]
Lipase	*Candida rugosa*	Coconut cake	[16]
Lipase	*Rhizomucor miehei*	Wheat bran	[17]
Lipase	*Penicillium restrictum*	Babassu oil cake	[18]
α-Galactosidase	*Humicola sp.*	Soya flour + wheat bran	[19]
Cellulases	*Bacillus subtilis*	Banana fruit stalk wastes	[20]
Cellulases	*Trichoderma reesei* + *Aspergillus phoenicis*	Sugar cane bagasse + soybean meal	[21]
Cellulases	*Trichoderma reesei* + *A. niger*	Alkali-treated sugar cane bagasse	[22]
Cellulases	*Trichoderma pseudokoningii*	Wheat bran	[23]
Pectinases	*Talaromyces flavus*	Citrus wastes	[24]
Pectinases	*Aspergillus niger*	Soy bran and wheat bran	[25]
Pectinases	*Aspergillus niger*	Apple pectin	[26]
Inulinase	*Staphylococcus sp.* or *kluyveromyces marxianus*	Wheat bran, rice bran, coconut oil cake and corn flour	[27]
Xylanases	*Aspergillus tamarii*	Corn cob or sugar cane bagasse	[28]
Xylanases	*Trichoderma longibrachiatum*	Wheat bran	[29]
Xylanase	*Trichoderma reesei* + *A. niger*	Sugar cane bagasse + soymeal	[30]
Xylanase	*Bacillus sp.*	Wheat bran	[31]
Lignolytic enzymes	*Phanerochaete chrysosporium*	Corn cob	[32]
Lignolytic enzymes	*Phanerochaete chrysosporium*	Foam impregnated with nutrients	[33]
Lignolytic enzymes	*Phanerachaete chrysosporium*	Corn cob	[34]
Biopesticides			
Bioherbicide	*Trichoderma virens*	Composted chicken manure	[35]
Bioinsecticide	*Colletotrichum truncatum, Alternaria sp., Paecilomyces fumosoroseus, A. flavus* or *A. parasiticus*	Rice flour	[36]
Bioinsecticide	*Coniothyrium minitans*	Impregnated hemp	[37]
Bioremediation			
Bioremediation	*Phanerochaete chrysosporium*	Sugarcane bagasse pith	[38]
Bioremediation	*Lentinula edodes*	Pentachlorophenol in soil	[39]
Biofilter	*Various*	Peat + volatile organics	[40]
Food and feed			
Fermented food	*Aspergillus orzyae* or *A. sojae*	Various fruit peel	[41]
Caffeine removal	*Aspergillus tamarii*	Impregnated sugarcane bagasse	[42]
Delignification	*White rot fungi*	Wheat straw	[43]
Improved nutrition	*Penicillium spp.*	Bergamot fruit peel	[44]
Phytic acid removal	*Lentinula edodes*	Wheat bran	[45]
Shiitake	*Lentinula edodes*	Sawdust	[46]
Protein enrichment	*Neurospora sitophila*	Sugar beet pulp or citrus waste	[47]
Aromas			
Aroma compounds	*Bjerkandera adusta*	Wheat bran	[48]
Pyrazines	*Bacillus subtilis*	Ground soybeans	[49]

Table 2 *(continued)*

Product or process	Organism	Substrate	Ref
Organic acids			
Citric acid	*Aspergillus niger*	Cane, beet pulp mol. imprg.	[9]
Citric acid	*Aspergillus niger*	Dry coffee husks	[211]
Citric acid	*Aspergillus niger*	Sweet potato	[53]
Citric acid	*Aspergillus niger*	Carob pod	[54]
Citric acid	*Aspergillus niger*	Pineapple waste	[55]
Citric acid	*Aspergillus niger*	Corn cobs	[56]
Amino acids	*Rhisopus oligosporus*	Seed hull	[226]
Kojic acid	*Aspergillus oryzae*	Steamed rice	[9]
Antibiotics			
Tetracycline	*Streptomyces iridifaciensis*	Sweet potato residue	[9]
Iturin	*Bacillus subtilis*	Wheat bran	[227]
Small organics			
Ethanol	*Saccharomyces cerevisiae*	Sweet sorghum or sweet potato	[50, 51]
Methane	*natural consortia*	Municipal solid waste	[52]
Mycophenolic acid	*Penicillium brevi-compactum*	Wheat bran	[57]
Cephamycin C	*Streptomyces clavuligerus*	Wheat rawa + cotton seed cake	[58]
Polymers			
Succinoglycan	*Agrobacterium tumefaciens*	Spent malt grains or ivory nut shavings or grated carrots	[59]
Succinoglycans	*Rhizobium hedysaris*	Impregnated spent malt grains	[60]
Xanthan gum	*Xanthomonas campestris*	Spent malt grains, citrus peels, apple pomace, or grape pomace	[61]
Xanthan gum	*Xanthomonas campestris*	Impregnated spent malt grains	[60]
Biopulping			
Pretreatment	*Phlebia radiata, Funalia trogii, Bjerkandera adusta* or *Poria subvermispora*	Eucalypt wood	[62]
Biopulping	*Pleurotus sp.*	Wheat straw	[63]

enzymes produced by SSF often have improved thermostability compared to those produced by the same microorganism in SLF systems. Likewise, in the production of fungal spores as biopesticides, sporulation is usually better in the environment provided in SSF systems than in that provided in SLF systems. Even when significant quantities of spores are produced in SLF, they are generally less robust and therefore do not survive as well when applied in the field. In other cases SSF may be favored for socioeconomic reasons, since it often uses low cost substrates which would otherwise be dumped as wastes, and is often appropriate for low technology applications in regions where labor costs are low. However, despite the high level of research activity there are still relatively few commercial processes, a situation which can largely be attributed to the complexity of SSF systems and our resultant poor understanding of how to design and operate processes successfully on a large scale.

In the future, SSF may play an important role in feeding the world's population, which reached six billion during the year 1999, and is expected to reach 8 to 12 billion people during the twenty-first century. At the present time the majority of the people in the developing world are vegetarians for economic reasons. Already meat substitutes are being produced by spinning soybean protein into fibers to give a meat-like texture. Production of microbial protein could be a strategic alternative for cheap future food production, and SSF has the potential to play a role here [5]. However, SSF technology must be improved before this potential can be fulfilled. This review shows that, although significant advances have been made in the development of SSF technology over the last decade, many further improvements are required.

1.1 Microbial Types

One of the most important features of SSF is the low availability of water in the system. Water activities, which are more important in controlling microbial growth than water content, are typically lower than those encountered in SLF. The water activity (a_w) of the moist solid substrate can easily be measured: it is the ratio of the vapor pressure of water above the substrate in a closed system to the vapor pressure of pure water at the same temperature. The water activity of the substrate is the measured relative humidity divided by 100. Values around 0.95 – 0.98 might be considered typical for solid substrates. These water activities are ideal for the growth of many fungi, especially filamentous fungi, which typically grow optimally at water activities of 0.96 – 0.98, and still grow reasonably well at water activities as low as 0.9, and, as a result, the majority of SSF processes involve filamentous fungi. In contrast many bacteria and yeasts grow best at water activities around 0.99, with growth rapidly decreasing as the water activity falls, and growth being completely inhibited at values around 0.9 [64].

Filamentous fungi have other features which give them advantages for SSF processes over unicellular organisms. The mycelial growth form is ideally suited to rapid colonization of the whole of a solid surface, which can later be followed by an increase in density. Fungal hyphae can also cross regions of low nutrient availability in search of nutrients, although the capability to do this does vary from species to species. The hyphal growth mode also allows fungi to penetrate into substrate particles, which may play an important role in degrading the particle structure and making nutrients available. Furthermore, many filamentous fungi can produce a range of hydrolytic enzymes to degrade the macromolecules found in solid substrates. Amylases and cellulases are the most important enzymes for growth on solid substrates of agricultural origin, although proteases and lipases aid in particle degradation and penetration. In fact, it is for these reasons that fungi are very commonly found growing naturally on solid materials in nature such as pieces of wood, leaves, and roots.

There are also a number of features of filamentous fungi which can be taken advantage of within SSF processes. A number of filamentous fungi grow well at low pH values, enabling the use in some SSF systems of a combination of low water activity and low pH to create an environment which is favorable for

fungal growth and selects against most bacterial and yeast contaminants. Also, most filamentous fungi produce spores. Spore inocula are easy to prepare and can be stored for longer periods than vegetative cells. This makes processes involving fungi more flexible since the synchronization of inoculum production with the rest of the process is not so crucial.

Despite the predominance of filamentous fungi, there are also several SSF processes which involve bacteria and yeasts. Yeasts generally grow on solid substrates only as minor members of the microflora, as is the case in the traditional processes of ensiling and tape manufacture [4]. However, some modern processes have involved monocultures of *Saccharomyces cerevisiae* for the production of ethanol (Table 2) and *Endomycopsis fibuligera* and *Schwanniomyces castelli* for protein enrichment of starchy solid substrates [65]. Bacteria play roles as the major or minor microorganisms in various SSF processes. Lactobacilli are the major microorganisms during ensilage and thermophilic bacteria predominate early during composting before being succeeded by thermophilic actinomycetes and fungi. Natto is a Japanese fermented food in which *Bacillus subtilis* is the major organism and forms a sticky coat on soybeans. In the production of many Asian fermented foods by traditional methods, in which neither the inoculum preparation nor the fermentation are carried out under aseptic conditions, bacteria may enter the process as contaminants. One example where this is advantageous is in the production of tempe in which an as yet unidentified bacterium is present and produces vitamin B_{12}.

1.2 Culture Methods

A range of different practices is used in SSF with respect to the organisms used and the use of aseptic procedures. These may be referred to as monoculture, defined mixed culture, sequential culture, and undefined mixed culture.

In monoculture the substrate is pasteurized or sterilized and inoculated with a pure culture. During the fermentation aseptic procedures may be used to prevent contamination. In some cases the conditions may select against contaminants and the process organism may grow vigorously so that any contaminants cannot compete. In these cases the process may be able to be carried out by unskilled operators.

In defined mixed culture the substrate is pasteurized or sterilized and inoculated simultaneously with more than one pure culture. This can be beneficial for complex substrates and where the various strains use different carbon sources. For example, mixed cultures of *Trichoderma reesei* or *Chaetomium cellulolyticum* with *Candida lipolytica* resulted in increased protein production from wheat straw because the yeast uses glucose and prevents catabolite repression of the fungal cellulase [66, 67].

Sequential culture is a type of mixed culture in which the second organism is added after growth of the first organism has ceased. This method can be used to maximize utilization of the nutrients in the substrate. For example, the protein content of wheat straw fermented by *Chaetomium cellulolyticum* or

Trichoderma reesei could be increased by inoculating with *Candida utilis* after 72 h, at which time the fungus had ceased growth but had not utilized all the sugars [68]. These excess sugars provided the substrate for growth of the yeast. Adding *C. utilis* at the beginning of the fermentation was less effective because it competed with the fungus for the sugars, retarding fungal growth and cellulase production. In other work, a novel method of sequential culture with five different fungal strains cultured successively on rice straw and wheat bran gave higher cellulase yields than monoculture [69].

In undefined mixed culture either the natural microflora of the substrate is allowed to develop or the substrate is inoculated with a mixed inoculum prepared by traditional methods. This type of process relies on the fermentation conditions to select for the desired microbial groups. Such processes are commonly used for traditionally prepared fermented foods and for waste treatment.

1.3 A General SSF Process

Solid-state fermentation processes involve the same general steps as are involved in SLF, namely upstream processing of substrate and inoculum, fermentation, and downstream processing and waste disposal, although there are differences in how some of the steps are carried out (Fig. 2). A typical process has the following features:

1. The substrate is usually of agricultural origin, and might be grains such as rice, tubers such as cassava, processed materials such as meals (e.g., corn meal) or byproducts such as straw. The carbon source is usually a macromolecule, such as starch or cellulose, although some solid substrates contain significant amounts of soluble sugars.
2. The substrate may require preparation or pretreatment such as chopping or grinding to reduce particle size, cracking to make the interior of the particles more accessible, cooking or chemical hydrolysis to increase the susceptibility of the macromolecules to degradation by microbial enzymes during the fermentation, and sterilization or pasteurization to eliminate or reduce contaminants present in the substrate.
3. The microorganism is usually a filamentous fungus, requiring aerobic conditions for growth and product formation. Spore inocula are commonly used because they are easy to prepare and are reasonably stable. Several culturing steps may be required to grow up sufficient amounts of inoculum from the stock culture.
4. The inoculum is mixed into the substrate to initiate the fermentation.
5. The bioreactor may or may not allow for mixing and aeration. If air is supplied it needs to be pretreated before entering the bioreactor to control the temperature and relative humidity, and treated upon leaving the bioreactor to prevent indiscriminate spreading of the process organism into the environment. One of the major challenges in operating the bioreactor is to prevent undesirable temperature rises in the fermenting substrate bed due to the production of waste metabolic heat by the microorganism.

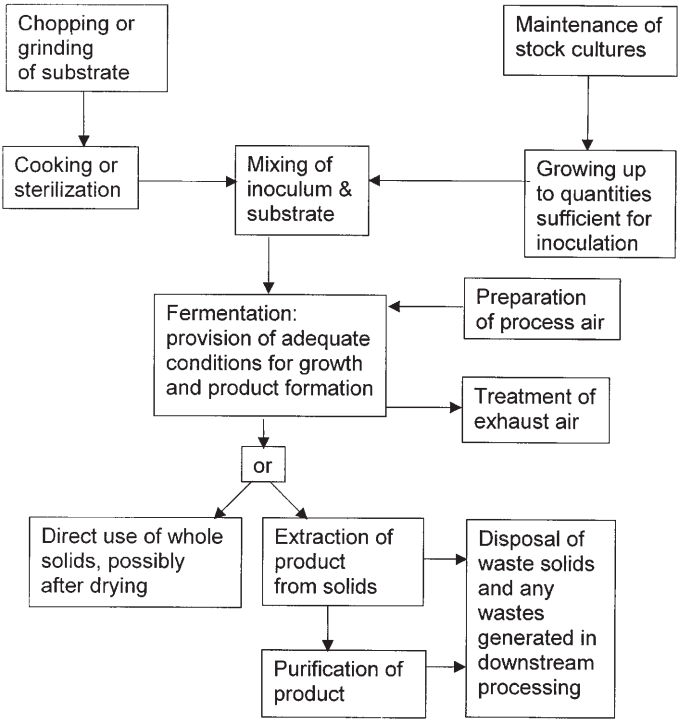

Fig. 2. The processes involved in a typical SSF process. Note that the general categories of substrate preparation, inoculum preparation, fermentation, downstream processing, and waste disposal also occur in SLF. However, the need to handle solids makes SSF more complicated

6. On completion of the process the whole fermented substrate comprises the product in the case of a food or feed, but other products must be leached out and recovered in downstream processes. After the recovery of products by leaching, the waste solids must be disposed of.

This review presents our current state of knowledge with respect to biochemical engineering aspects of these various steps of an SSF process. We define a biochemical engineering approach as a quantitative approach to characterizing the key phenomena controlling the performance of a process, with the aim of using this as a tool in process design and control and optimization of operation, including the scale-up of laboratory and pilot-scale results to commercial scale. As will become clear in the review, this biochemical engineering approach has been developed to the greatest degree for the bioreactor step of SSF processes.

2 Upstream Processing

2.1 Inoculum Preparation

The inoculum for an SSF process will typically be vegetative cells in processes involving bacteria or yeasts. For processes involving fungi, either vegetative mycelium or spores may be used. Spore inocula allow greater flexibility within the process since their dormancy enables them to be stored if necessary prior to inoculation, although spores should not be stored for extended periods since they gradually lose viability over time [70]. Spore inocula have the disadvantage of an extended lag phase required for germination and induction of appropriate extracellular enzymes. The spore inoculum may be pregerminated prior to mixing with the solid substrate if desired.

Spore germination may have different optimal conditions to vegetative growth or may need to be stimulated by some nutritional or environmental factor. Inocula can be prepared either as a dry powder by SSF or as a liquid suspension by SLF. Furthermore, liquid inocula can easily be prepared from a sporulating solid culture by suspending the spores in a liquid medium. The choice between inoculum preparation methods will depend partly on how easily the inoculum can be mixed in homogeneously with the solid substrate, although this issue has received little attention [71].

The inoculum density is of great importance. Too low a density may give insufficient biomass and permit the growth of undesirable contaminants, while for some processes high inoculum densities may produce too much biomass and deplete the substrate of nutrients necessary for product formation. Germination can also be inhibited at high spore densities. Typical densities used range from 10^4 to 10^8 spores per gram of substrate [72, 73].

On the laboratory scale, spore inocula are generally prepared by inoculating agar slants of suitable media, incubating them, and harvesting spores by adding 3–5 ml water or 0.01% sodium lauryl sulfate and aseptically scraping or shaking the slants. Spore density can be determined by colorimetric measurements at 540 nm, calibrated against hemocytometer counts. Typical methods for large-scale production of spores involve SSF of grains and drying of the fermented grains for use as inocula [74]. In drying processes the maintenance of viability of the spores is a crucial issue. The topic of drying of spores is discussed later in relation to the recovery of fungal spores as products.

2.2 Preparation of Substrates

Most substrates used in SSF are of agricultural origin and might be grains such as rice, tubers such as cassava, processed materials such as meals (e.g., corn meal) or byproducts such as straw. They are often relatively unprocessed, sometimes having only been ground or chopped from larger agricultural residues, which can give rise to particles of varying compositions. Furthermore,

the quality and composition of such substrates may differ from batch to batch since each plant grows in a particular microenvironment and has a particular genetic make-up. Plants obtained from different harvests have experienced different conditions, and their compositions can vary. The time of harvest and the length and conditions of storage can also affect substrate composition.

Substrates arising from agricultural raw materials typically consist of several macromolecules. A structural macromolecule may provide an inert matrix within which the carbon source, such as starch molecules or soluble sugars, are located, or the structural macromolecule itself may be the carbon source. The complexity of such substrates can lead to phenomena such as nutrient limitation, substrate inhibition, catabolite repression, and complex patterns of induction and repression of extracellular enzymes. This can have consequences for growth and sporulation.

Supplementation of the raw substrate may be required in order to stimulate growth, induce enzyme synthesis, or prolong secondary metabolite production. Most traditional food fermentations do not require nutritional supplementation. In cellulosic media, supplements of 0.5% of glucose or cellobiose, 0.5% peptone, asparagine, or yeast extract are in use [75].

Nitrogen is an important nutrient in SSF. Many solid substrates are supplemented with soluble sources of nitrogen during substrate preparation. The nitrogen source can play an important role in affecting the pH changes in the substrate during the fermentation. The ammonium ion is taken up as ammonia, thereby releasing a proton into the medium and causing a decrease in pH, a proton is taken up from the medium when nitrate is transported into the cell, and this causes the pH to increase, while pH increases also occur when urea is deaminated. A combination of these nitrogen sources can be used to reduce the pH changes during the fermentation [76, 77].

Some attention has been given to C:N ratios. However, note that overall C:N ratios do not necessarily reflect the relative availabilities of the carbon and nitrogen sources because the nutrients present are not necessarily equally accessible to the organism. Therefore optimal C:N ratios in SSF can potentially be quite different from those found in SLF. Also, even though the substrate may contain high levels of carbon, the provision of sufficient levels of the nitrogen source at the start of the fermentation to enable complete utilization of the carbon source can potentially cause substrate inhibition [78].

Natural solid substrates generally need some kind of pretreatment to make their chemical constituents more accessible and their physical structure more susceptible to mycelial penetration. Physical pretreatments involve chopping or grinding to reduce particle size, and cracking to make the interior of the particles more accessible. Chemical pretreatments such as high temperature cooking with acid or alkali can disrupt intraparticle barriers to diffusion, and may also be important in hydrolyzing macromolecules to produce soluble nutrients.

2.2.1
Size and Shape of the Particles

Particle size and shape are extremely important. They affect the surface area to volume ratio of the particle, the packing density within the substrate mass, and the size and shape of void spaces between the particles. Small particles, or particles with large flat surfaces, tend to pack together closely, making it difficult to aerate the substrate mass. If the microorganism can penetrate into the particle this increases the directly accessible substrate and decreases the distances over which diffusion needs to occur. In this case the optimal particle size will be influenced by the depth of penetration. The optimal particle size often represents a compromise between the accessibility of nutrients and the availability of oxygen. Particle sizes from less than 1 mm to almost 1 cm have often been used in SSF [79]. Many raw substrates, such as tubers or stalks, require processing in order to achieve particle sizes appropriate for the fermentation, which can be a costly operation. Methods for achieving this differ depending on the substrate, but may include chopping, grinding, or rasping.

Particle size may be difficult to characterize exactly, especially if the particles have irregular shapes. Possibly the best way to characterize particles is to determine the characteristic length (the ratio of volume to surface area) since this can be used to extrapolate between different shapes. Particle size distributions can be done by passing the substrate through a series of meshes with different aperture sizes, although this can be difficult with moist or sticky substrates, and in any case will work most effectively for roughly cubic or spherical particles.

Consistency and strength are also important characteristics since particles may deform due to the forces exerted by the agitator, or simply under the pressure of overlying substrate, causing the interparticle voids to disappear [79]. However, this aspect has received no attention, other than passing comments to the effect that if agitation during the fermentation was too frequent the substrate became compacted.

2.2.2
Substrate Types

Regarding the main carbon source used by the microorganism, substrates can be divided into three main groups: those that have starch, those which consist mainly of cellulose or lignocellulose, and those with soluble sugars as the main carbon source.

Starchy substrates that have been used in SSF processes include rice, cassava, wheat bran, rice bran, buckwheat seeds, rice bran, corn meal, sweet potato residue, and banana meal. Some of these substrates, such as rice, provide a nutritionally complete medium for microbial growth whereas others require addition of nutrients. For example, a nitrogen source must be added to cassava. Starchy substrates may need pretreatment such as:

1. Boiling or steaming to gelatinize the starch, unless the organism has a good potential to attack raw starch. On the large scale steaming is usually more practical.

2. Grinding, rasping, or chopping to reduce particle size.
3. Granulation to convert a fine meal into particles several millimeters in diameter to avoid the tight packing which occurs with powders.
4. Cracking to damage the surface of rice or wheat grains to make the interior more accessible.

Starchy substrates can suffer from problems of stickiness, which can cause substrate particles to agglomerate during the SSF process, especially if the substrate bed is mixed. This excludes air and is detrimental to growth.

Various different processes have been investigated for the utilization of lignocellulosic solid substrates such as wheat straw, corn and rice stover, wheat bran, sugar beet pulp, and wood. Some processes have the aim of degrading cellulose, and the microorganisms involved must be able to produce cellulolytic enzymes. Effective cellulose hydrolysis requires the synergistic action of several cellulases. Most studies emphasizing cellulose utilization have either aimed to increase the protein content of the substrate for feeding to ruminants, or to produce cellulases and other hydrolytic enzymes. Other processes aim to degrade the lignin preferentially to increase the ability of ruminants to digest the materials. Lignin peroxidase is the major enzyme involved in lignin degradation. Lignin is unable to act as a sole carbon and energy source, so lignolytic fungi also degrade some cellulose and hemicellulose.

Lignocellulosic substrates usually require significant pretreatment to disrupt the structure of cellulose and lignin molecules within the substrate. Substrates are often ground to particle sizes of 1–2 mm to increase the surface area for attack and to disrupt cell walls. In addition, the crystalline structure of cellulose may be disrupted by steaming under pressure. Sometimes the steaming is carried out in conjunction with chemical pretreatment with acid or alkali.

Solid substrates containing significant amounts of soluble sugars include grape pomace, sweet sorghum, sugar beet, pineapple waste, carob pods, and coffee pulp. Another strategy is to impregnate inert solid materials such as bagasse or hemp with soluble sugars in order to provide an SSF environment for growth [37].

2.2.3 *Substrate Sterilization*

If the process conditions are highly selective for the process organism or the process organism is extremely fast growing, then it may be possible to avoid a sterilization step or simply to pasteurize the substrate. However, for many SSF processes it is essential to sterilize the substrate.

During sterilization by heat there are two steps in the heat transfer process – heat transfer to the particle surface and intraparticle heat transfer. Due to the poor mixing characteristics of solid beds and the fact that intraparticle heat transfer is limited to conduction, it is more problematic to ensure sterility of a solid substrate than it is to ensure sterility of a liquid medium. In unmixed beds it is highly likely that the effectiveness of the sterilization process will vary with position.

Sterilization of solid substrates could be done in specialized vessels, in which case transfer into the bioreactor must be done aseptically. This is more problematic to achieve than with liquid media, and therefore it is preferable to sterilize in situ in the bioreactor, meaning that the bioreactor must be designed to enable this. In most processes batch sterilization will be used [80]. For processes operated in continuous mode a continuous sterilizer will be required at the inlet end of the bioreactor, with provision for sterile transfer into the inoculation chamber [81, 82].

3 Biochemical Engineering Approach to SSF Bioreactors

Both microscale and macroscale phenomena have the potential to control bioreactor performance. These are illustrated in Fig. 3 for an aerobic process. These processes occur within a spatially heterogeneous physical system, as was demonstrated in Fig. 1, a substrate bed consisting of moist solid particles between which are gas-filled voids. During the fermentation the bulk of the growth occurs at the particle surfaces.

The microscale phenomena include:

1. Microbial growth and death rates in response to the environmental conditions.
2. The microbial growth form, especially whether growth occurs as a mycelium or a biofilm of unicellular organisms.
3. The effect of microbial growth on the environment through the release of enzymes and end products and the uptake of nutrients.
4. Intraparticle diffusion of compounds such as O_2, CO_2, protons, enzymes, soluble nutrients, hydrolysis products, and products of metabolism.
5. Transfer between the interparticle regions and either the substrate particle or biomass of compounds such as O_2, CO_2, water, and volatile end products of metabolism.
6. Destruction of the particle due to growth if the carbon source contributes to the physical structure of the solid particle.

The macroscale phenomena include:

1. Bulk flow of air into and out of the bioreactor, carrying sensible energy and compounds such as O_2, CO_2, and water.
2. If the bioreactor is operated with forced aeration or mixing, bulk flow of air in the interparticle spaces, carrying sensible energy and compounds such as O_2, CO_2 and H_2O.
3. Natural convection, diffusion, and conduction, which are usually unimportant in the direction of airflow but can be important normal to the direction of airflow or in the absence of forced aeration.
4. Conduction across the bioreactor wall and convective cooling to the surroundings, which could be surrounding air, or could be water in a water jacket.
5. Shear effects caused by mixing within the bioreactor, including damage to either the microorganism itself, or to the integrity of the substrate particles.

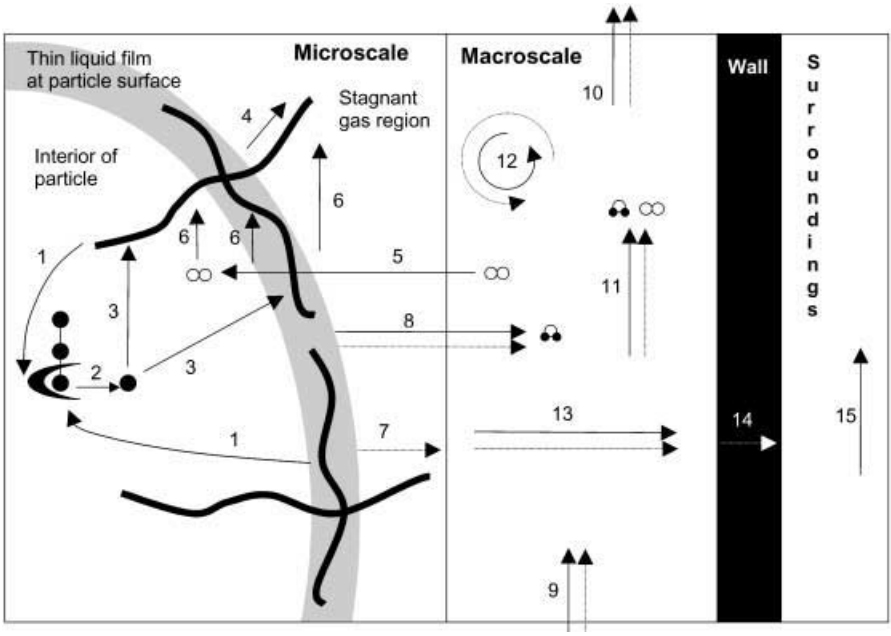

Fig. 3. Some of the microscale and macroscale phenomena occurring during an SSF process involving growth of an amylolytic fungus on a solid substrate containing starch, within an intermittently mixed SSF bioreactor with forced aeration. Note that the operational parameters of the bioreactor can only affect the macroscale phenomena. In SSF processes with bacteria or yeasts, growth occurs as a biofilm at the substrate surface. In this figure this could be represented by labeling the liquid film as a biofilm and removing the aerial and penetrative hyphae of the fungus and the phenomena associated with these hyphae. (●) Glucose units (oo) Oxygen (●O●) Water (⊂) Glucoamylase. The processes are: (*1*) Release of glucoamylase by the fungus and diffusion through the substrate; (*2*) Hydrolysis of starch by the glucoamylase; (*3*) Diffusion of glucose through the substrate and uptake by the fungus; (*4*) Translocation of biosynthetic precursors through the aerial hyphae; (*5*) Diffusion of oxygen through static gas layers, transfer to the thin liquid film at the surface, and diffusion within this film and the interior of the particle; (*6*) Uptake of oxygen by the fungus; (*7*) Release of waste energy by metabolism and conduction through static gas layers; (*8*) Evaporation of water and diffusion through static gas layers, carrying with it the enthalpy of vaporization of water; (*9*) Entry of water, oxygen, and enthalpy in inlet gases; (*10*) Exit of water, oxygen, and enthalpy in the outlet gases; (*11*) Convective flow of water, oxygen, and enthalpy in the direction of air flow; (*12*) Bulk mixing of material and energy during the periods of agitation; (*13*) Diffusion of oxygen and water and conduction of heat normal to the air flow; (*14*) Conduction across the bioreactor wall; (*15*) Natural or forced convective heat removal by the surrounding air or cooling water

Since the most powerful way to summarize our quantitative understanding is through the construction of mathematical models, the sections which follow will, in addition to giving a qualitative description, present key features of mathematical models which have been proposed to describe these microscale and macroscale phenomena. Furthermore, once constructed, such models can be used to explore system behavior, including making predictions about

phenomena for which it is not practical to make experimental measurements, and therefore these sections will also comment on what insights the mathematical models have given us as to what controls the performance of SSF systems.

Mathematical models can be applied to SSF bioreactors in two slightly different ways. First, predictive models can be proposed. These models predict system performance based on the initial conditions and the operating parameters of the bioreactor. Such models can be used to explore the likely performance of the bioreactor under conditions which have not yet been tried experimentally, and therefore can be useful tools in guiding the scale-up process. A model developed for a smaller scale bioreactor can be used to simulate performance at larger scales before the larger scale bioreactor is built. This increases the chances of identifying and avoiding operating problems on the large scale.

Second, interpretive models can be proposed. These models take as input operating variables of the bioreactor and measurements of those state variables which it is practical to measure, and give as output estimates of other state variables, including state variables which it may be impossible or impractical to measure during the fermentation. Such models are quite useful in SSF, because it is not practical to obtain direct measurements of the biomass, and parameters which can be measured on-line such as oxygen or carbon dioxide concentrations are only indirectly related to the amount of biomass. The accuracy of such models can be checked by predicting state variables which are easily measured experimentally, such as bed temperature. These models are interpretive and not predictive because they rely on the constant input of fermentation data; they cannot predict bioreactor performance simply on the basis of initial conditions. However, they are still quite useful since, if the measured variables can be measured on-line, the model can be used quite successfully in control schemes.

The application of interpretative models has been hampered by the technical challenges in collecting adequate data on-line, and as a result, to date bioreactor models have been of the predictive type. Some general comments can be made about such models First, due to the heterogeneity of SSF systems, a spatial variable is often involved, which leads to partial differential equations and therefore makes solution of the equations more difficult than would occur in perfectly mixed systems. Second, the sophistication of the model and the detail with which it describes the system depend on the complexity of the system and the motivation behind the modeling work.

4
Microscale Phenomena Occurring Within SSF Bioreactors

The microscale processes demonstrated in Fig. 3 are intrinsic to SSF due to the particulate nature of the substrate. They occur in all bioreactors and relatively little can be done to influence them in the way the bioreactor is designed and operated since they occur at the surface and inside the individual substrate particles. The most that can be achieved through bioreactor design and operational strategies is to promote exchange between the particle and air phases and to ensure that the transport processes within the air phase are not limiting.

However, the interparticle processes can be influenced by the manner in which the substrate particles are prepared. For example, the smaller the particle size the smaller the distance over which intraparticle mass transfer processes must occur. Unfortunately, small particle sizes can decrease the efficiency of the interparticle transfer processes.

Despite our very limited ability to influence these processes in the way we operate the bioreactor, it is still essential to understand their influence on the system. Understanding how and when microscale processes control process performance can prevent unfruitful attempts to improve performance by manipulating the operational variables of the bioreactor. Such understanding might point to more useful strategies. For example, for a process controlled by intraparticle mass transfer, it might be possible to disrupt barriers to diffusion within the substrate particle, such as plant cell walls. Independently of these reasons, characterization of at least some of the microscale phenomena is necessary for the construction of appropriate expressions to include in macroscale material and energy balances.

Although the various microscale processes are all interrelated, as shown in the diagram, they will be discussed one by one.

4.1 Microbial Growth in Response to its Environment

The important environmental variables which influence growth, and other growth related activities such as release of hydrolytic enzymes and of products, were described in detail by Prior et al. [76]. These variables include the concentrations of carbon and nitrogen sources, the oxygen concentration, product concentrations, temperature, pH and water activity. This section shows approaches which have been used to quantify the effects of these key environmental conditions on growth.

The basic equation for growth is

$$\frac{dX}{dt} = \mu X \tag{1}$$

where the question is essentially as to the effect of the environment on the value of μ.

4.1.1 *Effects of Nutrients, Oxygen, and Biomass Concentrations on Growth*

In mechanistic descriptions of the effect of nutrient concentrations on growth in SSF, it is not valid to relate the specific growth rate with the nutrient concentrations obtained by mashing the substrate particles prior to analysis. The mass transfer limitations within SSF particles cause concentration gradients of nutrients to arise and therefore the actual nutrient concentrations experienced by the organism are not equal to the average concentrations given by the mashing procedure (Fig. 4) [83–85]. In fact, microbial cells or hyphal tips

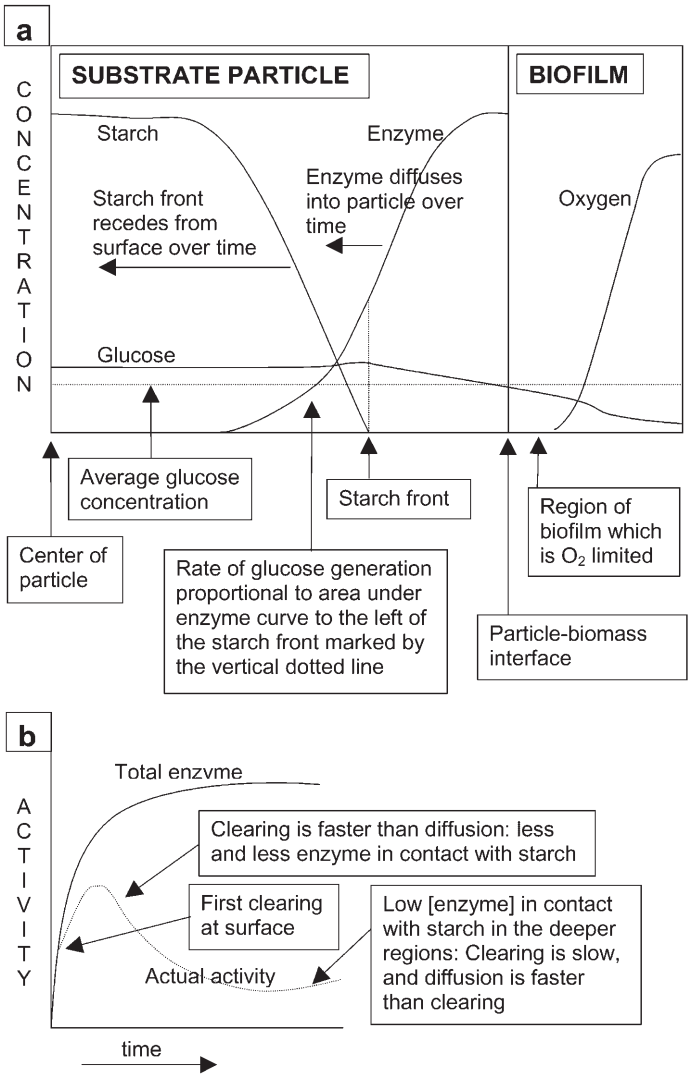

Fig. 4. **a** The concentration gradients which arise within substrate particles, shown for the growth of an amylolytic unicellular organism on a substrate containing starch. **b** The consequences that clearing of starch at the particle surface has on the rate of glucose generation within the substrate particle by the glucoamylase

located in different regions of the particle will be experiencing different nutrient concentrations. Likewise, there are oxygen concentration gradients within the substrate and cells or hyphal tips located in different regions of the particle will be experiencing different oxygen concentrations [86].

It is logical to express the specific growth rate of a cell or a hyphal tip at a particular location in the same manner that is common in SLF, namely by use

of the Monod equation. For example, the effect of oxygen on the growth of aerobic microorganisms can be described by a Monod relationship [87]:

$$\mu_{O_2}\big|_Z = \mu_{\max} \frac{C_{O_2}\big|_Z}{K_{O_2} + C_{O_2}\big|_Z} \tag{2}$$

where the notation $\big|_Z$ signifies that the value is for a particular location in space. The subscript O_2 signifies that this is the effect of oxygen on the specific growth rate. Other subscripts are used below to distinguish the effects of other environmental variables. The Monod equation can also be used to describe the effect on the specific growth rate of glucose as the sole limiting nutrient [84, 85]:

$$\mu_N\big|_Z = \mu_{\max} \frac{C_G\big|_Z}{K_G + C_G\big|_Z} \tag{3}$$

If the substrate is inhibitory at high concentrations then a substrate inhibition term can be included:

$$\mu_N\big|_Z = \mu_{\max} \frac{C_N\big|_Z}{K_N + C_N\big|_Z + \left(C_N\big|_Z\right)^2/K_i} \tag{4}$$

Although the last equation is presented here in terms of local nutrient concentrations, in the work in which it was used it was based on the average substrate concentration [88]. In this case the relationship between specific growth rate and nutrient concentration is purely empirical: it can only be determined from experiments done with the particular system modeled, and parameters are likely to change with small changes in the system, such as particle size. In contrast, the mathematical models in which Eqs. (2) and (3) were used included expressions describing the diffusion of glucose or oxygen or both. In this case the parameters of the equation can be determined in an independent system, such as liquid culture, in order to remove mass transfer limitations. Changes in system behavior due to changes in particle size would be taken into account by the diffusion equations, and there would be no need to adjust the parameters of the expression for the specific growth rate.

Models of bioreactor performance usually only take into account the intraparticle diffusion of nutrients if heterogeneity at the macroscale across the bioreactor can be ignored [89, 90]. For bioreactors in which there is heterogeneity at the macroscale, and even in some cases where there is no macroscale heterogeneity, to simplify the model it is common to use empirical equations that do not rely on nutrient or oxygen concentrations. These empirical approaches are commonly based on the logistic equation, which reasonably describes the biomass profiles found in many SSF systems, with extended periods of acceleration and deceleration of growth:

$$\frac{dX}{dt} = \mu_{\max} X \left(1 - \frac{X}{X_{\max}}\right), \quad \text{i.e.,} \quad \mu_X = \mu_{\max} \left(1 - \frac{X}{X_{\max}}\right) \tag{5}$$

with X corresponding to the biomass concentration (in kg-biomass kg-substrate^{-1}).

The deceleration of growth as X approaches X_{max} could be due to nutrient limitations, accumulation of inhibitory products, or maximum packing densities based on steric limitations [91] although in practice the value of X_{max} is usually simply taken directly from experimental biomass profiles. Note that μ_{max} is also typically determined empirically. However, with the assumption that each fungal hypha branches to give identical daughter hyphae which extend at the same rate as the mother hypha, these macroscopic parameters can be related to microscopic parameters such as hyphal branching frequencies and hyphal extension rates [92, 93].

Linear and exponential kinetics can also apply for a significant part of the growth phase. During an exponential growth phase μ remains at μ_{max}, whereas during a linear growth phase the growth rate itself is a constant. In this case there is a need to impose an external condition to prevent predictions of infinite growth; for example, that the growth rate equals zero when the biomass concentration reaches a particular value. In any case, linear or exponential growth profiles rarely persist for the whole of the fermentation time, and it may be necessary to divide the fermentation time into different phases. For example, to describe a fungal growth profile with early exponential growth followed by an extended period during which the growth rates slowly decelerates, the following empirical equations can be used [94]. First, during the exponential phase:

$$\frac{dX}{dt} = \mu_{max} X \tag{6}$$

At time t_a there is a switch to deceleration phase kinetics, described by

$$\frac{dX}{dt} = \mu_{max} L \cdot e^{-k(t-t_a)} \tag{7}$$

where the factor L describes an instantaneous decrease in the number of actively extending hyphal tips as the fungus enters the deceleration phase. During the deceleration phase there is a further first-order decay in the number of actively extending hyphal tips, with first order rate constant k.

The appropriate form of an empirical equation can only be decided after the collection of experimental data. This should be done with small substrate masses so that interparticle heat and mass transfer processes are not limiting. The integrated form of the growth equation can be fitted against the biomass fermentation profile by linear or non-linear regression to extract the parameter values. In doing this, it must be clear whether the biomass is expressed in absolute concentration terms (i.e., kg-biomass m^{-3}) or as in relative concentration terms (i.e., kg-biomass kg-dry-matter^{-1}). Since the amount of dry matter decreases during the fermentation due to the loss of carbon in the form of CO_2, these two expressions cannot simply be converted from one to the other by multiplying by a constant [95].

4.1.2 *Effect of Temperature on Growth*

Temperature is an important variable in SSF systems because the difficulty of removing waste metabolic heat from the substrate bed means that the temperature rises within the substrate bed, with the problem becoming more severe as the size of the substrate bed increases. As a result, in most large-scale bioreactors the microorganism at any location within the bed is subjected to a temporal variation in temperature, with the degree of variation depending on the effectiveness of cooling at that location in the bed. Usually there is an initial period of growth at the optimum temperature for growth, during the early period when the biomass density is low and therefore the rate of release of waste metabolic heat is low. However, as the biomass concentration increases the growth rate increases and therefore the rate of heat production increases. If the heat production rate exceeds the heat removal rate at that location in the bed, then the temperature increases. In poorly cooled regions of the bed, temperatures close to the maximum temperature for growth may be reached, with this temperature being maintained for periods as low as 1 h to as long as 50 h. Later, growth decelerates, possibly due to negative effects of the high temperature, but also possibly due to steric limitations on biomass density or nutrient exhaustion, and, as a result of the decreased heat production rate, the temperature falls again. As a result of the inevitability of temperature rises in almost all types of bioreactors, it is essential to incorporate a description of temperature effects on the growth kinetics.

To date, studies aimed at describing the effect of temperature on growth kinetics have obtained data using an experimental procedure which can be referred to as the "isothermal approach": a range of cultures are incubated at a range of temperatures, with each culture being maintained at a constant temperature throughout the fermentation. This can be achieved by using a small enough substrate sample (several grams) so that heat removal limitations are negligible. The specific growth rates are then plotted as a function of the incubation temperature and a mathematical expression, usually an Arrhenius-type expression but sometimes simply a quadratic fit, is fitted to the data. In those cases where temperature-related death of the biomass is not taken into account the expression describes the net growth rate and needs to be able to describe the decrease in growth rate above and below the optimum temperature for growth. Empirical expressions include the double Arrenhius expression [96]:

$$\mu_T = \frac{A.\exp\left(\frac{-E_{a1}}{R(T+273.16)}\right)}{1 + B.\exp\left(\frac{-E_{a2}}{R(T+273.16)}\right)} \tag{8}$$

where temperature is in °C. Alternatively, simple polynomial equations can be used [87, 97, 98]. The effect of temperature on the parameter X_{max} in Eq. (5) can also be described if data for this parameter is collected during the experiments. Typically this can be fitted with a quadratic function [96].

It is also possible to divide the biomass into living and dead biomass and to include equations for temperature-related death. Arrhenius-type relationships can be used to describe the effect of temperature on both the specific growth rate and the specific death rate, giving a net growth rate [99]:

$$\mu_T = \mu_{To} \exp\left(\frac{-E_g}{RT}\right) - k_{do} \exp\left(\frac{-E_d}{RT}\right) \tag{9}$$

In this case both of the rates increase with temperature, but the death rate is negligible below the optimal temperature. Above the optimal temperature the death term increases faster than the growth term, so the net specific growth rate falls. In this case the equation was fitted to data collected using the isothermal approach using non-linear regression.

A slightly different approach was taken by Smits et al. [100]. Rather than describing the death of biomass itself, they incorporated an inactivation term into their equation relating oxygen uptake to growth. This corresponds to a decrease in specific respiration activity as a result of aging processes. The inactivation term was expressed as an Arrhenius function of temperature:

$$m_d = m_{d0} + k_{md} \exp\left[-\frac{E_a}{R}\left(\frac{1}{T} - \frac{1}{T_{max}}\right)\right] \tag{10}$$

where m_{d0} is the basal specific inactivation rate.

As mentioned above, to date the effect of temperature on growth and death kinetics has been based on data obtained using the isothermal method. However, recent work indicates that the growth and death kinetics of a microorganism which starts growing at the optimum temperature for growth and is later subjected to a rise in temperature is not adequately described by the equations obtained using this isothermal approach. In the bioreactor model of Saucedo-Casteneda et al. [96], the model could not describe the experimental temporal temperature profiles if the specific growth rate was allowed to decrease as the temperature rose above the optimum temperature according to the expression obtained from isothermal approach data. Good agreement with the experimental results could only be obtained if the growth rate was assumed to remain constant as the temperature increased. Ikasari et al. [101] mimicked the temporal temperature profile in SSF of *Rhizopus oligosporus* by making a step upshift in temperature from 37 °C to 50 °C after 20 h of fermentation and a downshift back to 37 °C 10 h later. Growth rates close to the growth rate before the temperature upshift were maintained for several hours at the higher temperature. Furthermore, the upshift had delayed deleterious effects which were not reversed by returning the culture to 37 °C. More work needs to be done with a wider range of organisms and various temporal temperature profiles to obtain sufficient kinetic data to allow the effect of a varying temperature on growth to be modeled adequately.

4.1.3 *Effect of pH on Growth*

Microbial growth is usually significantly affected by the local pH. This has important consequences for SSF processes since pH gradients arise within the substrate particles, and although pH correcting solutions can be added to the substrate in mist form with some bioreactor designs, fine pH control in SSF is impracticable [84]. Models have been proposed which relate growth rate to pH based on empirical equations describing experimental data for the effect of pH on growth rate [102, 103]. However, the diffusion of protons within the substrate particles was not included in the equations, which raises questions as to the validity of such models, since the microbial growth response will depend on local pH and not some global average.

4.1.4 *Effect of Water Activity on Growth*

Relatively little effort has been made to incorporate the effects of water activity within bioreactor models, and it is done by using empirical expressions to obtain an expression for μ_w. Pitt [102] assumed that the specific growth rate fell linearly between an a_w of 1 and the minimum a_w for growth while Muck et al. [103] broke the curve into several linear segments. Data for the effect of water activity on the growth of fungi is commonly obtained by measuring the effect on the radial extension rate of colonies. Assuming that the width of the peripheral growth zone of the colonies is constant despite variations in water activity, then the radial extension rate will be directly proportional to the specific growth rate [104], and therefore such data can be adapted for SSF.

In colony extension rate data there is typically an optimum water activity at a value somewhat less than $a_w = 1$, with the radial extension rate falling off exponentially as the water activity decreases below this optimum [105, 106]. The following equation describes the exponential part of the curve:

$$r = A \ln \frac{a_w}{a_{w0}} + r_m \tag{11}$$

where A is a constant, and r_m is the radial extension rate at the optimal water activity for growth, a_{w0}.

4.1.5 *Combining Environmental Effects*

The simultaneous variation of various environmental variables within SSF systems raises the question of how their effects on growth should be combined. The best idea is to identify a value for μ_{max}, the specific growth rate at the optimum combination of T, pH, water activity, and with saturating nutrient concentrations. The relative effects of the different environmental variables can

then be expressed as fractions of this value:

$$f_V = \frac{\mu_V}{\mu_{\max}} = f(\text{variable}) \tag{12}$$

The actual specific growth rate μ can then be expressed as [102, 103]

$$\mu = \mu_{\max} f_{pH} f_{aw} f_T f_N f_X f_{O_2} \tag{13}$$

Various combinations which have been used in this manner in SSF models to date include simultaneous limitation by oxygen and glucose [85]:

$$\mu_N\big|_x = \mu_{\max} \frac{C_{O_2}\big|_x}{K_{O_2} + C_{O_2}\big|_x} \frac{C_G\big|_x}{K_G + C_G\big|_x} \tag{14}$$

simultaneous limitation by oxygen and high biomass concentrations [87]:

$$\mu = \mu_{\mathrm{m}} \left(\frac{\mathrm{C_{O_2}}\big|_x}{\mathrm{K_{O_2}} + \mathrm{C_{O_2}}\big|_x} \right) \cdot \left(1 - \frac{\mathrm{X}\big|_x}{\mathrm{X_m}} \right) \tag{15}$$

and simultaneous limitation by a growth inhibiting substrate and high biomass concentrations [88]:

$$\mu = \mu_{\max} \left(1 - \frac{X}{X_{\max}} \right) \frac{C_S\big|_x}{K_S + C_S\big|_x + C_S\big|_x^2 / K_i} \tag{16}$$

A slightly different rule for combining effects was used by Sargantanis et al. [107]:

$$\mu = f_X \sqrt{\mu_W \mu_T} \tag{17}$$

where $f_X = (1 - X/X_{max})$, μ_W was given by an empirical fit to data for the effect of moisture content (not water activity), and μ_T was given by an empirical fit to data for the effect of temperature.

4.2 Microbial Growth Forms Within SSF Bioreactors

In SSF processes the inoculum is spread over the surface of the substrate, with the intention of having a relatively high density of inoculated spores or cells in order to achieve rapid colonization of the substrate surface. This "overculture" technique differs from the approach in many microbiological studies in which low inoculum densities are often used in order to obtain well separated colonies. Overculture systems using flat substrate slabs have been used as model systems for some studies of growth kinetics in SSF [83, 84]. In overculture, separate colonies exist only very early in the process, while the colonies are at the microcolony stage. They soon merge to form an "overculture." With the

whole surface covered, further increases in density occur by growth above and below the surface.

The biomass in SSF is distributed spatially in one of two forms. Unicellular organisms such as bacteria and yeasts grow as a moist film on the surface of the substrate particle. This film will have a constant biomass density, and the intercellular spaces will be occupied by moisture. Mycelial organisms such as fungi and streptomycetes may extend above and below the substrate surface. Steric limitations associated with branching frequency and branch angles prevent high packing densities. Maximum packing densities can be 15–34% of available volume [91, 108]. In unmixed fungal SSF processes, within the substrate particle and within thin moisture films at the substrate particle surface, the spaces between hyphae will be occupied by an aqueous phase. However, the hyphae extending above the surface will typically be in direct contact with air [109]. In processes with mixing, the mixing action tends to squash the fungal mycelium to make a moist film at the surface, which will behave similarly to a biofilm of unicellular microorganisms [110].

Penetration into substrates is an important phenomenon which has been observed experimentally but has not yet received modeling attention. Ito et al. [111] showed that the concentration of penetrative hyphae decreased exponentially with depth in rice koji. Depths of penetration by hyphae of *Rhizopus oligosporus* into soybeans during the production of tempe vary from 0.4 mm to 2 mm, with the majority of penetrative hyphae extending to depths of 0.4–0.7 mm [112, 113]. The average frequency of penetration into the soybean was one penetration per 785 μm^2 of surface area. The majority of penetrations occurred in the intercellular spaces during growth on soybean cotyledons. Penetration into substrates where the cellular structure had been disrupted was easier. In soybean flour, *R. oligosporus* penetrated to depths of 0.5–1 mm, with a maximum depth of penetration of 5–7 mm [113].

Penetrative hyphae can potentially play an important role in making the substrate accessible to enzymes [113]. On the basis of expected molecular diffusion coefficients of proteins in solutions of 10^{-11} m^2 s^{-1}, enzymes would be expected to diffuse to depths of about 1 mm after 40 h, or even less if lower effective diffusion coefficients of around 10^{-12} m^2 s^{-1} occurred, such as might be expected within solid substrates [113]. Therefore enzyme diffusion occurs at a rate similar to hyphal penetration rates. As a result, the contribution of hyphal movement and release of enzyme from the hyphal tip would be significant in allowing the enzyme to reach greater depths than if the enzyme was simply released from the surface. Note that in modeling work to date enzyme release has been assumed to occur only at the interface between the substrate and biomass phases [84, 85, 114].

Early modeling studies of growth ignored the microbial growth form, simply expressing it as a concentration per area of substrate surface [83, 84]. Effectively these models assume that glucose crossing the surface is converted instantaneously into biomass. There is no diffusion of glucose in the biomass layer. Most of the more recent models have modeled growth in the form of biofilms, assuming a phase of constant density which increases in height during growth [85, 114, 115], and in which the value for oxygen diffusivity is that for

diffusion through water. Nopharatana et al. [116] developed a model more appropriate to describe the growth of a fungus. The existence of separate biomass and air phases is recognized, although the air and aerial biomass are treated as a single pseudohomogeneous phase, with each height simply being assigned a biomass concentration. The biomass concentration at any height can increase due to the movement of biomass into the region from lower heights, and the production of biomass within that region itself.

With the mycelial growth form there is also usually the phenomenon of differentiation. Many of the filamentous fungi used in SSF produce spores called conidia. Specialized aerial structures, called conidiophores, develop following initial colonization of the substrate surface by vegetative hyphae. Later conidia are produced on these structures. Differentiation within SSF systems has received some attention. Various workers have studied the stoichiometry of growth and differentiation, showing that the stoichiometry of production of vegetative biomass and conidia are different [117, 118]. However, differentiation has received very little attention to date in SSF models. In their model of fungal overculture growth Georgiou and Shuler [83] recognized four biomass forms – vegetative biomass, competent biomass, mature conidiophores, and conidia. The vegetative biomass become competent, i.e., able to differentiate, at 24 h. The rates of conversion of competent biomass into conidiophores, and of conidiophores into conidia were related to the nitrate and glucose concentrations. The model was able to describe the short lag of a few hours which occurs between the emergence of the first conidiophores and the appearance of the first conidia.

4.3 Effect of Microbial Growth on the Environment

The microorganism affects its environment through the release of extracellular enzymes and metabolic end-products and also by the uptake of a range of nutrients. As noted earlier, this leads to the establishment of concentration gradients of enzymes, nutrients, products, and oxygen within the particle. Approaches to describing these concentration gradients are described in the following section. The present section focuses on simpler modeling approaches.

In many bioreactor models intraparticle concentration gradients are ignored, and growth is modeled as depending only on the biomass concentration and temperature. In this case overall consumption of oxygen, production of CO_2, or consumption of nutrients can be calculated assuming that both growth-related and maintenance metabolism are involved:

$$R_A = Y_{AX}\frac{dX}{dt} + m_A X \tag{18}$$

where A is a compound associated with metabolism, Y_{AX} is the stoichiometric coefficient relating that compound with growth, and m_A is the maintenance coefficient for that compound. The rate R_A will be the rate of consumption if A is consumed during growth, and the rate of production if A is produced during growth.

Despite the fact that the goal of SSF processes is product formation, the modeling of production has received little attention. The products produced in SSF can be quite different in the way they are related to growth activities. Simple approaches which have been taken to modeling the production of a catabolic end product, extracellular enzymes, and secondary metabolites are described below.

Sato and Yoshizawa [119] modeled the production of ethanol, a catabolic end product, during SSF of *Saccharomyces cerevisiae*. The rate of ethanol production was assumed to be directly proportional to the rate of carbon dioxide formation, which had both growth and non-growth associated terms as shown in Eq. (18). The non-growth associated term represented maintenance metabolism and the non-growth associated rate constant was assumed to decrease exponentially as the ethanol concentration increased, in order to describe the inhibitory effect of ethanol on its own production.

Enzyme production kinetics in SSF have the potential to be quite complex, with complex patterns of induction and repression resulting from the multisubstrate environment. As a result, no mechanistic model of enzyme production in SSF has yet been proposed. Ramesh et al. [120] modeled the production of α-amylase and neutral protease by *Bacillus licheniformis* in an SSF system. They showed that production profiles of the two enzymes could be described by the logistic equation. However, although they claimed to derive the logistic equation from first principles, the derivation was based on a questionable initial assumption about the form of the equation describing product formation kinetics: They did not justify why the rate of enzyme production should be independent of biomass concentration but directly proportional to the multiple of the enzyme concentration and the substrate concentration. As a result their equation must be considered as simply empirical.

Perez-Correa and Agosin [121] modeled growth and production of gibberellic acid, a secondary metabolite, by *Gibberella fujikuroi*. Equation (18) was used to characterize gibberellic acid production. The non-growth associated rate constant was modeled as depending on the nitrogen concentration according to the Monod equation with a substrate inhibition term. Since the growth rate was also related to the nitrogen concentration by a Monod equation, these equations described the observed behavior that the gibberellic acid production is very slow until nitrogen is largely depleted, and then there is a period of production until the nitrogen is totally exhausted. As nitrogen concentration falls growth slows and the substrate inhibition of gibberellic acid production is progressively alleviated, but then as the nitrogen concentration falls to zero then both the growth and non-growth associated production terms fall to zero.

4.4 Intraparticle Diffusion of Enzymes, Nutrients, Hydrolysis Products, and Oxygen

It has been noted several times in the preceding sections that growth activities lead to intraparticle concentration gradients, with consequences for bioreactor performance. No attention has been paid to intraparticle product concentra-

tion, pH, or water activity gradients but some experimental and modeling work has addressed the diffusion of enzymes, oxygen, and soluble nutrients.

To date there has been little experimental effort to measure nutrient concentration gradients within particles. Mitchell et al. [109], by cutting slices off the faces of cubes of an artificial gel-based solid substrate, showed that starch and glucose concentrations were higher in the interior portion of the substrate particle than in the outer portion. Protein concentrations, used as a measure of biomass, were higher at the surface. Finer cuts would characterize the concentration profiles better, the fineness of the cut being limited by the sensitivity of the detection method for the compound whose concentration profile is being studied. Oxygen microprobe measurements demonstrate that during peak growth periods oxygen concentrations fall from atmospheric levels to zero within 100 µm depth for a fast growing organism such as *Rhizopus oligosporus* ($\mu = 0.3\,h^{-1}$) and within 200 µm depth for a slow growing organism such as *Coniothyrium minitans* ($\mu = 1\,day^{-1}$) [86]. The modeling studies described below have given more insight into these experimental results.

In overculture studies with a gel substrate in which starch was embedded, Mitchell et al. [84] showed that the diffusional limitation of the glucoamylase released by the fungus at the surface meant that the enzyme tended to be concentrated near the surface most of the time, and as a result the starch at the surface was quickly utilized (Fig. 4a). The boundary between the cleared region and the region containing starch receded from the surface. The glucoamylase in the cleared region lacked substrate to act upon. The cleared region receded from the surface faster than the glucoamylase diffused away from the surface, the result being that the rate of glucose production fell quite drastically (Fig. 4b). It could be as low as 20% of the activity that would be obtained if all the enzyme were in contact with starch. For much of the fermentation, growth can be limited by the rate at which this glucose is generated and diffuses to the surface. In this case growth can be assumed to be limited by enzyme diffusion, since the effect arises due to the low diffusivity of glucoamylase. At high diffusivities the glucoamylase would distribute evenly throughout the substrate and starch hydrolysis would occur throughout the substrate rather than being localized near the surface.

In this work of Mitchell et al. [84] the biomass had no structure and diffusion of glucose within the biomass layer was not considered. Furthermore the role of oxygen diffusion and consumption was not considered. The model was extended by Rajagopalan and Modak [85] for the growth of unicellular organisms in a biofilm of constant density (shown on the right of Fig. 4a). They concluded that oxygen is more likely to limit growth within the film than lack of glucose, even when high oxygen concentrations can be maintained at the outer edge of the film [85, 122]. After a short period in which neither glucose or oxygen are lacking, the oxygen becomes limiting within the lower parts of the biofilm. This situation is maintained until glucose becomes limiting later in the fermentation when the starch in the substrate is almost completely utilized. These results have been confirmed in a somewhat different SSF system in which glucose solution is sprayed onto the surface of yeast pellets in a gas-solid fluidized bed bioreactor [89, 90]. In the production of baker's yeast in this

system, glucose and oxygen are only available in the 100-µm layer at the surface of the particle.

The importance of oxygen transfer in limiting growth has led several authors to consider the measurement of the parameter $K_L a$ in solid state fermentation systems. Durand et al. [123], adapting a method used in liquid culture, used sulfite oxidation rates to estimate $K_L a$ in a packed bed bioreactor. Gowthaman et al. [124] estimated $K_L a$ simply on the basis of the inlet and outlet oxygen concentrations, although their results are questionable because they assumed that the decrease in oxygen concentration within the liquid film was always 10% of the saturation concentration, which will not be the case. More recently, Thibault et al. [125] suggest that this direct application of $K_L a$ concepts from submerged fermentation to SSF is conceptually incorrect. They point out the differences in the geometries of SLF and SSF systems: in liquid culture there are thin static gas and liquid films at the air-water interfaces of bubbles, there is assumed to be no consumption of oxygen within this thin static liquid film, and there is convective flow on the water side, whereas in SSF there is no convection on the liquid side, rather; as soon as the oxygen is transferred from the solid to the liquid phase, the oxygen diffuses through and is consumed within a static biofilm. As a result, rather than using $K_L a$ to try to describe oxygen limitations within SSF systems it is better to use a new term, the average biofilm conductance, $K_F a$, where K_F is the ratio of the dissolved oxygen diffusivity to the thickness of the aerobic portion of the biofilm [125]. Note that this is slightly different from $K_L a$, which in SLF represents the oxygen diffusivity divided by the thickness of the static liquid layer, where the major mass transfer resistance is assumed to occur.

For mycelial growth in SSF, it is probable that those fungal hyphae exposed directly to the air can take up oxygen directly from the air. In systems with forced aeration it is unlikely that transfer of oxygen to this aerial biomass will be limiting [116]. In this case nutrient movement within the aerial hyphae layer may be the factor controlling growth. Diffusion is probably the mechanism for translocation of at least some nutrients, such as glucose and orthophosphate, within the hyphae of some fungi, including *Rhizopus nigricans* [126]. Nopharatana et al. [116] showed that the diffusion of glucose within the aerial hyphae of a fungus has the potential to control the shape of the biomass concentration profile against height above the surface and how this develops over time. Of course, even for systems in which there is a significant amount of aerial mycelium, there will be hyphae in the liquid film at the substrate particle surface, and hyphae penetrating into the substrate. This region of the biomass can quickly suffer from oxygen limitation, so at least some of the biomass in SSF will always be under oxygen limitation.

In summary, intraparticle oxygen limitation is an intrinsic property of SSF systems, even if operation of a bioreactor enables high concentrations to be maintained in the interparticle air spaces [122]. At least some of the biomass will have little oxygen available for the majority of the fermentation. Of course this is one of the reasons why the density of penetrative hyphae quickly falls with depth below the particle surface [109].

4.5 Destruction of the Particle Due to Growth

If the carbon source used by the microorganism contributes to giving the particle its solid structure, then the structure of the particle will be degraded during growth. This can lead to a reduction in the size of the substrate particle during the fermentation. Note, however, that as the substrate particle itself is shrinking the biomass layer at its surface tends to expand outwards. Depending on the relative rates of these two phenomena, the overall particle (i. e., including both biomass and residual substrate) may either increase or decrease in size.

Decreases in particle size have been characterized experimentally. Nandakumar et al. [115] used perchloric acid to remove the fungal mycelium from wheat bran particles. During the fermentation the average size of the residual substrate particles decreased: At zero time 98% of the total substrate mass was composed of particles of greater than 1 mm. After 72 h this had fallen to 75%. Gumbira-Sa′id et al. [127] measured overall particle diameters (i. e., the particle plus the biomass film) for growth of *Rhizopus oligosporus* on spherical sago beads. With an initial particle diameter of 4.8 mm, the particle size increased to 5.4 mm at 24 h, but then decreased to 4.5 mm by the end of the fermentation at 54 h. With an initial particle size of 3.8 mm the diameter increased to 4.1 mm at 35 h and then decreased to 3.2 mm. With an initial particle diameter of 3.0 mm the diameter increased to 3.5 mm at 44 h and then decreased to 3.1 mm. In this last case, given that some of the diameter of the final particle was comprised of biomass, the substrate particle itself had probably shrunk.

Some modeling attention has been given to this phenomenon. Nandakumar et al. [115] assumed that the overall particle size was constant, meaning that biomass occupied the space liberated by the shrinking particle. The substrate consumption reaction was assumed to take place at the biomass-substrate interface and to be controlled by the availability of oxygen, the supply of which was restricted by diffusion through the biomass film. Note that since the oxygen consumption reaction occurred only at the interface, simultaneous diffusion and reaction of oxygen through the biomass film did not occur. With these assumptions an analytical solution was possible, relating the length of the substrate particle itself with time:

$$\frac{t}{T} = \left(1 + \frac{l_c^2}{L^2} - 2\frac{l_c}{L}\right) \tag{19}$$

where t is time, T_c is the time for complete particle degradation, l_c is the length of the residual particle core, and L is its original length.

The predictions agreed quite well with experimental measurements for growth of *Aspergillus niger* on wheat bran flakes for the first 60% of the fermentation time. Later the model predicted that the particle would disappear completely, whereas experimentally a residual length of 20% of the initial length was found. Later the same model was applied for the growth of *Bacillus coagulans* on wheat bran [128]. In this case different behavior was noted,

depending on the initial particle size. Wheat bran particles of initial flake length of 1 mm completely disappeared, and the decrease in flake length during the fermentation was described well by the model. As flake length increased there was a greater residual length. Particles of initial flake length of 2 mm and above were degraded to only 50% of this initial length in the 96 h of fermentation. In this case the model did not describe the degradation curve well. Nandakumar et al. [128] pointed out that smaller wheat bran particles contain mainly starch, while larger particles contain significant amounts of hemicellulose and cellulose, which cannot be degraded by *B. coagulans*.

A more sophisticated model was proposed for growth of biofilms of *B. coagulans* on reducing particles by Rajagopalan et al. [114], describing many other phenomena occurring such as oxygen reaction within the biofilm, expansion of the biofilm during growth, release of enzyme into the substrate, and diffusion of glucose through the substrate and biofilm. Their model also agreed well with the data of Nandakumar et al. [128]. They argued that the explanation of different compositions for particles of different sizes is not the only possible explanation. Instead, they suggested that the limited diffusion of glucoamylase into a particle, combined with the "clearing effect" noted by Mitchell et al. [84], could account for the different consumption rates for different particles sizes. Late in the fermentation, almost all the glucoamylase could be located in regions cleared of starch, preventing further particle degradation. However, they did not clearly propose a mechanism by which particle shrinkage was related to starch utilization.

4.6 Potential to Develop a Microscale Model of Growth

The preceding sections have highlighted the complexity of the microscale phenomena occurring during SSF, and our current understanding of how these phenomena can influence the process. Before describing approaches to modeling bioreactors, it is worthwhile to consider how these microscale phenomena might be handled in bioreactor models. There are basically two approaches – either to use empirical growth equations which ignore microscale mass transfer, or to attempt to incorporate the microscale mass transfer processes into the bioreactor model.

Due to the complexity of describing transfer phenomena at both the intraparticle and supraparticle scale, most bioreactor models use empirical equations, such as the logistic equation (Eq. 5), with the specific growth rate being expressed as an empirical function of temperature. However, if this is done the parameters of the empirical model must be determined for each small change in the system. The model may simply fail to describe data under different operating conditions where the factor limiting growth may be different. Additionally, the values of the fitted kinetic parameters will have no biological significance, although it still might be useful to compare values (e.g., of μ_{max} or X_{max} in the logistic equation) for different fermentations.

Combined intraparticle and interparticle diffusion of oxygen has been taken into account in a model of a tray bioreactor [122]. A "complete" bioreactor

model would include, in addition to those phenomena which have been mentioned above, the following microscale phenomena:

1. Diffusion of acidic and basic products of metabolism
2. Penetration and the role of penetrative hyphae in enzyme release
3. Mechanistic descriptions of the control of enzyme production, including induction and repression of synthesis
4. The effect of substrate structure on diffusion, since most work has been done with gel model systems, but real systems are likely to be more complex
5. Diffusion of products, especially those which can cause product inhibition, and for volatile products, exchange with the interparticle spaces
6. Metabolic production of water, diffusion of water within the substrate particle, exchange of water between the particle and the interparticle spaces, the effect of solute production and consumption on water activity, and the binding of water by capillary or absorptive forces

Such models might show how, at different times during a fermentation, and under different operating conditions, various of these phenomena may be limiting. However, the increased power of such a model and the benefits this brings in accuracy and flexibility would need to be weighed against the greater effort required to set up and solve the equations, the greater effort required to determine many of the parameters associated with the microscale transport and kinetic phenomena, and the experimental effort required to validate predictions of the model.

5
Bioreactor Design and Macroscale Phenomena Occurring in Bioreactors

The bioreactor is the central point of a fermentation process. It is here that the biotransformation takes place, that a raw material is turned into a desired and valued product. Optimization of the rate of formation and yield of product within the bioreactor is a key part of optimizing the production process. Although the field of bioreactor design for submerged liquid fermentation systems is well developed, many of the principles cannot be directly translated to SSF systems. Solid beds and liquid broths are different: solid beds are not as easy to mix as liquid broths, and due to poor heat transfer properties of solid substrate beds, heat removal is much more difficult in SSF than it is in SLF.

5.1
General Roles of a Bioreactor

A solid-state fermentation bioreactor must fulfill one or more of the following functions:

1. Contain the substrate bed
2. Prevent the uncontrolled release of the process organism into the environment
3. Prevent the entry of contaminants into the process

4. Enable the environmental conditions to be controlled at values which favor production of the desired product
5. Maintain homogeneity within the substrate bed
6. Facilitate other aspects of processing, including substrate preparation, sterilization, loading, unloading, and product recovery
7. Operate in the required mode, whether batch, fed-batch, or continuous

Some general points can be made about how these functions can be achieved in SSF bioreactors.

5.1.1 *Containing of the Substrate Bed*

The main criterion here is strength. This issue has not received direct attention in the literature concerning SSF bioreactors. However, some general rules can be outlined. First, although materials such as plastic, glass, and wood are used on the small scale, larger bioreactors, especially those containing hundreds of kilograms of substrate, will need to be constructed of metal. Considerations in the selection of the metal include cost, resistance to corrosion, and potential toxicity to the process organism. Stainless steel is a strong material, with good resistance to corrosion and a lack of toxicity. For this reason it is used extensively in the construction of bioreactors for SLF, and is also appropriate for large-scale SSF bioreactors. However, its major disadvantage is cost.

5.1.2 *Containing of the Process Organism*

Release of the process organism into the environment could be potentially dangerous, especially if pathogens are used in the process. Even if the process organism is not pathogenic, since the majority of SSF processes involve filamentous fungi, there is the potential for release of spores into the environment. Such release of fungal spores can cause allergic reactions and respiratory problems in the process workers. Prevention of release requires enclosed systems and filters on outlet air streams. Note that there is also potential for release of spores when the bioreactor is unloaded at the end of the fermentation.

5.1.3 *Protecting the Process Organism Against Contamination*

The importance of preventing the entry of contaminating organisms depends on the particular SSF system. If the process organism grows quickly, and if the low water content, or some other condition, such as a low pH, select against contaminants, then prevention of contamination may not be crucial. However, for slow growing organisms this will be quite important. As with liquid culture, entry of contaminants can be prevented by careful design of seals and filtration of the inlet air stream. However, such design features increase cost and can potentially negate one of the advantages usually quoted for SSF, namely that SSF

processes are cheaper and can be operated by people with low levels of technical skills. For such processes the extra cost of these anti-contamination measures must be covered by the value of the product.

5.1.4 *Controlling Environmental Conditions to Optimize Growth and Product Formation*

Important environmental conditions include pH, water activity, supply of oxygen, and temperature. Maintaining optimum temperatures and water levels is usually the main challenge in bioreactor design and operation. Aeration can be achieved by blowing air forcefully through the substrate, or passing air around a static or mixed bed. This air plays a key role in heat removal through convection and evaporation. Heat removal can also be promoted by having closely spaced cooling surfaces. Water transfer, air supply, and heat removal are tied together: aeration rates are typically determined by heat removal needs rather than oxygen supply needs, and the evaporation of water from the substrate bed into the process air can dry the bed to undesirably low levels if water is not replenished during the fermentation.

Although there is nothing that can be done in bioreactor operation to prevent intraparticle gradients from occurring, it is possible to prevent the interparticle transport phenomena from becoming limiting. Mixing and high aeration rates are the best strategies to achieve this. However, mixing is not always appropriate, and forced aeration in the absence of mixing leads to its own problems with temperature gradients in the bed. Evaporative heat removal can be promoted by aeration with dry air, but this tends to dry out the substrate in a system which already has a low water availability, and introduces problems of replenishing water evenly across the bed.

5.1.5 *Maintenance of Homogeneity Within the Substrate Bed*

This issue is linked to the previous issue. It is desirable for optimal conditions to be maintained over the whole bioreactor volume, since this will lead to optimal process productivity. The easiest way to achieve homogeneity is by mixing, which can be either intermittent or continuous. However, if the organism cannot tolerate mixing, meaning that the bed must remain static, then homogeneity is impossible to achieve. Thermal gradients across a bioreactor are more important than gas concentration gradients. Growth and product formation are quickly affected by deviations from the optimal temperature, whereas quite large changes in the oxygen and carbon dioxide levels can often occur with relatively little effect on process performance.

5.1.6 *Facilitating Other Aspects of Processing*

SSF processes involve not only the fermentation itself but also substrate preparation, inoculum preparation, loading and unloading of the bioreactor, and

product recovery. The bioreactor might be used for sterilization of the substrate. In-situ sterilization can reduce the risks of contamination during loading of the bioreactor, although the bioreactor then needs to be designed to enable this.

The issues of substrate loading and unloading have not received much attention in the SSF bioreactor literature. On the large scale, loading is probably best achieved by conveyor belts or screw augers. Unloading might be facilitated if the bioreactor can be opened, allowing the substrate bed to drop onto a conveyor belt or similar device. Pneumatic conveying may also be appropriate.

In some cases it might be desirable to use the bioreactor for processing of the final product. For example, for a product which simply needs to be dried, it is only necessary to blow warm dry air through the reactor. Alternatively, for a product which needs to be leached out of the solid, the leaching fluid can be sprayed onto the top of the substrate bed and withdrawn from the bottom.

5.1.7
Mode of Bioreactor Operation

Batch, fed-batch, repeated fed-batch, and continuous modes of bioreactor operation have been used in SSF processes, although batch processes are by far the most common. Fed-batch or continuous operations that involve the addition of fresh, uninoculated substrate particles require interparticle colonization to occur, which is a relatively slow process, and will lead to bioreactor dynamics very different from those obtained during similar processes in SLF. Despite this, laboratory studies have demonstrated potential advantages of such operation. Abdullah et al. [68] compared batch, fed-batch, and repeated fed-batch culture of *Chaetomium cellulolyticum* on wheat straw. Under optimal conditions in batch culture, protein production ceased after three days, with a maximum protein level of 12 g per gram of solids. In fed-batch culture fresh straw was added at three-day intervals. Protein productivity was maintained for 12 days at a slowly declining rate. In the repeated fed-batch culture half of the fermenting straw was removed and replaced with fresh straw at three-day intervals. Protein productivity was maintained for 12 days at a steady rate and the protein level reached a maximum level of 14 g per gram of solids.

Continuous SSF processes are usually operated in plug flow mode. Such processes will require pasteurization or sterilization of the substrate as it enters the bioreactor, mixing with an inoculum, and at the outlet end of the bioreactor, continuous removal of spent substrate. Such a process was operated on a pilot scale for the production of ethanol from fodder beets by *Saccharomyces cerevisiae* [81, 82]. The bioreactor had a screw within a 4.7 m long and 15.25 cm diameter tube. The screw was rotated intermittently to mix the substrate and move it along the tube. At the front end was a hammer-mill and a pasteurization chamber for substrate preparation and a port for inoculation. New substrate was added, inoculated, and the screw rotated at 12-h intervals, resulting in a residence time of 72 h.

Successful implementation of such fed-batch or continuous techniques on commercial scales will require development of effective technologies for solids

handling, automated or semi-automated measurement, control of environmental parameters, and prevention of contamination. Continuous supply of inoculum in an identical state would be a challenge in such a process: A non-dormant inoculum would change over time, while a dormant form of inoculum such as fungal spores would introduce a lag due to the time required for germination.

Fed-batch operations can also be operated where soluble nutrients are added to the bed. They can be sprayed onto the bed as a fine mist [89, 90, 129], or simply mixed in with the substrate, such as has been done with soluble starch during a fed-batch culture of *Gibberella fujikuroi* on wheat bran [130]. This technique of fed-batch operation is appropriate for soluble nutrients which cause substrate inhibition if added in sufficient amounts for the whole fermentation at the start of the fermentation.

Fed-batch and continuous modes of operation require agitation, either to mix in fresh substrates or nutrients, or to move the substrate bed along the bioreactor from inlet to outlet. Therefore these modes of bioreactor operation can only be used if the process microorganism tolerates mixing.

5.1.8
Key Considerations in Choosing a Bioreactor for a Particular Process

Depending on the particular substrate and organism used in the process, different considerations may become of overriding importance. For example, for a fast-growing organism the overriding problem is to remove sufficient heat from the bioreactor, whereas for a slow-growing organism the most important consideration is to protect the process against contaminants. For the slow-growing organism aseptic procedure is absolutely essential, whereas for the fast-growing organism, fermentations may not actually be carried out aseptically. The provision of high densities of an active inoculum leads to rapid growth which means that the process organism will compete well against any entering contaminants. For the fast-growing organism aeration plays a key role in achieving the desired heat removal.

The sensitivities of the microorganism and the substrate particles to shear forces generated by mixing are also crucial. Nothing quantitative is known about the magnitudes of the shear forces in mixed beds and their effects on the microorganism, although Stuart et al. [110] noted a steady decrease in the final protein content of the fermented substrate in a rotating drum bioreactor when the rotation speed was increased from 10 rpm to 50 rpm. Since the maximum substrate temperature was similar for all rotational speeds, it is likely that this decrease was related to shear forces. This is potentially quite an important issue for the growth of fungi, which are commonly used in SSF processes. In a mixed bed particles will rub against one another, which might damage hyphae. Intermittent mixing with long intervening periods of static operation will cause disruption of those hyphae which extend between particles during the static periods.

Growth rates and sensitivity to mixing can readily be determined in laboratory scale studies, and this information can be used to guide bioreactor selec-

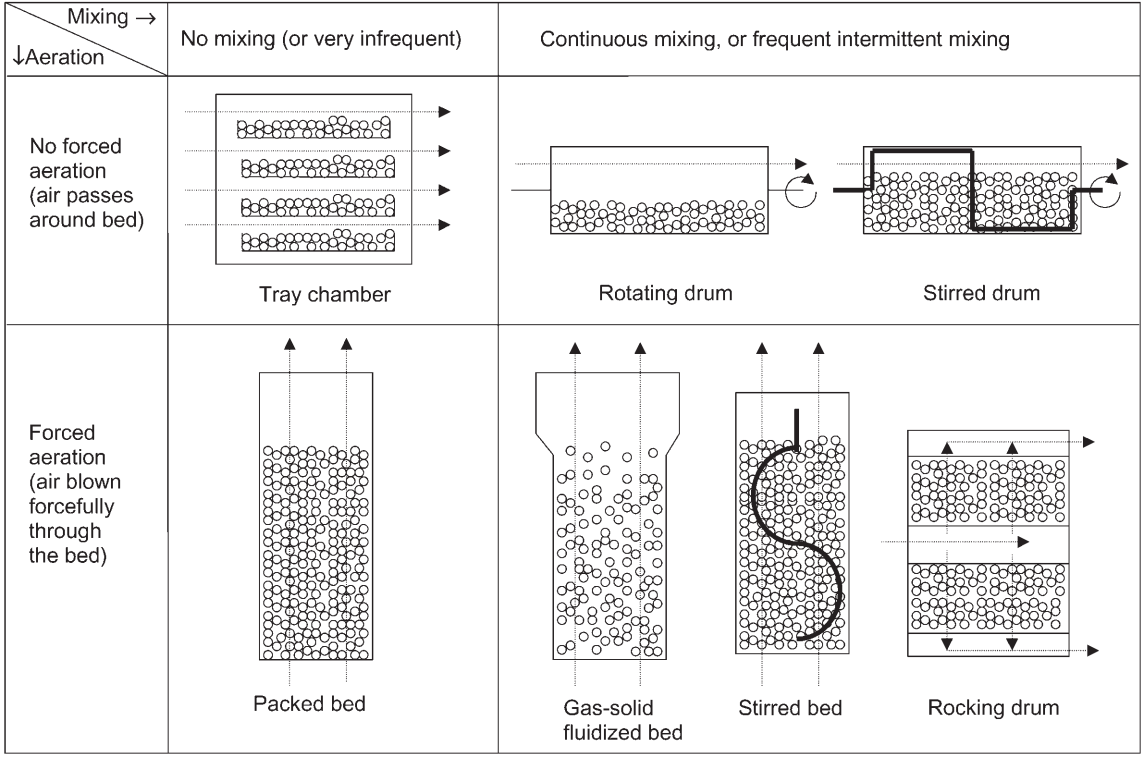

Fig. 5. The various bioreactors used in aerobic solid-state fermentations, categorized according to their aeration and mixing characteristics. Note that the drum bioreactors are all cylindrical drums lying horizontally. The bed bioreactors are typically upright cylinders, although they may have other shapes. The air flow in the system is indicated by the *dotted lines*

Table 3. Guide to the major considerations in the selection of an appropriate SSF bioreactor based on the characteristics of the process organism

	Fast growing organism (process of 1–5 days) – Prevention of entry of contaminants is less crucial – Continuous systems can be considered	**Slow growing organism (process of 1–4 weeks)** – Prevention of entry of contaminants is crucial – Continuous systems probably not suitable
Organism cannot tolerate mixing – Bed must be static, or mixed only infrequently – In static beds temperature and gas gradients are unavoidable	– Bioreactor choice essentially limited to **packed beds** – The **Zymotis** design (a packed bed with closely spaced internal heat transfer plates) is probably best [131]	– **Tray** fermentations may be appropriate, but even with a slow grower bed thickness will be limited to the order of 5–10 cm
Organism can tolerate mixing – Agitation helps in heat removal, prevents high pressure drops, allows even replenishment of water and provides homogeneity	– Available designs are **rotating drum, stirred drum, stirred bed, gas-solid fluidized bed and rocking drum** [107] – The stirred bed bioreactor of INRA [2] has already been proven at 25 tonne scale – **Rotating drums** might be required if the mixing must be gentle	– **Stirred bed** bioreactors designed for aseptic operation have already been proven at scales up to 200 kg – **Rotating or stirred drums** can probably be used even though aeration and heat removal may be poorer than other stirred designs

tion. It is therefore useful to divide the bioreactor types which have been used in SSF into four general categories, based on the mixing and aeration provided (Table 3 and Fig. 5) [2, 107, 131]. With respect to mixing, two strategies are available – the substrate bed may either be left static or mixed only infrequently, or alternatively might be mixed continuously or frequently. With respect to aeration two strategies are also available – the air can either be circulated around the substrate bed or blown forcefully through it.

5.2 Unmixed Beds and the Absence of Forced Aeration – Trays

A tray bioreactor consists of a chamber, which may be as small as an incubator or as large as a room, within which a number of trays are located. The environment is usually controlled by controlling the temperature and humidity of the air blown through the chamber. Individual trays may be constructed of plastic, wood, bamboo, or metal. Plastic bags have also been used. The bed in a tray may be left static or may be turned by hand once per day.

Tray processes have a long history in the production of traditional fermented foods such as soy sauce, koji, and tempe, and more recently have been used for commercial production of enzymes, but these processes are small- to medium-rather than large-scale [132, 133]. Due to the difficulty of automating the handling of trays, handling is usually done by hand, leading to relatively high labor costs. Therefore tray processes are only economical where labor costs are low.

The heat and mass transfer processes which occur in trays are shown in Fig. 6. Essentially, heat transfer within the tray is limited to conduction and

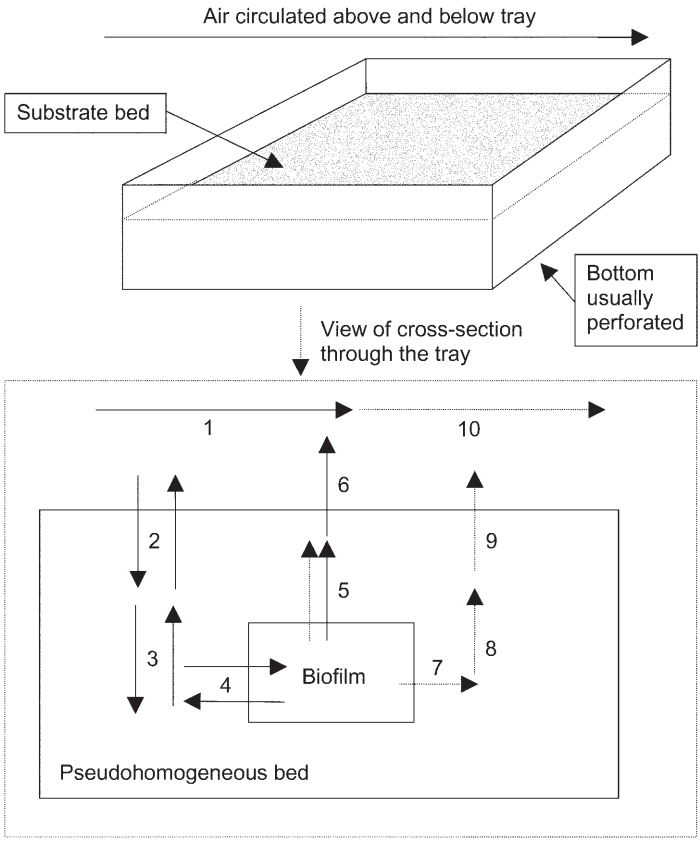

Fig. 6. The basic features of an individual tray, and some of the macroscale processes that have been included in various models of tray bioreactors, shown for a tray with an unperforated bottom. (*1*) Bulk flow of air around tray, maintaining O_2 and CO_2 concentrations in the headspace of the tray chamber; (*2*) Exchange of O_2 and CO_2 between headspace gases and interparticle spaces of trays; (*3*) Diffusion of O_2 and CO_2 within the interparticle spaces; (*4*) Transfer of O_2 and CO_2 between the interparticle spaces and the biofilm; (*5*) Generation of metabolic water, evaporation into the interparticle spaces, removing energy through the heat of vaporization, and diffusion within the interparticle spaces; (*6*) Transfer of water vapor from the interparticle spaces to the headspace; (*7*) Generation of waste metabolic heat; (*8*) Conduction through the bed; (*9*) Convective heat removal at the tray surface; (*10*) Bulk flow of air, carrying energy through the headspace of the tray chamber

mass transfer to diffusion. There is exchange at the tray surface between the bed and the headspace air. Within tray bioreactors several of factors appear to be potentially able to limit bioreactor performance – heat transfer, oxygen transfer, and water transfer.

Heat transfer has been identified as the major problem in tray bioreactors, by both experimental and modeling studies. Temperatures of the order of 20 °C above the external incubation temperature have been noted for bed depths as little as 8 cm [134]. This occurs because heat removal is essentially limited to conduction through the bed. Note that natural convection within the bed might also occur in response to the temperature profiles, and may affect not only heat transfer but also CO_2, oxygen, and water vapor transfer [100], but natural convection has received no experimental or modeling attention. These high temperatures cause corresponding low product yields. For example, Ghildyal et al. [134] noted yields only 20 % of those obtained in a bed with a 40-mm initial bed depth when a bed depth of 80 mm or more was used.

The modeling study of Rajagopalan and Modak [87] confirms that bed depths must be limited to the order of only a few centimeters, at least with relatively fast growing organisms. The most easily manipulated design and operating variables are the bed depth and the temperature of the surrounding air. Note that decreasing the humidity of the surrounding air to promote evaporation is not a feasible strategy because it will quickly lead to drying of the exposed surfaces of the bed, and it is likely that these regions will dry to such low values that growth and product formation will be limited. Best growth of *Aspergillus niger*, which has an optimum temperature of 35 °C, was predicted with relatively high surrounding air temperatures and relatively thin substrate slabs. For example, temperatures of 35 – 40 °C and bed heights of 0.8 – 1.6 cm gave maximal biomass yields at 100 h. At a bed height of 3.2 cm optimal growth occurred with surrounding air temperatures of 30 – 35 °C. With a bed height of 6.4 cm the yield at 100 h was at best 55 % of the maximum possible yield and the optimum surrounding air temperature was 30 °C. At lower temperatures some bed regions overcooled. At higher external temperatures too much of the bed overheated. The model suggested that temperature gradients are more important than oxygen gradients within trays, although oxygen limitations were predicted at the bottom of an unperforated tray.

Szewczyk [135] modeled the effect of convective and evaporative heat removal at the bed surface on tray performance. The mass transfer coefficient for evaporation was assumed to be related to the surface-to-surroundings convective heat transfer coefficient by the psychrometric ratio. The values of these coefficients can potentially be increased by increasing the flowrate of air past the tray surfaces, although the relationship was not explored. As the value of the convective heat transfer coefficient increases, the predicted surface temperature initially falls sharply – from values as high as 45 – 60 °C with a coefficient of 2 W m^{-2} K^{-1} to values around 35 °C with a coefficient of 10 W m^{-2} K^{-1}. Further increases up to 50 W m^{-2} K^{-1} are relatively ineffective in reducing the surface temperature further [135].

The importance of oxygen diffusion as a limiting factor depends on the values of the thermal conductivity of the bed and the effective oxygen dif-

fusivity within the bed. In modeling work, Smits et al. [100] showed that, for a bed depth of 10 cm from the surface, oxygen became limiting during the fermentation (i. e., reached zero concentration) at values of the thermal conductivity between 0.15 W m^{-1} K^{-1} and 0.6 W m^{-1} K^{-1} if the value of the effective diffusivity of oxygen was one-twentieth or less of the effective diffusion coefficient of oxygen in air. Such thermal conductivities can be expected in substrate beds and diffusivities this low can also be expected when high biomass densities are obtained [136, 137]. Thermal conductivities can potentially be much higher, of the order of 2.5 W m^{-1} K^{-1} [136]. As thermal conductivity increases, oxygen limitation problems increase because the better heat removal allows faster growth and therefore higher oxygen consumption rates [100].

Smits et al. [100] modeled the production, evaporation, and diffusion of water within the bed. Their model predicted that the water content inside the bed remained above the initial water content due to the production of water by metabolism, and the assumption that the surrounding environment was kept saturated in order to prevent drying of the substrate. Under these conditions water considerations were not important in controlling tray performance.

In conclusion regarding tray bioreactors, their future appears limited. Although oxygen limitation can be a problem depending on the time, location, and bed properties, it is the overheating problem which puts the main limitation on packed beds. There is little to be done to affect bioreactor operation except to remain with low bed heights. This means that processes can only be scaled up by increasing the number of trays, leading to the requirement for large surface areas. They will continue to be used where circumstances allow – on a small- to medium scale, and where labor costs are low.

5.3 Unmixed Beds with Forced Aeration Through the Bed – Packed Beds

Packed beds are the second type of bioreactor which is suitable for those situations in which the substrate bed must remain static during the process (Table 3). They consist of a column, which is commonly of rectangular or cylindrical cross-section, and usually have the air inlet and outlet at opposite ends, such that the air moves axially from one end to the other through the bed. The most commonly used packed beds have the substrate placed on a base plate and air blown upwards through the bed (Fig. 7). They may be water jacketed or not, or they may have internal heat transfer plates, such as in the Zymotis design [131].

Due to the forced aeration, oxygen supply in packed bed bioreactors is usually not a problem, even if quite low aeration rates are used [138]. In contrast, temperature control can be difficult, especially in packed beds above 15 cm diameter and lacking internal heat transfer plates. In such bioreactors, the main heat transfer mechanisms are axial convection and evaporation, and radial temperature gradients are negligible except close to the bioreactor wall. The dynamics of convective cooling mean that axial temperature gradients are established and temperatures over 20 °C higher than the inlet air temperature

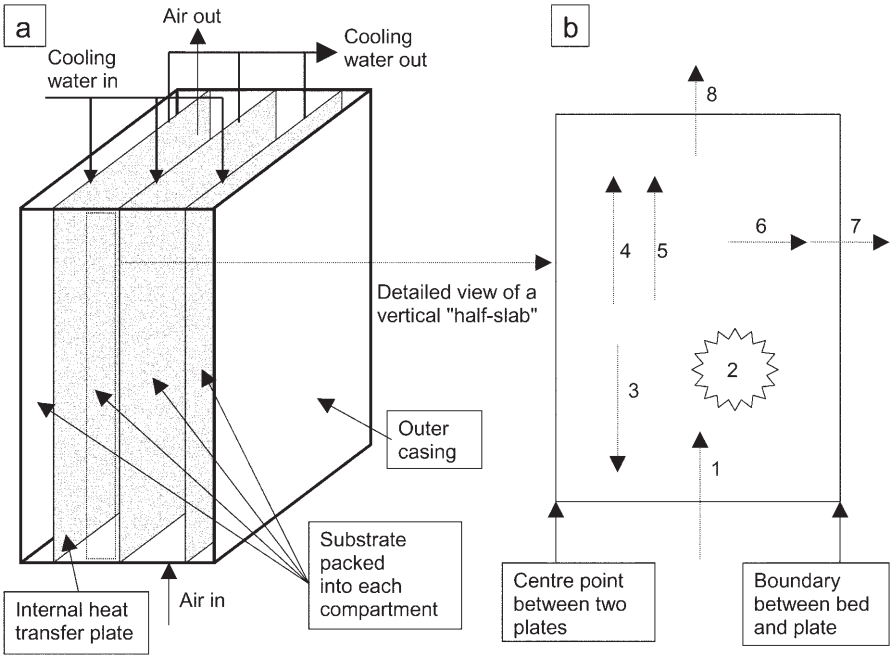

Fig. 7. **a** The main features of the Zymotis packed bed [131]. **b** A detailed view of the heat transfer processes that have been modeled in packed beds. Assuming that the outer case is insulated, there are no gradients from front to back, and therefore a plane, normal to the heat transfer plate, extending from the center point between two heat transfer plates to the bed-plate boundary, represents a repeating unit within the bioreactor. Note that b can also represent a cylindrical packed bed lacking internal heat transfer plates, with the rectangle representing a radial plane, with the left hand side corresponding to the central axis, and the right hand side to the bioreactor wall. The heat transfer processes in b are (*1*) Entry of sensible energy in the inlet air; (*2*) Release of waste metabolic heat by the microorganism; (*3*) Axial conduction, which works in the opposite direction to axial convection; (*4*) Axial convection; (*5*) Heat of vaporization of water as water evaporates to maintain the air saturated; (*6*) Radial conduction; (*7*) Conduction across the bioreactor wall and convection by the surrounding air or cooling water; (*8*) Exit of sensible energy in the outlet air

have been found experimentally [139]. This axial temperature gradient means that the water carrying capacity of the air increases as it travels up the bed. Therefore, even though saturated air is typically used to aerate packed bed bioreactors, it is impossible to prevent evaporation from occurring in this design [140]. Despite the fact that this evaporation contributes significantly to heat removal, being responsible for 65–78% of overall heat removal, it is undesirable due to the difficulty of replenishing water evenly within a packed bed [140, 141]. In contrast, in packed beds below 15 cm diameter and in the Zymotis bioreactor there is the extra heat removal mechanism of conduction normal to the direction of the air flow. As described below, this reduces axial temperature gradients and therefore reduces the amount of evaporation which occurs.

Heat transfer in packed-bed bioreactors has received a significant amount of modeling attention. In wide packed beds lacking internal heat transfer plates the design and operational variables available are the bioreactor height, and the aeration rate and the temperature of the inlet air [97]. Using unsaturated air to promote evaporation is not an option because the bed will dry out quickly. Of the operating variables, increasing the superficial velocity is the most effective in reducing axial temperature gradients [97]. Using low inlet air temperatures is not practical since, in order to achieve reasonable control of the temperature at the air outlet end, the air inlet temperature must be of the order of 10–15 °C below the optimum temperature for growth, and such low air temperatures cool the inlet region of the bed to temperatures which restrict growth [97]. Regarding bioreactor height, if it is possible to identify a temperature that should not be exceeded at any point in the bed during the fermentation, then, due to the steady rise in temperature with bed height, the bed can be no higher than the height at which this critical temperature is reached at the time of peak heat production [142]. This height can be denoted the critical height. It depends on the growth kinetics and the operating conditions used. For growth rates and operating conditions which have been reported in the literature, this height ranges from as low as 0.1 m to as high as 2.5 m [142].

The heat transfer dynamics are quite different in the case where a thin packed bed is used. The contribution to overall heat removal by radial heat conduction to the walls and convective removal by cooling water can be significant. This was observed experimentally by Saucedo-Castaneda et al. [96], who used a water-jacketed column of 6 cm internal diameter. There was a significant axial temperature gradient in the first 5 cm at the air inlet end of their 35 cm high column. Above this, the axial gradient was negligible but there was a significant radial gradient. An explanation for this behavior was provided by the modeling work of Mitchell and von Meien [143]. In the lower regions of the column the temperature is kept low enough by the incoming air that the organism grows rapidly. It grows so rapidly that the heat transfer to the cooling water cannot remove all the heat and therefore the air temperature rises as it moves up through the column. The less effective cooling by the warmer air means that there is an increase in bed temperature with height. As the bed temperature rises above the optimum, the growth rate slows. Once the growth rate slows to a value which gives a rate of heat production equal to the rate of heat removal to the cooling water, then there is no further increase in bed temperature with height. In those regions where the axial temperature gradient is negligible the evaporation will be negligible, so this design also reduces the importance of the water balance.

A Zymotis-type bioreactor with closely spaced internal heat transfer plates will perform similarly to the thin column of Saucedo-Castaneda et al. [96], in that, after a short distance near the air inlet in which there is a significant axial temperature gradient, there will be a negligible axial gradient with height [143]. This suggests that a Zymotis-type bioreactor can be of infinite height. However, as pointed out below, pressure drop considerations may limit the height of Zymotis-type bioreactors.

Thin packed bed columns of less than 10 cm are obviously impractical for large-scale applications because of the small capacity of individual columns,

even if they have heights of several meters. In contrast, the Zymotis bioreactor allows for large substrate loadings [131]. Theoretical modeling work done for the Zymotis bioreactor suggests that the best operational strategy is to have a control system for the cooling water, which reduces the temperature of the cooling water in response to the temperature measured at the air outlet end at the mid point between the heat transfer plates, which is where the maximum temperature is expected. Using such a strategy and using a low spacing between plates of 5 cm means that near optimal performance can be obtained [143].

Water balances have been noted as a potential problem in packed bed bioreactors [144], but they have received little attention. Most modeling work has ignored them, and experimental work has not been done to test how water contents vary with height. One strategy to minimize the importance of the water balance is to use a substrate in which large decreases in water content can occur before the water activity falls to undesirably low values [37]. Selection of such a substrate requires knowledge of sorption isotherms of the substrate and the influence of water activity on the growth of the process organism.

The other phenomena which are quite important are related to air flow through the column. Most modeling work has assumed plug flow of the air with a flat velocity profile across the column, but no experimental work has been done to confirm this. Pressure drop through the column is a potentially important phenomenon. At high biomass concentrations the intrinsic permeability of the bed can be less than 5% of the initial intrinsic permeability [108]. Pressure drops as high as 2.75 m of water per meter of bioreactor have been noted, during the growth of *Aspergillus niger* on a substrate consisting of a nutrient and sucrose solution adsorbed onto sugar cane bagasse and with a low aeration rate of only 3.5 vvm (air volumes per bioreactor volume per minute) [145]. Other systems with similar air flow rates (in vvm) have given maximum pressure drops ranging from 0.1 m to 0.7 m of water per meter of bioreactor [108, 145]. With a higher vvm of 11, Gumbira-Sa'id et al. [127] obtained a pressure drop of 1.45 m water per meter of bioreactor. Note that many of these studies have been done with relatively small laboratory reactors, where there might be significant effects of the walls and the bioreactor ends.

Pressure drops of 1 m of water per meter of bioreactor or higher could quickly put a limit on bioreactor height. These pressure drops need to be carefully considered in the design of the aeration equipment for packed bed bioreactors. If pressure drop is a problem and infrequent mixing can be tolerated, then this mixing can be used to limit the pressure drop [127].

A consequence of the decrease in particle size noted in Sect. 4.5 is that the substrate bed within a packed bed can shrink and may pull away from the bioreactor walls [127]. This is undesirable since air passes preferentially between the bed and the wall, rather than through the bed itself. Such shrinkage and its consequences can be avoided by using inert materials on which substrates are absorbed or by using a natural substrate in which the solid structure is provided by a polymer which is not attacked by the microorganism [37].

In conclusion regarding packed-bed bioreactors, the Zymotis design of Roussos et al. [131] is the most appropriate bioreactor for those processes in which the substrate bed must remain static throughout the fermentation, since

they allow better control over the conditions within the bed than can be achieved in tray bioreactors. However, the small spacing of only 5 cm between heat transfer plates which is required for optimal performance means that loading and unloading operations will be more difficult than in the case where there are no internal heat transfer plates. Despite the significant amount of attention that packed-bed bioreactors have already received, more attention is required with respect to pressure drops, the change in bed structure during the fermentation, and flow patterns of air through the bed.

5.4 Mixed Beds Without Forced Aeration – Rotating Drums, Stirred Drums and Screw Bioreactors

These bioreactors are horizontal or inclined cylinders. Their main feature is that air is not forcefully blown through the bed itself. Rather it is blown through the headspace above the bed, and gas exchange between the headspace and bed is promoted by the mixing of the bed (see Fig. 5). In rotating drum bioreactors, mixing within the substrate bed is caused by rotation of the bed, and may be promoted by the use of internal lifters. In stirred drum bioreactors, the drum itself remains static and the mixing action is caused by paddles or scrapers mounted on a shaft running through the central axis of the drum. Screw bioreactors have been used for continuous ethanol production in SSF, in which there is no need to blow air through the bioreactor. In this bioreactor a screw with a diameter equal to the internal diameter of the drum is operated intermittently to push the substrate from one end to the other. However, after some interest in the 1980s, the screw bioreactor has not received further attention [81, 82]. Only rotating drums have received modeling attention and the discussion below is limited to this design.

Heat removal from the substrate bed in rotating drums occurs by two main routes – transfer directly to the headspace air by convection and evaporation and transfer through the bioreactor wall by conduction followed by convective cooling of the bioreactor wall (Fig. 8) [146]. The mixing in rotating drum bioreactors allows the use of dry air to promote evaporation, because water can be replenished by spraying a fine mist of water onto the bed as it is being mixed [147]. Note that convective cooling of the drum wall occurs to both the surrounding air and the headspace air [146]. Although transfer to the headspace air is a minor contributor to overall heat removal, the resulting increase in headspace air temperature does increase the driving force for evaporation from the bed to the headspace. Unfortunately no work has been done to obtain experimental values for the various heat and mass transfer coefficients which are important in rotating drum bioreactors.

Transfer between the bed and headspace will be affected significantly by the mixing patterns of substrate particles within the bed and of air within the headspace. Note that transverse mixing considerations affect the substrate loadings that can be used in rotating drum bioreactors. In non-SSF applications optimal fill fractions, which maximize the amount of material within the drum but still allow good mixing, range from 17% to 22% of the drum volume [148]. In SSF

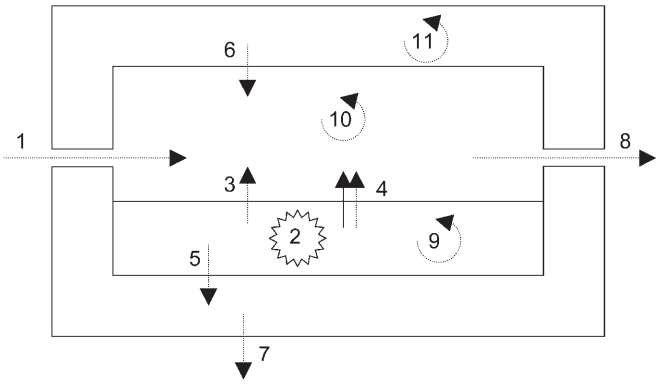

Fig. 8. Heat and mass transfer processes in a rotating drum bioreactor [146]. (*1*) Entry of sensible energy in inlet air; (*2*) Release of waste metabolic heat by the microorganism; (*3*) Convective heat transfer from the substrate bed to the headspace; (*4*) Evaporation of water from the bed to the headspace, carrying with it the heat of vaporization; (*5*) Conduction from the bed to the drum wall; (*6*) Convective cooling of the drum wall by the headspace gases; (*7*) Convection to the surrounding air; (*8*) Exit of sensible energy in the outlet air; (*9*) The substrate bed is assumed to be well mixed; (*10*) The headspace gases are assumed to be well mixed; (*11*) The high thermal conductivity of the drum wall is assumed to lead to thermal homogeneity

applications rotating drum bioreactors are typically operated with fractional fillings around 30 %. However, mixing patterns within the bed have not received any attention except to correlate transverse mixing regimes for drums without lifters with those observed in non-SSF applications of rotating drums. A critical speed can be identified for these rotating drums, which is the speed at which the solids are centrifuged against the drum wall. For horizontal drums the critical speed in rpm (N_C) is equal to $42.3D^{0.5}$, where D is the drum diameter in meters. For drum speeds up to about $0.1N_C$ there is little movement within the bed itself. Rather the bed as a whole tends to be dragged upwards by the drum rotation and then to slump back to the bottom. In this slumping regime the bed will perform similarly to a tray. Between $0.1N_C$ and $0.6N_C$ particles tumble down the face of the bed. Above $0.6N_C$ particles are thrown into the air. In practice, rotating drum bioreactors have only rarely been operated in the tumbling regime; rather they tend to be operated at speeds of a few rpm or even less. At these speeds transfer between the bed and headspace is greatly improved by the inclusion of lifters [149, 150].

Flow patterns within the headspace have been investigated by studying the residence time distributions of oxygen as a tracer gas [151]. In an unbaffled drum operated at various fractional fillings and air flow rates, the flow patterns were best described by either a plug flow with axial dispersion model or a model of several continuous stirred tanks in series. However, these flow patterns cannot simply be assumed to occur in other rotating drum bioreactors. Gas flow patterns will be greatly affected not only by the design of the rotating drum bioreactor itself, such as length to diameter ratio and

the presence or absence of baffles, but also by the design of the air inlet and outlet.

Discontinuous agitation of rotating drum bioreactors has been used in a few studies [152, 153]. In the work of de Reu et al. [152], when the temperature within the bed exceeded a setpoint, a one-minute agitation regime was initiated, with rotation alternately clockwise and counterclockwise at 4–6 rpm. In different fermentations adequate temperature control was achieved with mixing events being initiated at intervals from as short as 9 min to as long as 142 min.

The only modeling work available for the rotating drum bioreactor is the heat transfer model of Stuart [146]. The model treated the substrate bed, the headspace gases, and the bioreactor wall as separate phases, and assumed that each of these phases was thermally homogeneous, which is equivalent to assuming that the substrate bed and headspace gases are well-mixed and that the thermal conductivity of the bioreactor wall is high. Note that models of SSF bioreactors have to date rarely taken the bioreactor wall into account. It was only by doing so that Stuart [146] noted that the drum wall will be hotter than the headspace gases and therefore gives an indirect route for transfer of heat between the substrate bed and the headspace. The model predicts that for small scale bioreactors a significant proportion of the heat removal from the bed occurs by conduction from the bed to the bioreactor wall followed by convection to the surrounding air.

In conclusion regarding rotating drum bioreactors, although they have the potential to provide relatively gentle mixing, with less compaction and crushing of substrate particles than is likely to occur with agitators embedded within the substrate bed, their true potential is largely unexplored due to the lack of quantitative characterization of the mixing and heat and mass transfer phenomena occurring within them.

5.5
Mixed Beds with Forced Aeration – Gas-Solid Fluidized Beds, Stirred Drums, and the Rocking Drum

This group of bioreactors includes those in which air is blown forcefully through the bed and in which the bed is agitated either intermittently or continuously. The combination of mixing and forced aeration can help in avoiding the temperature and moisture gradients which occur in other bioreactor types. Note that this greatly simplifies modeling work because the bioreactor can be treated as a well-mixed system, eliminating the spatial variable (Fig. 9). There are several designs in which mixing with forced aeration can be achieved – stirred aerated beds, rocking drums, and gas-solid fluidized beds.

5.5.1
Gas Solid-Fluidized Beds

This bioreactor consists of a vertical chamber, with a perforated base plate through which air or some other gas is blown upwards at a sufficient velocity to fluidize the substrate particles (see Fig. 5). Note that not all solid substrates will

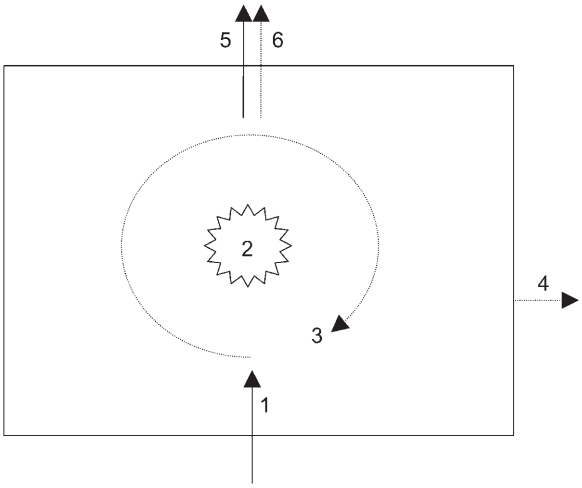

Fig. 9. Schematic diagram showing how heat transfer is typically modeled in a bioreactor with mixing and forced aeration. (*1*) Entry of sensible energy with the inlet air; (*2*) Generation of waste heat by the microorganism; (*3*) Mixing, which maintains equilibrium between the substrate bed and the headspace, and within each of these subsystems; (*4*) Convective heat transfer from the bioreactor wall to the surroundings; (*5*) Exit of sensible energy in the outlet air; (*6*) Exit of the heat of vaporization of water in the outlet air, which is assumed to be saturated

fluidize easily and therefore this bioreactor can only be used in those cases where the substrate has good fluidization behavior. There may be a mixer at the bottom to break up any substrate aggregates which form. Provision must be made for bed expansion upon fluidization and for the disengagement of particles from the gas stream. The disengagement space typically has a larger diameter than the lower region of the bed. A water sprayer can be incorporated, activated by the measurement of electric capacitance by a probe inserted at the bottom of the fluidized bed [154].

Reasonably large fluidized bed bioreactors have been built. Matsuno et al. [154] describe how a 16-l bioreactor was used for the production of proteases and amylases by *Aspergillus sojae* on wheat bran powder. The reactor had a height of 2 m, with a diameter of 20 cm in the lower region and 28 cm in the disengagement region. Higher productivities of these enzymes were obtained than for tray SSFs or submerged liquid fermentation. On the basis of these results, Kikkoman Corporation constructed an air solid-fluidized bed of 8000 l working volume in 1975 [154]. Bed diameter was 1.5 m in the lower region and 2 m in the upper disengagement region, with a bed height of 8 m. This bioreactor was used with 833 kg of wheat bran at 40% moisture content. Productivity was claimed to be the same as that obtained on a small scale. Unfortunately, little data is available regarding its performance.

More recently a pilot scale gas-solid fluidized bed, with a diameter of 55 cm, has been used for ethanol production. In this bioreactor a glucose solution is sprayed onto a fluidized bed of compressed pellets of *Saccharomyces cerevisiae*

[90]. This bioreactor has a capacity for approximately 20 kg of yeast biomass. This system can potentially relieve product inhibition problems since the ethanol is continuously stripped by the circulating gas.

The high gas flow rates required for fluidization means that temperature control of the bed is not difficult. High convective cooling rates occur, and if evaporation is required to boost cooling rates, the evaporated water can be replaced by spraying water onto the bed. As a result, models of gas-solid fluidized beds have ignored the energy balance [89, 90]. Rather, they have concentrated on the intraparticle diffusion phenomena, as mentioned in Sect. 4.1.1.

5.5.2 *Stirred Aerated Beds*

Stirred aerated beds typically have an appearance similar to packed beds, with air passing upwards through a perforated plate or screen which supports the substrate bed. The difference is that an agitator is embedded within the substrate bed (see Figs 1 and 5). This agitator can be operated either continuously or intermittently. Agitator design and operation becomes an important consideration in agitated beds. These bioreactors may sometimes be referred to as horizontal stirred beds or vertical stirred beds depending on whether the breadth or height dimension is larger.

Stirred beds have been used successfully on a large scale. A 50-l bioreactor with a planetary mixing device and a 50 kg capacity bioreactor in which the bed is held within a cylindrical basket which is rotated past stationary agitator blades have been designed for aseptic operation, making them suitable for processes involving slow growing organisms such as *Gibberella fujikori* [155–157]. Much larger bioreactors have been developed for non-aseptic aeration. The 1 tonne-capacity bioreactor of Durand and Chereau [2] consists of a steel box 2 m long, 0.8 m wide, and 2.3 m high (see Fig. 1). A 1 m thick substrate bed sits on a perforated base plate through which pre-humidified air is supplied. Three screw agitators are mounted across the breadth of the reactor on a trolley above the substrate bed, with the screws extending down into the substrate bed. The trolley moves backwards and forwards along the length of the bioreactor, such that each location in the bed is intermittently mixed. This bioreactor has been used successfully for protein enrichment and for the production of enzymes and biopesticides [158]. A larger version of this bioreactor was built by Xue et al. [159] and used for the production of microbial protein from sugar beet pulp by *Aspergillus tamarii*. The reactor was 17.6 m long, 3.6 m wide, and 2.0 m high. The bioreactor had a capacity of 25 tons of moist substrate. Little information was given on performance, although during the rapid growth phase with inlet air conditions of 88% relative humidity and a temperature of 33 °C, the outlet air was measured as 33 °C and 100% relative humidity, which suggests that adequate temperature control within the bed was achieved.

A variation of the stirred bed design involves a horizontal stirred drum, filled to two-thirds depth with substrate, with introduction of air through a perforated central shaft embedded in the substrate bed and upon which mixer blades are mounted (Fig. 10). This bioreactor has been successfully used for

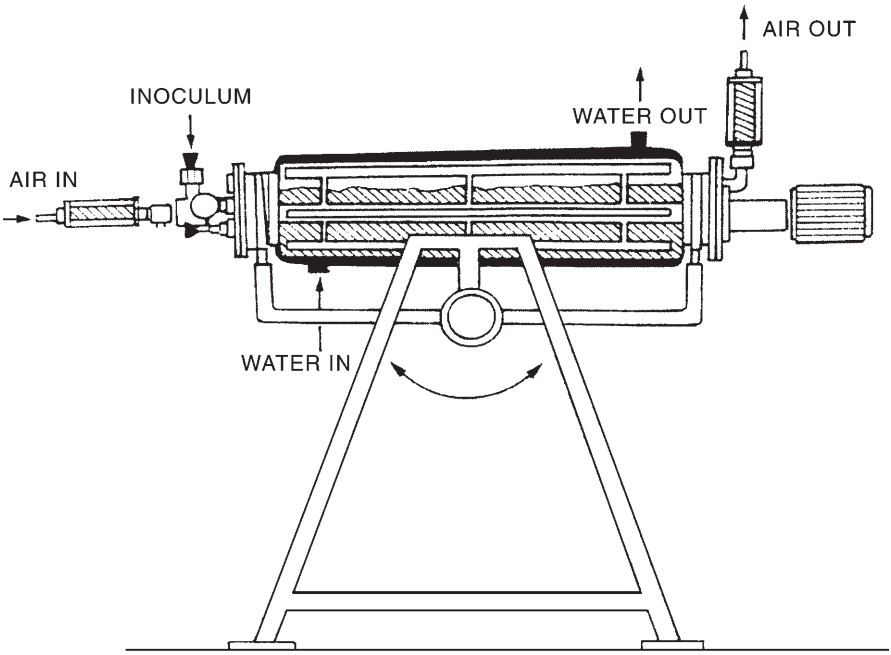

Fig. 10. The aerated-stirred bed bioreactor of Berovic and Ostroversnik [26]. Forced aeration and inoculation is provided through a central perforated hollow shaft. Sterilization and temperature control are enabled with a water jacket using microprocessor control

optimization of inoculation, sterilization, mixing, aeration, and temperature and humidity control during the production of pectinolytic enzymes by *Aspergillus niger* [26].

If stirred aerated beds are intermittently stirred then during the static periods they will behave like packed beds. Relatively little attention has been given to the mixing phenomena, with only one experimental study, done in a 28-l bioreactor constructed from a commercial solids mixer. The mixer consisted of a lengthwise Z-blade lying within a horizontal trough with a U cross section and was modified for use as a bioreactor by the drilling of four aeration holes along the bottom of the trough, through which air could be blown [160]. Mixing studies, done by observing the distribution of dye within the bioreactor during mixing, showed that mixing quality was directly proportional to the number of revolutions rather than being a function of the mixing speed itself.

Ashley et al. [161] modified a model for heat transfer in a packed bed to describe the performance of an intermittently stirred bed by assuming an instantaneous redistribution of biomass and energy within the bed at regular intervals. The model was used to explore whether mixing could decrease the maximum temperature achieved within the bed in comparison with static packed bed operation, in which the maximum temperature occurs at the outlet air end of the bed at the time of peak heat production. Interestingly, using

typical growth kinetics and operational conditions, namely a specific growth rate of 0.236 h^{-1} and a superficial velocity of 0.0236 m s^{-1}, they predicted that intervals between mixing of the order of one hour would lead to maximum bed temperatures 2.4 °C higher than those expected for completely static operation. This behavior occurs because, after a mixing event, the inlet air cools the bottom of the column back down to the air inlet temperature, but in doing so loses its capacity to cool the upper regions of the column. After each mixing event a cooling front travels up the bed, taking over 20 min to reach the top of a column only 35 cm high, during which period the waste heat generation at the top of the column has caused a significant increase in temperature [161]. The maximum temperature achieved in the bed could only be decreased relative to that for static operation if there were at least 10 mixing events per hour. At 30 mixing events per hour the predictions were quite similar to those for a continuously mixed bed [161].

5.5.3 *Rocking Drum Bioreactor*

The rocking drum bioreactor consists of three concentric cylinders lying horizontally [107, 162–164] (see Fig. 5). The inner and middle cylinders are perforated, and are contained within the outer unperforated cylinder. The substrate is loosely packed into the space between the inner and middle cylinders. Air and small amounts of water are introduced into the innermost cylinder with the air moving radially outwards through the substrate bed and the water percolating downwards due to gravity. When the air exits through the perforations in the middle cylinder it flows in the space between this cylinder and the outermost cylinder to the air outlet. The outer two cylinders rotate around the stationary inner cylinder, causing a gentle mixing action within the bed. Typical operation involves 3/4 turns backward and forth, hence the name of "rocking drum."

The rocking drum bioreactor has some similarities with a packed bed in that the air flowing radially outwards is like the air flowing axially within a packed bed. An advantage of the rocking drum reactor over the packed bed is that water can be replenished reasonably evenly with a reasonably gentle mixing action [107].

The work done to date with rocking drum bioreactors has addressed the question of automatic control of SSF bioreactors. Barstow et al. [162] used a control scheme where the air flowrate was increased from 6.2 l min^{-1} to 8.5 l min^{-1} whenever the temperature exceeded the set point of 37 °C, and between 9 h and 43 h of fermentation the inlet air was dry. Ryoo et al. [163] pointed out that finer control could be achieved by mixing dry and wet air to achieve the desired relative humidity at a constant overall air flowrate. They managed to maintain the fermentation temperature within 0.5 °C of the set point. However, this work was done in a bioreactor with a holding volume of only 1.3 l, and it is difficult to say how well the bioreactor will operate on a large scale.

The modeling work done for the bioreactor assumes that the bed held between the innermost and middle perforated drums is well mixed, although no

experimental work has been presented to confirm this [107]. In fact, in earlier studies, Barstow et al. [162] reported temperature differences of up to 3 °C across the bioreactor. The model was used to investigate the predicted effects on the performance of the laboratory scale bioreactor of variations in the inlet air flowrate, the overall heat transfer coefficient from the drum to the surrounding air, the inlet air relative humidity, and the inlet air flowrate. This model highlighted the importance of evaporation and the airflow rate in temperature control. In addition, through an analysis of the model, in which both the growth rate and the maximum biomass concentration were functions of moisture content and temperature, Sargantanis et al. [107] determined the optimal temporal profiles of substrate bed temperature and moisture content. Regarding temperature, optimum performance was predicted to be obtained with a temporal bed temperature profile in the shape of a rectangular hyperbola, with the temperature increasing from 33 °C to 38.8 °C during the first 15 h of the fermentation, and then a negligible increase after that. Regarding moisture content, optimum performance was predicted for a steady increase from 56.5 % to 64 % moisture over the first 25 h of the fermentation and then a negligible increase in moisture content after that. Such an analysis could be important in the design of on-line control strategies. However, they only identified the optimum profiles for the bed temperature and moisture content, the values of which depend on the operating conditions. They did not use their model to explore how the operating conditions should be manipulated in order to ensure that these optimum profiles would actually be obtained.

5.5.4
Evaluation of Mixed Aerated Bioreactors

The gas-solid fluidized bed gives the best heat transfer performance of all SSF bioreactors. However, relatively little information is available about design and operation. Any increases in productivity over other bioreactor types must also be weighed against the increased operating costs associated with the relatively high aeration rates needed to achieve fluidization. The stirred-bed design of Durand and Chereau [2] has been successfully demonstrated at a scales of 25 tonnes of moist substrate. It will probably remain the bioreactor of choice for those SSF processes in which mixing can be tolerated. Rocking drum bioreactors, on the other hand, have only been used on the laboratory scale, and there is no information about their performance on the large scale.

6
Approaches to Scale-Up of SSF Bioreactors

There has been a significant advance in our understanding of scale-up of SSF bioreactors since the largely qualitative review on this topic by Lonsane et al. in 1992 [165]. These advances have been achieved by applying mass and energy balances to describe the operation of SSF bioreactors. This work is still in progress. There are not yet any reports describing how such quantitative approaches have been used in the design of a commercial scale SSF bioreactor.

Rather the work has only shown theoretically how these approaches could be used to guide the design and operation of large-scale bioreactors.

The basic approach to using mass and energy balances as a scale-up tool was pointed out by Saucedo-Castaneda et al. [144]: if the dynamic balance equations for water and for energy can be equated to zero, then the water content and the temperature will not change with time. Furthermore if this equality with zero can be maintained as scale increases, then the large-scale bioreactor should operate equally as well as the small scale bioreactor. The challenge is then to find operating conditions for the bioreactor that will allow the water and energy balances to remain equal to zero as scale increases.

Regarding the prevention of undesirably high temperatures within the bioreactor, a relatively simple approach is to concentrate on the time of peak heat generation. This approach was demonstrated by Mitchell et al. [142] for packed bed bioreactors without internal heat transfer plates and Hardin et al. [166] for rotating drum bioreactors. Following the strategy of Saucedo-Castaneda et al. [144], estimates are made of the peak heat generation and heat removal terms. They are equated by taking a ratio of peak heat generation to peak heat removal and equating the ratio to one.

For packed beds without internal heat transfer a modified Damkohler number (Da_M) can be proposed assuming logistic growth kinetics without maintenance metabolism [142]:

$$Da_M = 1 = \frac{0.25\,\rho_s(1-\varepsilon)\,Y\mu_{opt}X_m}{\rho_a(C_{pa}+f\lambda)\,V_Z(T_{out}-T_{in})/H} \tag{20}$$

In the numerator ρ_s is the substrate density (kg m^{-3}), ε is the void fraction within the bed, X_m is the maximum biomass concentration (kg-biomass kg-substrate^{-1}) and Y is the heat yield coefficient (J kg-biomass^{-1}). The factor $0.25\,X_m$ arises from the assumed growth kinetics, for which the maximum heat production rate occurs at $0.5\,X_m$, with a specific growth rate of $0.5\,\mu_{opt}$ [142]. The denominator describes axial convection and evaporation, which are the major contributors to heat removal. If the air is assumed to remain saturated as it moves up the column, then the evaporation of water to maintain this saturation increases the effective heat capacity of the air from C_{pa} (J kg^{-1}°C^{-1}) by an additional factor of $f\lambda$, where λ is the heat of vaporization of water (J kg^{-1}) and f is the slope of a linear approximation to the humidity curve (kg-water kg-air^{-1}°C^{-1}). The bed height is given by H (m), V_Z is the superficial velocity of the air, and T_{IN} and T_{OUT} are the inlet and outlet air temperatures.

The easiest way to use the Da_M number is to identify a temperature which must not be exceeded within the bioreactor during the fermentation and to rearrange the equation to be explicit in H. Allowable bioreactor heights can then be calculated if an assumption is made about how V_Z varies as H increases. Note that this approach predicts that there are no limits on height if the ratio V_Z/H is maintained constant, although this is likely to lead quickly to unacceptably high pressure drops as scale increases [142]. More knowledge about the effects of pressure drop on packed bed operation is therefore required before this approach can be used effectively.

A similar approach applied to rotating drum bioreactors gives a dimensionless design factor [167]:

$$DDF = 1 = \frac{R_q}{F_a C_{pa}(T_B - T_{IN}) + F_a(C_{OUT} - C_{IN})\,\lambda + h_A(T_B - T_{SURR})} \quad (21)$$

where R_q is the peak rate of heat generation (J s^{-1}), F_a is the air flowrate (kg h^{-1}), T_B and T_{SURR} are the bed and surrounding air temperatures respectively, C_{IN} and C_{OUT} are the humidities of the inlet and outlet air (kg-water kg-dry air^{-1}), and h_A is the overall coefficient for heat transfer through the drum wall to the surroundings. Therefore the first term of the denominator represents convection to the headspace gases, the second represents evaporation to the headspace, and the third represents heat loss through the drum wall to the surroundings. By assuming that the outlet air leaves saturated at the same temperature as the bed, operating diagrams can be constructed to show how the maximum bed temperature increases as the drum diameter increases during scale-up according to rules-of-thumb such as maintaining geometric similarity and maintaining constant the superficial velocity of the air, or the vvm of air, or the DDF. Maintaining the vvm of air constant will be more effective in temperature control than maintaining the superficial velocity constant. Maintaining the DDF constant would mean that the maximum temperature within the bed would remain constant with scale, but might lead to unreasonably high air flowrates [167].

Regarding water balances, Weber et al. [37] applied a similar simplified approach to the water balance in a packed bed. They concluded that the rate of evaporation would be relatively constant along the bioreactor axis, meaning that no one region would tend to dry out more than any other. The challenge in scale-up was to ensure that a sufficiently high initial water content was used such that the substrate water activity did not fall to inhibitory levels during the fermentation.

Mathematical models promise to be more accurate and robust tools in the scale-up process, although this must be balanced against the extra difficulty of solving the model equations, especially where heterogeneity across the bioreactor means that the model contains partial differential equations. Theoretical demonstrations of how models can be used to guide the design and operation of large-scale bioreactors have been done for packed beds lacking internal heat transfer plates, Zymotis type packed beds, and rotating drum bioreactors [142, 143, 146]. For packed beds lacking internal heat transfer plates, the model predictions are similar to those given by the Da_M number [142]. In Zymotis type packed beds overheating problems with increase in scale are predicted to be negligible, but only as long as the gap between heat transfer plates is 5 cm, and if the cooling water temperature starts at the optimum temperature for growth but is decreased as the bed temperature rises above the optimum [143]. The importance of pressure drop considerations in influencing the scale-up process was not investigated. In rotating drum bioreactors the importance of evaporative heat removal is predicted to increase with scale. For a bioreactor of 20 m^3 volume, aeration rates greater than 8 vvm, using completely dry air, are

predicted to be necessary in order to obtain adequate temperature control [146].

In these mathematical models most attention has been paid to the heat transfer problem. Similar approaches need to be developed for the water balance to ensure that substrate beds do not dry out to levels which will decrease bioreactor performance.

These quantitative methods are potentially powerful tools in guiding the design and operation of large-scale bioreactors. They can be used in a rapid evaluation of designs before they are built, identifying those with the greatest potential to overcome overheating problems, and eliminating ideas which seem promising but in fact have no or poor potential. Use of these methods is more cost effective than relying solely on experimental data from large-scale bioreactors built on the basis of best guesses, although of course the most fruitful approach will be to run simultaneous modeling and experimental programs. Unfortunately, many of the mass and heat transfer coefficients are poorly characterized for SSF bioreactors. Rather, they are often estimated from the non-SSF literature. There is an urgent for experimental work, not only to determine these parameters for SSF bioreactors, but also to test these theoretical approaches by applying them in the development of real large-scale SSF bioreactors.

7
Measurement and Control Within SSF Bioreactors

The variables associated with bioreactor operation, whether SLF or SSF, can be divided into two groups – state variables and operating variables. Operating variables are those which can be varied directly through external control. State variables represent the state of the system or some part of it. They can only be controlled indirectly, through manipulation of the operating variables. State variables can be further divided into those which can be directly measured on-line, for example temperatures, and those which cannot be measured on-line, such as biomass concentrations. The basic goal of an on-line control system is to take the values of some state variables measured on-line, and to use these values to manipulate the values of the operating variables in order to influence the values of various state variables (which may or may not be directly measurable) in such a way as to optimize growth and product formation.

The key objective of a control system for an SSF bioreactor is typically to control the bed temperature and water content at values which will lead to optimal growth and product formation [167]. The operating variables which can be manipulated to achieve this in SSF bioreactors are, depending on the design, the temperature, flow rate and humidity of of the inlet air, and variables associated with the agitation system, such as the frequency and intensity of agitation. It may also be possible to manipulate the temperature and flowrate of the surrounding air or cooling water passing through jackets or heat transfer plates. If water or aqueous nutrient or pH-correcting solutions are added to the reactor the timing and quantity of these additions can be controlled.

The state variables which can be measured on-line and can therefore readily be used in such control systems are temperatures, and O_2 and CO_2 concentra-

tions in the outlet gas stream. On-line temperature measurements can be made with thermocouples, and it is usually practical to have a number located at different positions with the bioreactor. Outlet gas concentrations can be measured most conveniently on-line with paramagnetic oxygen analyzers and infrared carbon dioxide analyzers, which have in fact been used in SSF processes for many years, within control schemes regulating the inlet air flow rate and the passage of recycled air through KOH solutions to remove CO_2 [168, 169]. Other on-line measurements may be possible: a gas chromatograph with an automatic sampler can be used to measure volatile end product concentrations in the headspace gases [170]; on-line sensors can also be used to measure relative humidities in the outlet air stream [171]; meaningful pH measurements may be possible using normal pH electrodes, depending on the substrate properties [2]; and finally, in packed bed bioreactors, pressure drop measurements can give an indirect indication of the amount of growth [172].

7.1 Application of Advanced Control Techniques

Simple control schemes in which a single input variable is used to manipulate a single operating variable have been used in SSF for many years. However, the degree of control that can be achieved by such control systems is limited due to the complexity of the processes occurring within SSF bioreactors: airflow rates and humidities can be controlled to influence the bed temperature, but this also affects the level of water in the substrate bed. Sargantanis and Karim [164] showed that, although temperature in a rocking drum bioreactor can be controlled effectively using a single-input single-output algorithm, in which the dry air flow rate is varied in direct response to the measured temperature, water levels are best controlled by a multiple-input multiple-output scheme in which both total wet weight of the bioreactor and the carbon dioxide evolution rate are used to control the dry air flow rate and the water replenishment rate.

On-line measurements invariably contain noise, which may come from either variations in the process itself or from the measuring equipment [173]. In general it is necessary to process the data before it can be used in control algorithms, using mathematical filtering procedures such as Kalman filtering or Butterworth filtering to eliminate measurement noise [163, 164, 173]. The control schemes which control the operating variables such as inlet air temperature, flowrate, and humidity usually cannot prevent significant variations from occurring [167]. In the 50 kg stirred capacity bed of Fernandez et al. the inlet air temperature was controlled by electric air heaters with a selective on/off control algorithm and the humidity was controlled by steam addition through an on/off solenoid valve. Inlet air flowrate was set manually. Variations of ±10% RH occurred in the inlet air relative humidity and variations of 3 °C occurred in the inlet air temperature. Further smoothing algorithms may also be required to account for such variations in the values of these operating variables when processing data from on-line measurements [173].

7.2 Application of Off-Line Measurement Techniques

Off-line measurements of state variables are more difficult to integrate into control schemes due to the typically long delays in sample analysis. However, they are still crucial in post-fermentation analysis of the performance of the system, and can be used in the validation of both predictive and interpretive models. They may also be important to provide a check on on-line measurements, since off-line methods typically suffer from less noise than on-line methods. The most important off-line measurements are discussed below.

7.2.1 *Measuring Water Content and Water Activity*

Water content is much easier to measure than water activity. Most often the sample is dried at 100 – 105 °C for 24 h or until constant weight is attained. Some other methods as vacuum-oven drying, moisture evolution analysis, Karl Fischer titration, gas chromatography, near infrared analysis, and nuclear magnetic resonance could be also applied. Oven drying is the simplest and least expensive.

A wide range of methods can be used to determine the water activity of samples of solids removed from the bed, although electric hygrometers, in which the solids are placed in an enclosed chamber with a sensor that measures the equilibrium relative humidity, are the most convenient. Several commercial electric hygrometers are available, each of which works on a different principle. Hygrometers are usually accurate to within 2 %, but different hygrometers have different operating ranges.

7.2.2 *Measuring pH*

Flat-ended electrodes have been used to make off-line measurements directly on the surfaces of solid substrates [174, 175]. However, off-line measurements are usually made by measuring the pH of aqueous suspensions or extracts of the solid sample.

7.2.3 *Estimation of Biomass*

Growth of biomass is typically of crucial importance in SSF processes, even if the biomass itself is not the final product. The processes of nutrient consumption, oxygen consumption, carbon dioxide evolution, waste heat release, and product formation are intimately related to the growth process and therefore it is usually essential to characterize the growth curve. Unfortunately, on-line biomass measurement is still impossible in SSF, despite efforts to develop on-line sensors based on Fourier transform infrared spectroscopy [176].

Off-line measurements of biomass are also problematic because it is usually impossible to separate the fungal biomass from the substrate. Therefore indirect methods of following growth have to be used. A wide range of methods can be used, but most fall into three categories – direct separation of the biomass from the solid matrix, measuring metabolic activities, and measuring biomass components.

With a few substrates, most of the substrate can be digested enzymatically: this is especially true for substrates which predominantly consist of starch. After digestion the biomass can be recovered by filtration. Alternatively, for unicellular microorganisms the organisms can be washed from the substrate particles and estimated by viable count.

The most useful metabolic activities to measure for following growth are O_2 consumption and CO_2 evolution, which result from microbial respiration. Either one or both of these can be measured. If both are measured then it is possible to determine the respiratory quotient of the microorganism, which can give information about its metabolic state. These respiratory activities can be measured on-line with gas analyzers, although the calculations require knowledge of the aeration rate. It is usually assumed that CO_2 evolution and O_2 consumption are used both for growth and maintenance. Therefore the correlation equation for the oxygen uptake rate (OUR) is

$$OUR = \frac{dO_2}{dt} = \frac{1}{Y_{XO}} \frac{dX}{dt} + m_o X \tag{22}$$

where Y_{XO} is the yield coefficient for biomass from oxygen and m_o is the maintenance rate for consumption of oxygen. The equation for carbon dioxide evolution follows the same format.

In certain cases the production of extracellular enzymes can be used as an index of the amount of growth. For example, laccase (polyphenoloxidase) activities have been used to estimate growth of the mycelium of *Agaricus biosporus* in wheat straw [177].

Measurements of various biomass components have been used to follow growth in SSF systems. Protein measurements are simple if a predominantly starchy substrate is used, but cannot be used if the substrate contains significant amounts of protein, since the hydrolysis of substrate protein will counter balance the production of biomass protein. In addition, protein detection methods such as the Folin method can under- or overestimate fungal protein, with the amount of error depending on the strain [70]. Kjeldahl nitrogen analyses can be done, although since this gives the total nitrogen it is first necessary to acid-precipitate the protein in the sample [178].

Several compounds specific to fungi or subgroups of fungi can be used. *N*-Glucosamine, a component of the chitin in fungal cell walls, is produced by most fungi and absent in most substrates of agricultural origin. Unfortunately the extraction and hydrolysis of chitin and assay of glucosamine involves many steps and takes many hours, making the method inconvenient. Ergosterol is the predominant sterol in the cell membranes of fungi and can readily be measured by gas chromatography, high performance liquid chromatography, or ultraviolet spectrometry [179].

A problem with measuring components of the biomass is that the relationship between biomass and the component measured may change over time. This has been noted for protein, glucosamine, and ergosterol contents within fungal biomass [180–182]. Also the indirect methods of biomass estimation must be calibrated to establish the relationship with biomass, which can only be done in systems allowing direct measurement of the biomass. Some workers have calibrated indirect methods of biomass estimation using liquid culture; however, there is no guarantee that the biomass will have the same composition in the different environment in SSF. Membrane culture methods, where the fungus grows on a membrane overlaid on an artificial medium and in which the biomass can be readily removed, mimics SSF more closely, and can be used as the system for calibration [183].

8 Downstream Processing and Waste Disposal from SSF Processes

To date the downstream processing steps in SSF have received relatively little attention, due to the relatively few successful large-scale operations. Many of the studies of SSF simply show that the product can be produced within the fermented solid mass and do not consider recovery of the product. Although the product is often extracted for analysis, the objectives of extraction for analysis and extraction for product purification are different, and many processes used to extract products for analysis would not be economic. One current commercial product are microbial enzymes, and more attention has been given to enzyme recovery from SSF processes than has been given to the recovery of other products.

A review of downstream processing steps in SSF was written by Lonsane and Kriahnaiah in 1992 [184]. There has been relatively little progress since that time. This review briefly summarizes the main points of this earlier review, updating where appropriate. Since the purification of biotechnology products has already received extensive attention, this review concentrates only on aspects that are specific to solid-state fermentation, especially the step of extraction of product from the solids, a step which is not needed in submerged liquid fermentations, but is crucial in those SSF processes in which the product must be separated from the fermented material. In this extraction step there are two important criteria of success, which can have great effects on the economic performance of the process:

1. The percentage of the product that is extracted from the solid substrate. This is important because any product remaining in the solid residues represents a loss of potential income. This will be referred to below as the leaching efficiency, equal to the amount of product in the final extracted solution divided by the amount of product originally present in the solids.
2. The concentration of the product after extraction. Higher concentrations reduce the costs of further processing steps by reducing the costs of water removal.

8.1
Products for Which Extraction from the Fermented Solid is Not Needed

In these situations the whole fermented solid is used as the product. If a product is used fresh, it must be used soon after production. Examples include delignified wheat straw used as a feed supplement for ruminants and novel fermented foods such as tempe produced from indigenous Ethiopian beans, in which the fresh fermented product is cooked in a stew [185, 186].

If there is any processing, it is usually relatively simple, such as drying. In this case it may be stored for some time before use. Relatively little attention has been given to the drying of fermented materials for use as foods or feedstuffs. However, it is clear that the drying temperature should not reach levels which can cause undesirable changes in the material, such as charring. Many of the issues will be similar to those encountered in drying of food products.

Other examples in which the whole product is used include the production of animal feeds by the protein enrichment of sweet potato residue, cassava peel, or whole cassava, or when SSF is used to remove toxic or inhibitory compounds from feed materials, such as the reduction of phytic acid in canola meal, anti-digestive constituents in rye, or caffeine from coffee pulp [187–193]. In these studies it was not made clear whether the product would be used fresh or dried. This is because the research addressed the feasibility of the process itself, and not the use of the product as food or feed. The major consideration as to whether the product will be dried is the time the product must be kept before use, and the perishability of the product.

8.2
Methods for Recovery of Fungal Spores

Fungal spores are sometimes the products of SSF processes. They can be produced in medium-scale processes as inocula for large-scale SSF processes. They can also be produced as inocula for food fermentations, such as the production of spores of *Penicillium roqueforti* for inoculation into curds to produce blue cheese. Finally, spores may represent the active ingredient in the final product, as is the case with many fungal biopesticides.

The question of recovery has received most attention in the case of biopesticide production. In some cases the product can be dried and pulverized to a dust for direct application, or granules can be formulated from the dust [194]. These drying processes are similar to those described above for drying of other SSF products. In general rapid drying below 30–35 °C is essential to maintain high spore viabilities for many biopesticide fungi, although temperatures up to 50 °C can be used with *Trichoderma harzianum* [194, 195]. More recently, Daigle et al. [36] directly extruded a mixture of the fermented rice flour medium with various binding agents and then dried the granules at 50 °C in a fluidized bed to produce biopesticide granules.

In other cases it is desirable to recover the spores separately. This can be done by vacuuming the spores off directly, or partially drying the solid mass and then tumbling it to knock off spores which are then recovered by aspiration.

The product can be spread on trays and dried in a flow hood [196]. However, note that drying operations can readily be carried out in the bioreactor if packed beds are used. All that is necessary is to change the conditions of the inlet air [195]. For the production of *Beauvaria bassiana* on clay microgranules, which are well suited to direct harvesting and drying without further formulation, Desgranges et al. [197] increased the air flow rate twofold and decreased the relative humidity of the inlet air to 17%.

8.3 Leaching of Enzymes

Leaching involves contacting either the fresh fermented solid, or dried fermented solid, with a leaching solution. The difference in concentration of the product between the liquid phase held within the solid and the extraparticle leaching solution drives the transfer of the product from the solid phase into the leaching solution.

For the production of extracellular fungal enzymes, it is best not to disrupt cell walls by using overly vigorous blending or agitation during the leaching process, because this would release intracellular enzymes and make the enzyme purification step more difficult [198]. This is not such an important issue with unicellular microorganisms, which are much more difficult to disrupt.

It is common that, in addition to the product, substrate components such as polysaccharides are extracted from the fermented substrate [199]. These can make the extract quite gummy and interfere with further purification steps. In general polysaccharides can be precipitated by adding calcium chloride to a final concentration of 2% (w/v), but this can only be done when the calcium chloride does not precipitate the product as well [200].

Various issues associated with leaching are discussed below.

8.3.1 *Properties of the Leaching Solution*

Enzyme solubility depends on pH and ionic strength. As a general principle the pH of the leaching solution should be away from the isoelectric point of the enzyme so that the enzyme is charged, and the leaching solution should contain salts in order to increase the solubility of the charged enzyme. Higher enzyme concentrations in the leachate were demonstrated using salt (NaCl) in comparison with water, under otherwise identical extraction procedures, for the recovery of protease from rice bran [201]. Likewise, recovery of *Mucor bacilliformis* acid protease was higher with aqueous solutions of NaCl in comparison with water and with solutions of non-ionic detergents such as Triton X-100 or Tween 80 [202]. However, in some cases the presence of salt can increase the extraction of undesirable co-solutes. For the extraction of enzymes from fermented wood, distilled water or dilute buffers are preferable, because adding salts, organic solvents, or mild wetting agents, although sometimes extracting more activity, results in increased extraction of polyphenols and decreased enzyme recovery in subsequent purification steps [198].

In an interesting variation of leaching, more recently an aqueous two-phase system was used for recovery of amyloglucosidase produced by SSF of wheat bran by *Aspergillus niger* [203]. The two-phase system consisted of a PEG 6000 phase and a potassium phosphate phase. Here 95% of the glucoamylase was recovered in the potassium phosphate phase, while all the visible particles of bran collected at the interface. This combined extraction and separation step gave a purification factor of 11.

8.3.2
Retention of Leaching Solution in the Substrate Particles

Normally SSF processes are carried out with moist substrates at less than their maximum water holding capacity. During the leaching process these substrates will tend to retain sufficient leaching solution to reach their maximum water-holding capacity. Any leaching solution retained in the solids will contain enzyme, which represents a loss during the recovery process. Increasing the amount of leaching solution would decrease the fractional loss of enzyme, assuming that there is equilibrium between the retained and extraparticle leaching solution, because the fraction of overall liquid retained would be lower. However, this is not a feasible option because it leads to more diluted leachate. In fact, the advantage that SSF processes have in producing high product concentrations compared to SLF would be lost if large dilutions occurred in the extraction step. Alternatively, the solids can be pressed to minimize the amount of liquid retained in the product.

8.3.3
Leaching Mode

Various types of leaching can be undertaken – direct extraction, percolation, pulsed flow extraction, and countercurrent extraction.

In direct extraction leaching solution is added to the solids in a vessel which is then agitated. This type of extraction is common in the laboratory, but it requires large solvent to solids ratios. In percolation the solids are placed in a column and the leaching solution is added to the top. A valve in the outlet at the bottom is opened and the liquid slowly drains through the solids bed. In pulsed-flow extraction the solids are placed in a column and a dosing pump is used to add leaching solution at the top at a controlled rate [199]. A four-stage countercurrent extraction involves four vessels which contain solids at different stages of leaching. Fresh leaching solution is added to the solids which have already been leached three times. After this leaching the solids are thrown out and replaced by a new batch of solids which have already been leached three times and the leachate is fed into the vessel containing solids which have already been leached twice. The leaching process is repeated until liquid which has passed through three batches of solids is finally used to leach fresh solids. The leachate from this step represents the final leachate product.

Of these methods, multiple-stage countercurrent extraction enables the highest efficiencies and lowest ratios of leaching solution to solid, thereby

resulting in the highest enzyme concentrations in the leachate. With four to five contact stages, leaching efficiencies of 85% can be achieved using leaching solution to dry solids ratios as low as 1 l of leaching solution per kg of dry solids [130, 204]. These high efficiencies are obtained because the countercurrent movement of solids and liquid through the process increases extraction efficiency: the liquid leaves in equilibrium with the fresh solids, rather than in equilibrium with the spent solids, as occurs in the other methods. Pressing of the solids between extraction stages can help to improve recovery [205]. Recently this method has been applied to the recovery of pectinolytic enzymes using three extraction stages [206].

The disadvantage of counter current leaching is the number of contact stages. For example similar extraction efficiencies can be obtained in one-step pulsed-flow extraction, although the final leachate has a twofold lower enzyme concentration [199].

In a variation of the counter current method called "semi-continuous multiple contact forced percolation", six-fold higher concentrations of fungal rennet were claimed in comparison with five-stage counter-current extraction [207]. However, it is difficult to reconcile a six-fold increase in concentration with the fact that the leaching solution to solids ratios were similar, and the percentage recoveries were similar.

8.4 Recovery by Direct Pressing

Enzymes can also be recovered by direct pressing. Hydraulic pressing without leachate addition was done by Roussos et al. [208]. They applied 220 bar pressure for 1 min, then added a volume of water equal to the leachate volume released in the first pressing, and repeated the pressing. They were able to recover 80% of the water originally present in the solids on the first pressing, although the fraction of water retained will obviously depend on the type of solid. After the second pressing, enzyme recoveries of 85–95% were obtained. These recoveries are possible with the addition of relatively little liquid. In total the ratio of final leachate to initial mass of fermented solids (fresh weight) was only 1.2. Despite the apparent success of this method, and the widespread use of industrial scale presses in the fruit processing industry, the use of direct pressing to recover products from SSF has not received further attention [208].

8.5 Recovery of Non-Volatile Small Organic Molecules

Small, non-volatile, organic molecules which have been produced in SSF include pigments, antibiotics, plant growth factors, and simple organic acids such as lactic and citric acids. As for enzymes the only extraction methods available are pressing and leaching. However, in contrast to the work done in the leaching of enzymes, relatively little attention has been given to the extraction of these small non-volatile organic molecules.

Leaching solutions are likely to be similar to those used for extraction for the purpose of assaying the product concentrations. Water has been used for extraction of oxytetracycline, cephamycin C, citric acid, and lactic acid; 95% ethanol has been used for extraction of *Monascus* pigment; both phosphate buffer and ethyl acetate have been used for extraction of penicillin [209–215]. However, since high concentrations in the extract are usually not crucial in the assays, direct extraction is used, and therefore high leaching solution to solids ratios of 5:1 to 10:1 have been used. These are not appropriate for recovery during downstream processing since they lead to low product concentrations in the leachate.

Within this group of products the exception is gibberellic acid, for which downstream processing has received some attention. Kumar and Lonsane [130] pointed out that one of the reasons for exploring gibberellic acid production in SSF is the low concentrations achieved within fermentation broths in SLF. However, SSF processes would lose any advantages of high concentrations in the fermented mass if large liquid volumes had to be used for extraction. Therefore they used a four-stage countercurrent leaching system, which allows low leaching solution to solids ratios. Before extraction, the fermented bran was dried at 50 °C. The loss of gibberellic acid during this drying was negligible, not exceeding 5% of the total. Extraction was best at low pH values, being optimal at the lowest value tested, pH 2.5. Aqueous solutions of methanol, ethanol, acetone, and ethyl acetate were tested. Water containing 10% ethanol gave the highest degree of extraction. The use of four contact stages in a countercurrent leaching system led to 87% recovery and a gibberellic acid concentration of 0.9 mg ml^{-1}.

Supercritical fluid extraction has also been investigated for the removal of undesirable co-products after production of gibberellic acid on wheat bran by *Gibberella fujikuroi* in SSF [216]. In this case the gibberellic acid remained within the solid mass, although the method can potentially be used for extraction of products. However, although supercritical fluid extraction has high leaching efficiencies, it involves high capital and operating costs and therefore will only be feasible for high value products [184].

8.6 Recovery of Volatile Products by Stripping

Volatile products such as ethanol and aroma compounds can potentially be recovered during the fermentation by stripping them out of the solids with a flowing gas stream.

In the case of ethanol, extraction with water is undesirable due to the dilution of the ethanol, whereas direct pressing gives poor yields [184]. Direct distillation from the fermented solids performs relatively poorly, although distillation is economically feasible if combined with animal feed production from the solid wastes [217, 218]. As an alternative, forced gas circulation can be used to strip ethanol from the substrate. This has been shown for a gas-solid fluidized bed and for a stirred bed [90, 219, 220]. A further advantage is that continuous stripping during the fermentation, rather than simply recovering the ethanol at the end of the fermentation, avoids the product inhibition

problems which plague ethanol production processes. The off-gases can be passed through a water cooled condenser before being returned to the bed. At the end of the fermentation ethanol concentrations in the condensed phase can be as high as 16.7% (v/v) [219]. However, little further attention has been given over the last decade to ethanol production and recovery by stripping in gas-solid fluidized beds.

In contrast to ethanol production, no attention has been paid to the recovery of aroma compounds. However, the presence of volatile compounds such as acetaldehyde, ethyl acetate, ethyl propionate, and 3-methyl butanol in the headspace above substrates on which *Rhizopus oryzae* is growing [221] suggests that such recovery could be attempted, although the economics of such a recovery process are unclear, given that the compounds are present at very low concentrations of less than 0.5 mmol l^{-1}.

In a related system, during growth of baker's yeast on a semi-solid substrate, homogenized whole potatoes predigested with α-amylase, within an air-fluidized bed bioreactor, proteins were entrained in the exit air from the bioreactor [222]. These proteins could be recovered by sparging the exit air through a water chamber. Interestingly, the entrainment of proteins was selective, suggesting the possibility of on-line protein fractionation [222]. Of course, unlike small organic compounds, the proteins are not volatile. The fractionation occurs as a partitioning between the aqueous phase within the substrate and microdroplets of water which exit with the exit gas stream [223].

8.7 Waste Treatment and Ecological Aspects

One of the claimed advantages of SSF is that it often uses agricultural wastes which would otherwise be dumped. However, for those SSF processes in which the whole product is not used, but rather the product is extracted from the solids, there is the important question of how the spent solids are disposed of. Relatively little attention has been given to this question, probably because there are relatively few large-scale SSF processes generating solid wastes. However, if the technology does manage to become established on the large scale, waste disposal will become a key problem, especially since governments around the world are imposing stricter environmental controls.

Despite the lack of attention to this issue in the literature, some general principles can be outlined here. First, one of the important considerations is the impact of the solids on the environment Second, there is the question of economics. It is better to take some advantage of a waste material rather than pay to have to dump it, and it is likely that dumping fees will increase with increasing shortage of conveniently located suitable dump sites.

Spent solids can potentially generate undesirable odors, or release leachates rich in organic material. Since extraction will often involve wetting, the solids may have a high water content, especially if the solids are not pressed, which can allow the growth of bacteria. The interior regions of piles of solids can quickly become anaerobic, giving the potential for the production of undesirable odors by anaerobic bacteria.

There are two main ways to utilize the waste solids – either compost them or convert them into useful products. Since composts often have relatively little value, the second route is preferable. Mehta et al. [224] cultivated *Pleurotus florida* on rice straw to produce mushrooms. They used the waste solid for biogas production. In fact they noted that the growth of the fungus increased the production of biogas from the straw. Singh et al. [225], in reviewing the traditional production of mushrooms from cereal straws in Asia, pointed out that residues are often used as animal feeds. However, the acceptance of the residue by ruminants varied with the type of mushroom produced.

9 Evaluation of the Current Status and Future Prospects

This review has investigated the state of the art of biochemical engineering aspects of solid state fermentation. It is clear that the development of large-scale processes is problematic, owing to the limitations of heat and mass transfer which are intrinsic to the system. Any of a range of factors can potentially be limiting at different times and places during a fermentation, such as temperature, nutrient concentration, oxygen concentration, pH, and water activity. Due to this complexity, until recently our quantitative understanding of the system has been poor, which has limited our ability to design successful large-scale processes.

Solid-state fermentation technology must be seen as complementary to SLF technology. In a majority of cases SLF is superior, if not for product yields then for the ease of handling and control on the large scale. However, there is a need for SSF technology, because certain products are either not produced in SLF, or if produced, do not possess desirable features possessed by the product from SSF. SSF may also be favored in some instances simply because a low technology process is sufficient and labor costs are low, or because a waste solid material needs to be utilized for profit rather than simply dumped.

Routine commercialization of those products for which SSF is the superior technique will require better knowledge about how to design equipment and how to operate the process. The application of biochemical engineering approaches to SSF is still in its early stages. Despite this, our knowledge of bioreactor design and operation has advanced considerably over the last decade. Mathematical models of the microscale have given us insights into how intraparticle diffusion of enzymes, hydrolysis products, and oxygen have the potential to limit process performance. Further, mathematical models have been developed to describe the operation of most types of bioreactors. Although these mathematical models need many further improvements, they have already given us valuable insights into how to design and operate bioreactors on the larger scale.

Much more needs to be done. More attention needs to be given to the auxiliary operations such as substrate preparation, sterilization, aseptic transferal of substrate, preparation of inoculum, and downstream processing. With respect to the bioreactor step itself, mathematical models need to be improved in order to improve their usefulness as tools in the design process.

First, they need to be extended to describe more phenomena: Most attention has been given to the energy balance, and more attention needs to be given to the water balance. Second, better values of system parameters must be determined. Until very recently there has been a tendency to borrow values of parameters from other systems. These parameters are sometimes even borrowed from non-SSF systems which operate under quite different conditions (e.g., high temperatures) than those under which SSF systems operate. Finally, there is no description in the literature of how mathematical modeling has actually been used to guide the scale-up from laboratory through pilot scale to commercial scale. This is the crucial test of the usefulness of the biochemical engineering approaches discussed in this review, and will greatly accelerate the refinement of the models.

Also, there is a need to develop effective systems for the measurement and control of large-scale processes, a task made challenging by the microscale and macroscale heterogeneity within the substrate bed: It is difficult not only to obtain reliable on-line measurements but also to achieve fine control over system parameters.

Finally, relatively few efforts have been made to analyze the economic performance of SSF processes relative to SLF processes. Urgent attention must be given to this aspect since it is on economic performance criteria that the future of the technology will ultimately rest.

Achievement of these improvements will greatly improve our ability to operate SSF processes reliably and reproducibly near their maximum potential, allowing us to use SSF technology routinely for those products for which it has better potential than SLF.

References

1. Cannel E, Moo-Young M (1980) Proc Biochem 15(5):2
2. Durand A, Chereau D (1988). Biotechnol Bioeng 31:476
3. Knapp JS, Howell JA (1977) Solid substrate fermentation. In: Wiseman A (ed) Topics in enzyme and fermentation biotechnology, vol 4. Ellis Horwood, Chichester, p 85
4. Moo-Young M, Moreira AR, Tengerdy RP (1983) Principles of solid-substrate fermentation. In: Smith JE, Berry DR, Kristiansen B (eds) The filamentous fungi, vol 4. Edward Arnold, London, p 117
5. Steinkraus KH (1984) Acta Biotechnol 4:83
6. Stanton WR, Wallbridge A (1969) Proc Biochem April:45
7. Ralph BJ (1976) Food Tech Aust 28:247
8. Takamine J (1914) J Ind Engng Chem 6:824
9. Mial LM (1975) Historical development of the fungal fermentation industry. In: Smith JE, Berry DR, Kristiansen B (eds) The filamentous fungi, vol 1. Edward Arnold, London, p 104
10. Stentiford EI, Dodds CM (1992) Composting. In: Doelle HW, Mitchell DA, Rolz CE (eds) Solid substrate cultivation. Elsevier, London, p 211
11. Doelle HW, Mitchell DA, Rolz CE (eds) (1992) Solid substrate cultivation. Elsevier, London
12. Selvakumar P, Ashakumary L, Pandey A (1998) Biores Technol 65:83
13. Arasaratnam V, Mylvaganam K, Balasubramaniam K (1997) Int J Food Sci Technol 32:299

14. Mamo G, Gessesse A (1999) J Ind Micro Biotech 22 : 622
15. Kamini NR, Mala JGS, Puvanakrishnan R (1998) Proc Biochem 33 : 505
16. Benjamin S, Pandey A (1997) Acta Biotechnol 17 : 241
17. Uvarani G, Jaganathan L, Shridas P, Boopathy R (1998) J Sci Ind Res 57 : 607
18. Gombert AK, Pinto AL, Castilho LR, Freire DMG (1999) Proc Biochem 35 : 85
19. Kotwal SM, Gote MM, Sainkar SR, Khan MI, Khire JM (1998) Proc Biochem 33 : 337
20. Krishna C (1999) Biores Technol 69 : 231
21. Gutierrez-Correa M, Tengerdy RP (1999) Agro Food Ind Hi-Tech 10 : 6
22. Gutierrez-Correa M, Portal L, Moreno P, Tengerdy RP (1999) Biores Technol 68 : 173
23. Nirmala PJ, Ramakrishna M (1997) Adv Food Sci 19 : 140
24. Crotti LB, Jabor VAP, Chellegatti MAD, Fonseca MJV, Said S (1999) J Basic Microbiol 39 : 227
25. Castilho LR, Medronho RA, Alves TLM (2000) Biores Technol 71 : 45
26. Berovic M, Ostroversnik H (1997) J Biotechnol 53 : 47
27. Selvakumar P, Pandey A (1999) Proc Biochem 34 : 851
28. Ferreira GL, Boer CG, Peralta RM (1999) FEMS Microbiol Lett 173 : 335
29. Ridder ER, Nokes SE, Knutson BL (1998) Trans ASAE 41 : 1453
30. Gutierrez-Correa M, Tengerdy RP (1998) Biotechnol Lett 20 : 45
31. Gessesse A, Mamo G (1999) Enz Microb Technol 25 : 68
32. Couto SR, Longo MA, Cameselle C, Sanroman A (1999) Acta Biotechnol 19 : 17
33. Rodriguez S, Longo MA, Cameselle C, Sanroman A (1999) Bioprocess Eng 20 : 531
34. Rodriguez S, Santoro R, Cameselle C, Sanroman A (1998) Bioprocess Eng 18 : 251
35. Hutchinson CM (1999) Biol Control 16 : 217
36. Daigle DJ, Connick WJ, Boyette CD, Jackson MA, Dorner JW (1998) Biotechnol Tech 12 : 715
37. Weber FJ, Tramper J, Rinzema A (1999) Biotechnol Bioeng 65 : 447
38. Rodriguez-Vazquez R, Cruz-Cordova T, Fernandez-Sanchez JM, Roldan-Carrillo T, Mendoza-Cantu A, Saucedo-Castaneda G, Tomasini-Campocosio A (1999) Folia Microbiol 44 : 213
39. Okeke BC, Paterson A, Smith JE, Watson-Craik IA (1997) Appl Microbiol Biotechnol 48 : 563
40. Wu G, Chabot JC, Caron JJ, Heitz M (1998) Water Air Soil Poll 101 : 69
41. Sardjono, Zhu Y, Knol W (1998) J Agr Food Chem 46 : 3376
42. Hakil M, Voisinet F, Viniegra-Gonzalez G, Augur C (1999) Proc Biochem 35 : 103
43. Dorado J, Almendros G, Camarero S, Martinez AT, Vares T, Hatakka A (1999) Enz Microb Technol 25 : 605
44. Scerra V, Caridi A, Foti F, Sinatra MC (1999) Animal Feed Sci Technol 78 : 169
45. DiLena G, Patroni E, Quaglia GB (1997) Int J Food Sci Technol 32 : 513
46. Ohga S (1999) J Wood Sci 45 : 337
47. Shojaosadati SA, Faraidouni R, Madadi-Nouei A, Mohamadpour I (1999) Resources Conservation and Recycling 27 : 73
48. Lapadatescu C, Bonnarme P (1999) Biotechnol Lett 21 : 763
49. Larroche C, Besson I, Gros JB (1999) Proc Biochem 34 : 667
50. Sree NK, Sridhar M, Suresh K, Rao LV (1999) Bioprocess Eng 20 : 561
51. Sree NK, Sridhar M, Rao LV, Pandey A (1999) Proc Biochem 34 : 115
52. Rodriguez-Iglesias J, Castrillon L, Maranon E, Sastre H (1998) Biores Technol 63 : 29
53. Leangon S, Maddox IS, Brooks JD (1999) World J Microbiol Biotechnol 15 : 493
54. Roukas T (1999) Enz and Microb Technol 24 : 54
55. Tran CT, Sly LI, Mitchell DA (1998) World J Microbiol Biotechnol 14 : 399
56. Hang YD, Woodams EE (1998) Biores Technol 65 : 251
57. Sadhukhan AK, Murthy MVR, Kumar RA, Mohan EVS, Vandana G, Bhar C, Rao KV (1999) J Ind Microbiol Biotechnol 22 : 33
58. Kota KP, Sridhar P (1999) Proc Biochem 34 : 325
59. Stredansky M, Conti E (1999) Appl Microbiol Biotechnol 52 : 332
60. Stredansky M, Conti E, Navarini L, Bertocchi C (1999) Proc Biochem 34 : 11

61. Stredansky M, Conti E (1999) Proc Biochem 34:581
62. Gutierrez A, Del Rio JC, Martinez MJ, Martinez AT (1999) Appl Env Microbiol 65:1367
63. Camarero S, Barrasa JM, Pelayo M, Martinez AT (1998) J Pulp Paper Sci 24:197
64. Scott WJ (1957) Adv Food Res 7:83
65. Rossi J, Clementi F (1985) J Food Technol 20:319
66. Viesturs UE, Apsite AF, Laukevics JJ, Ose VP, Bekers MJ, Tengerdy RP (1981) Biotechnol Bioeng Symp 11:359
67. Tengerdy RP, Murphy VG, Wissler MD (1983) Annals New York Acad Sci 413:469
68. Abdullah AL, Tengerdy RP, Murphy VG (1984) Biotechnol Bioeng 27:20
69. Shamala TR, Sreekantiah KR (1987) Enz Microb Technol 9:97
70. Daubresse P, Ntibashirwa S, Gheysen A, Meyer JA (1987) Biotechnol Bioeng 29:962
71. Mitchell DA (1992) Microbial basis of processes. In: Doelle HW, Mitchell DA, Rolz CE (eds) Solid substrate cultivation. Elsevier, London, p 17
72. Huang SY, Wang HH, Wei CJ, Malaney GW, Tanner RD (1986) Kinetic responses of the koji solid state fermentation process. In: Wiseman A (ed) Topics in enzyme and fermentation biotechnology, vol 10. Ellis Horwood, Chichester, p 88
73. Raimbault M, Alazard D (1980) Culture method to study fungal growth in solid fermentation. Eur J App Microbiol Biotechnol 9:199–209
74. Wang HL, Swain EW, Hesseltine CW (1975) J Food Sci 40:168
75. Mudgett RE (1986) Solid-state fermentations. In: Demain AL, Solomon NA (eds) Manual of industrial microbiology and biotechnology. ASM, Washington DC, p 66
76. Prior BA, Du Preez JC, Rein PW (1992) Environmental parameters. In: Doelle HW, Mitchell DA, Rolz CE (eds) Solid substrate cultivation. Elsevier, London, p 65
77. Torrado A, Gonzalez MP, Murado MA (1998) Biotechnol Techniques 12:411
78. Mitchell DA, Berovic M (1998) Solid state fermentations. In: Berovic M (ed) Bioprocess engineering course. National Institute of Chemistry, Ljubljana, p 128
79. Mitchell DA, Targonski Z, Rogalski J, Leonowicz A (1992) Substrates for processes. In: Doelle HW, Mitchell DA, Rolz CE (eds) Solid substrate cultivation. Elsevier, London, p 29
80. Berovic M, Logar-Derencin M (1993) J Chem Technol Biotechnol 56(2):209
81. Gibbons WR, Westby CA, Dobbs TL (1984) Biotechnol Bioeng 26:1098
82. Gibbons WR, Westby CA, Dobbs TL (1986) Appl Env Microbiol 51:115
83. Georgiou G, Shuler ML (1986) Biotechnol Bioeng 28:405
84. Mitchell DA, Do DD, Greenfield PF, Doelle HW (1991) Biotechnol Bioeng 38:353
85. Rajagopalan S, Modak JM (1995) Chem Eng Sci 50:803
86. Oostra J, le Comte P, de Heer N, van den Heuvel JC, Tramper J, Rinzema A (1997). 8th European Congress on Biotechnology, Budapest, p 283
87. Rajagopalan S, Modak JM (1994) Chem Eng Sci 49:2187
88. Gutierrez-Rojas M, Auria R, Benet JC, Revah S (1995) Chem Eng J 60:189
89. Bahr D, Menner M (1995) Bioforum 18:366
90. Rottenbacher L, Schossler M, Bauer W (1987) Bioprocess Eng 2:25
91. Laukevics JJ, Apsite AF, Viesturs US, Tengerdy RP (1985) Biotechnol Bioeng 27:1687
92. Viniegra-Gonzales G, Saucedo-Castaneda G, Lopez-Isunza F, Fevela-Torres E (1993) Biotechnol Bioeng 42:1
93. Viniegra-Gonzalez G, Larralde-Corona CP, Lopez-Isunza F (1994) A new approach for modelling the kinetics of mycelial cultures. In: Galindo E, Ramirez OT (eds) Advances in bioprocess engineering. Kluwer Academic Publishers, Dordrecht, p 183
94. Ikasari L, Mitchell DA (2000) Biotechnol Bioeng (in press)
95. Mitchell DA, Stuart DM, Tanner RD (1999) Solid-state fermentation – microbial growth kinetics. In: Flickinger MC, Drew SW (eds) The encyclopedia of bioprocess technology: fermentation, biocatalysis and bioseparation, vol 5. Wiley, New York, p 2407
96. Saucedo-Casteneda G, Gutierrez-Rojas M, Bacquet G, Raimbault M, Viniegra-Gonzalez G (1990) Biotechnol Bioeng 35:802
97. Sangsurasak P, Mitchell DA (1995) J Chem Tech Biotechnol 64:253
98. Kaiser J (1996) Ecological Modelling 91:25
99. Szewczyk KW, Myszka L (1994) Bioprocess Eng 10:123

100. Smits JP, van Sonsbeek HM, Tramper J, Knol W, Geelhoed W, Peeters M, Rinzema A. (1999) Bioprocess Eng 20:391
101. Ikasari L, Mitchell DA, Stuart DM (1999) Biotechnol Bioeng 64:722
102. Pitt RE (1993) J Food Protection 56:139
103. Muck RE, Pitt RE, Leibensperger RY (1991) Grass Forage Sci 46:283
104. Prosser JI (1982) Growth of fungi. In: Bazin MJ (ed) Microbial population dynamics. CRC Press, Boca Raton, p 125
105. Gervais P, Simatos D (1992) Modelling of water relations in fermentation processes. In: Thorne S (ed) Mathematical modelling of food processing operations. Elsevier, London, p 137
106. Gervais P, Molin P, Grajek W, Bensoussan M (1988) Biotechnol Bioeng 31:457
107. Sargantanis J, Karim MN, Murphy VG, Ryoo D, Tengerdy RP (1993). Biotechnol Bioeng 42:149
108. Auria R, Ortiz I, Villegas E, Revah S (1995) Proc Biochem 30:751
109. Mitchell DA, Greenfield PF, Doelle HW (1990) World J Microbiol Biotechnol 6:201
110. Stuart DM, Mitchell DA, Johns MR, Litster JD (1998) Biotechnol Bioeng 63:383
111. Ito K, Kimizuka A, Okazaki N, Kobayashi, S (1989) J Ferment Bioeng 68:7
112. Jurus AM, Sundberg WJ (1976) Appl Env Microbiol 32:284
113. Varzakas T (1998) Proc Biochem 33:741
114. Rajagopalan S, Rockstraw DA, Munson-McGee SH (1997) Biores Technol 61:175
115. Nandakumar MP, Thakur MS, Raghavarao KSMS, Ghildyal NP (1994) Proc Biochem 29:545
116. Nopharatana M, Howes T, Mitchell DA (1998) Biotechnol Tech 12:313
117. Desfarges C, Larroche C, Gros JB (1987) Biotechnol Bioeng 29:1050
118. Larroche C, Gros JB (1992) Biotechnol Bioeng 39:815
119. Sato K, Yoshizawa K (1988) J Ferment Technol 66:667
120. Ramesh MV, Charyulu NCLN, Chand N, Lonsane BK (1996) Bioprocess Eng 15:289
121. Perez-Correa JR, Agosin E (1999) Automation of solid-substrate fermentation processes. In: Flickinger MC, Drew SW (eds) The encyclopedia of bioprocess technology: fermentation, biocatalysis and bioseparation, vol 5. Wiley, New York, p 2429
122. Rajagopalan S, Modak JM (1995) Bioprocess Eng 13:161
123. Durand A, Pichon P, Desgranges C (1988) Biotechnol Techniques 2:11
124. Gowthaman MK, Raghava Rao KSMS, Ghildyal NP, Karanth NG (1995) Proc Biochem 30:9
125. Thibault J, Pouliot K, Agosin E, Perez-Correa R (2000) (in preparation)
126. Olsson S, Jennings DH (1991) Experimental Mycology 15:302
127. Gumbira-Sa'id E, Greenfield PF, Mitchell DA, Doelle HW (1993) Biotechnol Adv 11:599
128. Nandakumar MP, Thakur MS, Raghavarao KSMS, Ghildyal NP (1996) Enz Microb Technol 18:121
129. Tao S, Beihui L, Zuohu L (1997) J Chem Technol Biotechnol 69:429
130. Kumar PKR, Lonsane BK (1987) Proc Biochem 22:139
131. Roussos S, Raimbault M, Prebois JP, Lonsane BK (1993) Appl Biochem Biotechnol 42:37
132. Pandey A (1991) Proc Biochem 26:355
133. Lonsane BK, Ghildyal NP, Budiatman S, Ramakrishna S (1985) Enz Microb Technol 7:258
134. Ghildyal NP, Ramakrishna M, Lonsane BK, Karanth NG, Krishnaiah MM (1993) Chem Eng J 51:B17
135. Szewczyk KW (1993) Acta Biochimica Polonica 40:90
136. Costa JAV, Alegre RM, Hasan SDM (1998) Biotechnol Techniques 12:747
137. Auria R, Palacios J, Revah S (1992) Biotechnol Bioeng 39:898
138. Gowthaman MK, Ghildyal NP, Raghava Rao KSMS, Karanth NG (1993) J Chem Technol Biotechnol 56:233
139. Ghildyal NP, Gowthaman MK, Raghava Rao KSMS, Karanth NG (1994) Enz Microb Technol 16:253
140. Sangsurasak P, Mitchell DA (1998) Biotechnol Bioeng 60:739

141. Gutierrez-Rojas M, Amar Aboul Hosn S, Auria R, Revah S, Favela-Torres E (1996) Proc Biochem 31:363
142. Mitchell DA, Pandey A, Sangsurasak P, Krieger N (1999) Proc Biochem 35:167
143. Mitchell DA, von Meien OF (2000) Biotechnol Bioeng 68:127
144. Saucedo-Castaneda G, Lonsane BK, Krishnaiah MM, Navarro JM, Roussos S, Raimbault M (1992) Proc Biochem 27:97
145. Auria R, Morales M, Villegas E, Revah S (1993) Biotechnol Bioeng 41:1007
146. Stuart DM (1996) PhD Thesis. University of Queensland, Brisbane, Australia
147. Ziffer J (1988) Wheat bran culture process for fungal amylase and penicillin production. In: Raimbault M (ed) Solid state fermentation in bioconversion of agro-industrial raw materials. ORSTOM, Montpellier, p 121
148. Khakhar DV, McCarthy JJ, Shinbrot T, Ottino JM (1997) Phys Fluids 9:31
149. Fung CJ, Mitchell DA (1995) Biotechnol Techniques 9:295
150. Marsh AJ, Mitchell DA, Stuart DM, Howes T (1998) Biotechnol Lett 20:607
151. Stuart DM, Mitchell DA, Howes T (1995) Proceedings of the 4th Pacific Rim Biotechnology Conference, Melbourne, Victoria, p 262
152. de Reu JC, Zwietering MH, Rombouts FM, Nout MJR (1993) Appl Microbiol Biotechnol 40:261
153. Kalogeris E, Fountoukides G, Kekos D, Macris BJ (1999) Biores Technol 67:313
154. Matsuno R, Adachi S, Uosaki H (1993) Biotechnol Adv 11:509
155. Chamielec Y, Renaud R, Maratray J, Almanza S, Diez M, Durand A (1994) Biotechnol Techniques 8:245
156. Agosin E, Perez-Correa R, Fernandez M, Solar I, Chiang L (1997). An aseptic pilot bioreactor for solid substrate cultivation processes. In: Wise DL (ed) Global environmental biotechnology. Kluwer Academic Publishers, Dordrecht, p 233
157. Bandelier S, Renaud R, Durand A (1997) Proc Biochem 37:141
158. Durand A, Renaud R, Maratray J, Almanza S, Diez M (1996) J Sci Ind Res 55:317
159. Xue M, Liu D, Zhang H, Hongyan Q, Lei Z (1992) J Ferment Bioeng 73:203
160. Ellis SP, Gray KR, Biddlestone AJ (1994) Trans Inst Chem Eng Part C 72:158
161. Ashley VM, Mitchell DA, Howes T (1999) Biochem Eng J 3:141
162. Barstow LM, Dale BE, Tengerdy RP (1988) Biotechnol Techniques 2:237
163. Ryoo D, Murphy VG, Karim MN, Tengerdy RP (1991) Biotechnol Techniques 5:19
164. Sargantanis JG, Karim MN (1994) Ind Eng Chem Res 33:878
165. Lonsane BK, Saucedo-Castaneda G, Raimbault M, Roussos S, Viniegra-Gonzalez G, Ghildyal NP, Ramakrishna M, Krishnaiah MM (1992) Proc Biochem 27:259
166. Hardin MT, Mitchell DA, Howes T (2000) Biotechnol Bioeng 67:274
167. Fernandez M, Perez-Correa JR, Solar I, Agosin E (1996) Bioprocess Eng 16:1
168. Bajracharya R, Mudgett RE (1980) Biotechnol Bioeng 22:2219
169. Narahara H, Koyama Y, Yoshida T, Pichangkura S, Ueda R, Taguchi H (1982) J Ferment Technol 60:311
170. Ramstack JM, Lancaster EB, Bothast RJ (1979) Proc Biochem 14:2
171. Gervais P, Bazelin C (1986) Biotechnol Lett 8:191
172. Auria R, Revah S (1994) Pressure drop as a method to evaluate mold growth in solid state fermentors. In: Galindo E, Ramirez OT (eds) Advances in bioprocess engineering. Kluwer Academic Publishers, Dordrecht, p 289
173. Pena y Lillo M, Perez-Correa R, Latrille E, Fernandez M, Acuna G, Agosin E (2000) Bioprocess Eng (in press)
174. Levonen-Munoz E, Bone DH (1985) Biotechnol Bioeng 27:382
175. Mitchell DA, Greenfield PF, Doelle HW (1986) Biotechnol Lett 8:827
176. Greene RV, Freer SN, Gordon SH (1988) FEMS Microbiol Lett 52:73
177. Wood DA (1979) Biotechnol Lett 1:255
178. Matcham SE, Wood DA, Jordan BR (1984) Appl Biochem Biotechnol 9:387
179. Seitz LM, Sauer DB, Borrougs R, Mohr HE, Herbard JD (1979) Pathology 69:1202
180. Nout MJR, Bonants-van Laarhoven TMG, de Jongh P, de Koster PG (1987) Appl Microbiol Biotechnol 26:456

181. Mitchell DA, Gumbira-Sa'id E, Greenfield PF, Doelle HW (1991) Biotechnol Techniques 5:437
182. Farley PC (1991) Biomed Lett 46:227
183. Mitchell DA, Doelle HW, Greenfield PF (1989) Biotechnol Techniques 3:45
184. Lonsane BK, Kriahnaiah MM (1992) Product leaching and downstream processing. In: Doelle HW, Mitchell DA, Rolz CE (eds) Solid substrate cultivation. Elsevier, London, p 147
185. Valmaseda M, Martinez MJ, Martinez AT (1991) Appl Microbiol Biotechnol 35:817
186. Ashenafi M, Busse M (1991) World J Microbiol Biotechnol 7:72
187. Yang SS (1993) Biotechnol Adv 11:495
188. Ofuya CO, Nwajiuba CJ (1990) World J Microbiol Biotechnol 6:144
189. Balagopalan C (1996) J Sci Ind Res 55:479
190. Nair VC, Duvnjak Z (1990) Appl Microbiol Biotechnol 34:183
191. Nair VC, Duvnjak Z (1991) Acta Biotechnologica 3:211
192. Weichert D, Zakordonets L, Klappach G, Charkevitch E, Koval EZ (1991) Acta Biotechnologica 11:115
193. Aquiahuatl MA, Raimbault M, Roussos S, Trejo MR (1988) Coffee pulp detoxification by solid state fermentation: isolation, identification and physiological studies. In: Raimbault M (ed) Solid state fermentation in bioconversion of agro-industrial raw materials. ORSTOM, Montpellier, p 13
194. Bartlett MC, Jaronski ST (1988) Mass production of entomogenous fungi for biological control of insects. In: Burge MN (ed) Fungi in biological control systems. Manchester University Press, Manchester, p 61
195. Roussos S, Olmos A, Raimbault M, Saucedo-Castaneda G, Lonsane BK (1991) Biotechnol Techniques 5:415
196. Silman RW, Bothast RJ, Schisler DA (1993) Biotechnol Adv 11:561
197. Desgranges C, Vergonian C, Lereec A, Riba G, Durand A (1993) Biotechnol Adv 11:577
198. Leatham GF, Forrester IT, Mishra C (1991) Enzymes from solid substrates: recovering extracellular degradative enzymes from *Lentinula edodes* cultures grown on commercial wood medium. In: Leatham GF, Himmel ME (eds) Enzymes in biomass conversion. ACS, Washington DC, p 95
199. Ghildyal NP, Ramakrishna M, Lonsane BK, Karanth NG (1991) Proc Biochem 26:235
200. Lonsane BK, Ramesh MV (1990) Adv Appl Microbiol 35:1
201. Ikasari L, Mitchell DA (1996) Enz Microb Technol 19:171
202. Fernandez-Lahore HM, Fraile ER, Cascone O (1998) J Biotechnol 62:83
203. Ramadas M, Holst O, Mattiasson B (1995) Biotechnol Techniques 9:901
204. Karanth NG, Lonsane BK (1988) Laboratory and pilot scale production of enzymes and biochemicals by solid state fermentation at CFTRI Mysore. In: Raimbault M (ed) Solid state fermentation in bioconversion of agro-industrial raw materials. ORSTOM, Montpellier, p 113
205. Thakur MS, Karanth NG, Nand K (1990) Appl Microbiol Biotechnol 32:409
206. Castilho LR, Alves TLM, Medronho RA (1999) Proc Biochem 34:181
207. Thakur MS, Karanth NG, Nand K (1993) Biotechnol Adv 11:399
208. Roussos S, Raimbault M, Saucedo-Castaneda G, Lonsane BK (1992) Biotechnol Techniques 6:429
209. Yang SS, Yuan SS (1990) World J Microbiol Biotechnol 6:236
210. Kota KP, Sridhar P (1998) J Sci Ind Res 57:587
211. Shankaranand VS, Lonsane BK (1994) World J Microbiol Biotechnol 10:165
212. Xavier S, Lonsane BK (1994) Appl Microbiol Biotechnol 41:291
213. Johns MR, Stuart DM (1991) J Ind Microbiol 8:23
214. Barrios-Gonzalez J, Castillo TE, Mejia A (1993) Biotechnol Adv 11:525
215. Barrios-Gonzalez J, Tomasini A, Viniegra-Gonzalez G, Lopez L (1988) Penicillin production by solid state fermentation. In: Raimbault M (ed) Solid state fermentation in bioconversion of agro-industrial raw materials. ORSTOM, Montpellier, p 39
216. Kumar PKR, Sankar KU, Lonsane BK (1991) Chem Eng J 46:B53

217. Jaleel SA, Srikanta S, Ghildyal NP, Lonsane BK (1988) Starch 40:55
218. Joshi VK, Sandhu DK (1996) National Acad Sci Letts India 19:219
219. Moebus O, Teuber M (1982) Eur J Appl Microbiol Biotechnol 15:194
220. Sato K, Miyazaki SI, Matsumoto N, Yoshizawa K, Nakamura KI (1988) J Ferment Technol 66:173
221. Bramorski A, Christen P, Ramirez M, Soccol CR, Revah S (1998) Biotechnol Lett 20:359
222. Hong K, Tanner RD, Malaney GW, Danzo BJ (1989) Bioprocess Eng 4:209
223. Kokitkar PB, Hong K, Tanner RD (1990) J Biotechnol 15:305
224. Mehta V, Gupta JK, Kaushal SC (1990) World J Microbiol Biotechnol 6:366
225. Singh K, Puniya AK, Singh S (1996) J Sci Ind Res 55:472
226. Bau H, Villaume C, Lin C-F, Evrard J, Quemener B, Nicolas J-P, Mejean LJ (1994) Sci Food Agric 65:315
227. Ohno A, Ano T, Shoda M (1992) Biotechnol Lett 14:817

Received February 2000

Multistage Magnetic and Electrophoretic Extraction of Cells, Particles and Macromolecules

K. S. M. S. Raghavarao[1], Marc Dueser[2], Paul Todd[2]

[1] Department of Food Engineering, Central Food Technological Research Institute (CFTRI), Mysore-570 013, India
[2] Department of Chemical Engineering, University of Colorado, Boulder, CO-80809-424, USA
E-mail: raghava@cscftri.ren.nic.in

Improved techniques for separating cells, particles, and macromolecules (proteins) are increasingly important to biotechnology because separation is frequently the limiting factor for many biological processes. Manufacturers of new enzymes and pharmaceutical products require improved methods for recovering intact cells and intracellular products. Similarly isolation, purification, and concentration of many biomolecules produced in fermentation processes is extremely important. Often such downstream processing contributes a large portion of the product cost. In conventional methods like centrifugation and even modern methods like chromatography, scale-up problems are enormous, making them uneconomical and prohibitively expensive unless the product is of very high value. Therefore there has been a need for efficient and economical alternative approaches to bioseparation processes to eliminate, reduce, or facilitate solids handling. Magnetic and electric field assisted separations may hold considerable potential for providing a future major improvement in bioseparation technology.

In the present review the merits and demerits of the existing methods are discussed. We present mainly our own research on the development of unified multistage extraction processes that are versatile enough to handle cells and particles as well as macromolecules as described below. We describe multistage methods, namely ADSEP (Advanced Separator), MAGSEP (Magnetic Separator), and ELECSEP (Electrophoretic Separator), for quantitatively separating cells, particles, and solutes by using magnetically and electrophoretically assisted extraction processes. To the best of our knowledge, multistage magnetic and electrophoretic separations have not been reported in the earlier literature. The theoretical underpinnings of these separations are crucial to their success and to the identification of their advantages over other separation processes in particular applications. Hence mathematical modeling is stressed here, presenting our own models while also reviewing models reported in the literature. We also present suggestions for future work while analyzing the scale-up and economic aspects of these extraction processes. Commercial uses of the magnetic and electrophoretic processes, having both ground- and space-based research elements, also are presented in this review.

Keywords. Magnetic extraction, Electrophoretic extraction, Aqueous two-phase extraction, Multistage extraction, Counter-current distribution

Advances in Biochemical Engineering/
Biotechnology, Vol. 68
Managing Editor: Th. Scheper

List of Abbreviations and Symbols

a_{cell}	cell radius (m)
a_p	particle radius (m)
A	area over which the field is applied (m^2)
A_T	effective surface (heat transfer) area of the chamber (m^2)
ADH	alcohol dehydrogenase
ADSEP	advanced separator
AP	affinity partitioning
ATPE	aqueous two-phase extraction
ATPF	aqueous two-phase fermentation
ATPS	aqueous two-phase system
B	applied magnetic field (kg A^{-1} s^{-2} or tesla, T)
B_r	magnetic field component in r direction (kg A^{-1} s^{-2} or tesla, T)
B_z	magnetic field component in z direction (kg A^{-1} s^{-2} or tesla, T)
C	cell concentration (cells ml^{-1})
C_p	specific heat of the media carrying the current (kJ kg^{-1} K^{-1})
C_{pc}	specific heat of the coolant (kJ kg^{-1} K^{-1})
CCD	counter-current distribution

CZE	capillary zone electrophoresis °C
d	diameter of the solute or droplet sphere (m)
dB/dz	magnetic field gradient in the direction of motion
dy/dt	velocity of the bioparticle in electric field (m s^{-1})
dz/dt	one-dimensional particle motion
D	diameter of the chamber or distance (perpendicular to g) from the high temperature to the closest lateral boundary (m)
DX	dextran
e	electrical charge (C)
E	electric field strength (V m^{-1})
E_p	parameter in Eq. 27 ($E_p = KR$)
ECCD	electrophoretic counter current distribution
ELECSEP	electrophoretic separator
F	total force on a particle (N)
F_b	buoyancy force (N)
F_d	drag force (N)
F_g	gravitational force (N)
F_m	magnetic force (N)
g	acceleration due to gravity (m s^{-2})
Gr	Grasshof number
G-6-PDH	glucose-6-phosphate dehydrogenase
h	total depth of chamber (m)
h_T	heat transfer coefficient (kW m^{-2} °C^{-1})
H	magnetic field strength (A m^{-1})
H_c	chamber height (m)
H_P	volume of the heavy phase (m^{-3})
HGMSs	high gradient magnetic separations
i	unit vector in the z direction
I	current (A)
J	flux of cells in magnetic field (cell m^{-2} s^{-1})
k_E	electrical conductivity of the medium (S m^{-1})
k_T	thermal conductivity of the medium (kW m^{-1} °C^{-1})
K	solute partition coefficient ($K = x_s/y_s$)
l	length of element (in Eq. 1)
L_P	volumes of the light phase (m^{-3})
LDH	lactate dehydrogenase
m	number of bioparticles that would migrate during a single step
m_p	mass of the particle (kg)
$(m_1)_{n,r}$	number of type-1 particles with mobility μ_{1E}
M	induced polarization (Eq. 3)
M_c	flow rate of the coolant that is to be circulated to remove the required heat (kg s^{-1})
MAGSEP	magnetic separator
MDX	maltodextrin
n	stage or chamber number
N	total number of bioparticles initially ($t = 0$) present in the first bottom chamber ($N = N_1 + N_2$)

$[N_1]_{r-1}$	number of particles of mobility μ_{E1} in stage 'n' at transfer or step (r – 1)
N_1	number of bioparticles with mobility μ_{1E} $[N_1 = x_1(N)]$
N_2	number of bioparticles with mobility μ_{2E} $[N_2 = x_2(N)]$
Nu	Nusselt number
ORSEP	organic separator
p	parameter in Eq. (27) [p = E/(E + 1)]
Pd	palladium
6-PGDH	6-phosphogluconate dehydrogenase
PEG	poly(ethylene glycol)
PPE	phase partition experiment
PTK	phophofructokinase
Pr	Prandtl number
Q	heat to be removed from the system (kW)
r	transfer or step number
r_c	radius of chamber (m)
R	phase volume ratio (R = L/H)
Ra	Rayleigh number
Ra_c	critical Rayleigh number
Re	Reynolds number
RME	reverse micellar extraction
t	time of application of electric field(s)
u_m	magnetic energy density
U_m	magnetostatic potential energy
v	drop velocity (m s^{-1})
v_{cell}	velocity of the cell (m s^{-1})
v_E	drop velocity due to electric field (m s^{-1})
v_{medium}	velocity (circulation) of the medium (m s^{-1})
v_p	velocity and can be assumed to be equal to $\Delta z/\Delta t$ (m s^{-1})
V_b	volume of the lower cavity half (m^3)
V_{cell}	volume of the cell (m^3)
V_p	particle volume (m^3)
V	volume of the chamber (m^3)
V*	mis-alignment volume (m^3)
W	power density (kW m^{-3})
x_s	mass concentration of the solute in the light phase (kg m^{-3})
x_1	fraction of type 1 particles
y_s	mass concentration of the solute in the heavy phase (kg m^{-3})
y	distance of electrophoretic migration by bioparticles during the electric field application of time τ
z	distance of unidimensional motion (m)
β	coefficient of thermal expansion ($°C^{-1}$)
λ	function of the conductivities of the dispersed or droplet phase and continuous phase (Eq. 26)
μ	chemical potential
μ_0	magnetic permeability of free space
μ_E	electrophoretic mobility of bioparticle (m^2 V^{-1} s^{-1})

μ_{1E}	electrophoretic mobility of type 1 particles ($m^2\ V^{-1}\ s^{-1}$)
μ_{2E}	electrophoretic mobility of type 2 particles ($m^2\ V^{-1}\ s^{-1}$)
$\Delta\chi_m$	magnetic susceptibility difference
$\Delta\chi_c$	bulk magnetic susceptibility between the particle and the surrounding medium
χ_{cell}	magnetic susceptibility of cell
χ_m	magnetic susceptibility
χ_{medium}	magnetic susceptibility of medium
τ	time of application of the electric field(s)
$\partial B/\partial r$	rate of change of the magnetic field along the vertical axis r
$\partial B/\partial z$	rate of change of the magnetic field along the vertical axis *z*
ρ	density of the system ($kg\ m^{-3}$)
ρ_{cell}	density of the cell ($kg\ m^{-3}$)
ρ_{medium}	density of the medium ($kg\ m^{-3}$)
ρ_C	density of solvent or the continuous phase ($kg\ m^{-3}$)
ρ_D	dispersed or droplet phase density ($kg\ m^{-3}$)
ρ_o	medium density ($kg\ m^{-3}$)
ρ_p	particle density ($kg\ m^{-3}$)
ρ_S	density of solute sphere or dispersed phase droplet ($kg\ m^{-3}$)
$\Delta\rho$	density difference ($kg\ m^{-3}$)
σ_E	surface charge density ($C\ m^{-2}$)
Δt	time interval required for particle separation (s)
ΔT	rise in temperature (°C)
Δz	vertical height of particle migration (m)
η	viscosity ($kg\ m\ s^{-1}$)
η_C	viscosity of the solvent or continuous phase ($kg\ m\ s^{-1}$)
η_D	viscosity of the dispersed phase ($kg\ m\ s^{-1}$)

1 Introduction

Separation science and technology is one of the most complex and important area of biotechnology and biochemical engineering. New separation technologies, capable of treating dilute solutions in both small and large-scale processes, even in the presence of particulate matter, are necessary. Electrophoretic and magnetic separation techniques appear to have potential in this area with a wide range of applications. Manufacturers of new enzymes and pharmaceutical products require improved methods for recovering intact cells and intracellular products. There is an increasing need for efficient methods to recover cells selectively from other bioparticles to generate a feedstock for product separation processes involving chromatography and membrane separations. Similarly, isolation, purification, and concentration of many biomolecules produced in fermentation processes are extremely expensive. Often such downstream processing contributes a large portion of the product cost [1, 2]. Many methods of cell separation have been reviewed in the literature [3, 4]. In the present review we briefly discuss the suitability of various methods for different applications.

Magnetic separation technologies, though conventionally being used for ore and chemical industries, have gained importance for biotechnological applications quite recently [5, 6]. Similarly, aqueous two-phase extraction and reverse micellar extraction have recently gained prominence for the downstream processing of macromolecules. In the present review these methods are analyzed especially in terms of the reasons for not realizing their full market potential. We present mainly our own research on the development of unified multistage extraction processes that are versatile enough to handle cells as well as macromolecules as given below.

We describe multistage methods, namely ADSEP (Advanced Separator), MAGSEP (Magnetic Separator), and ELECSEP (Electrophoretic Separator), for quantitatively separating cells, particles, and other macromolecules by using magnetically and electrophoretically assisted extraction processes. These methods are expected to cost much less in comparison with the competing technologies at similar scale and precision. These multistage methods build on the counter-current distribution technology of classical chemical engineering separations, stemming from the seminal work of Craig and Craig [7] and later applied to aqueous two-phase extraction (ATPE). Earlier exploitation of this sliding chamber concept has been attempted with only partial success due to some shortcomings related to convenience and practicability. In the present review we indicate how these shortcomings can be alleviated by combining concepts, so that more efficient and convenient automated magnetic and electrophoretic bioextraction processes can be developed. We also presented a few suggestions for future work while analyzing the scale-up and economic aspects of these extraction processes. Commercial uses of the magnetic and electrophoretic processes, having both ground and space based research elements, also are presented in this review.

To the best of our knowledge, multistage magnetic and electophoretic separations have not been reported in the earlier literature. While other processes involve some element of trial and error (e.g., identifying an appropriate solution), the theory behind magnetic and electric field assisted separations provide the ability to predict how unknown cells, particles, and macromolecules will react to magnetic and electric fields. Hence mathematical modeling is stressed in the proposed review, discussing our own models while reviewing the models reported in the literature.

2
Cell and Particle Separations

2.1
Magnetic Extraction

Magnetic extraction has been used in various biological processes such as biochemistry, biotechnology, and environmental technologies. Magnetic extraction, based on magnetic sorbents, carriers, and modifiers, has been used for isolation, modification, detection, immobilization, and removal of a variety of biologically active compounds, xenobiotics, cellular organelles, and cells.

The developments that aroused fresh technical interest in magnetic separations are:

1. New methods for generating high magnetic field gradients.
2. The introduction of reasonably priced efficient and superconducting magnets [8].
3. New developments in magnetic labeling techniques for cells and microspheres that have extended the useful range of High Gradient Magnetic Separations (HGMSs) into many important areas of biotechnology [1].

No widely-used magnetic method has yet been developed to separate cells on the basis of the amount of ligand bound. By combining magnetic extraction, used as a rate process, with countercurrent extraction, it is now possible to use magnetic separation of cells as a quantitative technique, separating on the basis of the number of ligands bound per cell. This could be qualitative, based on the amount of ligand bound to each kind of cell, or quantitative, based on the amount of ligand bound to cells of the same type, some with high receptor content and some with low.

There are numerous examples of potential uses of magnetic extraction methods. Separation of high CD4 from low CD4 binding cells from all other cells in whole blood is a very significant procedure for the study of immune function in leukemia, AIDS, and immunomodulation caused by environmental stresses. Research laboratories have recently used receptor number as a dependent variable in a variety of scientific applications, such as endocrinology [9], growth regulation [10, 11], virology [12, 13], carcinogenesis [14, 15], infectious diseases [16], neurology [17], and nutrition [18].

2.1.1
Existing Methods – Brief Summary

Magnetic separation methods can be classified into two main types. In the first type, separand is intrinsically magnetic so that magnetic separation can take place without any modification. There are only a few examples of such materials in biotechnology, such as red blood cells containing high concentrations of paramagnetic hemoglobin, magnetotactic bacteria containing small magnetite particles within their cells, and magnetic particles used in waste water purification systems. In the second type, one or more non-magnetic components of a mixture have to be rendered magnetic by the attachment of a magnetically responsive entity. The newly formed complexes have magnetic properties and can be manipulated using an external magnetic field [5].

Magnetic properties include ferromagnetism, paramagnetism, and diamagnetism, and specific materials including cells and biomolecules can exhibit these properties [8]. The most naturally labeled cells that are separated by HGMS are probably the magnetoactive aquatic bacteria [19]. These organisms contain small single-domain crystals of magnetite, and the ability to be oriented in a magnetic field remains even when the organism dies. Several patents have already been granted in the USA and Japan describing potential uses of these rare organisms in medical applications [1].

The simplest technique for adding ferromagnetic properties to biological matter is to supplement the solution with small magnetite particles and using the natural surface and colloidal properties of both the magnetite and the biological material to obtain the desired separation from the solution [1]. Although this technique is not very selective, it works very well in cases where total removal of cell mass is required, for example, from fermentation broth or waste water. The technique can be further improved by adjusting surface and/or colloidal properties and/or by adding a flocculating agent [6]. Ferrofluids (surfactant stabilized magnetite colloids) had also been extensively used for ferromagnetic labeling as reviewed by Rosenberg [20] and their application in affinity chromatography was discussed by Mosbach and Anderson [21].

Most of the applications of HGMS of paramagnetic material pertain to red blood cells (erythrocytes) [6, 22]. The technique relies on the paramagnetic properties of hemoglobin groups in erythrocytes when they are in the reduced state (Fe^{2+}). When hemoglobin combines with oxygen it becomes diamagnetic. No evidence of damage to erythrocytes was found when they were separated from whole blood by HGMS [22]. This opened up a wide range of clinical and research uses of HGMS of red blood cells as this method has advantages over centrifugation in that it is completely selective and can be made a continuous process. The low magnetic susceptibility of erythrocytes [22] is compensated by using lower flow rates than in the other (magnetically labeled cells) applications of HGMS to maintain the level of adsorption [1]. There are other ways to induce paramagnetism. For instance, large positive susceptibilities can be introduced into biological particles by their adsorption of magnetic cations. The trivalent cations of the lanthanide series are especially effective at relatively low magnetizing fields compared to hemoglobin. It was demonstrated that cells from whole blood, yeast cells, bacteria and *Vistna* virus can be magnetically recovered from Er^{3+}-containing solutions with an efficiency greater than 80% [23]. The binding of the ion is affected by the pKa of the binding group, the pH, and the ionic strength and hence these parameters could be varied to magnetize a specific material preferentially [1].

Diamagnetic materials can be separated by using a strongly paramagnetic background fluid which increases the contrast. White blood cells and platelets have been extracted by this method though in general the range of concentration of the carrier medium is limited by the osmotic pressure effects on the cell membrane [6].

Two possible modes – direct and indirect – are available for the isolation of target cells or compounds. The former is often employed, in which magnetic particles with immobilized affinity ligands are directly suspended in the solution or suspension. During the course of incubation the target cells bind with the immobilized ligand and the whole complex can then be separated using a magnet. In the indirect mode, the target cells interact with the affinity ligand, usually a primary antibody, that has first been added to the solution or suspension in the free form, to form a complex during incubation. Magnetic particles with immobilized secondary antibodies are then added. Finally the magnetic complex formed is separated in a magnetic separator.

Magnetic particles with immobilized lectins can be used for the isolation of polysaccharides or structure containing sugar moities. This technique has been used for the isolation of various microbial cells from culture media [24]. Immunomagnetic particles – magnetic particles bearing immobilized specific antibodies against the target structures – can be used for the selective isolation of specific cells such as prokaryotic and eukaryotic [25, 26].

Magnetic modifications of standard immunoassays can be successfully used for the determination of microbial cells [26], parasites [27], and viruses [28]. Cells to which magnetic carriers are attached can be removed from the system simply by using an external magnetic field, or can also be targeted to the desired place. Non-porous magnetic supports with a diameter of 1 μm or smaller are advantageous as they are more resistant to fouling, diffusional limitations, and attrition than porous supports [1, 29]. There are many ways to immobilize the cells or compounds of interest and practically all the standard procedures used in affinity chromatography can be used for this purpose. Again, similar to the chromatography methods, a spacer must often be inserted between the magnetic particle and the ligand to overcome steric hindrance at the cell surface. Several microorganisms have been immobilized on magnetic carriers or have been entrapped in biopolymers containing magnetic material. These methods are useful in applications where suspended particles and viscous substances are present in the fermentation medium. The magnetic material usually does not interfere with the catalytic function of the cells, as shown for *Saccharomyces cerevisiae* immobilized in calcium alginate together with magnetite [30]. HGMS of yeast cells by means of irreversible adsorption of very fine particles of maghemite (gamma-Fe_2O_3) on the cell wall was reported [31]. Binding of paramagnetic erbium ions on various surface structures of microbial cells also leads to the formation of magnetized microorganisms [32]. Many other applications in different biorelated areas, apart from the specific ones given in this section, are discussed by Safarik and Safarika [33], in an excellent review article on magnetic separations.

Gravity-dependent phenomena associated with separation processes have been studied in the low-gravity environment of space flight [34]. Magnetic field-based separations, on the other hand, have not been pursued in microgravity research. In general, gravity assists the separation of magnetized from unmagnetized separands [35], or magnetic stabilization is designed to avert effects of gravity [36, 37]. Flowing systems [38] can be considered relatively gravity independent. However, certain gradient-dependent separations have a meaningful gravitational component, and Owen's work suggests that enhanced separation could be achieved in a ferrofluid relieved of the gravity vector [39].

The method of cell separation using a magnetic field has been implemented as a binary separation between cells that have and have not bound magnetic microspheres on the basis of a cell receptor (a specific type of surface ligand), as shown in Fig. 1.

Apart from the above-mentioned interests in low-gravity research applied to separation science and technology, there is an interest in performing separations in support of low-gravity biotechnology, immunology, cytology, serology, microbiology, and chemical procedures on the International Space Station

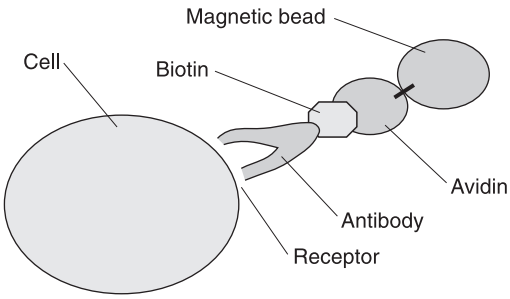

Fig. 1. Magnetic bead attached to cell receptor

Alpha [40]. Addressing this concern is likely to require innovative research on separation processes that require a body force but will function independently of the gravitational vector, yet possibly be enhanced by gravitational unloading.

Continuous collection and processing of blood samples from animals and crew members is best done by analyzing samples for cell types when the samples are fresh. Methods available for separating cells for characterization are sedimentation, flow cytometry, electrophoresis, differential adsorption, and magnetic separation [41]. Sedimentation can provide only a binary separation unless elutriation or a density gradient is used. Elutriation is complicated and requires fraction collecting capability. Density gradients are difficult to form in low gravity and on a centrifuge while it is operating at moderate speed for cell separation, and, in any case, differential sedimentation would be a multistep process. Flow sorting produces small sample sizes and requires unnecessarily complex and expensive equipment ($200,000 on the ground). Electrophoresis, like sedimentation, separates cells on the basis of an intrinsic physical property. Adsorption and magnetic separations are usually based on affinity ligands immobilized to adsorbents in the former case and magnetic microspheres in the latter.

It is easy to argue that magnetic cell separation methods are the easiest to implement in low gravity, and that they can be made quantitative; that is, cells with low amounts of microspheres bound by ligand can be separated from cells with high amounts of microspheres bound by ligand.

2.1.2
Multistage Magnetic Method

Magnetic field gradients can be set up as shown in Fig. 2, but many configurations of magnetic poles can be used to create the gradient; for example, N and S poles could be placed on opposite sides of the upper cavity, and a metal hairpin could hang into the cavity to create a gradient around the hairpin [38]. Additional configurations are considered below.

The development of user-friendly devices that are capable of separating particles according to quantity of ligand on their surfaces appears to be the area of greatest need in improving magnetically-assisted separation devices. The

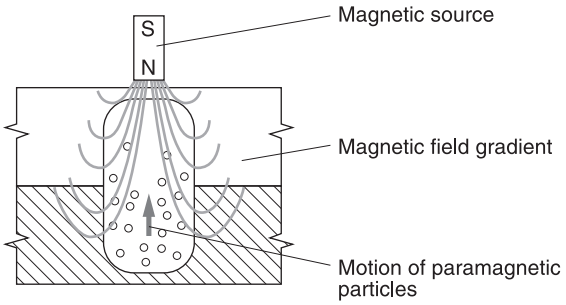

Fig. 2. Single stage of the magnetic separation process

magnetic separation industry has made considerable progress in this regard, but the commercial technology to date has been limited to binary separation methods. The innovation presented here represents progress by finally providing a reliable method for differential magnetic separation on the basis of small differences in surface composition.

The model equations (discussed in Sect. 2.1.3) are used as the basis for the design of a multistage separation system where the separation driving force is electromagnetic (Fig. 3). In staged magnetic separation, the final distribution of separands can be calculated from a simple relationship involving the number of transfers and the equivalent of a partition coefficient, K, defined as the ratio of upper and lower compartment concentrations.

Capture could be isocratic (magnets in all stages having equal strength) or gradient (magnets at increasing stage numbers having increasing field strength). In the latter case, in a typical application the first stage has no magnet and no upper cavity and serves the purpose of homogenizing the cell mixture by stirring just before the beginning of transfers. The second stage also has no magnet and serves the purpose of adding magnetic particles to the cell suspension from a low-volume upper cavity, mixing them together, and allowing them to react. The third stage has a very weak magnet in the upper cavity, and attracts only the most highly magnetized cells, namely those with the most receptors for bonding with the magnetic microspheres. The fourth stage has a

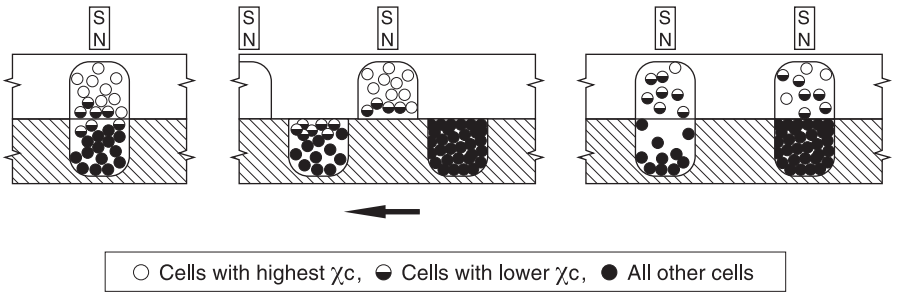

Fig. 3. One transfer in the multistage electromagnetic separator process

stronger magnet than the third in its upper compartment and attracts more weakly magnetized cells, etc., until, at the last-but-one stage the strongest magnet of all captures the cells with the fewest receptors. The final stage also has no magnet and will contain any remaining completely unmagnetized cells after the final transfer. In the presence of gravity, uncaptured cells settle into the lower cavities by gravitational sedimentation if the transfer times are made sufficiently long. In the absence of gravity, uncaptured cells would remain in both the upper and lower cavities at each transfer. However, continued mixing with each transfer would have the effect of removing the uncaptured cells in each cavity.

This method can separate both particulate (cells) and soluble (proteins) separands. The electromagnetic method for separating solute molecules resembles the magnetically stabilized fluidized adsorption bed developed by Noble and co-workers [36, 37]. The separand will bind to magnetized chromatography beads, and these will be drawn to the upper chamber by the electromagnetic field. If the binding is due to specific affinity, then K will be very high, as non-binding solutes will be quickly diluted away by subsequent transfers.

A comprehensive mass-balance model of multistage separation has been developed [42]. Figure 4 graphically represents how the multistage separator is equivalent to a tall separation column.

The electromagnetically-assisted separation process was employed by modifying a multistage technology previously developed ADSEP. The ultimate objective is to design and fabricate a prototype of a multistage electromagnetic separator for purifying cells and proteins. The combination of these two innovative technologies promises to provide a unique new method for performing cell and particle separations and meeting a growing commercial demand.

In order to establish the feasibility of multistage electromagnetic separation, the following technical objectives were addressed:

1. Determination of how closely a theoretical model can predict the outcome of an electromagnetically-assisted separation.
2. Optimization of magnetic field, stirring procedure, and magnet design to capture magnetized cells and particles.
3. Resolve if (and how) the existing multistage configuration may need to be altered to accommodate the electromagnetic separation process.
4. Establish the effectiveness of separating and classifying model particles and model cells in a multistage process, which has magnets of gradually increasing strength at each successive stage.
5. Determine optimal number of cavities to accommodate various degrees of separation in the electromagnetic separation process.
6. Evaluate user requirements, applications, and commercial potential for a multistage electromagnetic separator.

A preliminary concept for magnetic separation (MAGSEP) has been developed and the feasibility of the concept was established.

MAGSEP is designed to operate based on separation governed by particle migration rates rather than static binary separations. Due to the non-static nature of MAGSEP, there is no equilibrium point constant or partition coef-

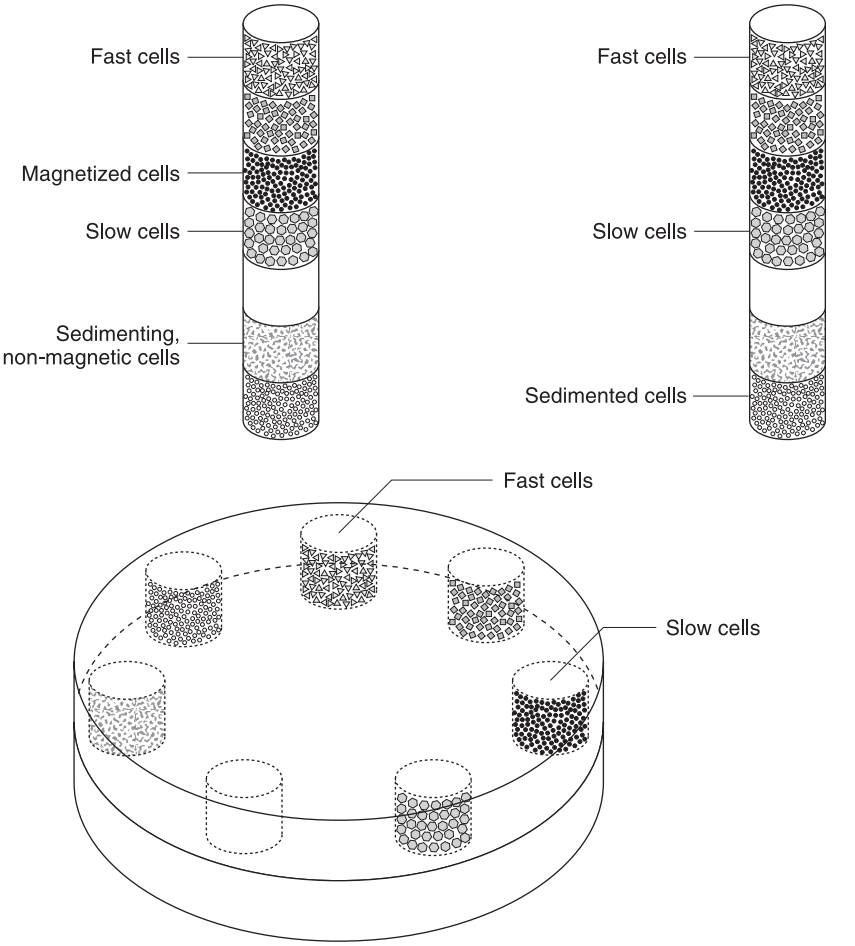

Fig. 4. Multistage electromagnetic separator compared with a magnetic chromatography column

ficient that can be predetermined. By determining a specific set of conditions (i. e., constant geometry, magnetic field, materials, etc.), the selected volumetric susceptibility range becomes a function of the time that the particles are in motion. The relationship between the susceptibility range separated and time could then be condensed into a single mathematical equation. The constant produced as a result of the fixed variables would give an indication of the ratio of particles in the upper cavity compared with the number of particles in the lower cavity at the separating time.

Experiments using inactivated magnetotactic bacteria and a single permanent magnet repeatedly confirmed that rather weak magnetic particles could be translated at a controlled velocity through an aqueous medium over distances up to 2 cm.

A magnetically adapted ADSEP was used to reduce the above principle to practice. Using large (1–2-μm) paramagnetic beads from Polysciences, Inc. (Warrington, PA, cat. no. 19131), a series of cylindrical magnets of increasing strength with increasing cavity number was positioned above six consecutive cavities of the ADSEP upper plate in the programmable ADSEP base device. These commercial particles have a broad distribution in size and susceptibility (shown in Fig. 5). The permanent-magnet pole pieces were of the same diameter as the cavities. In the example described below, particles were magnetically attracted to the upper cavity, without agitation, during 5-min intervals of exposure to successively increasing magnetic fields. The number of particles captured in each upper cavity was then counted using a microscope and hemacytometer. The results at various field strengths and gradients are given in Table 1.

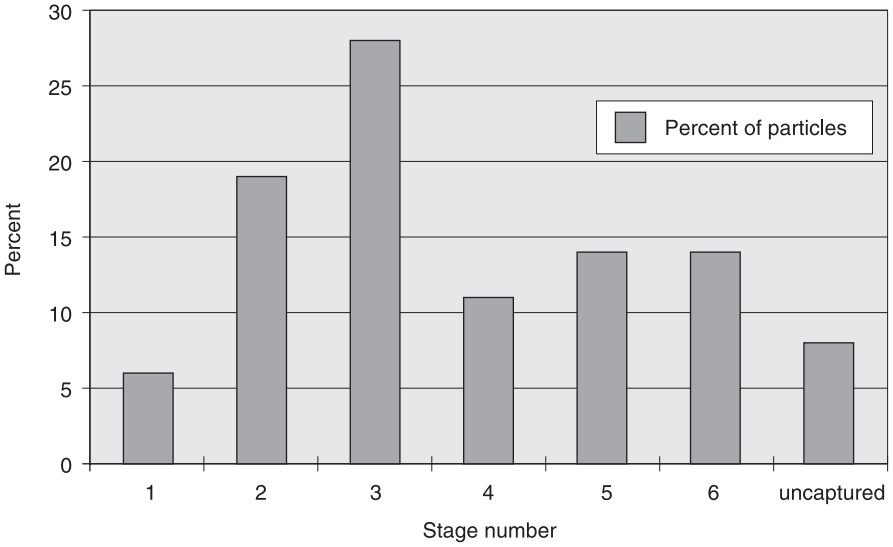

Fig. 5. Histogram of particles separated in each stage of MAGSEP using increasing fields and gradients, and $\Delta t = 5$ min

Table 1. Particle separation test data for MAGSEP

Stage number	Pole Flux (Mt)	Gradient (TM^{-1})	Gradient ($kg\,m^{-1}$)	Percent of particles
1	1.70	0.105	0.0105	6 + 2
2	10.81	0.672	0.0672	19 + 3
3	10.25	0.629	0.0629	28 + 4
4	15.75	0.918	0.0918	11 + 3
5	260	15.76	1.576	14 + 3
6	320	19.19	1.919	14 + 3
Uncaptured				8 + 2

The effect of adjusting exposure time was explored, and it was found that short exposures result in less particle capture at early stages and aggregation by stronger magnets at later stages. This important discovery that proper temporal programming can prevent aggregation makes the MAGSEP concept feasible. In addition, the magnets used in the above experiment had pole fluxes ranging over two orders of magnitude, and the weak magnets were shown to attract large beads while, in separate experiments, the strong magnets were shown to attract weak particles such as magnetotactic bacteria (data not shown).

2.1.3 *Theory and Mathematical Models*

The range of magnetic field required for cell separation is obviously decided by the magnetic and mechanical properties of the cells. A review of the mathematical formulae that are relevant to cell extraction and their illustration by selected examples was presented well by Zborowski [43].

The magnetic field is a space domain where an electrical charge 'e' moving with velocity 'v_e' experiences a magnetic force 'F_m', given by

$$F_m = IlB \tag{1}$$

where 'I' is the current intensity, l is length of element, and B is the magnetic field intensity (kg A^{-1} s^{-2} or Tesla, T) given as

$$B = \mu_o H \tag{2}$$

where μ_o is magnetic permeability of free space and H is the magnetic field strength (A m^{-1}). The presence of matter in the magnetic field modifies the field fluxes at given constant field strengths. The magnetic properties of matter are defined by induced polarization M to account for the variation in magnetic flux. For isotropic media

$$M = \chi_m H \tag{3}$$

where χ_m is magnetic susceptibility. In the uniform magnetic field the magnetic particle undergoes rotation until Maxwell stress tensor becomes zero and then remains stationary with respect to the medium. In the non-uniform field, differences in the Maxwell stresses result in a net force F_m acting on the magnetic particle given as

$$F_m = V_p (M \cdot \nabla) B \tag{4}$$

where V_p is the volume of the particle. In the simplest one-dimensional case, using Eq. (3), it can be written as

$$F_m = V_p \chi_m H \frac{dB}{dz} \tag{5}$$

In homogenous media, magnetic field B is parallel and proportional to the magnetic field strength H. Magnetic force lines are defined as curves which are

tangent to the direction of vector F_m. In general, due to non-linear relationship between the magnetic force F_m and the magnetic field H, the lines of magnetic force do not follow the lines of magnetic field B. In other words, even in homogenous media, the lines of magnetic field do not represent the lines of force exerted on the elementary dipole. The correct representation of such forces are the lines of the magnetic force F_m. This is drastically different from the static electric field, in which electric force lines are synonymous with electric field lines.

Now the work required to bring all the components of the magnetic system from infinity to their given spatial position is defined as magnetostatic potential energy U_m, which with the help of Eqs. (2) and (3) can be given as

$$U_m = V_p \chi_m u_m = -\frac{V_p \chi_m B^2}{2\mu_o} \tag{6}$$

where u_m is magnetic energy density, given by $-B^2/2\mu_0$. The relationship between the force and the potential energy leads to the following expression of the magnetic force:

$$F_m = -\nabla U_m = -V_p \chi_m \nabla u_m = \frac{V_p \chi_m \nabla B^2}{2\mu_o} \tag{7}$$

The direction of the magnetic force F_m relative to the energy density gradient ∇B^2 depends on the sign of χ_m. For paramagnetic substances, $\chi_m > 0$ and the force vector points toward the direction of the maximum increase in magnetic field energy density, termed magnetic attraction. For diamagnetic substances $\chi_m < 0$ and the force vector points in the opposite direction to the maximum increase in the field energy density, termed magnetic repulsion. When the particles are suspended in a medium of magnetic susceptibility χ_m, then in the above expression χ_m is to be replaced by $\Delta\chi_m$. Consequently the above discussion applies to $\Delta\chi_m$ rather than χ_m.

Thus the very basis for all magnetic cell extractors is the observation that forces acting on small magnetic particles follow the lines of gradient of the magnetic field energy density.

2.1.3.1 Model for Viscous Medium

A simple mathematical model is developed based on the theory discussed, till now, for the motion of magnetically labeled cells in a viscous medium in the presence of magnetic field [43]. The following assumptions are involved:

1. Cells are small compared to the characteristic magnetic field and fluid flow dimension
2. Cells are treated as magnetized rigid spheres while calculating magnetic and fluid drag forces
3. Specific density of the cell is similar to that of the medium
4. Inertial forces are too small to be considered when compared with the viscous ones

With these assumptions the equation of motion – involving the forces magnetic (F_m), drag (F_d), and buoyancy (F_b) – is written as

$$F_m + F_d + F_b = 0 \tag{8}$$

where

$$F_m = \frac{(\Delta\chi_m)\, V_{cell} \nabla B^2}{2\mu_o} \tag{9}$$

$$F_d = 6\pi\eta a_{cell}(\upsilon_{cell}) \tag{10}$$

$$F_b = V_{cell}(\Delta\rho)\, g \tag{11}$$

when the circulation in the medium is neglected (v_{medium}) due to high viscosity. It may be noted that $V_{cell} = 4\pi a_{cell}^3/3$, $\Delta\chi_m = (\chi_{cell} - \chi_{medium})$ with magnetic susceptibility replaced by volume average cell susceptibility and $\Delta\rho = (\rho_{cell} - \rho_{medium})$. On solving for v_{cell},

$$\upsilon_{cell} = -\frac{(\Delta\chi_m)\, a_{cell}^2 \nabla B^2}{9\mu_o\eta} - \frac{2(\Delta\rho)\, a_{cell}^2 \nabla B^2}{9\eta} \tag{12}$$

In order to obtain the flux J, both sides are multiplied by concentration of cells C:

$$J = -\frac{C(\Delta\chi_m)\, a_{cell}^2 \nabla B^2}{\mu_o\eta} = C\upsilon_{cell} + \frac{2(\Delta\rho)\, a_{cell}^2 g}{9\eta} \tag{13}$$

This equation states that the flux of magnetically labeled cells relative to the medium follows the lines of magnetic energy density gradient. Here the mass flux of small magnetic particles (cells) is coupled to the driving force of the magnetic energy density gradient. As the magnetic particles are assumed to be rigid bodies of finite volume such that convective, gravity, and buoyancy forces can be neglected, the magnetic particles are expected to accumulate forming layers around the magnetic surfaces. Furthermore, the surfaces of the magnetic layers follow the surfaces of constant magnetic energy density or B2 is constant. Zborowski [43] has given examples, illustrating this observation, based on the literature reports on particle accumulation on wires and solid surfaces exposed to the magnetic field.

This model [43] could be easily adapted for our MAGSEP. Additional assumptions made at this point include:

1. All particle motion is vertical.
2. The drag force is negligible except for in the vertical direction.
3. The axial magnetic field is constant over the radius of the cylindrical cavity of the MAGSEP.
4. Creeping flow conditions (low Re).
5. Particle velocity is constant and is equal to the mean velocity of migration ($d^2z/dt^2 = 0$).

Magnets with large cross sections (relative to the cavity cross section) were selected and, as a result, the magnetic field was considered to be constant over

the radial cross section, or

$$\frac{\partial B}{\partial r} = 0 \tag{14}$$

By taking the dot product of the magnetic field and the gradient of the magnetic field, the following differential relationship is determined:

$$B \cdot \nabla B = B_z \cdot \frac{\partial B_z}{\partial r} + B_r \cdot \frac{\partial B_z}{\partial z} \tag{15}$$

This relationship, combined with the above assumptions to simplify the magnetic force equation, yields the scalar magnetic force relationship similar to that given in Eq. (9). If all variable parameters for the MAGSEP experiment in this equation (B and particle size a_p) are set, then the susceptibility difference, $\Delta\chi_m$ is the controlling variable governing the magnetic force. Based on this calculation, the separation of the cells as it relates to the susceptibility difference can be governed by controlling the magnetic field B, the vertical height of separation Δz, and the time interval required for separation, Δt.

The volumetric susceptibility difference $\Delta\chi_m$ can be measured by sampling a distribution of particle positions (which is a function of their velocities). If the particles are placed in a thin flat layer across the bottom of a cavity and covered with a solution to a depth Δz, the particles can then be aligned below a shallow upper cavity with an activated magnet. The magnetic field of the upper magnet can then attract particles for a time Δt, and when a sufficient amount of particles have migrated into the shallow upper cavity, the cavities can be half-stepped to separate the particles as shown in Fig. 3. The volumetric susceptibility can then be calculated by the following relationship:

$$\Delta\chi_m = \frac{9\upsilon_p \eta / a_p^2 + 2g(\Delta\rho)}{B \cdot \dfrac{dB}{dz}} \tag{16}$$

where v_p is the velocity, and can be assumed to be equal to $\Delta z/\Delta t$. The number of particles transferred represents a distribution of the total particles and is also a representation of the number of particles within a volumetric susceptibility range. If enough separation in these stages takes place, then this volumetric susceptibility range can be assumed to be an absolute volumetric susceptibility. Further modeling of magnetic extraction in MAGSEP is in progress.

Continuous flow magnetic cell sorting using soluble immunomagnetic label and the corresponding theory was presented by Zborowski et al. [44].

2.2
Electrophoretic Extraction

2.2.1
Existing Methods – Brief Analysis

Electrophoresis is a leading method for resolving mixtures of charged macromolecules (either proteins or nucleic acids) or cells. The electrophoretic separation of proteins without gels has been a long-standing goal of separation research [45, 46]. Electrophoretic separations are influenced by many factors including the size (or molecular weight), shape, secondary structure, and charge of the macromolecule or cell. These features can influence electrophoretic properties either separately or jointly. In order to achieve the required scale-up scientists and engineers resort to flowing methods [46–48]. Scale-up of electrophoresis is hindered by ohmic heating. The heat generated is equal to the product of the current and voltage, and this heat can cause free convection and mixing within the system. Too much heat can also denature the labile biomolecules or cells.

Decades of research in free electrophoresis have identified thermal convection [49], electro-osmosis [50], particle sedimentation [51], droplet sedimentation [52], particle aggregation [53], and electro-hydrodynamic zone distortion [54] as the major obstacles to scale-up. Free electrophoresis has not gained popularity as a preparative or industrial separation method owing to these gravity-dependent characteristics. Density gradients [52, 55] or elaborate flowing devices have been required up to now to stabilize free fluid systems and/or the particles suspended in them while they are non-isothermally heated by the passage of an electric current. Without the need to prepare density gradients and/or use elaborate flowing systems, free electrophoresis could enjoy more widespread use, because it is a high-resolution separation method that does not require adsorption to solid media and the subsequent solids handling. Furthermore, it can handle particles (cells) as well as solutes (macromolecules) alike. To name a few, specific applications of free electrophoresis include the separation of different cells of peripheral blood and bone marrow in hematological and immunological research and potentially in clinical therapeutic applications [56], and the separation of proteins from body fluids, tissue extracts, and fermentation broths in biotechnology [57].

None of these principal gravity-dependent and gravity-independent processes have been investigated in multistage electrophoresis, which is designed to minimize the impact of these processes on separation quality. All of these processes have been studied in the past in applications to other forms of free electrophoresis as reviewed by Todd [34, 41].

Thermal convection, which in turn causes mixing, is induced by ohmic heating when current passes through the buffer and heats the buffer non-uniformly [49]. Above a critical Rayleigh number (Ra_c), convective circulation sets in, and it occurs in both static and flowing electrophoresis systems [54, 58]. The Ra_c is unexpectedly low in certain flowing electrophoresis applications, so that thermal convection is a significant deterrent to the development of electro-

phoresis as an industrial separation tool [59]. Under most circumstances in particle separations, conditions can be arranged so that the sedimentation of individual particles, say cells, can be minimized, but not always [51]. Finally, the diffusion-driven formation of droplets containing high concentrations of particles or solutes [60] results in 'droplet sedimentation', and at very high concentrations of particles in density-gradient electrophoresis [52] but not in low-gravity electrophoresis [54].

Another type of mixing problem encountered in free electrophoresis, although less critical compared to ohmic heating, is the mixing caused by gas release at the electrodes. This problem is addressed by employing non-gassing electrodes [61] or membrane-separated electrodes [62]. This experience points to the possibility of using non-gassing Pd electrodes (as in the present work) rather than the more complicated membrane based system of Tulp et al. [63].

A score of methods has been developed to effect free electrophoresis [41]. These methods can be broadly divided into static and flowing methods, neither of which has satisfactory capacity for application as a manufacturing tool. Batch and continuous methods have also been developed. In almost all cases maximum sample input rates have been of the order of a few milliliters per hour. In one important case, Tulp et al. [63] designed a re-orienting free electrophoresis device consisting of a flat disk-shaped container with thin sample bands and a short migration distance. The top and bottom electrode fluids served as coolant, the total height of the separation column was 1–2 cm, and its diameter was greater than 15 cm. The distance between unrelated separands was about 1–2 mm, and this distance was increased during fractionation after electrophoresis by re-orienting the disk.

Based on research experience and needs identified for free electrophoresis in various fields of bioprocessing and analysis such as virology, endocrinology, enzymology, hematology, and mammalian cell culture [64–69], in the present study an attempt is made to overcome the major bottlenecks of free electrophoresis.

2.2.2
Multistage Electrophoretic Method

The multistage electrophoretic method has been developed by combining free electrophoresis and multistage extraction and is explored as an improved alternate method for the purification and concentration of cells or macromolecules. The present discussion is restricted to cells and particles. The present design is based on a derivative of the thin-layer multistage extractor design of Albertsson [70] and Treffrey et al. [71] and called ADvanced SEParation apparatus (ADSEP), designed by SHOT, Inc. [42].

To test this method extraction of fixed human red blood cells and latex suspended in 0.01 mol l^{-1} phosphate buffer was performed at different electric field strengths such as 0.05 V m^{-1} or 0.1 V m^{-1}. A simple mathematical model was developed (discussed in Sect. 2.2.3) to describe the mass and heat transfer during the electrophoretic separation process in the countercurrent extractor employed. The experimental results agree reasonably well with those predicted

by the model, which suitably predicts separations of mixtures of cells or molecules having different electrophoretic mobilities as well.

The latest version of the ADSEP fabricated in collaboration with SHOT, Inc [42] is described in detail in Figs. 6 and 7. The extractor consists of a 22-cavity multi-stage thin layer extraction system [71]. Half-cavities oppose each other in disks that are sealed together and rotate with respect to each other. The half cavities are disk shaped, and top cavities have flat tops while bottom cavities have flat bottoms. Both contain palladium (Pd) metal electrodes that produce an electric field when the two cavities are in phase with each other. This extractor, like the Tulp device [63], takes advantage of short column height to maintain isothermal conditions. Each cavity is only a few mm in height so that the fluid within it remains isothermal during the application of an electric field that transfers the separand particles or molecules from the bottom to the top cavity. As each separand is transferred to a new cavity, it is either drawn into the upper cavity by the electric field or left in the lower cavity, depending on its

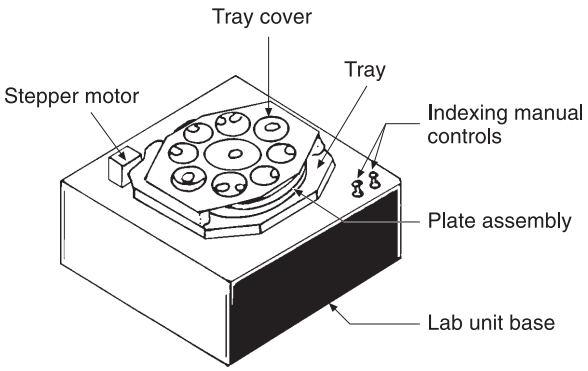

Fig. 6. ADvanced SEParation (ADSEP) apparatus

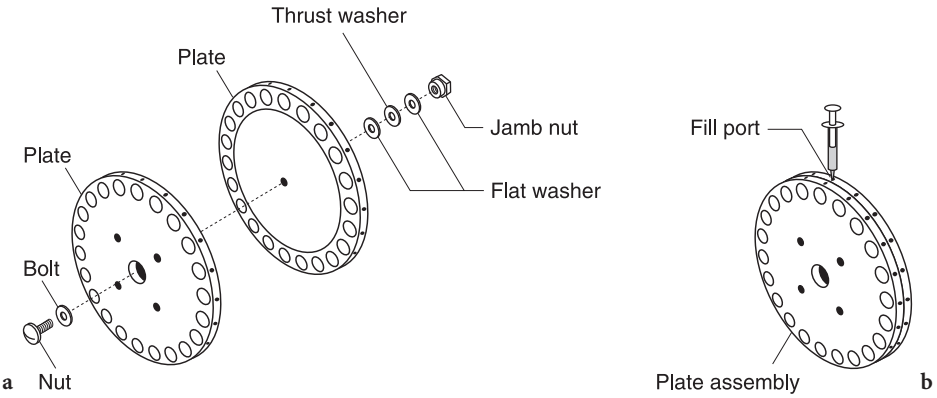

Fig. 7 a, b. Assembly of multistage extraction plates containing the chambers: **a** plates; **b** filling ports

electrophoretic mobility. The assembly of the plates containing the chambers is shown in Fig. 7a. Identically designed plates assure uniform loading and sealing when the plates are clamped together. The experimental samples are loaded and withdrawn through the fill ports located on the side of each plate as shown in Fig. 7b. ADSEP is driven by an independent power supply (Lamda, Model No. LP-532-FM) for rotating the plates to bring the chambers into interfacial contact with each other. This ADSEP was modified to use as ELECSEP by replacing the chamber bottoms with metal cover plates. Electrodes are kept over these cover plates with gaskets in between them.

Preliminary electrophoretic transfer experiments were carried out [72] with two types of particles, fixed human red blood cells and latex particles (average diameter is 3.5 µm and 2.3 µm, respectively). The particles were counted by hemacytameter with a minimum of three counts per fraction. Average values of duplicate experiments were reported.

Fixed human red blood cells, in the concentration range of $90 - 245 \times 10^4\,ml^{-1}$, were placed in suspension in 0.01 mol l^{-1} phosphate buffer (pH 8.0) in the lower cavity of stage 1 in a total volume of about 0.4 ml. A field of known intensity ($0.05\,V\,m^{-1}$ or $0.01\,V\,m^{-1}$) was applied for a specified time period (30 s or 60 s) then a fresh top chamber containing buffer only was aligned with the bottom chamber of stage 1. This process was repeated until several transfers had been completed. Cells were then removed from the top cavities, and the fraction of the original population transferred at each step was obtained by counting the suspended cells with a hemacytameter.

Precautions are required when using sliding chambers. Swapping of the liquids between the chamber liquid surfaces occurs during the time period while the chambers approach each other for the extraction transfer step and depart after the transfer. The swapping of liquid and enhanced mass transfer associated with such hydrodynamic flow for similar equipment was reported [73]. The schematic diagram indicating the swapping of liquid and flow pattern during the alignment and separation of the chamber is shown in Fig. 8 [73]. In order to assess the magnitude of cell migration due to this phenomenon, a few control experiments were performed without the application of an electric field. Results are shown in Table 2.

Considerable numbers of cells are transferred due to the hydrodynamic flow during transfer steps, especially in the initial steps. This problem is alleviated by giving sufficient settling time for the cells to settle toward the bottom of the lower cavity and by considerably reducing the speed at which the cavities are aligned during the transfer steps.

Table 2. CCD without application of electric field

S No.	Initial cells	Transfer #1	Transfer #2	Transfer #3	Residual cells
1	273	178	29	5	52
2	328	200	32	4	46

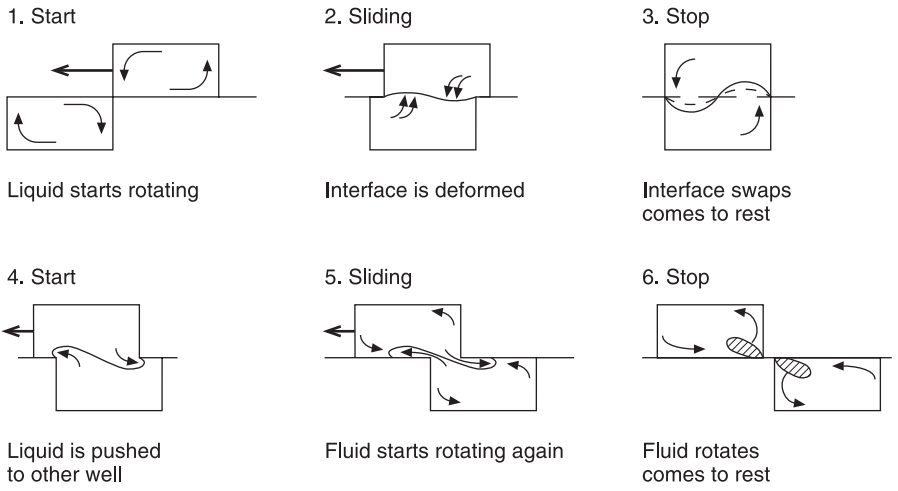

Fig. 8. Schematic diagram indicating the swapping of liquid and flow pattern during alignment and separation of the chambers

The electrophoretic extraction runs at field strengths of 5 $V\,m^{-1}$ and 10 $V\,m^{-1}$, indicated by the bar diagrams in Fig. 9a, b, respectively.

Electrophoretic extraction results of the latex particles are shown in Fig. 10a, b. From these figures it can be noted that when the field strength was doubled the cell extraction was completed in a much lower number of transfers. For instance, in case of latex particles (size 3.4 µm) at 0.05 $V\,m^{-1}$ field strength, about 450 particles were extracted in 5 transfers (Fig. 10a) and when field strength was increased to 0.01 $V\,m^{-1}$ the similar number was extracted in 3 transfers only (Fig. 10b). This can be appreciated from the fact that in Eq. (20) (in Sect. 2.2.3), the cell transport velocity increases proportional to the applied electric field strength under otherwise similar conditions. An almost equal number of cells/particles are electrophoretically extracted in each transfer step as described by the physical model in Fig. 14 (in Sect. 2.2.4) and also by Eq. 20). The exception for this was observed in case of smallest latex particles (size 2.6 µm, data not shown). This is due to the carry over of small particles by the electrode gassing at higher field strength and the extent of this effect being prominent at initial transfers where the particle concentration will be high.

The parity plot of the predicted and experimental values of the electrophoretically extracted cells/particles is shown in Fig. 11. A good agreement can be seen for fixed blood cells but not for latex particles, especially those of lower size range. Two main reasons for this situation are gassing near the cathode and heating of the buffer. Gassing results in a gas/liquid dispersion instead of liquid buffer between the electrodes, distorting the effective electric field. Further, it is causing carryover of smaller latex particles into the top chambers, causing the extracted particles to be higher than the predicted ones. Heating of the buffer causes convection current, which will have more effect on smaller particles in being swapped to the top chambers during transfers. Heating may also lower

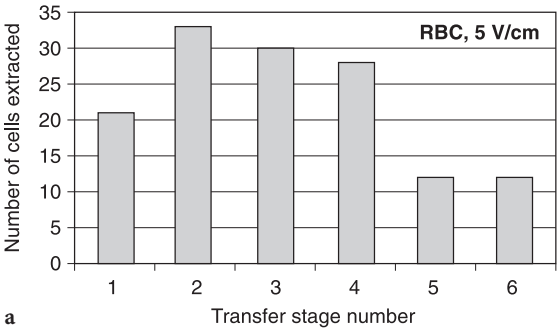

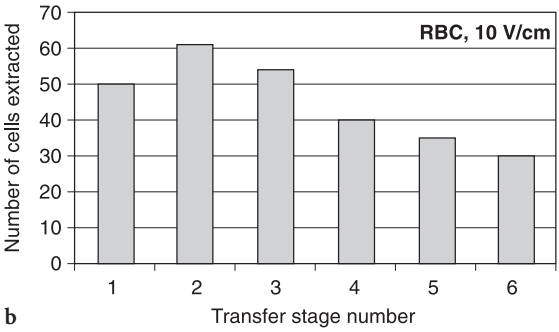

Fig. 9. Bar diagram of electrophoretic extraction of fixed human red blood cells

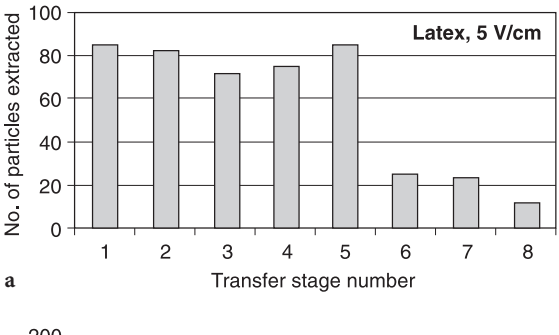

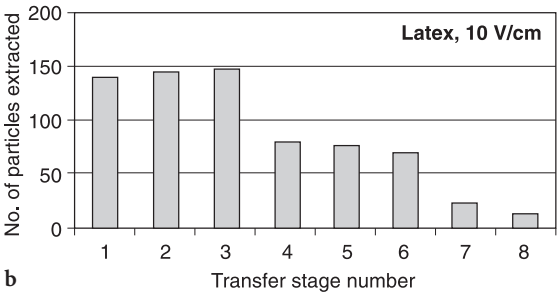

Fig. 10. Bar diagram of electrophoretic extraction of latex particles

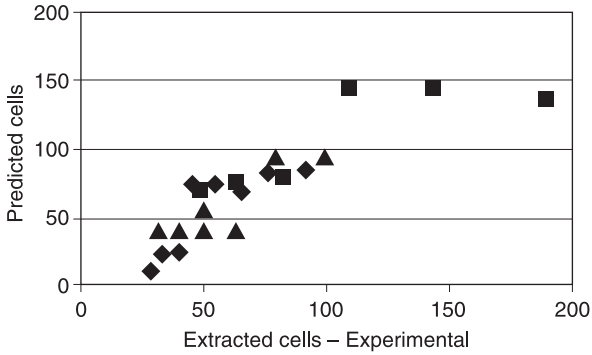

Fig. 11. Parity plot for the electrophoretic extraction of cells and particles. ◆ Latex particles (3.5 µm); ■ latex particles (2.6 µm); ▲ fixed blood cells (4.6 µm)

the effective field strength due to the variation in its conductivity with temperature. In order to overcome this problem the strength of the phosphate buffer is reduced from 0.01 mol l^{-1} to 0.002 mol l^{-1}. Note that the electrophoretic mobility of any given species increases with decreasing buffer ionic strength [74]. This enhancement at lower concentration enables the separation of cells/particles whose mobilities are only slightly different from each other. The electrophoretic extraction results of latex particles with lower ionic strength buffer are encouraging (data not show). As already discussed, the most useful application of ADSEP electrophoresis is to fractionate mixed cells/particles, exploiting the differences in their mobilities. The fractionation of a mixture containing fixed blood cells and latex particles is to be carried out.

Calculations predicted heating rates of the order of millidegrees per second for the applied current using a field that would affect motion of particles with electrophoretic mobilities around $10^{-4}\,m^2\,V^{-1}\,s^{-1}$ [72]. Theoretical values of temperature-increase (predicted values) were calculated using buffers of known conductivity and compared with exact measurements. In 0.01 mol l^{-1} phosphate buffer, $k_E = 3.6\,S\,m^{-1}$ (which is considered a high conductivity buffer for use in an electrophoretic instrument) a field of approximately 0.05 V m^{-1} was applied [72]. The Joule-heating calculation with t in seconds is given by

$$\Delta T = (IE/\rho C_p)t = 0.017\,(t) \tag{17}$$

The plot depicting the above relationship, indicating the variation of ΔT with the time of application of field at various values of electric currents, is shown in Fig. 12. The above relationship was counter checked by measuring the temperature with a thermistor probe over a 2-min period (twice the typical time period of one electrophoretic transfer) and obtaining the following linear relationship:

$$\Delta T = (1.2\,°C/120) = 0.01\,(t) \tag{18}$$

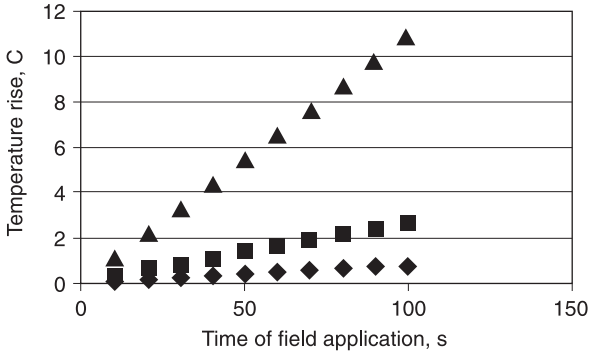

Fig. 12. Rise of temperature with the time of application of electric field. ◆ 2.5 mA; ■ 5.0 mA; ▲ 10.0 mA

Interestingly the observed temperature rise was less than the expected rise. This relationship scales linearly with conductivity and applied field (the product EI contains conductivity). The actual experimental temperature profile consisted of a rise from 23.0 °C to 24.2 °C in 120 s. In this extreme case a temperature rise of 0.6 °C per transfer (60 s of field application) could be expected. In a typical experiment involving 20 transfers, the total temperature rise would be 12 °C, typically from 23 °C to 35 °C. Thus when low-conductivity buffers are used there is no obvious reason to resort to thermoregulation since this temperature rise will be much lower.

One significant application of ADSEP electrophoresis is direct measurement of electrophoretic mobilities as demonstrated in the present work. Capillary zone electrophoresis (CZE) is normally used to measure the electrophoretic mobility of solutes in free solution. Several undesirable features of CZE are absent in the present version of ADSEP, namely:

1. Limited to solutes (particles can not be evaluated)
2. Need of a calibration standard due to electroosmotic backflow
3. Non-absolute mobility values as all measurements are relative
4. Small sample volume and hence lack of recoverable amounts of separands
5. No recovery of fractions is possible as both the ends of the capilllary are submerged in buffer

In the present case the cells/particles that move electrophoretically to the top chamber are collected and counted, and by using the following equation (derivation is shown in Sect. 2.2.3) the electrophoretic mobility can be estimated, as m is experimentally determined and other parameters except μ_E, are known:

$$m = (\mu_E E \tau / h)\,[N] \tag{19}$$

In order to confirm the validity of this approach, the electrophoretic mobilities of fixed blood cells, which are well known from the literature, are estimated by this method. The values of estimated mobilities of different cells/particles are in

good agreement with the reported values. For instance, the average value for fixed blood cells that we observed is $2.0 \times 10^{-4}\ m^2\ V^{-1}\ s^{-1}$ with the reported value at similar buffering ion concentration being $2.1 \times 10^{-4}\ m^2\ V^{-1}\ s^{-1}$.

2.2.3
Theory and Mathematical Models

In an electrophoretic counter current distribution (ECCD) apparatus, the separation of bioparticles having different electrophoretic mobilities is achieved by contacting the buffer solutions of top chambers with bottom chambers containing the bioparticles in buffer or fermentation broth, and then applying an electric field (E) at regular, predetermined intervals. The combination of electrophoresis and CCD involves the evaluation of the resulting novel instrument in terms of Joule heating, electric field development, and its ability to transfer particles. Modeling studies were undertaken in these areas, and these were followed by experimental studies [72].

2.2.3.1
Mass Transfer

Electrophoretic extraction of cells is a rate process (not an equilibrium process) and the particles having higher electrophoretic mobility are separated ahead of those having relatively lower mobility. An ECCD apparatus has 'n' extraction stages. Let us consider a situation in which all particles of electrophoretic mobility μ_E are initially in one (first) bottom chamber.

The physical description of the multistage extraction is shown in Fig. 13. In the first extraction step, the top and bottom chambers of stage 1 are brought into interfacial contact with each other. Then the field of pre-selected strength,

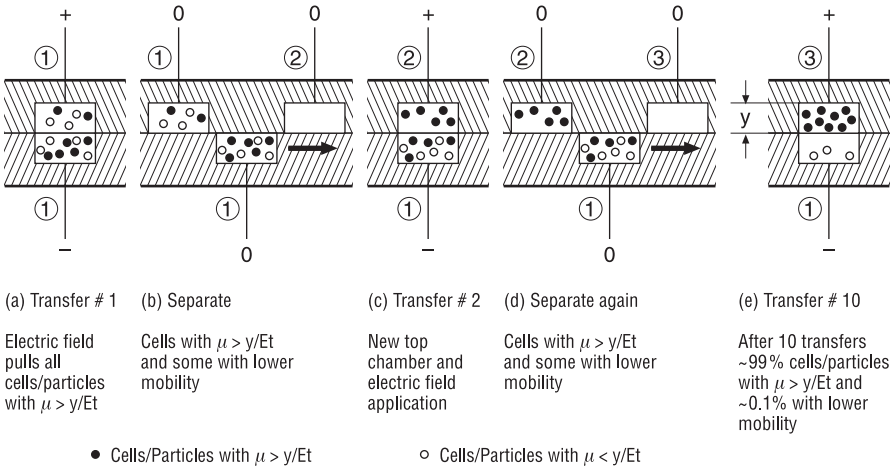

Fig. 13 a–e. Physical description of multistage extraction of cells/particles

E ($V m^{-1}$) is switched on. Cells having negative mobility move to the top chamber (each of which has an anode). After applying the field for a predetermined time period τ, the field is switched off. The bottom cavity is moved to a position to be in contact with a new top cavity having buffer. This process is repeated as many times as necessary to achieve the desired separation. Even when one type of particle is used, the particles usually have an approximately normal electrophoretic mobility distribution and not a single value. However the average mobility can be estimated under actual conditions without the drawbacks of the conventional methods. Particles can thus be fractionated from a mixture according to their mobility to meet desired purity demands. In addition cell partitioning can be controlled by modifying the electric filed strength, E as the separands pass from stage to stage.

The quantity of bioparticles initially (t = 0) present in the first bottom chamber is denoted by N. Now let us consider one chamber, whose total depth is h and radius is r_c with the bioparticles suspended in buffer solution filling the chamber. When a vertical electric field is applied the bioparticles move upward as a slug due to their electrophoretic mobility and the conceptual description of this multistage extraction of cells/particles is depicted in Fig. 14

Their velocity will be proportional to the applied field. In other words

$$\frac{dy}{dt} \propto E \tag{20}$$

$$\frac{dy}{dt} = \mu_E E \tag{21}$$

where the proportionality constant μ_E is electrophoretic mobility, a characteristic of the bioparticle, and its magnitude is determined by the surface charge of the bioparticle. Integrating the above equation between the limits y = 0 to y and t = 0 to τ, where τ is the time of application of the electric field, results in

$$y = \mu_E E \tau \tag{22}$$

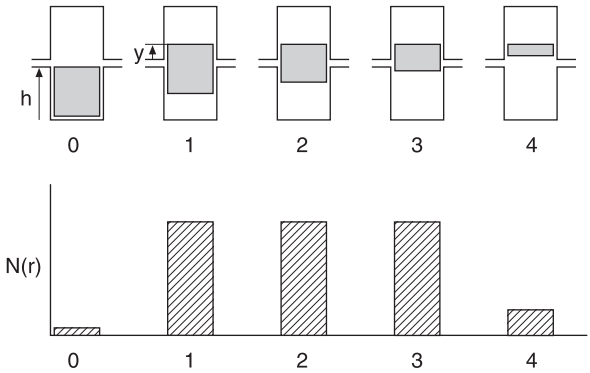

Fig. 14. Conceptual description of multistage extraction of cells/particles

so that a bioparticle of mobility μ_E moves a distance y in an electric field of intensity E applied for a time of τ. It is obvious that if E is increased τ can be decreased to achieve the same distance of migration and vice-versa, under otherwise similar conditions.

The bioparticles are randomly distributed in space over the volume of the bottom chamber. However, the time required for any individual particle to move into the top chamber increases as its distance from the top surface of the bottom chamber increases, under a given set of experimental conditions of E and τ. That is, the ratio of these heights gives the relative number of bioparticles that migrate to the top chamber at any given set of E and τ. To calculate the absolute number of particles transferred to the top chamber, the ratio of the distance to the top of the chamber to the total height h, has to be multiplied by the concentration of the particles (i.e., number of particles per unit volume), since the ratio of the heights is nothing but the ratio of the volumes of the chamber corresponding to the location considered.

Therefore, when an electric field is applied to capture the particles with mobility μ_E located at distance y from the top surface of bottom chamber, the number of bioparticles that would migrate during a single step is

$$m = (y/h)\,[N] = (\mu_E E \tau/h)\,[N] \tag{23}$$

where $N = (C)(\pi r_c^2 h)$ and C is the cell concentration (cells ml^{-1}) and $\pi r_c^2 h$ is the volume of the chamber and since $y = \mu_E E \tau$ [from Eq. (22)]. This movement of particles has already been depicted in Fig. 14

2.2.3.2 Mixed Cells/Particles

The bottom chamber contains two types of particles having electrophoretic mobilities μ_{1E} and μ_{2E}. The change in the number of type-1 particles in a stage n during step r will be equal to the number of bioparticles that migrated to the top chamber during step r. So the general equation can be written for this situation by material balance as

$$-[x_1 N]_{n,r} + [x_1 N]_{n,r-1} = (m_1)_{n,r} \tag{24}$$

where $(m_1)_{n,r}$ is number of type-1 particles with mobility μ_{E1} that migrated from stage n during step r to the top chamber; N is the total number of bioparticles present in any of the n bottom chambers, at t = 0; N_1 is the number of bioparticles with mobility μ_{1E}; N_2 is the number of bioparticles with mobility μ_{2E}; $N = N_1 + N_2$ and $x_1 = N_1/[N_1 + N_2] = N_1/N$. Now using Eq. (22), Eq. (24) can be written as

$$-[x_1 N]_{n,r} + [x_1 N]_{n,r-1} = (\mu_{1E} E \tau/h)\,[N_1]_{n,r-1} \tag{25}$$

where $[N_1]_{n,r-1}$ = number of bioparticles with mobility μ_{1E} in stage n at step (r – 1), i.e., $(C_1)(\pi r_c^2 h)$ where C_1 is the concentration of type-1 cells. Alternatively the number of type 1 particles remaining will, since $N_1 = x_1(N)$,

be given by

$$[N_1]_{n,r} = -(\mu_{1E} E \tau/h)\,[N_1]_{n,r-1} + (N_1)_{n,r-1} \tag{26}$$

This is a general equation, which enables us to estimate the fraction of bioparticles having mobility μ_{1E} at any stage provided their concentration is known in the previous stage. Similar equations can be written for other particles having mobility μ_{2E}. It can be easily extended to any number of cell/particle types in the initial sample mixture in the bottom cavity of stage 1.

The bioparticles are assumed to be uniformly distributed in the chamber and they move in a plug flow under the influence of the applied electric field (Fig. 14). Therefore in each step the same number of particles migrate to the top chamber (that are contained by the slug of height y of Eq. 22), and hence the following material balance equation can be written:

$$[x_1 N]_{n,r} = -(r)\,(\mu_{1E} E \tau/h)\,[N_1] + [N_1] \tag{27}$$

where r is the step number. With this model we can predict, for example, the number of bioparticles of different mobilities that migrated during each electro-extraction step and thereby the concentration of these particles in a given chamber during the process of multistage extraction. The model calculations are already shown in the previous section and more details are given elsewhere [72].

2.2.3.3 Heat Transfer

A major problem in the scale-up of electrokinetic processes is known to be heating which in turn causes mixing. However, the major advantage of the multistage process is the speed at which it performs separations. Hence our aim is to determine design modifications (such as provision for proper heat transfer/removal) in order to reduce the adverse effects of heating, while scaling up the process based on the basic laws of heat generation and transmission. Electrical energy is dissipated as heat according to the equation

$$W = IE/A \tag{28}$$

where W is the power density ($kW\,m^{-3}$), I is the current (A), E is the electric field strength ($V\,m^{-1}$), and A is the area (m^2) over which the field is applied. For a system that obeys Ohm's law,

$$W = I^2/A^2 k_E \tag{29}$$

where k_E is the electrical conductivity of the medium ($S\,m^{-1}$). It may be noted that the heat generation increases as the square of the current passed. For this reason, nearly all electrokinetic applications are performed in the most resistant media compatible with the unit operation meaning that low-conductance solutions must be used to have low current in order to operate for

longer periods of time. In an adiabatic stagnant system the temperature gradually increases uniformly with time as

$$\Delta T = \frac{IE\tau}{C_p\rho} = \frac{I^2\tau}{k_E A^2 C_p \rho} \tag{30}$$

where τ is the time of application of electric field, C_p is the specific heat of the media carrying the current (kJ g^{-1} °C^{-1}), and ρ is the density of the system (kg m^{-3}). The above equation represents the maximum (adiabatic) temperature increase in the electrophoretic system.

In the cases where the temperature rise is higher than a typical case, it will be necessary to calculate further how much heat needs to be removed. For this purpose, the temperature and the circulation flow rate of the coolant needs to be determined. Presuming that the system boundaries remain at the initial temperature, the Grasshof number is given as [57]

$$Gr = \frac{g\beta\Delta T D^3\rho^2}{\eta^2} \tag{31}$$

where β is coefficient of thermal expansion (°C^{-1}), D is the diameter of the chamber (m) or distance (perpendicular to g) from the high temperature in the system to the closest lateral boundary; ρ and η are the same as defined earlier. The Rayleigh number is the product of Gr and Pr (Prandtl number), that is

$$Ra = \frac{g\beta\Delta T D^3\rho^2}{\eta^2} * \frac{C_P\eta}{k_T} = \frac{g\beta\Delta T D^3\rho^2 C_p}{\eta k_T} \tag{32}$$

where k_T is the thermal conductivity of the medium (kW m^{-1} °C^{-1}). In case of the jacketed slit the critical Ra was reported to be 6.1 by Ivory [75] and around 8.0 by Rhodes and Snyder [58]. In general Ra and Gr should be minimized which usually means minimizing D. However, in the present case D is practically fixed. The only way to reduce these numbers is to reduce g (by operating at low gravity) or minimize ΔT (close to zero using low I/A).

At normal gravity, the Nusselt number, Nu (hD/k_T), can be obtained from these two dimensionless numbers, from which h_T (kW m^{-2} °C^{-1}), the heat transfer coefficient, can be calculated. Then the heat that is to be removed from the system can be calculated as

$$Q = h_T A_T \Delta T \tag{33}$$

where ΔT is already available from the above calculations, and A_T is the effective surface (heat transfer) area of the chamber. Then from Q (kW) the flow rate, M_c (kg s^{-1}), of the coolant (with specific heat C_{pc}) that is to be circulated to remove the required heat can be calculated:

$$Q = M_c C_{pc} \Delta T \tag{34}$$

The following conclusions can be drawn based on the work carried out to date. The multistage electrophoretic extraction concept was shown to be capable of electrokinetic transport of cells and particles. Although the depth of the chambers hampers the resolution of cell extraction, studies to date have paved way for new generation equipment. Resolution can be increased by decreasing the depth of the chamber and increasing the diameter or cross sectional area of the chambers.

The heat transfer analysis presented here has led to the design of the next generation of multistage electrophoretic separators. Two types of ADSEP could be designed for the market:

1. An inexpensive version without temperature control, to be used with low conductivity buffers.
2. A more expensive, thermostated instrument that can be used with high conductivity buffers.

3 Extraction of Macromolecules

The world market for industrial enzymes has been estimated at $1.2 billion in 1995 [76]. Production methods, such as fermentation of genetically engineered microorganisms, have advanced tremendously in recent years. This has promoted work on the development of macromolecule products such as recombinant blood proteins, which require production on the multi-ton scale at low cost (only a few dollars per gram) [77].

Generally many unit operations are used in combination, such as filtration (normal or membrane), centrifugation, precipitation, crystallization, etc. for the separation and purification of macromolecules. Chromatography in its various forms (ion exchange, reversed-phase, hydrophobic interaction, affinity, and gel filtration) has proved to be a general purification technique that can achieve the desired product purity. Although individual unit operations for large-scale purification of macromolecules are generally considered to be well developed and satisfactory, the high degree of complexity (and large number) of steps involved in a complete process are often a source of excessive cost and other problems. Because of this, many of the recent developments in this field have been directed at combining and eliminating different process steps [77].

In conventional methods like centrifugation, and even modern methods like electrophoresis and column chromatography, scale-up problems are enormous, making them uneconomical or prohibitively expensive unless the product is of high value. Therefore there has been a need for alternative approaches to bioseparation problems.

Liquid-liquid extraction is one such method. This technology has been successfully used in separation of compounds in chemical and related industries for many years. However, it is only recently that liquid-liquid extraction technology has been recognized as potentially useful in biotechnology [78, 79]. Two classes of two-phase extraction system are suitable for biomolecule recovery:

1. Aqueous two-phase systems (polymer-polymer type and polymer-salt type).

2. Systems in which an organic reverse micellar solution is in equilibrium with a conjugated aqueous phase.

Both the systems are based on the differential partitioning of biomolecules between the immiscible phases. However, the principles of solubilization differ greatly. These two developing techniques will be discussed briefly here.

3.1 Existing Methods – Brief Analysis

Even though aqueous two-phase extraction (ATPE) has been known for quite some time, it has gained importance for industrial exploitation only recently. Unlike conventional liquid-liquid extraction involving organic and aqueous phases or pairs of organic phases, ATPE employs two aqueous phases. ATPE has been successful to a large extent in overcoming the limitations of conventional extraction such as poor solubility of proteins in organic solvents and the tendency of organic solvents to denature proteins/enzymes. ATPE has been recognized as a versatile technique for downstream processing of biomolecules such as proteins, enzymes, viruses, cells, cell organelles, and other biological materials [70, 80–82]. Its applications for cells and particles was discussed in the earlier sections. ATPE offers many advantages such as biocompatible environment, low interfacial tension, low energy, easy scale-up, and continuous operation. More importantly, partitioning depends on differences in surface properties and does not depend on size, shape, or density of the separand except under specific conditions [78, 83]. Further, the equipment and methods of conventional organic aqueous phase extraction used in the chemical industry can be easily adapted to ATPE. However, ATPE is not selective enough to provide the extreme purity usually desired. The main reasons for ATPE not reaching industry are perhaps the high cost of the phase forming polymers and slow demixing rate of the phases. Thus, ATPE has been recognized as a potential primary purification step in the overall protein/enzyme recovery train [84, 85] in which the final purification is achieved by methods such as chromatography or crystallization. ATPE is also effective and efficient for the removal of contaminating materials and undesirable byproducts such as nucleic acids and polysaccharides [83].

Temperature induced phase separation, proposed by Galaev and Mattiasson [86] and studied extensively by Tjerneld and coworkers [87–90] enables the recovery and recycling of the polymers so the economics have improved to a large extent. It also improves the yield, degree of selectivity, etc. Methods for faster demixing of the phases were developed by employing electric fields [91, 92] and by acoustic fields [93]. In the near future ATPE is expected to enjoy further commercial adaptation.

Some recent developments in this area, which resulted in either increase in selectivity or improvement in yield, are briefly discussed here. Affinity partitioning (AP) is based on the preferential/biospecific interaction between the molecule and affinity polymer derivative which results in a biomolecule-polymer derivative complex which selectively partitions to one of the phases leaving the contaminating substances or proteins in the other phase. Most of the reported investigations regarding affinity partitioning pertain to polymer/

polymer type aqueous two-phase systems (ATPSs) [78] and very few reports are available on polymer/salt type ATPSs, [94] mainly due to the interference of high salt concentrations with the biospecific interactions. More details such as the theory available for AP, future trends, and its other applications are given elsewhere [84, 95, 96].

Metal affinity partitioning exploits the affinity of transition metal ions for electron-rich amino acid residues, such as histidine and cysteine, accessible on the surfaces of proteins. When the metal ion is partially chelated and coupled to a linear polymer, such as polyethylene glycol (PEG), the resulting polymer-bound metal chelate can be used to enhance the partitioning of metal binding proteins into the polymer-rich phase of a PEG-salt or PEG-dextran (DX) ATPS. Since most proteins favor the salt-rich heavy phase of an aqueous two-phase system, metal affinity partitioning can be a very efficient and selective means of isolating and purifying a metal-binding protein from a crude mixture [97].

In most cases, the desired protein has been isolated in a single chromatographic step from clarified cell lysate, without further pretreatment [98]. Guinn [95] and Sulkowski [99] successfully achieved the partitioning of recombinant hemoglobin from crude cell lysate using Cu (II) IDA-PEG in a two-phase system of PEG and magnesium sulfate. To our knowledge, this is the first recorded successful attempt to apply metal affinity partitioning techniques to the isolation of a recombinant protein from crude cell lysate. Successful demonstration of this technology sets the stage for its potential commercial use in the isolation of native and non-native metal-binding proteins. More details in this area can be found in a recent review article [96].

Extractive fermentation/bioconversion involves the integration of fermentation/bioconversion with one or more downstream processing step(s), such as extraction using ATPS, ultrafiltration, etc. An opportunity is thus created to explore new types of industrially relevant bioreactor designs [100, 101]. Many examples are given in the review articles by Diamond and Hsu [78] and Raghavarao et al. [79]. Most of the bioconversions have been performed using polymer/polymer type ATPSs. Lee and Chang [102] were among the first to employ the PEG/potassium phosphate system successfully for the production of acrylamide from acrylonitrile using *Brevibactrium* sp. The selective partitioning of the product into the top phase was found to reduce the inhibition of the active bacterial enzyme by both the substrate and the product. The same strategy is gaining popularity under the name of aqueous two-phase fermentation (ATPF) [103, 104].

Over the past few years there has been considerable interest in the use of the micro-gravity environment of earth orbit as a laboratory for understanding the role of surface forces in liquid-liquid phase separation. The importance of surface wetting forces on the phase separation of ATPSs in microgravity was observed during Space Shuttle flight STS-26 in October 1988. Separation experiments were performed in a Plexiglas hand-held phase partition experiment (PPE) module consisting of 18 chambers filled with PEG and DX in plastic extraction cavities [105, 106]. Evidence of surface tension-driven phase separation in microgravity and its potential processing advantages led to the development of a reusable platform, the ORSEP, for conducting multi-stage extraction using ATPSs for both terrestrial and space-based processing applications [95, 96].

In microgravity, the coalescence of dispersed phase droplets results in a decrease in dispersed phase volume. Since the continuous phase is incompressible, the decrease in droplet volume induces a flow of the continuous phase toward the droplet. In the absence of buoyancy forces, assuming the dispersed phase droplets are uniformly distributed, there would be an increase in the collision efficiency of droplets due to the effect of local flow. Thus in microgravity, as in unit gravity, coalescence and phase separation is spontaneous and enhanced by the local flow induced by droplet coalescence. This would help to explain why phase separation was possible for some of the systems in STS-26 using the PPE module but not for others and why low viscosity and surface tension had such a large positive effect on demixing rates [107]. Due to the combined effects of Brownian motion and the local flow induced by droplet coalescence there is a greater probability that PEG-rich phase droplets (typically the dispersed phase in PEG/DX systems) would impact the container walls and remain there. If the continuous phase were DX it would prevent the dispersed phase from contacting the container walls. The sole effect of surface wetting forces in microgravity would seem to be giving the phase separation directionality.

Reverse micellar extraction (RME) has been gaining popularity as an attractive liquid-liquid extraction process [108–111]. This is mainly due to the fact that enzymes can be solubilized in organic solvents with the aid of reverse micellar aggregates [112, 113]. Their inner core contains an aqueous microphase, which is able to solubilize polar substances, e.g., hydrophilic enzymes [114]. In many cases not only the enzymes retained their activity in organic environment; in some cases they seem to perform even better if they are entrapped into reverse micellar aggregates [111]. One of the remarkable findings that gave this field a major boost is that the solubilization of different proteins into micellar solutions is a selective process [112].

3.2
Magnetic and Electro-Extraction Methods

3.2.1
Magnetic Extraction

Affinity techniques appear currently to be among the most powerful tools available for downstream processing both in terms of their selectivity and recovery. Conventional porous affinity supports are mostly applicable for work in clarified solutions and not suitable for work in early stages where suspended solids and other fouling compounds are present in the system. Non-porous support particles, which are easier to clean and less prone to fouling, are more useful for the purification from feed streams [29, 115]. However, in order to obtain similar surface area of typical microporous particles of 100 µm, the size of non-porous support particles have to be in the range of 0.1–1 µm [116]. It appears that the only feasible method for the recovery of such small particles in the presence of biological debris of similar size is magnetic separation, which eliminates many time-consuming steps and is easy to carry out. The direct and

Table 3. Magnetically assisted separation of enzymes

Enzyme	Magnetic system	Reference
ADH, LDH, 6-PGDH	Ferrofluid-modified 5′-AMP-sephadex 4B	[117]
Hexokinase, G-6-PDH	Magnetic aqueous two-phase system ADH, PTK	[118]
Asparaginase	Magnetic polyacrylamide gel with immobilized D-asparagine	[119]
β-Galactosidase	Silanized magnetite with immobilized *p*-aminophenyl-*b*-D-thiogalactopyranoside	[119]
Chymostrypsin	Chitosan-magnetic beads	[120]
G-6-PDH	Ferrofluid-modified 2′,5′-ADP-Sepharose 4B	[121]
LDH	Magnetic agarose with immobilized triazine dye	[122]
Lysozyme	Magnetic chitin	[123]
Pectinase	Alginate-magnetite beads	[124]
Trypsin	Magnetic polyurethane-polystyrene beads with immobilized soy trypsin inhibitor	[125]
Trypsin	Sub-micron ferrite particles with immobilized soybean trypsin inhibitor	[29]

indirect methods described in the section on cell separation (Sect. 2.1.1) are equally valid for macromolecules as well. Although both the direct and indirect methods perform well, the direct method is generally more controllable. However, the indirect method may perform better for antibodies with poor affinity or when antigen is rare or less accessible [33].

Many magnetic adsorbents have been used for the isolation of various biologically active macromolecules such as enzymes, enzyme inhibitors, DNA, RNA, antibodies, antigens, etc. from different sources such as nutrient media, fermentation broth, tissue extracts, body fluids, and others. However, the present discussion is restricted to enzymes only.

In the case of enzymes, an appropriate affinity ligand is usually immobilized on a magnetic carrier such as silanized magnetite or on polymeric magnetic (chitin) or magnetizable particles. Alternatively, it is possible to begin with a standard affinity chromatography gel and to modify it magnetically by passing ferrofluid through the gel column [117]. Examples of magnetically assisted separation of enzymes are shown in Table 3.

3.2.2 *Electro-Extraction*

As both the phases of ATPSs are electrically conductive, application of electric fields in these systems gives rise to electrokinetic mass transfer of charged species. Thus ATPS was shown as a medium for electrophoretic separation with two aqueous phase interfaces providing the stability against convection and facilitating product recovery [126]. Proteins have been directed into either the

top or the bottom phases of PEG/DX system employing 20 – 50 $V\,m^{-1}$ electric fields perpendicular to the phase interfaces. They could achieve separation of binary mixtures in both batch and continuous modes by operating between isoelectric points and directing oppositely charged proteins into opposite phases.

Recently several studies have been reported regarding improved extractive separation by the application of electric fields to both traditional organic solvent extraction systems and ATPSs [126–130]. Scott and Wham [127] applied an electric field to create emulsion with high interfacial area and contacting with the continuous phase and also to induce coalescence in a novel counter current extractor. Increased mass transfer was achieved due to the altered convection currents within and around the oscillating aqueous drops dispersed in a continuous, nonconducting, organic phase under the influence of a pulsating electric field [129]. Electroextraction with an applied field of 250 $V\,m^{-1}$ was successfully employed to recover citric acid from water using *n*-butanol (saturated with water) as solvent [131].

Levine and coworkers [132, 133] have reported that electrophoretic transport of proteins across the interface of ATPS is greatly impeded in one direction. They have indicated that the electrophoretic transfer of proteins is readily achieved if the protein is migrating from its less-preferred phase (which is not favorable according to its equilibrium partition behavior) to the more-preferred phase. They also observed that the protein does not migrate in the opposite direction, that is, from the more-preferred phase to the less-preferred phase under similar conditions. However, Theos and Clark [126] have shown that the protein can be made to transfer across the aqueous two-phase boundary in both directions.

Scale-up of ATPE, which is useful in the isolation and purification of bioproducts [134, 135], depends to a large extent upon the rapid demixing of the phases with the desired product concentrated in one of them. Pairs of phases involved in ATPE are characterized by high viscosities, low interfacial tensions, and similar densities [70, 80]. These properties lead to slow demixing rates of these phases which has been counteracted by centrifugation, column contacting, or electrokinetic demixing – each having its own drawbacks [85]. Electrokinetic demixing has been shown to increase demixing rates of ATPSs (up to 100 ml) more than fivefold in a manner that depends on field strength, field polarity, concentration of partitioning anion, and phase composition [91, 92]. Electrokinetic demixing is also potentially useful in situations such as low gravity where an additional force has to be introduced for the demixing of the equilibrated phases [136]. Operation of electrokinetic demixing on a commercial scale requires further understanding of the fundamentals involved in the process, which is the motivation for our recent work where the objective was to identify the mechanism of enhanced demixing [137].

When two polymers are dissolved in aqueous solution at concentrations that cause phase separation, certain dissolved ions such as phosphate are unequally partitioned between the phases [138] leading to an electrical potential across the interface [139] and an apparent electrokinetic potential at the surface of the dispersed phase droplets [140, 141]. As a consequence of the latter, droplets of dispersed phase move in the continuous phase in the presence of an externally

applied electric field [141–143]. It is therefore possible to control demixing rates by application of an electric field to ATPS emulsions of appropriate ionic composition. Brooks and Bamberger [136] initially demonstrated enhanced emulsion clearing on a 1-ml scale. They demonstrated qualitatively, by monitoring the system turbidity in a 1-ml chamber, that electrophoretic mobility of the phase droplets enhances the phase demixing.

The effects of the electric field strength, phosphate ion concentration, temperature, field polarity, and phase composition on the demixing rate of PEG/DX system were evaluated quantitatively. It was found that an optimum field strength of around 25 $V\,m^{-1}$ exists at which the demixing is most rapid. In an optimized system this causes a twofold decrease in demixing time relative to that at zero field using normal polarity and a sixfold decrease in demixing time relative to that at zero field in the case of reverse polarity (electric field opposing gravitational settling). Normal polarity refers to anode at the top of the column and reverse polarity refers to anode at the bottom. Paradoxically, both normal and reverse polarity fields increased the demixing rate [91, 92].

Brooks and coworkers [136, 141] measured drop electrophoretic mobilities in ATPSs. They were surprised to discover that the sign of the droplet mobilities was opposite to that predicted from the phosphate partition and the Donnan potential. They also found mobility to be directly proportional to drop radius, which is a contradiction of standard colloid electrokinetic theory [144]. Levine [140] and Brooks et al. [141] hypothesized that a dipole potential at the phase boundary oriented in a way that reverses the potential gradient locally is responsible for the paradox of the sign of electrophoretic mobilities of ATPS droplets.

In our recent study [137], it was confirmed that the droplet electrophoretic mobility increased with increasing drop diameter and the increase was explained based on the electroosmotic flow generated due to the additional internal diffuse double layer of the droplet. These values were compared with the predicted mobilities obtained from the electrophoresis theory. The effect of field strength, polarity, and pH on phase demixing rate was studied. These dependencies were found to be consistent with a model based on the electroosmotic flow:

$$-v = \left(\frac{d^2(\rho_D - \rho_c)\,g}{18\,\eta_c}\right)\left[\frac{3\eta_D + 3\eta_c}{3\eta_D + 2\,\eta_c}\right] + \left(\frac{d\sigma_E E}{2(3\eta_D + 2\eta_c + \sigma_E^2/\lambda}\right) \tag{35}$$

and electrophoretic mobility (μ_E) can be obtained from the electrophoretic velocity [137] as

$$\mu_E = -\frac{v_E}{E} = \left(\frac{d\sigma_E}{2(3\eta_D + \eta_c + \sigma_E^2/\lambda)}\right) \tag{36}$$

Raghavarao et al. [91, 92] have also measured the electrophoretic mobilities of the individual phase droplets suspended in the other phase for PEG/DX system using a micro-electrophoresis unit. These values compared well with the predicted mobilities obtained from the electrophoresis theory. Analysis of these

data by the electroosmotic flow model [137] was found useful in resolving two paradoxes:

1. The direction of migration of drops is the opposite of that predicted by colloid electrokinetics.
2. The phase demixing rate increased irrespective of the sign of the applied electric field.

In the case of normal polarity the field supplements the buoyant rise or fall velocities of the phase drops thereby enhancing phase demixing rate over that in the absence of a field. Interestingly, in reverse polarity, though the field works against the buoyancy of the phase drops, it assists their growth in the dispersion zone until buoyancy takes over causing faster phase demixing. As the buoyant velocity of a drop is proportional to the square of its diameter while the electrophoretic velocity is proportional to its diameter, the demixing rate is faster in reverse polarity than in normal polarity.

3.3 Multistage Method

A schematic representation of the ORSEP is shown in Fig. 15. The extractor consists of two disk-shaped plates into which 24 cylindrical cavities have been machined along the space between two concentric circles of the plate faces. When the plates are joined and securely bolted together to form a leak-tight seal, the cavities can be aligned to form an extraction chamber. Access to the chambers is through a small, stoppered port above each cavity of the top plate.

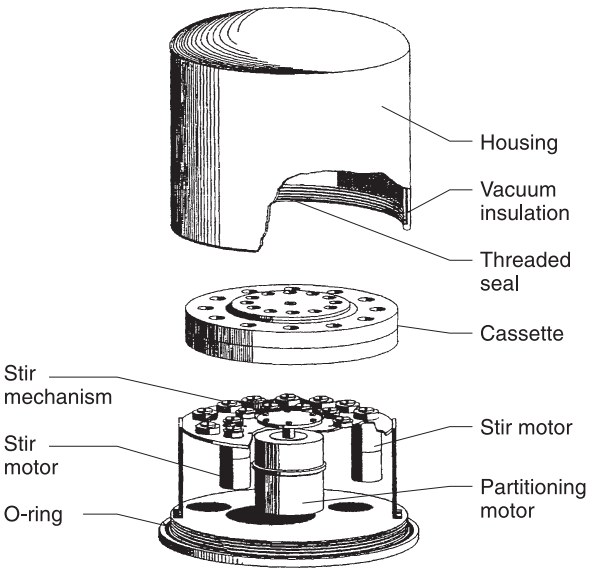

Fig. 15. ORSEP multi-stage countercurrent distribution apparatus

In order to exploit surface tension driven phase separation, the top cover plate is fabricated from a hydrophobic plastic (e.g., Plexiglas, Lexan, etc.) while the bottom plate is machined from stainless steel. The entire unit is mounted to a base consisting of 24 miniature stirbar drivers, which are intended to provide adequate mixing by means of a stirbar installed in each chamber.

Multi-stage extraction using the ORSEP [95] is intended to mimic the procedure known as 'Craig extraction' or counter-current distribution (CCD). As illustrated in Fig. 16, this technique provides a means of isolating and purifying a mixture of solutes by sequentially contacting the top phase of each chamber with the bottom phase from the adjacent chamber, in a manner that mimics counter-current extraction.

The fraction of original solute, added in the first stage, in chamber n after r total transfers is

$$f(n,r) = \frac{r!}{n!\,(n-r)!}\, p^n (1-p)^{n-r} \tag{37}$$

where p = E/(E + 1) and E = KR. The phase volume ratio, R, is defined as the ratio of the top phase volume to the bottom phase volume, and the solute partition coefficient, K, is defined as the ratio of the concentration of solute in the top phase to that in the bottom phase. Multi-stage partitioning of a solute results in a solute concentration profile that closely approaches a Gaussian distribution. Suitable mixing design was provided in a second-generation extractor, ADSEP, for the necessary vertical bulk motion required to achieve adequate momentum transfer between the two fluid phases.

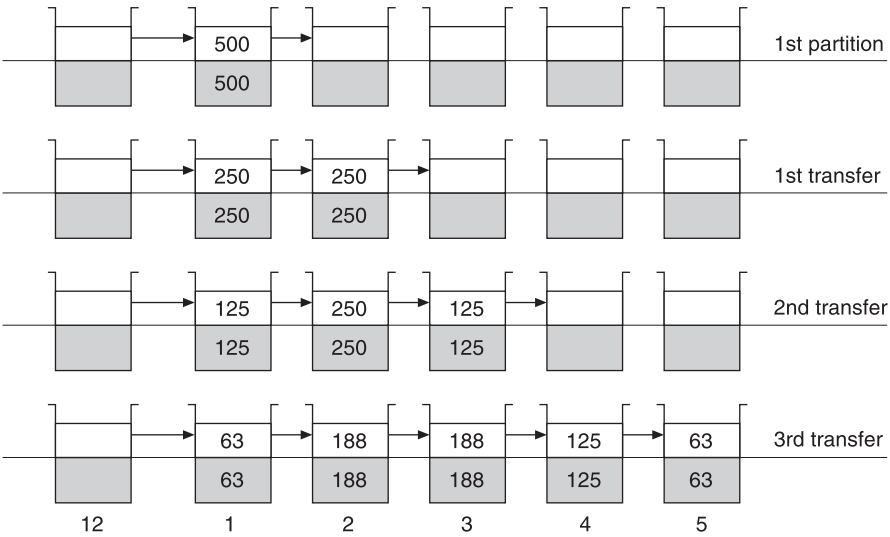

Fig. 16. A schematic representation of Craig extraction

3.4
Theory and Mathematical Models

Counter-current distribution has gradually evolved into a preferred multi-stage contacting method for aqueous two-phase partitioning of biological materials [71]. However, scale-up of this technique beyond the laboratory has been hampered by the lack of a comprehensive model that accounts for the influence of non-idealities on the partitioning process. Counter-current distribution of a mixture of solutes has been modeled as an equilibrium staged process which generates a solute concentration profile that can be represented by a Gaussian error distribution. However, aqueous two-phase CCD is an inherently non-equilibrium process and can result in non-ideal behavior. This is mainly due to factors such as non-alignment of the phase interface and phase cut location, incomplete phase demixing, incomplete solute mass transfer, and perturbation of the phase system composition as a result of solute loading and system dilution. In general, a perturbation of the phase composition in the feed stage due to these and other factors will result in a stage-to-stage variation in the solute partition coefficient (K), the phase volume ratio (R), and the total system volume (V_T). This can translate into a significant deviation from ideal CCD performance. Guinn [95] has developed a comprehensive material balance model for non-ideal CCD and tested it using the ORSEP multi-staged extractor described earlier.

In stage-independent CCD operation K, R, and V_T do not vary from stage to stage. However, stage-independent CCD operation is approached only for those limited cases for which solute loading has a negligible impact on phase system composition, total system volume, and phase volume ratio and for which mass transfer and phase demixing have reached equilibrium. Our objective is to begin with the assumption of stage-independent partitioning in order to develop the general equations which describe solute partitioning in CCD but take into account the effect of liquid interface and phase cut nonalignment on CCD performance. The model will then be systematically generalized for non-ideal operation by applying an empirical demixing model to account for non-equilibrium phase demixing and a model to account for the effect of solute partitioning and feed stage dilution on the perturbations of the phase volume ratio. Perturbation of the feed stage due to any of these non-equilibrium events will be conveyed as a deviation from ideal CCD operation to each successive stage.

In a CCD apparatus, phase transfer is accomplished by slicing the two-phase system along the plane joining the upper and lower chamber halves. In the unlikely event that the phase interface is aligned with this phase cut plane, Eq. (37) can be applied to predict the solute composition in each phase. A more general treatment takes into account the non-alignment of the liquid interface and phase cut.

Three distinct volume regions are defined as shown in Fig. 17 for two adjacent extraction stages of a typical CCD apparatus containing a total of n extraction stages. Light phase is transferred from the left adjacent cavity (n – 1) to the right cavity (n) by slicing the phase system at the junction of the two

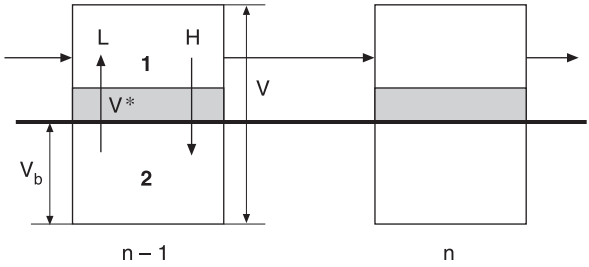

Fig. 17. CCD extraction model

extractor rings (along the heavy horizontal line in the figure). In general, the liquid-liquid interface may be above or below the phase system cut as indicated by the volume V*. The total liquid volume, V_T and the volume of the lower cavity half, V_b, is fixed by the geometry of the extractor.

If x_s and y_s are the mass concentrations of the solute in the light and heavy phases respectively and L_P and H_P are the volumes of the light and heavy phases, then the solute balance over stage n following transfer r is

$$[(V_T - V_b - V^*)\, x_s + V^* y_s]_{n-1,r-1} - [(V_T - V_b - V^*)\, x_s + V^* y_s]_{n,r-1} = [L_P x_s + H_P y_s]_{n,r} - [L_P x_s + H_P y_s]_{n,r-1} \tag{38}$$

Rearranging, an equation for x in stage n after the r transfer is obtained:

$$(x_s)_{n,r} = \frac{\left\{\left[V_T - V_B - V^*\left(\frac{K-1}{K}\right)\right] x_s\right\}_{n-1,r-1} - \left\{\left[V_T - V_B - V^*\left(\frac{K-1}{K}\right) - \frac{(RK+1)\,V}{K(R+1)}\right] x_s\right\}_{n,r-1}}{\left\{\frac{(RK+1)\,V_T}{K(R+1)}\right\}_{n,r}} \tag{39}$$

where the partition coefficient $K = x_s/y_s$ and the phase volume ratio $R = L_P/H_P$. The misalignment volume $V^* = H_P - V_B$ is zero by definition when the liquid interface is at or below the plane of the phase cut. For stage-independent operation, K, V_T, and R are constant and Eq. (39) can be rewritten as

$$(x_s)_{n,r} = \frac{\left[V_T - V_B - V^*\left(\frac{K-1}{K}\right)\right](x_s)_{n-1,r-1} - \left[V_T - V_B - V^*\left(\frac{K-1}{K}\right) - \frac{(RK+1)\,V_T}{K(R+1)}\right](x_s)_{n,r-1}}{\left[\frac{(RK+1)\,V_T}{K(R+1)}\right]} \tag{40}$$

4 Scale-Up and Economic Aspects

A limited number of biotechnological applications are available at present where magnetic extraction techniques were successfully used both in a laboratory and large-scale. Recent developments such as new methods of generating high magnetic field gradients and availability of reasonably priced efficient and superconducting magnets enabled the use of magnetic extraction technology even on a large-scale [1]. Batch HGMS machines are in commercial use and continuous separators are also developed [1]. Some of the following are already commercialized or have very high possibility in near future.

Magnetic affinity adsorbents are now widely accepted in immunoassay techniques [145, 146]. The main advantage of magnetic separation here is to eliminate the need for centrifugation with its many associated disadvantages [145]. Further magnetic separations are cheaper, faster, allow many samples to be handled simultaneously, and help to lend the process towards automation. Ease of conjugation of magnetic immunomicrospheres having the required size with antibodies paved the way for large-scale immunological cell sorting [1]. Development of new polymers simplified the handling of water insoluble enzymes and use of immobilized magnetic enzymes for reaction on a large-scale has been investigated [1]. Performance data in simple and complex matrices for the process-scale cell separation with the help of bioreceptor ferrofluids and HGMS was reported [147].

Commercially introduced by Dynal A/S (Oslo, Norway) and Miltenyi Biotech (Bergish Gladbach, Germany), immunomagnetic cell separation has become an established method for cell analysis in clinical diagnostics. Its low price makes it an alternative to flow-cytometry and very handy for the rare cellular events [148].

On analyzing the available information, it appears that electro-extraction may pose more scale-up problems when compared to magnetic extraction for cells, particles, and macromolecules. However, the actual situation varies depending on the application and each method has its own advantages and disadvantages. For instance, the advantages of using the magnetic rather than electric field are: no need for medium modifications, no biological effects in the range of practical static magnetic field intensities, no joule heating and therefore no flow distortion and thus no need for a complex cooling system [149]. On the other hand, the disadvantages are: its complex interaction with paramagnetic and ferromagnetic labels, adding to the cost of research and development and its dependency on chemical reagents antibodies and magnetic colloids while all other methods are based on cellular immunoreactivity [44].

Practically no reports are available in the literature up to the present date regarding economic aspects of magnetic and electro-extractions. One report was available on costing, albeit based on 1977 data, of a HGMS unit for cleaning of wastewater from a steel mill [150]. However, we are optimistic about the prospects for the electrophoretic methods in processing of cells and macromolecules due to two main factors. As a source of energy, electrons are cheap and equilibrate quickly. As a force, electric fields are tunable to a very fine degree and involve no moving parts. Small-scale applications are already

making a major impact on analytical and preparative separations. However, large-scale processes, while enjoying the same mass transfer advantages as their small-scale counterparts, suffer from poor heat rejection. Hence the prospects for electrophoretic extraction of cells/macromolecules and electrokinetic demixing of biphasic systems to some extent depend also on the economic success of their parent processes.

One of the critical factors in the industrial purification of enzymes and proteins using ATPE is the selection of the appropriate system. Most of the large-scale purifications reported in the literature use either PEG/DX or PEG/salt systems. These systems have a number of desirable characteristics, such as suitable physical properties, non-toxicity, and biodegradability, and are approved by the regulatory authorities. However, the high cost of fractionated DX (approximately $500/kg) and the high salt concentrations (of the PEG/salt systems) have necessitated a search for suitable alternatives. Technical feasibility as well as the cost effectiveness of crude DX ($15/kg) [151], hydroxy propyl starch (HPS) ($20/kg)[152], along with PEG was successfully demonstrated for large-scale enzyme purification.

At this juncture, the PEG/maltodextrin (MDX) system [153, 154] appears to be the most cost-effective ATPS (cost of MDX is $1/kg) though the large-scale operations using real systems have yet to be carried out using this system. The productivity of the purification process increases considerably, especially for intracellular enzymes, which in turn improves the economics of the process, when ATPE is employed instead of conventional methods as indicated by Kroner et al. [151].

The cost of waste treatment is another important factor as rightly indicated by Kula [155]. Phase-forming polymers like PEG, DX, and MDX are biodegradable and non-toxic; however, salt (sulfates and phosphates) disposal is problematic. Hence phase-forming components have to be recycled a few times before discarding, thus improving the economics [156].

5 Other Applications

Magnetic extraction being a potential method needs thorough exploration for its application in other areas, including food processing. Some possible applications are cited here, which will prompt researchers to look for similar applications elsewhere.

Purification of water in hydrocyclones in a magnetic field is reported [157] to meet the high water recirculation demand (640 – 800 m^3/day) for hydrothermal processing of wheat in a 320 t/day capacity mill.

Separation of an ethanol-water system was achieved by magnetic field where ethanol yield was 2% higher over the conventional method. Magnetic field was found to increase aluminum sulfate dissolution coefficient by 10 – 20%, depending on the quality of the treatment. Theoretical elucidation of the effect of the magnetic field on aqueous solutions is also given [158].

High gradient magnetic separation (HGMS) was observed to be a potential treatment for food processing wastewater. HGMS treatment of composite waste

water from processing of turnip greens, green beans, and corn showed significant reductions in color plus turbidity, COD, total P, and suspended solids [159].

Casein hydrolysis in stirred tank reactors using chymotrypsin immobilized on magnetic supports was studied. A comparison was made of the kinetics in batch and continuous stirred tank reactors [160]. Two types of commercially available magnetic separation devices were tested for use in catalyst recovery. HGMS enabled paramagnetic particles to be removed from a rapidly flowing liquid. The filamentary matrix materials used (steel wool or expanded metal lath) provided a large volume for trapping magnetic particles. In this way, Ni particles (3–7 μm in diameter) can easily be separated from an aqueous suspension.

The ability of immobilized lectin-magnetic separation to improve methods for the detection of *Staphylococcus aureus*, *Salmonella enteritidis* and *Listeria monocytogenes* was reported [161]. A new assay, called Lister Screen method, was developed to detect *Listeria* spp. in food [162]. This method separates *Listeria* cells from enriched food samples by means of immunomagnetic beads. After magnetic capture, the beads are spread on PALCAM agar. The analysis time, including an 18-h enrichment and plate incubation, is 48 h for positive samples and 72 h for negative samples.

Recently, continuous production of daizein and genstein from soybean in a magnetically stabilized fluidized bed bioreactor was reported [163]. Brodelius [164] previously demonstrated the use of plant cells in MSFB bioreactor.

Another potential application of magnetic particle separation technology is the use of magnetically delivered therapeutics. Carrier systems for the delivery of chemotherapeutic agents by magnetic means have already been developed. Carrier holding the drug can be concentrated at the desired site in vivo by a magnetic field. Such a delivery system achieves a local accumulation of the drug, which is comparable to that achieved by administration of a 100-fold higher dose of the free drug [165].

Similarly, electrophoretic methods are also finding increasing applications in other areas. For instance, electrophoretic processes are established techniques for the dewatering of fine clays and latexes. Electrically enhanced liquid-liquid extraction was reported by Thornton [166]. Adaptation of this method for the extraction of biochemicals was reported [167]. Greater clarification and faster floc formation were claimed using electrocoagulation in comparison with conventional chemical methods [4].

6 Suggestions for Future Work

Development of equipment is a continual process involving development of prototype models, testing, and elimination of unfeasible models and unworkable alternatives. The complexities of using an internal magnet (such as a stir bar), namely the collection of particles having widely different characteristics and magnetically induced particle aggregation, discouraged this approach, and a more traditional dipole constant field and gradient approach was chosen. The migration time at each station was found to be critical, both for the prevention of aggregation in the field and for the free capture of specific particles.

Only a few attempts at proportional magnetic particle separation have been made. The technical shortfall is related to the distance over which field gradients must be maintained. Using the pre-existing ADSEP technology, these distances can be kept short, the apparatus is manageable, and the separation can be of adequate resolution. The market appears to require a product that can separate particles according to volumetric susceptibility and/or size with a precision of +6% [17]. Although the technical feasibility of MAGSEP has been established, more research is to be carried out to deliver the economically feasible design of multistage magnetic extractor.

Identification of applications is one of the major aspect that needs attention in the immediate future. A need for proportional (vs binary) magnetic separation was identified in the areas of immunological research, pharmaceutical delivery, and biomedical applications. The need for proportional (vs binary) separations was identified in each case. It was found that the pharmaceutical delivery field has an immediate need for the separation of magnetic particles for the delivery of drugs.

There is a need for magnetic extraction of cells on the basis of receptor density. The relatively small sample of recent findings [11–18] clearly indicates that the tools for studying cells with modified receptor densities would be welcome. More effort is required for standardizing and scaling-up magnetic as well as electrophoretic methods in the area of environmental technologies, which usually involves processing of dilute solutions and suspensions at various scales at a reasonable cost.

Our research work in electrophoretic extraction has confirmed the technical feasibility of multistage extraction of cells using electric fields. However, a good amount of research needs to be done to bring the ADSEP to the market as ELECSEP (electrophoretic separator). For example, immediate study is required to examine the efficacy of the unit for the fractionation of mixtures of cells. Preliminary experiments have indicated that the resolution is being hampered by the depth of the chamber. So in the future design the depth of the chamber is to be reduced while increasing the diameter/cross sectional area of the chambers.

Similarly, the heat transfer analysis has led to the design of the next generation of multistage electrophoretic extractors for the market: an inexpensive version without temperature control and a more expensive, thermostated instrument for precise temperature control.

Scale up studies of electrokinetic and acoustic field assisted demixing of ATPSs [91–93] are to be undertaken. Demixing rate can also be enhanced by the addition of fine magnetite particles or ferrofluids to the system followed by the application of magnetic field. Initial studies on a 10-ml scale have shown encouraging results [168]. Detailed study is required on the large scale, examining the effect of phase volume ratio, phase physical properties, etc., with and without cells and macromolecules in the system. It was observed that addition of ferrofluids and/or iron oxide particles usually have no influence on enzyme partitioning and enzyme activity [169].

In this context, electrophoretic extraction, unlike magnetic extraction methods, has influence on the partition behavior of cells and macromolecules

as well as on phase demixing rates. Hence, there is a need for systematic investigation for the fractionation of mixtures of cells, selective differential partitioning of macromolecules, and phase demixing in multistage electrophoretic extractors and counter current distribution electrophoretic extractors.

7 Conclusions

Separation technology is one of the most complex and important areas of biotechnology. It had been estimated that downstream processing accounts for 40% or more of the added value of a fermentation product [1]. Some of the new separation technologies, which show considerable promise for the near future, for the effective extraction of cells, particles, and macromolecules are presented in the present review. It is encouraging to note that some successful applications of magnetic extraction are commercialized [148]. Advanced Magnetics, Cambridge, MA is making large super paramagnetic particles for cell separation [38, 39] and a few companies have commercialized single-stage magnetically assisted separators [35]. There are enough indications that electrophoretic extraction will also soon reach the market. For example, commercial electrophoretic separation of cells and particles has already been carried out by the Bender and Hobein Company by its VaP series free flow electrophoretic separators, and apparatus for proteins is commercially available [170]. Electrokinetic demixing and electroextraction appear to overcome the main drawbacks of ATPE, namely slow rate of phase demixing and selectivity and control over the partitioning behavior of the desired biomolecule. Unfortunately, information in the literature on the engineering aspects of these field-assisted extraction methods involving heat and mass transfer is scant or remains proprietary, and only a few reports are available.

Magnetic and electrophoretic extraction techniques are undoubtedly complementary to other methods that are in use at present in the area of biotechnology. Furthermore, they could be attractive alternatives, especially in the cases of dilute solutions and suspension systems, where other conventional methods normally tend to fail. The use of magnetic and electrophoretic extraction methods often results in relatively faster and more selective separation of the target cells and macromolecules [1].

Some of the important aspects on which future research efforts need to be focused in these areas are suggested in the present review article. In order to develop effective field-assisted separation processing methods, an interdisciplinary effort involving a combination of physical, chemical, and engineering aspects is very essential. Although enough attention has been paid to the physical and chemical aspects, the engineering aspects have been largely neglected. Mathematical modeling, which is highlighted in this review, will be of immense use in predicting the amount of cells or macromolecules extracted without the measurement of an inordinately large number of parameters and, hence, due importance should be given to this aspect.

The scope of possible applications of magnetic and electrophoretic extraction methods is very broad and obviously not limited only to those discussed in

this review. Many more newer applications will certainly be identified and studied in the near future.

Although in principle magnetic and electrophoretic extractions offer the advantage of easy adaptation of the extraction equipment used in the chemical/pharmaceutical industry to achieve efficient extraction, the cell mobilities and mass and heat transfer aspects of this contacting equipment should be studied in detail, employing different base solutions (buffers etc.) as well as real systems involving the actual cells and macromolecules. Even if some of these aspects are addressed in greater depth by future researchers, the objective of this review article can be considered fulfilled in view of the recognized scientific and industrial potential of magnetic and electrophoretic extraction methods.

Acknowledgements. The authors acknowledge the support of this work by SHOT. Inc., Floyd Knobs, IN. One of the authors (KSMSR) gratefully acknowledges the Department of Biotechnology (DBT), Government of India for sponsoring his sabbatical stay at University of Colorado, Boulder, USA.

References

1. Setchell CH (1985) J Chem Tech Biotechnol 35B:175
2. Scott MW (1987) Bio/Technol 5:790
3. Todd P, Pretlow TG (1991) In: Kompala DS, Todd P (eds) Cell separation science and technology. American Chemical Society, Washington, p 1
4. Bowden CP (1985) J Chem Tech Biotechnol 35B:253
5. Whitesides GM, Kazlauskas RJ, Josephson L (1983) Trends in Biotechnol 1:144
6. Dunlop EH, Feiler WA, Mattione MJ (1984) Biotech Adv 2:63
7. Craig LC, Craig D (1956) In: Weissberger (eds) Techniques of organic chemistry. Interscience, New York, vol 4, part 1
8. Hirschbein BL, Brown DW, Whitesides GM (1982) Chemtech 3:172
9. Cremaschi CA, Cazaux L, Sterin-Borda (1994) Internat J Immunopharm 16:12
10. Kuszynski KA, Miller AR (1993) In Vitro 29:708
11. Lokeshwar SS, Huang JS (1989) J Biol Chem 264:19,318
12. Mitamura R, Iwamoto TU (1992) J Cell Biol 118:1389
13. Johnson RL, Burke TG (1990) J Virol 64:2569
14. Filmus JZ, Buick RN (1992) Oncogene 7:521
15. Martin JL, Marvaldi J (1989) Eur J Biochem 180:435
16. Barg RS (1990) Neuroscience Lett 111:222
17. Reddy S, Moore LR, Sun L, Zborowski M, Chalmers JJ (1995) Chem Eng Sci 51:947
18. Rickard DL (1989) Am J Clin Nutrition 49:641
19. Blackmore RP, Frankel RB, Wolfe RS (1979) Science 203:1355
20. Rosenberg RE (1982) Sci Am 247:124
21. Mosbach K, Anderson L (1977) Nature 270:259
22. Melville D, Paul F, Roath S (1975) Nature 255:706
23. Graham MD, Selvin PR (1982) IEEE Trans Magn MAG 18:1523
24. Palchett RA, Kelly AF, Kroll RG (1991) J Appl Bacteriol 71:271
25. Olsvik O, Popovic T, Skjerve E (1994) Clinical Microb Rev 7:43
26. Safarik I, Safarikova M, Forsythe SJ (1995) J Appl Bacteriol 78:575
27. Seesod N, Lunderberg J, Hedrum A (1993) J Clinical Microb 31:2715
28. Grinde B, Jonnesen TO, Ushijima H (1993) J Virol Meth 55:327
29. Halling PJ, Dunhill P (1979) Eur J Appl Microbiol Biotechnol 6:195
30. Larsson PO, Mosbach K (1979) Biotech Lett 1:501
31. Dauer RR, Dunlop EH (1991) Biotechnol Bioeng 37:1021

32. Zborowski M, Malchesky PS, Jan TF, Hall GS (1992) J Gen Microbiol 138:63
33. Safarik I, Safarika M (1997) In: Hafeli U, Schutt W, Teller J, Zborowski M (eds) Scientific and clinical applications of magnetic carriers. Plenum, New York
34. Todd P (1990) In: Koster JN, Sani RL (eds) Progress in astronautics and aeronautics: progress in low-gravity fluid dynamics and transport phenomena. AIAA, Washington, vol 130, p 539
35. Miltenyi WM, Weichel W, Radbruch A (1990) Cytometry 11:231
36. Nixon R, Koval CA, Xu L, Noble RD, Slaff GS (1991) Bioseparation 2:217
37. Nixon R, Koval CA, Noble RD, Slaff GS (1992) Chem Matter 4:117
38. Liberti PA, Feeley BP (1991) In: Kompala DS, Todd P (eds) Cell separation science and technology. ACS Symposium Series, American Chemical Society, Washington, p 268
39. Owen CS, Liberti PA (1987) In: Pretlow TG, Pretlow TP (eds) Cell separation: methods and selected applications. Academic Press, New York, vol 4, p 259
40. Todd P, Hymer WC, Morrison DR, Goolsby CL, Hatfield JM, Kunze ME, Motter K (1988) The Physiologist 31(1) Suppl S52
41. Todd P (1991) In: Kompala DS, Todd P (eds) Cell separation science and technology. ACS Symposium Series, American Chemical Society, Washington, p 216
42. Deuser MS, Vellinger JC, Naumman RJ, Guinn MR, Todd P (1995) Apparatus for aqueous two-phase partitioning for terrestrial and space application. AIAA Life Sciences and Biomedical Conference, April, Houston, TX, Book of Abstracts 95-LS-42, p 65
43. Zborowski M (1997) In: Hafeli U, Schutt W, Teller J, Zborowski M (eds) Scientific and clinical applications of magnetic carriers. Plenum Press, New York, p 205
44. Zborowski M, Moore LR, Sun L, Chalmers JJ (1997) In: Hafeli U, Schutt W, Teller J, Zborowski M (eds) Scientific and clinical applications of magnetic carriers. Plenum Press, New York, p 247
45. Bier M (1989) In: Bier M, Sikdar SK, Todd P (eds) Frontiers in bioprocessing. CRC Press Boca Raton, FL, p 235
46. Ivory CF (1983) Sep Sci Technol 23:875
47. Strickler A (1967) Sep Sci 2:335
48. Hannig K (1972) In: Glick D, Rosenbaum RM (eds) Techniques of biochemical and biophysical morphology. Wiley, New York, vol 1, p 191
49. Ostrach S (1977) J Chromatogr 140:187
50. Hjerten S (1962) Free-zone electrophoresis. Almqvist and Wiksells Boktr. AB, Uppsala
51. Plank JD, Hymer WD, Kunze ME, Todd P (1983) J Biochem Biophys Meth 8:273
52. Boltz RC Jr, Todd P (1979) In: Righetti PG, Van Oss CJ, Vanderhoff JW (eds) Electrokinetic separation methods. Elsevier/North Holland, Amsterdam, p 229
53. Hjerten S (1977) In: Bloemendal H (ed) Cell separation methods. Elsevier/North-Holland, Amsterdam, p117
54. Snyder RS, Rhodes PH (1989) In: Bier M, Sikdar SK, Todd P (eds) Frontiers in bioprocessing. CRC Press, Boca Raton, FL, p 245
55. Griffith, AL, Castimopoolas N, Wortis HH (1975) Life Sci. 16:1693
56. Preece AW, Light PA (1981) Cell electrophoresis in cancer and other clinical research (vol 6 of Developments in cancer research). Elsevier/North-Holland, Amsterdam
57. Rudge SR, Todd P (1990) In: Protein purification. ACS Symposium Series, ACS, Washington DC, p 427
58. Rhodes PH, Snyder RS (1982) In: Rindone GE (ed) Material processing in the reduced gravity environment of space. North Holland, New York, p 217
59. Belter PA, Cussler EL, Hu WS (1988) Bioseparations: downstream processing for biotechnology. Wiley, New York
60. Mason DW (1976) Biophys J 16:407
61. Agarwala JP (1994) Inclined settler classification of particles and transport of ions through liquid membranes with an electric field. Ph.D. Thesis, University of Colorado
62. Cole KD, Todd P, Srinivasan, Dutta BK (1995) J Chromatogr A707:77
63. Tulp A, Timmerman A, Bornhorn MG (1983) In: Stathakos D (ed) Electrophoresis. W. de Gruyter, Berlin, p 317

64. Boltz RC Jr, Todd P, Streibel MJ, Louie MK (1973) Preparative Biochem 3:383
65. Thomson CJ, Docherty JJ, Boltz RC Jr, Gains RA, Todd P (1978) J Gen Virol 39:449
66. Hymer WC, Barlow GH, Cleveland C, Farrington M, Grindeland R, Hatfield JNM, Kunze ME, Lanham JW, Lewis ML, Morrison DR, Olack D, Richman M, Rose J, Scharp D, Snyder RS, Todd P, Wilfinger W (1987) Cell Biophysics 10:61
67. Todd P, Elsasser W (1990) Electrophoresis 11:947
68. Todd P, Hjerten S (1985) In: Schutt W, Klickmann H (eds) Cell electrophoresis. Walter de Gruyter, Berlin, p 23
69. Wang H, Zeng S, Loenberg MG, Todd P, Davis RH (1996) Preprints of 3rd Microgravity Fluid Physics Conference, June, Cleveland, OH
70. Albertsson PA (1986) Partition of cell particles and macromolecules. Wiley-Interscience, New York
71. Treffey TE, Sharp PT, Walter, H, Brooks DE (1985) In: Walter H, Brooks DE, Fisher D (eds) Partitioning in aqueous two-phase systems. Academic Press, Orlando, FL, p 132
72. Raghavarao KSMS, Doyle J, Todd P (1998) AIChJ (submitted)
73. Pollman (1992) Master's Theses, University of Colorado
74. Platsoucas CD, Griffith AL, Cartsimpoolas N (1983) J Immunol Methods 13:145
75. Ivory CF (1990) In: Asenjo JA (ed) Separations in biotechnology. Marcel Dekker, p 153
76. Neidleman SL (1994) Cur Opinion in Biotech 5:206
77. Scott PF (1994) Cur Opinion in Biotech 5:201
78. Diamond AD, Hsu JT (1992) Adv Biochem Eng/Biotechnol 47:89
79. Raghavarao KSMS, Rastogi NK, Gowthaman MK, Karanth NG (1995) Adv Appl Microb 41:97
80. Walter H, Brooks DE, Fisher D (1985) Partitioning in aqueous two-phase systems. Academic Press, New York
81. Fisher D, Sutherland IA (1989) In: Separation using aqueous two-phase systems: applications in cell biology and biotechnology. Plenum, New York
82. Zaslavsky BY (1995) Aqueous two-phase partitioning: physical chemistry and bioanalytical applications. Marcel Dekker, New York
83. Kula MR, Kroner KH, Hustedt H (1982) Adv Biochem Eng 24:73
84. Abbott NL, Blankschtein D, Hatton TA (1990) Bioseparation 1:191
85. Sikdar SK, Cole KD, Stewart RM, Szlag DC, Todd P, Cabezas H Jr (1991) Bio/Technol 9:253
86. Galaev I, Matiasson B (1993) Enzyme Microb Technol 15:354
87. Alred PA, Kozlowski A, Harris JM, Tjerneld F (1994) J Cromatogr 659:289
88. Harris PA, Karlstorm G, Tjerneld F (1991) Bioseparation 2:237
89. Johansson HO, Karlstorm G, Tjerneld F (1997) Biochim Biophys Acta 1335:315
90. Persson J, Nystrom L Ageland H, Tjerneld F (1998) J Chromatogr 711:97
91. Raghavarao KSMS, Stewart RM, Todd P (1990) Sep Sci Technol 25:985
92. Raghavarao KSMS, Stewart RM, Todd P (1991) Sep Sci Technol 26:257
93. Raghavarao KSMS, Scovazzo P, Todd P (1998) Biotechnol Bioeng (submitted)
94. Menge U, Morr M, Mayr U, Kula MR (1983) J Apl Biochem 5:75
95. Guinn MR (1996) Ph.D. Thesis, University of Colorado, USA
96. Raghavarao KSMS, Guinn MR, Todd P (1998) Sep Pur Meth 27:1
97. Johansson G (1985) In: Walter H, Brooks DE, Fisher D (eds) Partitioning in aqueous two-phase systems. Academic Press, New York, p 61
98. Mrabet NT (1992) In: Frances HA (ed) Methods in metal affinity protein separations, vol 4, p 14
99. Sulkowski E (1985) Trends Biotechnol 3:1
100. Larsson M, Arusuratnam V, Mattiasson B (1989) Biotechnol Bioeng 33:758
101. Sonsbeek HM, Beeftink HH, Tramper J (1993) Enzyme Microb Technol 15:722
102. Lee YH, Chang HN (1989) Biotech Lett 1:23
103. Kuboi R, Umakoshi H, Komasava I (1995) Biotech Prog 11:202
104. Jin Z, Yang ST (1998) Biotech Prog 14:457

105. Brooks DE, Bamberger SB, Harris JM, Van Alstine JM, Snyder RS (1986) In: Proceedings of the 6th European Symposium on Materials Science under Microgravity Conditions. Bordeaux, France, December 2, ESA Publication No. SP-256, p 131
106. Van Alstine JM, Karr LJ, Harris JM, Snyder RS, Bamberger SB, Matsos HC, Curreri PA, Boyce JF, Brooks DE (1987) Adv Exp Med Biol 225 : 305
107. Bamberger S, Van Alstine JM, Brooks DE, Boyce J (1990) In: Koster JN, Sani RL (eds) Progress in astronautics and aeronautics. AIAA, Washington DC, vol 130
108. Kadam KL (1986) Enzyme Microb Technol 8 : 266
109. Abbott NL, Hatton TA (1988) Chem Eng Progr 8 : 31
110. Sadana A, Raju RR (1990) BioPharma 3 : 53
111. Dekkar M, Leser ME (1994) In: Street G (ed) Highly selective separation in biotechnology. Blackie Academic and Professional, Glasgow, UK
112. Luisi PL, Bonner PJ (1979) Helv Chim Acta 62 : 740
113. Menger FM, Yamada K (1979) J Am Chem Soc 101 : 6731
114. Misiorowsky RL, Wells MA (1974) Biochemistry 13 : 4921
115. O'Brien SM, Thomas ORT, Dunhill P (1996) J Bacteriol 50 : 13
116. Groman EV, Wilcheck M (1987) Trend Biotech 5 : 220
117. Mosbach K, Andersson L (1977) Nature 270 : 259
118. Flygare S, Wikstrom P, Johansson G, Larsson PO (1990) Enzyme Microb Technol 12 : 95
119. Dunhill P, Lilly MD (1974) Biotechnol Bioeng 16 : 987
120. Ghosh M, Tyagi R, Gupta MN (1995) Biotech Tech 9 : 149
121. Griffin T, Mosbach K (1981) App Biochem Biotechnol 6 : 283
122. Ennis MP, Wisdom GB (1991) App Biochem Biotechnol 30 : 155
123. Safrik I, Safarikova M (1993) J Biochem Biophy Meth 27 : 327
124. Tyagi R, Gupta MN (1995) Biocatalysis Biotrans 12 : 293
125. Lochmuller CH, Wigman LS (1987) Sep Sci Technol 22 : 2111
126. Theos CW, Clark WM (1995) Appl Biochem Biotechnol 54 : 143
127. Scott TC, Wham RM (1989) Ind Eng Chem Res 28 : 94
128. Scott TC, Basaran OA, Bayers CH (1990) Ind Eng Chem Res 29 : 901
129. Marando MA, Clark WM (1993) Sep Sci Technol 28 : 1561
130. Clark WM (1992) Chemtech 22 : 425
131. Stichlmair J, Schmidt J, Proplescher R (1992) Chem Eng Sci 47 : 3015
132. Levine ML, Bier M (1990) Electrophores 11 : 605
133. Levine ML, Cabezas H Jr, Bier M (1992) J Chromatogr 607 : 113
134. Kula MR (1979) In: Wingard LB Jr, Katchalski-Latzir E, Goldstein L (eds) Applied biochemistry and bioengineering. Academic Press, New York, vol 2
135. Flanagan JA, Huddleston JG, Lyddiatt A (1991) Bioseparation 2 : 43
136. Brooks DE, Bamberger S (1982) In: Materials processing in the reduced gravity environment of space. Elsevier Science Publishing, New York, p 233
137. Raghavarao KSMS, Stewart RM, Rudge SR, Todd P (1998) Biotechnol Prog 14 : 922
138. Johansson G (1970) Biochim Biophys Acta 221 : 387
139. Bamberger S, Seaman GVF, Brown JA, Brooks DE (1984) J Colloid Interface Sci 99 : 187
140. Levine SA (1982) In: Rindone GE (ed) Material processing in the reduced gravity of space. North Holland, New York, p 241
141. Brooks DE, Sharp KA, Bamberger S, Tamblyn CH, Seaman GVF, Walter H (1984) J Colloid Interface Sci 102 : 1
142. Van Alstine JM, Karr LJ, Harris JM, Snyder RS, Bamberger SB, Matsos HC, Curreri PA, Boyce JF, Brooks DE (1987) Adv Exp Med Biol 225 : 305
143. Rudge SR, Todd P (1990) In: Ladisch MR, Willson RC, Painton C-DC, Builder SE, (eds) protein purification from molecular mechanisms to large-scale processes. ACS Symposium Series 427, American Chemical Society, Washington, p 244
144. O'Brien RW, White LR (1978) J Chem Soc, Faraday Trans 2 74 : 1607
145. Pourfarzaneh M, Sandy K, Johnson C, Landon MD (1982) Ligand Q 5 : 41
146. Rembaum A, Dreyer WJ (1980) Science 208 : 364

147. Liberti EA, Feeley BP (1991) In: Kompala DS, Todd P (eds) Cell separation science and technology. American Chemical Society, Washington, p 268
148. Uhlen M, Hornes E, Olsvik O (eds) (1994) Advances in biomagnetic separation. Eaton Publishing
149. Vanderhoff JW, Micale FJ, Krumrine PH (1979) In: Rigetti PG, van Oss CJ, Vanderhoff JW (eds) Electrokinetic separation methods. Elsevier/North Holland Biomedical Press, New York, p 121
150. Collan HK, Kokkala MA, Toikka OE (1982) IEEE Trans Magn MAG 18:827
151. Kroner KH, Cordes A, Shelper A, Marr MA, Buckman AF, Kula MR (1982) In: Visser E (ed) Affinity chromatography and related techniques. Elsevier, Amsterdam, p 491
152. Tjernaeld F, Johansson G, Joelesson M (1987) Biotechnol Bioeng 30:809
153. Szlag DC, Guiliano KA (1988) Biotechnol Tech 2:277
154. Mattiasson B, Ling TGI (1986) J Chromatogr 37:235
155. Kula MR (1990) Bioseparation 1:181
156. Greve A, Kula MR (1991) J Chem Tech Biotechnol 50:27
157. Pirko VF, Goergi NV, Kotlyar LI (1974) Pishchevaya-Promyshlennost 19:81
158. Velikodnyi PL (1975) Pishchevaya-Promyshlennost' 21:117
159. Petruska JA, Perumpral JV (1978) Trans ASAE 21:993
160. Munro PA, Dunnill P, Lilly MD (1981) Biotechnol Bioeng 23:677
161. Payne MJ, Campbell S, Kroll RG (1993) Food Microbiol 10:75
162. Avoyne C, Butin M, Delaval J, Bind JL (1997) J Fd Protection 60:377
163. Amea TT, Worden RM (1997) Biotechnol Prog 13:336
164. Brodelius P (1990) In: Nijkamp H, Van der Plas L, Van Aartrijk J (eds) Progress in plant cellular and molecular biology. Kluwer Academic Publishers, Boston, MA, p 567
165. Widder KJ, Senyei AE, Ovadia H, Paterson PY (1981) J Pharm Sci 70:387
166. Thornton JD (1976) Birmingham Univ Chem Eng J, p 6
167. Weatherley LR, Campbell I, Slaughter JC, Sutherland KM (1987) In: Verrall MS, Hudson MJ (eds) Separations for biotechnology, p 341
168. Wikrostorm P, Flygare S, Grondalen A, Larrson PO (1987) Anal Biochem 167:331
169. Larsson PO (1994) Meth Enzymol 228:112
170. Hong J, Lee CK (1986) In: Biochemical Engineering IV, Anals NY Acad Sci 469:131

Received June 1999

Recovery of Proteins and Microorganisms from Cultivation Media by Foam Flotation

Karl Schügerl

Institute for Technical Chemistry, University of Hannover, Callinstrasse 3, D-30167 Hannover, Germany
E-mail: Schuegerl@mbox.iftc.uni-hannover.de

Foaming is often present in aerated bioreactors. It is undesired, because it removes the cells and the cultivation medium from the reactor and blocks the sterile filter. However, it can be used for the recovery of proteins and microorganisms from the cultivation medium.

The present review deals with the characterization of model protein foams and foams of various cultivation media. The suppression of foaming by antifoam agents and their effect on the oxygen transfer rate, microbial cell growth and product formation are discussed. The influence of process variables on the recovery of proteins by flotation without and with surfactants and mathematical models for protein flotation are presented. The effect of cultivation conditions, flotation equipment and operational parameters on foam flotation of microorganisms is reviewed. Floatable and non-floatable microorganisms are characterized by their surface envelope properties. A mathematical model for cell recovery by flotation is presented. Possible application areas of cell recovery by flotation are discussed.

Keywords. Foaminess, Protein foams, Flotation of proteins, Flotation of microorganisms, Foam suppression, Antifoam agents, Characterization of cell surface

Advances in Biochemical Engineering/
Biotechnology, Vol. 68
Managing Editor: Th. Scheper

List of Abbreviations

AFA	antifoam agent
BSA	bovine serum albumin
CFU	colony forming units
CMC	critical micelle concentration
CPR	CO_2 production rate
DOC	dissolved oxygen concentration
GUR	glucose utilization rate
HBB	hemoglobin
HPMC	(hydroxypropyl)methyl cellulose
IEP	isoelectric point
LB	Luria-Bertani medium
OTR	oxygen transfer rate
OUR	oxygen uptake rate
PEO	poly(ethylene oxide)
POE	poly(oxyethylene)
POP	poly(oxypropylene)
PPL	potato protein liquor
RQ	respiration quotient
SPA	specific product activity
SPR	specific production rate
UDV	ultrasound Doppler velocimeter
XPS	X-ray photoelectron spectroscopy
a_i	interfacial area

A_d	down-comer cross-sectional area
A_r	riser cross-sectional area
C_P	protein concentration in feed
C_R	protein concentration in residue liquid
C_S	protein concentration in foam liquid
C_P^*	cell concentration in feed
C_R^*	cell concentration in residue liquid
C_S^*	cell concentration in foam liquid
D	dilution rate in reactor
E	protein enrichment factor (Eq. 6)
E*	cell enrichment factor (Eq. 13)
f_q	signal activity coefficient
g	acceleration of gravity
H	foam height
$k_L a$	volumetric mass transfer coefficient of oxygen
m_{corr}	coalescence index (Eq. 3)
N	stirrer speed
P	product concentration
q_G	aeration rate of the reactor
R	protein recovery (Eq. 8)
R*	cell recovery (Eq. 15)
S	protein separation factor (Eq. 7)
S*	cell separation factor (Eq. 14)
SG	specific glucose uptake rate
SP	specific product concentration with regard to the cell mass
t	time
u	drainage velocity of Plateau borders
V_{tP}	volumetric flow rate of feed
V_{tS}	volumetric flow rate of foam liquid
V_{tR}	volumetric flow rate of residue liquid
V_S	equilibrium volume of the foam above the liquid layer
v_B	actual bubble velocity
v_{B0}	original bubble velocity
V_{tg}	volumetric gas flow rate
w_{SG}	superficial gas velocity in the flotation column
x	antifoam concentration
X	(dry) cell mass concentration
$Y_{X/S}$	yield coefficient of growth with respect to substrate consumed
ε	liquid holdup
Γ	surface concentration of protein
μ	specific growth rate
μ_P	viscosity of protein solution
ρ	density of protein solution
Σ	foaminess for batch operation (Eq. 1)
Σ*	foaminess for continuous operation (Eq. 10)
σ	surface tension
σ_o	volumetric concentration of AFA

1 Introduction

Foams play an important role in several fields of human life: in food technology, medicine, cosmetics, oceanography, environmental technology, fire extinguishing technology, etc. Therefore, foams were investigated very early by natural scientists. Foam films and Plateau borders were characterized, and the formation and structure of foams were described. The mechanical, optical and electrical properties of foams and theories for foam stability were presented [1].

Most of the physicochemical investigations were carried out with surfactant foams. However, in biotechnology, protein foams in combination with surfactants play a role. The properties of these protein and protein/surfactant foams differ considerably from those of pure surfactant foams. Therefore, the results evaluated by surfactant foams can only be partially applied to protein foams. Since proteins adsorb at interfaces at very low concentrations, protein concentrations of as little as $1\,mg\,l^{-1}$ can influence foaming [2]. Protein concentration in industrial cultivation media are far above this limit, because of the high protein content of complex nutrient media and because the microorganisms produce proteins and excrete them into the cultivation medium. In this chapter model protein foams and protein/surfactant foams formed in cultivation media, and their effect on flotation of proteins and microorganisms, are discussed. The results with model protein foams are compared with those of cultivation foams.

Foam flotation during biological waste water treatments is not considered, because of the undefined properties of these systems. Aqueous media have unknown and often changing compositions and the mixed cultures consist of uninvestigated and only partly identified organisms, respectively.

2 Characterization of Biological Foams

The main components of foam formation in cultivation media are proteins. Therefore, several authors have applied solutions of particular proteins and used them as model media to investigate the behavior of biological foams. In this section foams formed by various protein solutions and foams produced by cultivation media are characterized. In addition, the properties of foams suppressed by antifoam agents (AFAs) are described.

2.1 Protein Foams

The high foaming capacity of protein solutions is explained by the stabilization of the gas/liquid interface due to the denaturation of proteins, in particular due to their strong adsorption at the interface. According to Cumper et al. [3] the adsorption process takes place in three main stages: (1) diffusion of the native protein molecules to the interface and their adsorption, (2) uncoiling of the polypeptide chains at the interface (surface denaturation), and (3) aggregation

of the surface-denaturated protein into a coagulum largely devoid of surface activity (coagulation). The polar groups in the protein cause the molecules to spread and denature at the interface, the hydrophobic groups of the molecule keep the film coherent. The foam stability is mainly caused by the film cohesion and film elasticity [4]. Since only the surface-denaturated protein is effective in stabilizing the foam, and only this protein is able to reduce the surface tension of the medium, the rate of the complex adsorption process can be evaluated by means of surface tension measurements.

2.1.1 *Definition of Foaminess*

The foam capacity of the surfactant or protein solution is characterized by the foaminess. The foaminess Σ is defined as:

$$\Sigma = \frac{V_S}{V_{tG}} \tag{1}$$

where V_s is the equilibrium volume of the foam above the liquid layer and V_{tg} is the volumetric gas flow rate.

The foaminess Σ is an unequivocal function of the time t_{DG} which is needed to obtain equilibrium surface tension. e.g. $\Sigma = 1.85 \times 10^5 \times 1.00^{-tDG}$ for BSA foams [5]. The area requirement of a single surface adsorbed molecule was obtained from dσ/dc, where c is the protein concentration, by the Gibbs relationship. By assuming the existence of a hydrate ion complex, which consists of protein and water molecules, the coordination numbers were estimated. By applying the phase change model from ref [6] for the adsorption and surface denaturation of BSA, a simple relationship was found between the dimensionless surface tension y and the time t:

$$\ln\left(\frac{1}{1-y}\right) = bt^n \tag{2}$$

where

$$y = \frac{(\sigma_0 - \sigma_{se})}{(\sigma_0 - \sigma_{st})} \tag{2a}$$

where σ_0 is the surface tension of the pure solvent, σ_{st} is the surface tension of the surfactant solution at time t, σ_{se} is the equilibrium surface tension, and n and b are constants. The unequivocal relationship between Σ and n, as well as between Σ and nb, indicate the applicability of this model.

The same relationships hold true for other proteins, such as bacterium protease and amyloglucosidase, only the constants n and b are different [7].

2.1.2
Investigations with Bovine Serum Albumin

Bovine serum albumin (BSA), a globular protein, is often applied as a model protein for foam formation. The surface tension of BSA solutions as a function of time indicates that, depending on the BSA concentration, it can take 15 to 20 h to attain an equilibrium surface tension which is independent of the BSA concentration. The coagulation rates are slight and the loss of native protein in the surface film due to adsorption and denaturation is compensated by the quick and continuous diffusive transport of native protein to the surface. Therefore, the critical micelle concentration (CMC) and σ_{CMC} can be evaluated from these measurements.

2.1.3
Influence of Protein Structure

A comparison of foams formed by various proteins indicates that the foaminess is related to the rate of decrease in the surface tension of the air/water interface by protein molecules whereas foam stability is related to the structure of adsorbed protein films. Thus flexible protein molecules, which can rapidly reduce the surface tension of the air/water interface, give good foaminess whereas highly ordered global molecules with slow surface denaturation rates give poor foaminess. Rapid build-up of film pressure by proteins tends to lead to formation of a coarse foam (with large bubbles) whereas a slow increase favors small air bubbles, i.e. a creamy foam. Globular protein foams are more stable than foams prepared with proteins of flexible structure. Therefore, the foaminess of proteins with more-or-less random coil molecules (e.g. β-casein) differs from that of globular proteins (e.g. BSA) [8].

2.1.4
Influence of Protein Environment

The solubility of proteins as well as the protein type influences the foaminess. The solubility of proteins is lowest at their isoelectric point (IEP) and, therefore, their foaminess is the highest at their IEP, if the proteins do not precipitate. However, BSA has an anomalous behavior. In the acidic pH range BSA exhibits a non-folded configuration, the size of the albumin molecule changes. In the pH range between 4.5 and 10.5 the protein molecule has a compact shape. In this range no change in configuration or molecular weight occurs [9]. Below and above this range the protein molecule expands. This expansion is accompanied by a change in secondary and tertiary structures. In accordance with this behavior maximum foaminess is found at the beginning of these changes. Why the foaminess exhibits a minimum at pH 3 and below 3 increases again is not yet clear [10].

It is well known that inorganic salts influence protein solubility [11]. The efficiency of various salts is characterized by means of the position of the salts in the lyotrophic or Hofmeister series [12]. By means of the turbidity temperature, measured with poly(ethylene oxide) NP-10 (PEO) solution, the influence of the water structure variation on the protein solubility can be deter-

mined [13]. By means of a change in the turbidity temperature of the protein solution with the salt concentration, a specific constant k can be determined for each salt. The change in the foaminess with the salt concentration was calculated by means of this constant k and the dependence of the turbidity temperature on the PEO concentration. The calculated and measured foaminess values were in good agreement [14]. The applicability of the turbidity temperature for the calculation of foaminess indicates that the influence of salts on the foaminess is mainly due to their effect on the structure of water.

The influence of organic solvents on the foaminess is more complex. They control not only the water structure, and by that the protein solubility, but also the protein structure. In spite of this, it is possible to calculate the foaminess as a function of the concentrations of various alcohols by means of the turbidity temperature change, which is corrected by a factor for the direct alcohol/protein interaction [15].

2.1.5
Influence of Foam Stability

Foam stability is important for foam suppression as well as for foam flotation. According to Mokrushin and Zhidkova [16], foaminess and foam stability are complementary properties. This was proved by Bumbullis and Schügerl [17] for BSA foam. They found that salts which increase the foaminess reduce the foam stability. There is a relationship between the foam stability and the drainage rate of liquid from the foam lamellae [1]. With increasing viscosity of the bulk liquid, the drainage rate diminishes. To evaluate the influence of the surface viscosity of the liquid on the drainage rate, surface rheological measurements were performed according to the method of the authors [18–20].

Highly viscoelastic surface viscosity was found with BSA solutions [21]. Above the threshold concentration, the surface viscosity is independent of the BSA concentration. Below this critical concentration the surface viscosity increases with diminishing BSA concentration. This could be caused by an increase in the coordination number of the hydration complex of the protein [5]. The surface viscosity increased with time, during which the surface tension remained constant. This may be caused by the conformation change and denaturation of the protein on the surface [21]. With increasing concentration of a structure forming salt (Na_2SO_4), foaming and surface viscosity are enhanced and surface tension is diminished [22].

2.2
Foams of Cultivation Media

All industrial biotechnological production processes use complex cultivation media which consist of agricultural by-products (beet or cane molasses, cornsteep liquor, cottonseed meal, whey permeate, peanut flour, soybean meal, distillation residues, etc.). In addition polysaccharides (starch, dextrose, malt extract, maltodextrins, etc.) and proteins (e.g. caseinate, yeast autolysates, etc.) are used as energy sources for the microorganisms and cells. These systems

contain many proteins and surfactants besides several poorly defined components (e.g. solid particles) which influence the formation and properties of foams [1, 23] in (volume-aerated) submersed cultures. However, because protein foams dominate in cultivation media, it is expected that properties of protein foams and cultivation foams will be similar and that results obtained with model protein foams can be applied for foams of cultivation media.

2.2.1
Foaminess of Components of Cultivation Media

Szarka and Magyar [24] investigated the foaminess of various cultivation medium components such as corn-steep liquor, peanut meal, soybean meal and casein solutions and their dependence on the pH value and sterilization. The foaminess passes a maximum with increasing concentration of these components in the range 3 to 5% and as a function of the pH value. The maximum is at pH 4 in the case of soybean meal solutions. With increasing sterilization time the foaminess is enhanced. After 100 min heat treatment at 125 °C, the foaminess Σ increased by a factor of 7 in the case of a model cultivation medium consisting of glucose soybean meal and $CaCO_3$ in water.

2.2.2
Foaminess of Microbial Cell Cultivation Systems

In this section the foam behavior of various cultivation media is investigated. The surface tension σ and foaminess Σ of cultivation media of *Hansenula polymorpha* with unlimited, substrate limited and oxygen transfer limited growth in the presence and absence of antifoam agents were investigated using methanol, ethanol and glucose substrates, respectively. The time dependence of σ can be described by the Avrami relationship: $\ln y = bt^n$, where y is the dimensionless surface tension. The constants n and b are functions of the cultivation time t_F as long as the growth is unlimited, but they are constant in the state of limited growth. With the glucose substrate, Σ can be presented as a definite function of the time t_{DG}, as in model protein foams. However, with methanol and ethanol substrates, no definite $\Sigma(t_{DG})$ function was found, because their concentration varied during the cultivation [25]. In the main, alcohols considerably influence foaminess, as shown by Bumbullis and Schügerl [15]. Surface tension (about 45 mN m^{-1}) and surface viscosity (0.55 cP) were constant during the cultivation time with methanol as substrate in the presence of an antifoam agent. During cultivation with ethanol as substrate, and in the presence of an antifoam agent, the surface tension diminished slightly and the surface viscosity increased with the time.

During *Escherichia coli* cultivation on casein peptone, yeast and meat extract as medium components and in presence of an antifoam agent, the surface tension (36 mN $m^{-1)}$ and surface viscosity (1.9 cP) were constant and did not depend on the cultivation time.

Similar investigations were performed with *Penicillium chrysogenum* cultivation medium in the absence and presence of antifoam agents [26]. Again the Avrami relationship was applied for the antifoam-free system. The foami-

ness is a simple function of t_{DG}. As a function of the cultivation time, Σ passes a maximum during the transition from the growth to the production phase. By addition of an antifoam agent the maximum of Σ could be eliminated. Foaminess increases with the aeration rate V_{tG} in the presence of a small amount of antifoam agent, it attains a maximum, then it diminishes. Obviously at high aeration rates the foam is gradually destroyed.

Saccharomyces cerevisiae was cultivated with potato protein liquor (PPL) and glucose (starch hydrolysate) as substrate. Before the start of the cultivation PPL was sterilized at various temperatures between 80 and 120 °C for different periods between 5 s and 30 min [27]. The foaminess of PPL was very low before the sterilization. The foaminess increased with the temperature and time during sterilization and, at 120 °C and 30 min, Σ was enlarged by a factor of 2×10^3. This effect is due to the denaturation of proteins [4] and the formation of Maillard reactions between reducing sugars and amino acids [28].

Similar results were obtained with two partly soluble substrates: soy flour and sugar beet cossette [29]. By autoclaving at 121 °C for 15 min, the medium foaminess increased considerably.

Noble et al. [30] cultivated *Penicillium herqueii* and identified ingoldian fungus on a synthetic medium in the presence of Tween 80 and determined the relative foaminess (foam index) as a function of the cultivation time. During the cultivation of *P. herqueii*, foam formation started at 20 h and strongly increased at 60 h. They found that surfactants (extracellular lipophilic compounds) were enriched in the foam and, at the same time, the surface tension in the medium increased. In the case of the other fungus the foam formation started at 70 h and strongly increased at 100 h. In this case also the lipophilic compounds enriched in the foam and at the same time the surface tension increased in the medium.

2.3 Prevention, Breaking and Suppression of Foams

The best way to avoid foaming is to choose cultivation conditions which circumvent foam formation. Often foaming is caused by cell lysis due to substrate or oxygen transfer limitation, lack of an essential medium component or by a rapid change in the cultivation conditions. The initiation of the production phase at the end of the growth phase by reduction of the easily consumable substrate during the production of secondary metabolites often causes foam formation, which diminishes after the microorganisms have adapted to the new cultivation conditions. Of course, foam formation can be diminished by reducing the aeration rate. However, this can cause oxygen transfer limitation, which enhances the cell lysis and foam formation. Ghildyal et al. [31] diminished foam formation by reducing the temperature from 32 to 28 °C. This control was more effective than the use of chemical agents. However, it is often not possible to change the cultivation temperature without reducing the growth and production rate considerably. By the use of spargers with large holes, which produce large bubbles, unstable foam was formed and the flotation of hybridoma cells was reduced [32]. However, especially in the case of animal cells, large bubbles can impair the viability of cells.

If foam formation cannot be avoided, it can be destroyed mechanically by foam breakers, physically by ultrasound, heat or electrical methods, or chemically by antifoam agents [33]. In industrial production, with a few exceptions, mechanical foam breakers (e.g. steroid biotransformation [34]) are not used because of their high power input demand, which is often higher than the power input by the stirrer. Physical methods are not used either, because ultrasound, heat or electric treatment can impair the viability of the microorganisms. Therefore, only chemical methods are considered in this review.

2.3.1
Foam Suppression by Chemical Antifoam Agents

For foam suppression during antibiotic production often antifoam agents (AFAs) are used which can be metabolized (e.g. soy oil). For enzyme production, inert antifoam agents, which cannot be metabolized by the microorganisms, are preferred [35].

According to Ross [36] and Robinson and Woods [37], AFAs may affect foam in two different ways: (1) The antifoam agent is dispersed into very small droplets which penetrate into the foam lamellae and form a duplex film. This film spreads on the lamellae. It bursts because of the strain caused by the extension of the duplex film. (2) The antifoam agent penetrates into the lamellae and forms a mixed monolayer on the lamellae which has less cohesion than the lamellae-stabilizing protein film in the absence of antifoam.

Antifoam agents destroy the surface elasticity and surface viscosity of the foaming system. The antifoam agent must have, therefore, low surface tension to spread on the foam lamellae. To be active at low concentrations, they must also be insoluble in the foaming medium [38].

Vardar-Sukan [29] evaluated the efficiency of different natural oils with unsterilized and sterilized model media consisting of soybean flour and sugar beet cosette. Soybean was most efficient in unsterilized and cotton seed for sterilized soybean model media. Sunflower oil was most efficient in unsterilized and cotton seed in sterilized sugar beet model media. Their optimum concentrations are in the range 0.1 to 0.6% v/v.

In the following sections, a few examples of the effect of antifoam agents on the properties of cultivation medium and foam are considered. Most of the authors evaluated the effect of antifoam agents on the volumetric mass transfer coefficients in bioreactors.

2.3.2
Influence of Antifoam Agents on the Oxygen Transfer Rate

Systematic investigations were carried out by Adler et al. [39–41] and König et al. [26] with various cultivation media. The volumetric mass transfer coefficients k_La were determined by a steady state method with distilled water, nutrient salt solution and various cultivation media in the presence and absence of antifoam agents. Volumetric mass transfer coefficients are strongly enhanced by increasing aeration rate. At low superficial gas velocities ($< 2.5\,cm\,s^{-1}$) the

bubble coalescence can be neglected. It was assumed that below this gas velocity the difference between k_La values in distilled water, in cultivation media in the presence and absence of AFA, is caused by only k_L and that this difference in k_L holds true for higher gas velocities as well. Above this critical superficial gas velocity the volumetric mass transfer coefficient due to the specific interfacial area is enhanced, but the bubble coalescence is also increased, which reduces the specific interfacial area. In order to compare the specific interfacial area of the investigated systems in the presence and absence of AFAs, the coalescence index m_{corr} was defined, which was corrected by the difference in k_L values in water, nutrient medium and cultivation medium [39].

$$m_{corr} = \frac{(k_L a)_{corr}}{(k_L a)_{ref}} \tag{3}$$

where $(k_La)_{ref}$ is the volumetric mass transfer coefficient in the reference system.

$$(k_L a)_{corr} = k_L a - \Delta(k_L a) \tag{3a}$$

and k_La is the volumetric mass transfer coefficient in the cultivation medium:

$$[\Delta k_L a = k_L a - (k_L a)_{ref}] \text{ at } w_{SG} = 2 \text{ cm s}^{-1} \tag{3b}$$

A nutrient salt solution with an antifoam agent had the lowest k_La value, and therefore it was chosen as the reference system.

In Table 1, m_{corr} values for various biological systems and nutrient salt solutions with an antifoam agent [Desmophen 3600, Bayer AG, a poly(propylene

Table 1. Values of m_{corr} for biological systems and nutrient salt solution in a bubble column at $w_{SG} = 4$ cm s^{-1}. The reference is the nutrient salt solution with Desmophen which has the lowest k_La value [40]

Biological system	Substrate	(Antifoam)	m_{corr}
Chaetomium cellulolyticum	glucose	(no antifoam)	2.56
C. cellulolyticum	glucose	(small amount of Desmophen)	1.21
Escherichia coli	casein peptone	(small amount of Desmophen)	1.40
Saccharomyces cerevisiae	glucose	(small amount of Desmophen)	1.22
Hansenula polymorpha	glucose	(small amount of Desmophen)	2.29
H. polymorpha	glucose	(small amount of Desmophen)	(with substrate limitation 2.17)
H. polymorpha	ethanol	(small amount of silicon oil)	1.52 (with oxygen transfer limitation)
H. polymorpha	ethanol	(small amount of Desmophen)	1.52 (with substrate limitation)
Nutrient salt solution		(no antifoam)	2.29

oxide) with a mean molecular weight of 2000] and silicone oil at $w_{SG} = 4\ cm\ s^{-1}$ are compared [40].

With increasing gas velocity, the volumetric mass transfer coefficient and bubble coalescence are enhanced and the efficiency of antifoam agents are enlarged, i.e. in the presence of an antifoam agent the m_{corr} values decrease. For example, during the cultivation of *Hansenula polymorpha* on ethanol substrate under oxygen transfer limitation with silicone oil, the corrected coalescence index m_{corr} reduces from 1.52 at $w_{SG} = 4\ cm\ s^{-1}$ to 1.23 at $w_{SG} = 6\ cm\ s^{-1}$. The same m_{corr} values were obtained during the cultivation of the same yeast on ethanol substrate under substrate limitation with the Desmophen AFA.

With increasing amounts of AFA in *Hansenula polymorpha* cultivation medium, k_La passes a maximum at 1.0‰ (w/w) Desmophen. However, gas holdup attains the maximum at 10‰ (w/w) Desmophen [41]. The surface tension diminishes and the surface viscosity increases with increasing antifoam concentration in distilled water and in BSA solution. Foaminess Σ drops from 200 to 1 s already at low concentrations of Desmophen ($< 1\ mg\ l^{-1}$). In a cultivation media of *Hansenula polymorpha* and *E. coli,* the surface tension and surface viscosity remain constant during the entire cultivation time in the presence of Desmophen [22]. As already pointed out, the maximum of foaminess which arises at the transition from the growth phase to the production phase during the production of penicillin V by *Penicillium chrysogenum* can be eliminated by adding Desmophen to the cultivation medium. The foaminess is reduced from 400 to 100 s [26].

Several AFAs (various silicone emulsions produced by Wacker, Goldschmidt, Dow Corning and Bayer, and others) were tested under standardized conditions with regard to their foam-reducing effect on BSA solutions. The surface tension and foaminess were measured at 0.0, 0.0005, 0.001, 0.005 and 0.01% of the active components of antifoam agents [42]. BSA foams exhibit equilibrium surface tensions in the range of $40\ mN\ m^{-1}$ with most of the AFAs. The foaminess Σ decreased with increasing antifoam concentrations and, at an antifoam concentration of $1\ mg\ l^{-1}$ (Desmophen) and $5\ mg\ l^{-1}$ (Wacker silicones), respectively, the foam disappeared. The silicones from other manufacturers only had partly the same efficiency. Because of the various types of antifoam agents and their different composition, no general relationship could be obtained with respect to their efficiency. However, particular results were published.

Al-Masry [43] investigated the effects of silicone antifoams in tap water in airlift reactors with an external loop with regard to the gas holdup and volumetric mass transfer coefficient. They recommend the following relationship for this special case:

$$k_L a = a w_{SG^b} (1 + x)^c \left(1 + \frac{A_d}{A_r}\right)^d \tag{4}$$

where x is the antifoam concentration, A_d the down-comer cross a sectional area and A_r the riser cross-sectional area. For the investigated system, a = 0.041, b = 0.083, c = 0.017, and d = 0.414.

The gas holdup and volumetric mass transfer coefficients were determined in a bubble column of 150 mm diameter and 3 m height as a function of the aeration rate in tap water and a nutrient solution of *Candida boidinii* in the presence and absence of an antifoam agent [Ucolub N 115, a water-insoluble poly(oxyethylenepropylene) copolymer]. Up to a superficial gas velocity $w_{SG} = 3$ cm s^{-1} the gas holdup was not influenced by the antifoam agent. Above that the gas holdup approached a constant value of 0.15. The volumetric mass transfer coefficient was more sensitive to the AFA. Above $w_{SG} = 1$ cm s^{-1}, $k_L a$ did not change with the gas velocity. Depending on the antifoam concentration it had a value 0.15 s^{-1} (0.1% Ucolub + 1% methanol + 1% salt solution) and 0.1 s^{-1} (0.1% Ucolub in water and in 1% methanol solution). Without an antifoam agent the gas holdup was a factor of three higher at $w_{SG} = 3$ cm s^{-1} and the $k_L a$ a factor of four higher at w_{SG}=2 cm s^{-1} [44].

During the production of penicillin G by *Penicillium chrysogenum*, the addition of lard oil to the cultivation medium increases the dissolved oxygen concentration below 25% of saturation and reduces it above this value [45]. After addition of an antifoam agent to the cultivation medium, the balance between oxygen uptake rate (OUR) and oxygen transfer rate (OTR) is disturbed. The increase in the DOC is probably caused by the stronger reduction of OUR of the fungus (due to its diminished respiration of the fungus) than OTR. The decrease in DOC above this value is due to the stronger reduction of the OTR than the OUR.

The respiration rate of microorganisms can be evaluated by means of the O_2 and CO_2 balances. Nyiri and Lengyel [46, 47] observed that DOC was reduced and OUR increased after addition of an antifoam agent to the medium. CO_2 entrapped inside the bubbles is released changing the composition of the off-gas, if the foam is destroyed. This can reduce the dissolved CO_2 concentration in the medium and enhance the respiration of the microorganisms, which causes an increase in OUR and a decrease in DOC.

2.3.3
Influence of Antifoam Agents on Fluid Dynamics, Cell Growth and Product Formation

It is well known that fluid dynamics influence the process performance. Therefore, bubble velocity and gas/liquid interfacial area were monitored during the cultivation of *E. coli.* The effect of an AFA on the bubbles was determined by monitoring the bubble velocity with an ultrasound Doppler velocimeter (UDV) in situ [48, 49]. By adding an AFA to the cultivation medium, the mean bubble velocity instantaneously increased by a factor of about two in the airlift tower loop reactor during the cultivation of *E. coli* [50] (Fig. 1a).

After about half an hour, the bubble velocity dropped to the original value, which indicates that the antifoam had disappeared from the cultivation medium. However, after several antifoam additions, the base line and the maxima of the bubble velocity gradually increased. The cultivation medium became more and more coalescence promoting. Monitoring the intensity of the reflected ultrasound allowed the specific gas/liquid interfacial area a to be measured in situ (Fig. 1b). The specific interfacial area a

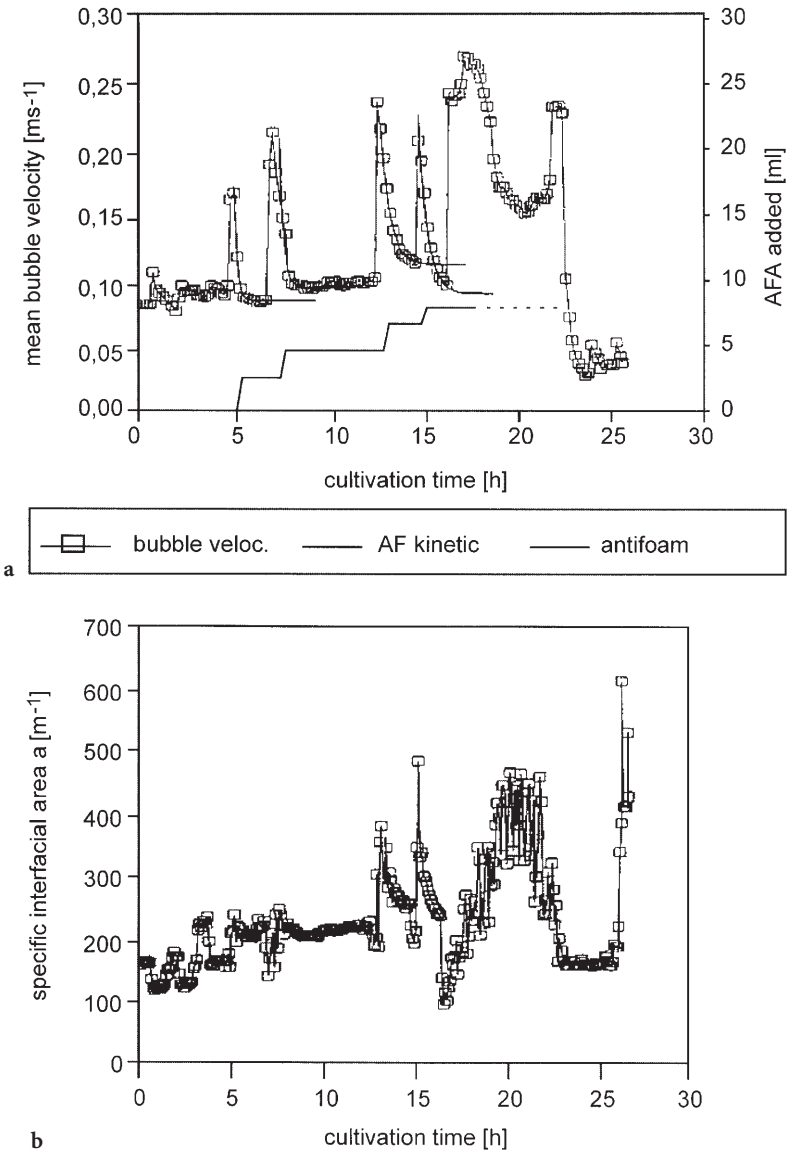

Fig. 1. Measurements during the cultivation of recombinant *E. coli* K-12 MF cells in a 60-l working volume air lift tower loop reactor without gene expression using SE9 antifoam agent (AFA) [50, 51]. **a** Variation in the mean bubble velocity. Bubble velocity measured in situ by an ultrasound Doppler technique. AFA added to the medium. **b** Variation in the specific interfacial area (m^{-1}) measured in situ by an ultrasound technique

instantaneously reacted to the addition of an AFA (SE9) to the medium [51].

Most research groups have determined the oxygen transfer rate as a function of the AFAs, and only a few have investigated their influence on the cell growth and viability [51–54]. The toxicity of different antifoam agents on *Aspergillus niger* was tested in Petri dishes [52]. In addition respiration tests were performed in a Warburg apparatus. Most of the antifoam agents inhibited the growth of the fungus. The respiration of *A. niger* was diminished by AFAs as well; unfortunately, too high AFA concentrations (1%) were applied in these investigations. In practice, the applied AFA concentrations are orders of magnitude lower.

Only Koch et al. [51] monitored the fluid dynamic properties of a two-phase system and the biological behavior of the cells during the same cultivation. They investigated the influence of four different AFAs (Table 2) on the foaminess, oxygen transfer rate and growth of recombinant *Escherichia coli* and the production of recombinant protein. The specific growth rate μ, the colony forming units CFU, the CO_2 production rate CPR, the specific glucose uptake rate GUR, and specific production rate (activity of β-galactosidase) SPR, and yield coefficient $Y_{X/Glu}$, were monitored during the cultivation using four different AFAs (Table 3). The OTR and the volumetric mass transfer coefficient k_La were also monitored [51]. Each of the AFAs was used in different initial concentrations to suppress foaming during the batch cultivation of *E. coli*.

The surface tension of the cultivation medium decreased when the antifoam agent was added. Above a critical AFA concentration the surface tension was independent of AFA concentration. SE9: $\sigma = 24.5$ mM m^{-1} (at. 5 ppm), S184: $\sigma = 26$ mM m^{-1} (0.5 ppm), VP1133: $\sigma = 33$ mN m^{-1} (0.5 ppm), SLM 54474: $\sigma = 36$ mN m^{-1} (2.0 ppm). Above a concentration of 150 ppm VP1133, SE9 or S184, the foaminess of the model medium (with casein peptone and yeast extract) was reduced to below 50 s, and above 200 ppm SLM54474 it was reduced to 100 s [51].

Escherichia coli was batch cultivated in a 2.5-l working volume stirred tank reactor (Biostat; M Braun, Melsungen) and in a 60-l working volume airlift

Table 2. Characterization of AFAs applied during the recombinant *E. coli* cultivation [51]

S184	(pure silicone oil) consists of 95% diethylsiloxane with viscosity of 1000 cP at 298 K and 5% highly dispersed silicone oxide. Viscosity of the mixture at 298 K: 2000–4000 cP (Wacker Chemie)
SLM54474	Pure poly(propylene glycol) (PPG) with a molecular weight of 2000 g mol^{-1} (Wacker Chemie)
VP1133	(silicone oil/PPG mixture) consists of 20% branched dimethylsiloxane with viscosity of 200–600 cP at 298 K, 3.5% highly dispersed silicon dioxide and 76.5% PPG with molecular weight of 2000 g mol^{-1}. Viscosity of the mixture at 298 K: 1000–3000 cP (Wacker Chemie)
SE9	(emulsion) consists of 85.4% de-ionized UV-sterilized water, 0.1% sorbic acid, 4.5% non-ionic emulgators, 10% S184. Viscosity of the emulsion at 293 K; 5000–20000 cP (Wacker Chemie)

Table 3. Parameter maxima of the cultivations of *E. coli* with various AFAs [51]

AFA	AFA (ppm)	X (l^{-1})	μ (h^{-1})	$P \times 10^{-3}$ ($U\ l^{-1}$)	$SP \times 10^{-3}$ ($U\ g^{-1}$)	$Y_{X/S}$ ($g\ g^{-1}$)	SG ($g\ h^{-1}\ g^{-1}$)
SLM54474	125	1.59	0.34	27.8	13.7	0.43	0.90
SML54474	250	1.66	0.28	28.9	14.7	0.35	1.00
SLM54474	1000	1.96	0.23	41.0	24.5	0.57	0.78
S184	63	1.69	0.35	26.0	16.0	0.93	0.75
S184	250	1.78	0.35	20.0	10.0	0.45	n.d.
S184	2000	2.10	0.32	19.0	9.0	0.70	0.85
VP1133	50	1.60	0.39	12.4	7.4	0.41	0.70
VP1133	500	1.7	0.42	15.5	9.0	0.53	n.d.
VP1133	1000	1.8	0.28	22.4	14.5	0.48	0.90
MV.GrA		1.76	0.33	23.7	13.2	0.54	0.84
SD.GrA		0.16	0.06	8.0	5.0	0.17	0.30
SE9	70	4.15	0.64	n.d	n.d.	0.80	1.55
SE9	555	3.94	0.41	n.d	n.d	0.40	1.55
SE9	5000	4.98	0.64	4.8	12.0	2.3	1.35
MV.Gr.B		4.36	0.56	n.d	n.d	1.16	1.45
SD.Gr.B		0.49	0.11	n.d	n.d	0.82	0.14

MV: mean value; SD: standard deviation; Gr.A: group A [pure silicone oil and poly(propylene glycol) PPG and silicone oil/PPG mixture]; Gr.B: group B (aqueous emulsion with only 10% S184); X: cell mass concentration; $Y_{X/S}$ yield coefficient of growth with respect to substrate; P: productivity of β-galactosidase; SP: specific productivity: SG: specific glucose consumption rate [51]

tower loop reactor. In the 60-l airlift tower loop reactor, S184 had no foam-suppressing effect, but VP1133 was very effective. The foaminess was controlled and maintained below 140 s by the appropriate feeding of VP1133 to the reactor. Gas holdup, OTR, and respiratory quotient RQ = CPR/OTR varied slightly during the addition of the AFA. However, the mean bubble velocity increased immediately after the addition of silicone oil containing an AFA to the reactor (Fig. 1).

In Fig. 2 the key parameters are presented for recombinant *E. coli* batch cultivation in a 60-l working volume airlift tower loop reactor at constant aeration rate up to 16 h, whereupon the temperature was increased from 30 to 42 °C and gene expression was induced. At the same time concentrated Luria-Bertani (LB) medium was added to the reactor. To avoid oxygen limitation, the aeration rate was increased (Fig. 2a). At 12 h the foaming increased and SE9 was added to the medium. The bubble velocities (Fig. 2b) and the specific gas/liquid interfacial area (Fig. 2c) quickly increased and passed a narrow maximum, but k_La dropped and the OTR was not influenced (Fig. 2d). After the induction of the gene expression by a temperature increase and medium supplement the dissolved oxygen concentration with respect to the saturation increased due to the elevation of the aeration rate (Fig. 2a); the mean bubble velocity (Fig. 2b) and specific interfacial area (Fig. 2c) decreased, OTR increased and k_La remained at low values (Fig. 2d). The mass transfer coefficient with respect to the liquid phase k_L dropped from about 1.67 to 0.67 m s^{-1} after the addition of SE9 to the medium [51].

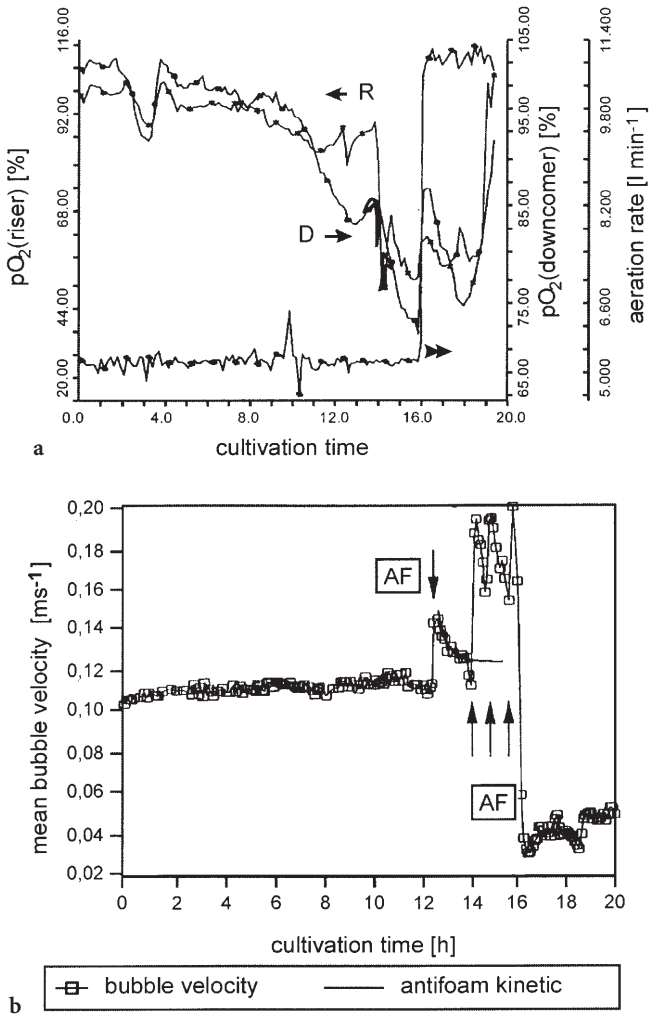

Fig. 2 a, b. Variations in the process parameters during the cultivation of recombinant *E. coli* K-12 MF cells in a 60-l working volume air lift tower loop reactor. At 12 h addition of SE9 AFA to the medium. At 16 h induction of the gene expression by a temperature increase from 30 to 42 °C. At the same time concentrated LB medium is added to the reactor [51]. **a** Aeration rate and dissolved oxygen concentration with respect to the saturation (pO_2) in down-comer and riser, **b** mean bubble velocity

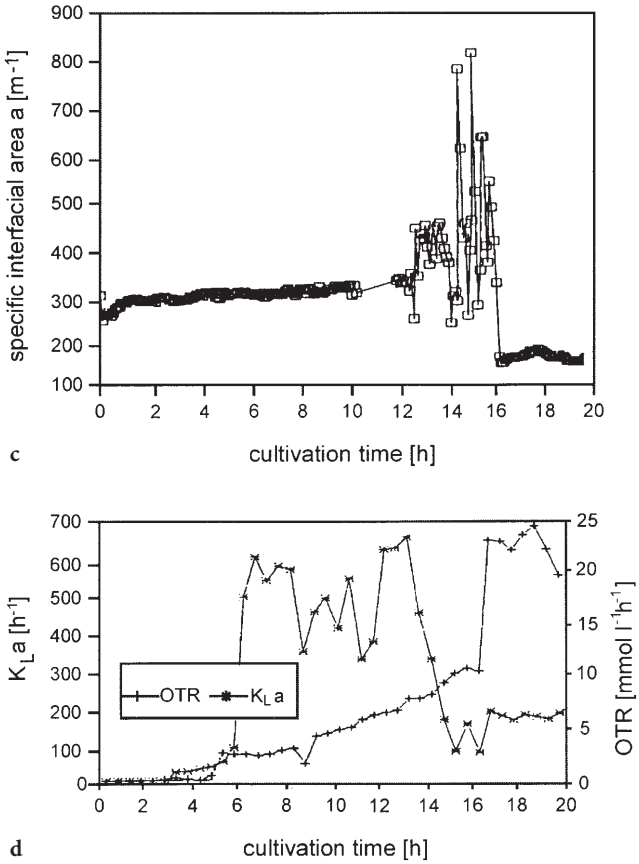

Fig. 2 c, d **c** specific gas/liquid interfacial area, and **d** oxygen transfer rate (OTR) and volumetric mass transfer coefficient k_La of oxygen

In Fig. 3 the variations in the specific growth rates of recombinant *E. coli* during cultivation in a 2.5-l stirred tank reactor at different AFA concentrations are shown. With SLM54474 the specific growth rate decreased with increasing AFA concentration, but with S184, VP1133 and S9 no change of μ was observed below 250 ppm AFA concentration. In addition, the number of cells which were able to propagate (colony forming units CFU) and the CO_2 production rate CPR were determined as a function of the cultivation time for all four AFAs. The results of these measurements are in good agreement. They decrease with increasing SLM54474 concentration and with SE9 their highest values were obtained for 5000 ppm AFA. The AFA concentration did not influence them up to 500 ppm AFA with S184 and VP1133, but above that they decreased. The specific product activity (SPA) was the highest at high SE9 concentrations. With other AFAs no clear concentration dependence was observed.

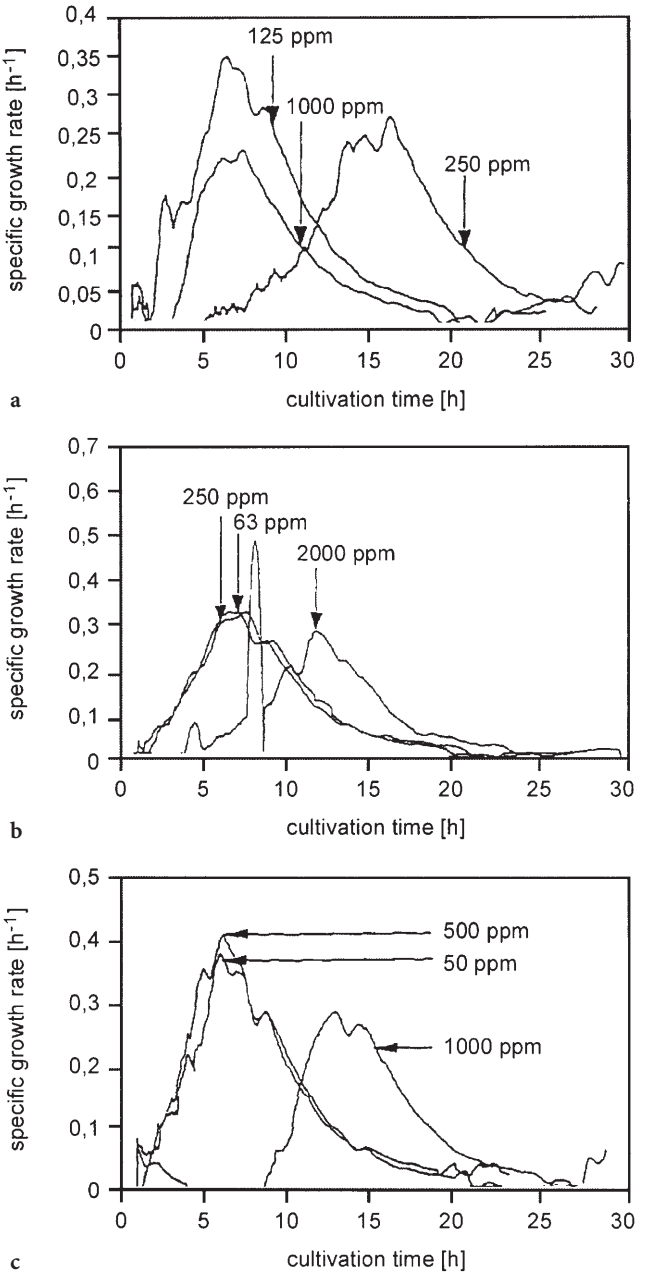

Fig. 3 a–c. Specific growth rate μ of recombinant *E. coli* K-12 MF cells as a function of the cultivation time at different AFA concentrations. **a** SLM54474, **b** S184, **c** VP1133

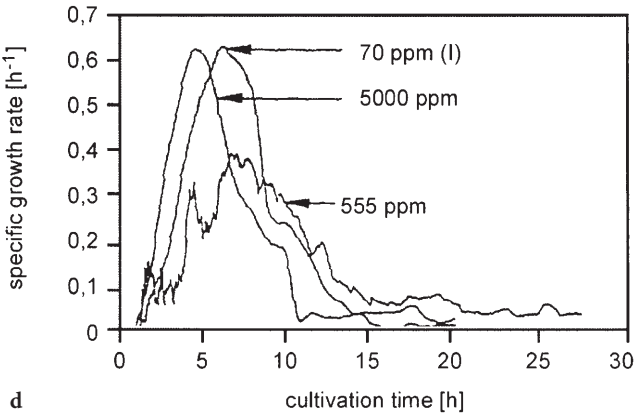

d

Fig. 3 d SE9 [51]

Silicone-oil-free AFAs influence the OTR only slightly. Silicone-oil-containing AFAs considerably reduce OTR in the early stages of the cultivation, but later on they have only a slight effect. The same holds true for their influence on $k_L a$. When a silicone-oil-containing AFA was added to the reactor, the bubble velocities suddenly increased, but within 60–100 min they dropped to their original values, which indicated the removal of AFA from the medium. The removal rate is a first-order process [51] (Fig. 4):

$$\upsilon_B = \upsilon_{Bo} \sigma_o f_A \exp(-kt) \tag{5}$$

where υ_B and υ_{B0} are the actual and original bubble velocities ($m\,s^{-1)}$, σ_o the volumetric concentration of the AFA ($ml\,l^{-1}$), f_A the signal activity coefficient ($ml\,s^{-1}\,ml^{-1)}$, k the time constant ($h^{-1)}$ and t the time since the maximum of the bubble velocity was attained (h). At the beginning of the cultivation the removal rate is the highest, later this process decelerates.

The addition of an AFA to the medium caused a short increase in the CO_2 concentration in the off-gas and the pH value in the medium. Since the solubility of CO_2 and the pH value are not influenced by the AFA, the change in their values is due to a short decrease of dissolved CO_2 concentration in the medium by foam destruction, which is in agreement with earlier results [46, 47].

The following amounts of AFAs are necessary to complete foam depression in a small stirred tank reactor: S184 (2000 ppm), SE9 (1000 ppm), SLM54474 (300 ppm) VP1133 (100 ppm). The pure silicone oil (S184) is not effective for foam depression in large reactors, due to a low dispersion rate, while pure PPG is not an effective AFA at all. The PPG/silicone oil mixture (VP1133) and the silicone oil emulsion (SE9) are very effective. AFAs in large reactors only slightly influence the cell concentration and product formation. SE9, a silicone oil emulsion, caused a significant increase in the concentration of *E. coli* and intracellular product and did not impair the CFU and plasmid stability, which was 100% during these investigations. The effect of AFAs on the OTR and $k_L a$ is significant at the beginning of the cultivation. Later, this effect is gradually decreased [51].

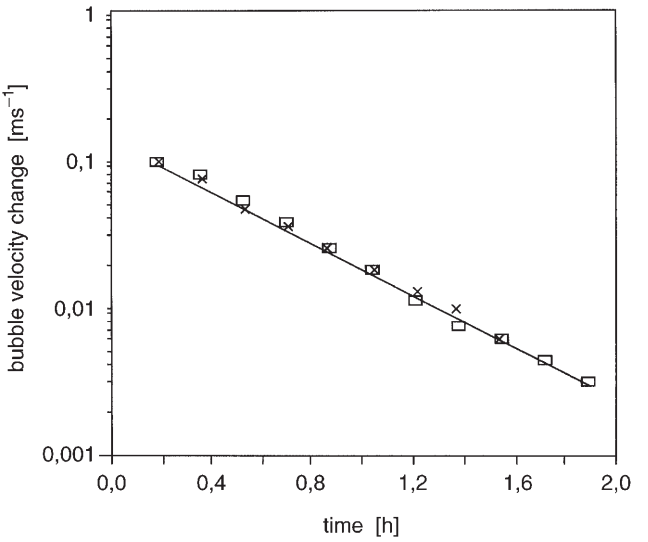

Fig. 4. Variations in the bubble velocity in recombinant *E. coli* culture at 13 and 16 h as a function of the time after the maximum velocity had been attained with SE9 AFA addition [51]

Animal cells are sensitive to direct bubble aeration, as several author have observed (e.g. [55, 56]). Pluronic F-68 (BASF, Ludwigshafen) is a copolymer of poly(oxyethylene) (POE) and poly(oxypropylene) (POP) with a relative molecular weight of about 8400, of which 80% is POE. In the molecule the hydrophobic POP moiety is flanked by two hydrophilic POE moieties. This surfactant have been widely used as a protective agent against hydrodynamic cell damage, because the direct cell–bubble interaction is eliminated. However, in medium supplemented with Pluronic F-68, the foaminess considerably increased. The highest foaming was observed in the middle of the exponential growth rate, with less foam being produced in the stationary and dying phases. To suppress the foam formation a silicone AFA (30% antifoam C emulsion; Sigma, USA) was used. Foam was completely eliminated in a medium supplemented with greater than 50 ppm AFA and 0.2% (w/v) Pluronic F-68. Relatively constant cell growth was found both in the bioreactor until 200 ppm AFA concentration; a marked reduction in cell growth was observed above that. Contrary to cell growth, relatively high monoclonal antibody (MAB) concentration was found in medium containing 200 ppm AFA. This enhancement effect on MAB concentration is attributed to the increased specific antibody production rate observed in the presence of Pluronic F-68 under lower cell growth. However, the cell damage by bubbles increased, probably because the AFA reduces the protective effect of Pluronic F68.

Van der Pol et al. [54] investigated the influence of a silicone AFA on the shear sensitivity of hybridoma cells in sparged cultures. They supplemented the medium with 1 g l^{-1} poly(ethylene glycol) PEG 6000 and PEG 20,000 to protect the cells from hydrodynamic damage. To suppress the foaming caused by the

PEG, a poly(dimethylsiloxane) AFA (JT Baker, USA) was used, which increased the death rate.

3 Protein Flotation

Flotation has been used for centuries in the mining industry for the dressing and concentration of mineral ores and in waste water engineering. Despite many publications and several books on the use of flotation in the industry, only a few papers and short chapters in books have dealt with the application of flotation for protein and cell recovery [57, 58]. The theory of flotation has been discussed by Schulze [59] and Loewenberg and Davis [60]. Some biotechnological applications of flotation were presented in the handbook written by Rousseau [61].

The recovery of proteins from cultivation medium is usually performed by precipitation, adsorption, flocculation, extraction and ultrafiltration [62–64]. The adsorptive bubble separation techniques were considered in a book by Lemlich [65]. Foam flotation was described by Wilson and Clark [66]. However, in these books, no systematic investigations on the influence of equipment and operating parameters on protein enrichment and separation factors were published.

Foam flotation is especially suitable for protein recovery from aqueous solutions at low protein concentrations. BSA was used as a model protein in batch [67] and continuous operation [68–71]. β-Casein recovery [72] and binary mixtures (BSA/lysozyme, β-casein/lysozyme and β-casein/BSA) and their separation were also investigated [73].

The most common mode of operation of foam fractionation employed by various investigators is the single stage semibatch flotation: the protein solution used in batch mode and aerated continuously [71]. However, continuous multistage operation has the highest performance [70]. Therefore, this operation mode is discussed in detail.

3.1 Continuous Flotation of Proteins

Typical continuous laboratory flotation equipment has been described by Gehle and Schügerl [70], who investigated the recovery of BSA from aqueous solution by foam flotation. The thermostatted flotation setup consisted of a column with a 23-mm internal diameter, 49-cm bubbling liquid height and 30-cm foam layer height. Nitrogen gas saturated with water was distributed by perforated and porous plates, respectively. The protein solution was fed into the column at the height of the interface between the bubble column and the foam column. The interface was controlled by an overflow. The foam left the column at the top. The foam liquid was recovered by a mechanical foam breaker. The remaining liquid at the bottom was disposed of through the overflow (Fig. 5). Another thermostatted setup consisted of a column 25 mm in diameter, 44 cm bubbling liquid height and 18 cm foam layer height operated in the same way as the other

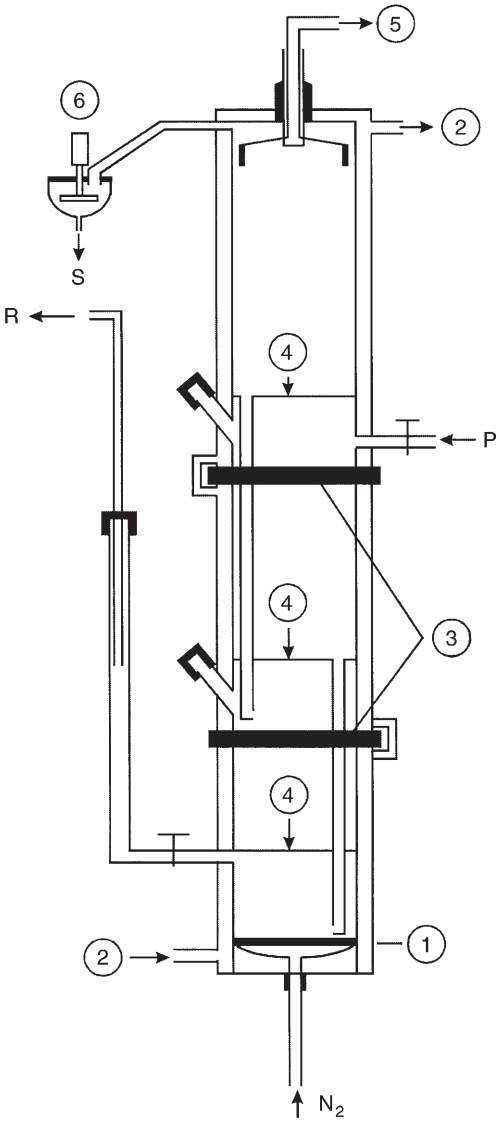

Fig. 5. Three-stage thermostatted flotation column (25 mm diameter). *P* feed; *R* liquid outlet with protein residue; *S* foam liquid outlet; N_2 gas inlet; *1* glass frit; *2* thermostat; *3* perforated plates with overflow and down-comer; *4* liquid level in the three stages; *5* electrical conductivity probe; and *6* foam breaker (3000 rpm) [70]

apparatus. This piece of equipment was operated as a three- and four-stage bubble column, respectively. The pH value of the feed solution was controlled by a pH meter.

The electrical conductivity of the foam was measured on-line to control the steady state of the process. Results were only accepted if they had been obtained under steady state conditions. The protein concentrations were determined by a photometer at 275.5 and 320 nm and the difference was used for to correct for the error due to the turbidity of the solution.

3.1.1 *Characterization of Process Performance*

The process performance was characterized by the protein enrichment (E), the protein separation (S), as well as by the protein recovery (R), i.e. the partition of protein between the foam liquid and residue liquid. Protein enrichment (E) is defined as:

$$E = \frac{C_S}{C_R} \frac{\textit{protein concentration in foam liquid}}{\textit{protein concentration in feed}} \tag{6}$$

protein separation (S) as:

$$S = \frac{C_S}{C_R} \frac{\textit{protein concentration in foam liquid}}{\textit{protein concentration in residue liquid}} \tag{7}$$

and protein recovery (R) as:

$$R = \frac{\textit{Mass of protein in the foam}}{\textit{Mass of protein in the initial feed}} \times 100\,(\%) \tag{8}$$

where C_P is the protein concentration in the feed, C_S the protein concentration in the foam liquid and C_R the protein concentration in the residue liquid.

The results of protein analysis were controlled by the protein balance:

$$C_P V_{tP} = C_S V_{tS} + C_R V_{tR} \tag{9}$$

where V_{tP}, V_{tS} and V_{tR} are the volumetric flow rates of the feed, the foam liquid and the residue liquid, respectively.

The foaminess Σ was determined according to Bikermann [74]. However, since the foaminess in a continuous flotation cannot be defined according to Eq. (1), the foam liquid volume flow V_{tS} was used to characterize the foam property. This modified foaminess Σ^* is approximately proportional to Σ defined according to Eq. (1) and for continuous operation is defined by Eq. (10):

$$\Sigma^* = \frac{V_{tS}}{V_{tg}} \tag{10}$$

Table 4. Examples of the performance of columns A, columns (single stage) B (four stage) and C (three stage), C_P = 75 mg l^{-1} at 30 °C and pH 4.8 [70]

Column	A	B	C
$S = C_S/C_R$	7.9	11.1	19.5
C_S (mg l^{-1})	237.5	282.3	870.0
C_R (mg l^{-1})	30.2	25.4	45.0
V_{tS} (ml min^{-1})	2.0	2.2	0.4
R (% BSA in S)	66	80	43
Mean residence time τ (min)	19.3	18.4	n.d

The recovery, i.e. the partition of protein between foam and residue, was also determined. Typical results are shown in Table 4. In the three-stage column the highest enrichment (E) was achieved, whereas in the four-stage column it was the best recovery (R) that was obtained. Under optimum operational conditions the performance of the protein recovery was considerably improved (Table 4).

BSA was also used as a model protein by Brown et al. [75] for protein recovery by foam flotation. They investigated the influence of feed concentration, superficial gas velocity, feed flow rate, bubble size, pH and ionic strength on the enrichment and recovery of BSA in a single-stage continuous flotation column.

3.1.2
Influence of Process Variables

The concentration of the protein in the foam liquid and in the residue depends on several parameters which interact in a complex way. It is difficult to develop a quantitative relationship between them for cultivation media. However, some qualitative interrelations can be recognized [70].

1. Parameters which increase the foam liquid volume flow, i.e. the water content in foam, diminish C_S. Thus, V_{tS} is increased and C_S diminished by a reduction in:
   - foam layer height (drainage is reduced)
   - temperature (drainage is reduced)
   - concentration of „structure breaker“ ($NaClO_4$) and ethanol (above 1 vol%) (foaminess increased)

   and by an increase in

   - protein concentration in feed (foaminess increased)
   - concentration of „structure maker“ (Na_2SO_4) and ethanol below 1 vol% (foaminess increased).
2. Some of the effects which increase the foam liquid volume flow diminish C_R as well:
   - concentration of ethanol above 1 vol% (solubility of protein decreased)
   - aeration rate
   - porosity of aerator (specific gas/liquid area is increased)
   - concentration of „structure maker“ (Na_2SO_4) and ethanol below 1 vol%.

3. When C_S and C_R change in the same direction, then:
   – C_S/C_R increases if the aeration rate is reduced
   – C_S/C_R diminishes if Na_2SO_4 or ethanol is added to the solution.
4. The separation (C_S/C_R) can be increased by a decrease in:
   – aeration rate
   – protein concentration in feed
   – ethanol concentration above 1 vol%

   and by an increase in

   – porosity of the aerator
   – temperature
   – liquid and foam layer heights
   – concentration of „structure breaker“ and ethanol concentration below 1 vol%, and
   – at the isoelectric point (pH 4.8 – 5.0).

3.2 Separation of Protein Mixtures

Ostermaier and Dobiás [76] investigated the possibility of separating proteins with different isoelectric points (IEPs) by flotation from mixtures by varying the pH of the solution, together with certain concentrations of structure maker and structure breaker. They applied a mixture of the following proteins: fetuin, BSA, hemoglobin, myoglobin, chymotrypsinogen A and cytochrome c with IEPs in the range 3.5 to 10.2. Measurements of solutions of the same proteins at various pH values showed that the minimum surface tension occurs at the IEP of the protein concerned. The surface tension of the protein mixture as a function of the pH indicated that IEPs of particular proteins are nearly the same as the IEPs of the single proteins. Therefore, protein separation should be possible

Table 5. Performance of some protein flotations under optimum operational conditions

Protein	pH	T (°C)	C_P (mg l^{-1})	R (%)	E (–)	S (–)	Ref.
BSA	4.8	40	40	90	50	450	[70]
β-casein	5.3	25	20	62.4	54.7	181.3	[72]
β-casein	5.3	25	30	92.1	1.5	7.4	[72]
Mixture of β-casein	6.25	25	40	63.5	79.4	31.8[a]	
Lysozyme	6.25	25	500	2.0	2.5		[73]
Mixture of BSA	4.6	25	10	41.9	74.2	53.0[b]	
Lysozyme	4.6	25	500	0.9	1.4		[73]
Mixture of β-casein	5.3	25	40	49.4	23.5	0.6[c]	
BSA	5.3	25	10	89.4	42.9		[73]

[a] β-casein/lysozyme ratio.
[b] BSA/lysozyme ratio.
[c] β-casein/BSA ratio.

by means of the surface tension vs. pH diagram. However, because of a strong overlapping of the protein peaks their separation was not possible.

Liu et al. [77] investigated the separation of BSA and hemoglobin by flotation in batch operation. An optimal separation factor $\alpha = S_1(\text{BSA})/S_2(\text{HBB}) = 14$ was obtained at pH 3.9. Brown et al. [73] investigated the separation of binary mixtures of β-casein, lysozyme and BSA and obtained fairly good separations (Table 5).

The isolation and purification of human placental homogenate was investigated by Sarkar et al. [78] in a batch foam column. They found the optimum near to the IEP (pH 8.0). Column diameter and height were optimized. At a low gas flow rate the best separation from accompanying proteases was obtained.

3.3
Application of Additives

Miranda and Berglund [79] used a food grade polymer, (hydroxypropyl)methyl cellulose (HPMC), and ammonium sulfate as additives for the recovery of recombinant α-amylase by flotation. The enzyme was removed from the liquid phase by partition to a salted-out HPMC phase and the enzyme-containing polymer flocs were recovered by flotation. This system behaved in a manner similar to the flotation of mineral systems. The problem with this technique is the cost of the polymer and the separation of the enzyme from the polymer phase. Both of them complicate the process and increase the separation cost. In general, for protein recovery and separation, especially in the pharmaceutical industry, it is not proper to add chemicals to the feed, because they have to be removed from the product completely and this separation causes problems and additive costs.

3.4
Protein Denaturation

The application of foam flotation for the recovery of enzymes is often impaired by their denaturation and activity loss. By using nitrogen or carbon dioxide as sparging gas, respectively, instead of air, low volumetric flow rates (0.79 cm s^{-1}) and operating at 16 °C and pH 3, denaturation can be suppressed. In the case of catalase the loss of enzyme activity was reduced to 0% and in the case of trypsin to 10% [80].

Varley and Ball [81] investigated the activities of lysozyme, pepsin and trypsin during foam separation. They found that with increasing protein concentration the enzyme activity loss diminished. According to Graham and Phillips [82, 83] the surface concentration of a protein at the gas/liquid interface changes with its bulk concentration. At higher bulk concentrations a multi-protein layer with high surface coverage is formed. A bubble surface covered by a multi-layer obviously reduces the residence time of the protein in the foam phase and protects the enzymes from denaturation. With increasing flow rate, the activity loss was reduced. 99% of the initial activity of lysozyme, 92% of

pepsin and 90% of trypsin were retained at high flow rates, above 300 $cm^3\,min^{-1}$, at 2.2 $mg\,ml^{-1}$ lysozyme, 0.2 $mg\,ml^{-1}$ pepsin and 0.1 $mg\,ml^{-1}$ trypsin initial concentrations [81].

3.5 Mathematical Modeling

To describe and quantify the effects of the various operational variables on the performance of foam flotation, several authors have developed mathematical models. Earlier investigators assumed equal-sized bubbles, infinite surface viscosity and accounted only for the gravity drainage [84–86]. Later on, the influence of the surface viscosity on the liquid drainage was also considered [87–89] and the liquid holdup profile in a foam column was predicted by considering the liquid drainage from the Plateau border [90]. The change in the bubble size distribution due to inter-bubble gas diffusion was also taken into account [91–94]. Uraizee and Narsimhan [95, 96] developed an advanced model for continuous foam concentration of protein which accounts for (i) kinetics of the adsorption of proteins in the liquid pool and in the foam, (ii) the liquid drainage from this film due to Plateau border suction, (iii) the gravity drainage of liquid from the Plateau border, and (iv) the bubble coalescence in the foam. The mass balances of liquid in the film and Plateau border, the protein balances in the film and Plateau border, and the balance of the bubbles are used with appropriate boundary conditions. The protein concentration in the liquid pool, the kinetics of adsorption of protein, the time of bubble formation, the residence time of the bubbles in the liquid pool and the coalescence rate are needed for the calculation.

In order to solve the balance equations, the velocities of the film and Plateau border drainage as well as the kinetics of the protein adsorption in the films are used. The velocity of drainage of Plateau borders, u, depends on the flow due to gravity and due to the gradient of Plateau border suction. By neglecting the latter one obtains:

$$u \approx \frac{C_v a_p \rho g}{20\sqrt{3\mu_P}} \tag{11}$$

where C_v is the velocity coefficient for gravity drainage of the Plateau border, a_P is the cross-sectional area of the Plateau border (m^2), ρ is the density of the protein solution, g is the acceleration of gravity, and μ_P is the viscosity of the protein solution.

Since the velocity of the film drainage is small, protein adsorption in films is assumed to be diffusion controlled. The enrichment was calculated by using the protein concentration in the feed for its pool concentration. The surface concentration of a protein at the foam/liquid interface was calculated by the following equation:

$$\Gamma = \Gamma_{formation} + \int_0^{\theta_p} \left(\frac{d\Gamma}{dt}\right)_{pool} dt \quad \text{at} \quad z = 0 \tag{12}$$

where Γ is the surface concentration of protein, θ_P the residence time of the bubble in the liquid pool, $\Gamma_{formation}$ the protein concentration at the end of the bubble formation, $\left(\frac{d\Gamma}{dt}\right)_{pool}$ the rate of protein adsorption onto the bubble during its travel through the liquid pool, and z is the axial distance from the foam/liquid interface (m).

The film thickness and area of the Plateau border at the foam/liquid interface were obtained from the knowledge of the gas velocity and bubble size. The coupled partial differential equations of the balances were solved using a differential equation solving package. The surface concentration of the protein at the film interface is calculated by assuming a diffusion-controlled adsorption rate. From the mass balance the bottom flow rate and the liquid pool concentration were evaluated. Using these data the enrichment and recovery were calculated. This model predicts the enhancement of protein enrichment with increasing liquid pool height, decreasing gas velocities, increasing bubble size due to coalescence, high feed flow rates and low feed concentrations in good agreement with the measurements with BSA solution. The extension and application of this mathematical model for complex cultivation media is still to be achieved.

4 Flotation of Microorganisms

Centrifugal separators are applied in industry for the recovery of microbial cells from cultivation media. In waste water engineering a combination of flocculation and sedimentation is practiced. In the laboratory, cross-flow membrane separation is often used for retention of the cells. Some microorganisms and cells are enriched in the foam; therefore, flotation is suited for the recovery of particular microbial cells from cultivation medium.

Dognon and Dumonte [97] and Dognon [98] were the first to observe the enrichment of microorganisms in foam. To enhance the separation quaternary ammonium ions [99–101] or flocculants [102] were applied. Cell recovery without additives (collectors) was seldom used [103–107]. All of these investigations were performed in batch operation.

Several investigations were carried out to remove toxic heavy metal ions from waste water by biosorption. Microbial cells loaded with heavy metals were recovered by flotation, e.g. *Streptomyces griseus* and *S clavuligerus* loaded with Pb [108] and *Streptomyces pilosus* loaded with Cd [109]. In these flotation processes the microbial cells were dead; therefore, they are not considered here. The removal of pyritic sulfur from coal slurries such as coal/water mixtures by *Thiobacillus ferrooxidans* and recovery of this iron-oxidizing bacterium by flotation is a special technique in the presence of high concentrations of solid particles (see e.g. [110]). The flotation of colloid gas aphrons was used for the recovery of yeast in continuous operation [111] for the recovery of micro algae, and in the presence of flocculants in batch operation [112]. These special techniques are not discussed here.

4.1
Flotation of Yeast Cells

Systematic investigations of microbial cell recovery by foam flotation were performed by *Hansenula polymorpha* [113–117] and *Saccharomyces cerevisiae* [118–123] in continuous operation. The equipment used for flotation was often identical to that used for protein flotation. The microorganisms were cultivated in laboratory reactors on synthetic media in the absence of antifoam agents in continuous operation and the cell-containing cultivation medium was collected in a buffer storage and was fed into the middle of the column, at the top of the interface between the bubble and the foam layers. The height of the interface was controlled by an overflow. The foam left the column at the top. The cells were recovered from the foam liquid by a mechanical foam destroyer. The liquid residue left the column through an overflow [113] (Fig. 6).

Hansenula polymorpha was cultivated in synthetic medium in the absence of an antifoam agent in stirred tank reactors (B20; B Braun, Melsungen and LF 14; Chemap), as well as in the 45-l tower loop reactor described by Buchholz et al. [124]. The foam was controlled by a mechanical foam destroyer (Fundafoam; Chemap) and by a destroyer constructed and built at the Institute of Technical Chemistry, University of Hannover, respectively. The influence of substrate type (glucose, ethanol and methanol) and concentrations of substrates and cells, the growth limiting component (O_2, P, and N), pH value, temperature, and presence of flocculation agent ($CaCl_2$) on the process performance was investigated.

4.1.1
Characterization of Process Performance

The cell recovery process was characterized by the cell enrichment factor E*, cell separation factor S* and cell recovery factor R*:

$$E^* = \frac{C_S^*}{C_P^*} = \frac{\textit{cell concentration in foam liquid}}{\textit{cell concentration in medium}} \tag{13}$$

$$S^* = \frac{C_S^*}{C_R^*} = \frac{\textit{cell concentration in foam liquid}}{\textit{cell concentration in residue liquid}} \tag{14}$$

$$R^* = \frac{C_S^* V_{tS}^*}{C_R^* V_{tP}^*} = \frac{\textit{cell mass flow in foam}}{\textit{cell mass flow in medium}} \tag{15}$$

The cell mass balance

$$C_P^* V_{tS}^* = C_S^* V_{tS}^* + C_R^* V_{tR}^* \tag{16}$$

was used to control the accuracy of the cell mass analysis.

In Eqs. (10–12), C_P^*, C_S^* and C_R^* are the cell concentrations in the feed, the foam liquid and the residue liquid, and V_{tP}^*, V_{tS}^* and V_{tR}^* are the flow rates of the

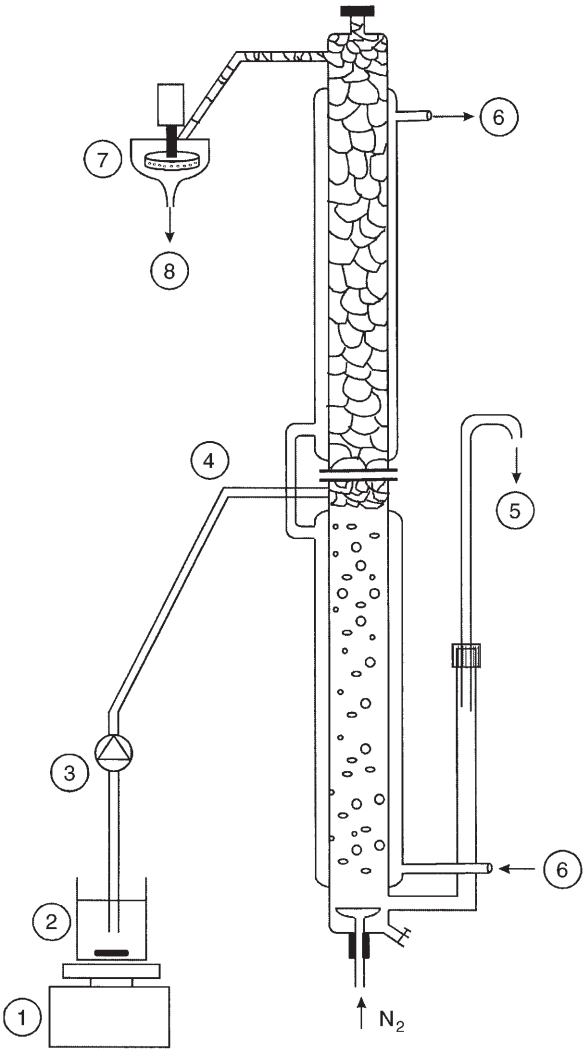

Fig. 6. Continuous cell flotation column. *1* magnetic stirrer; *2* cell suspension; *3* pump; *4* feed; *5* liquid outlet with cell residue; *6* thermostat; *7* foam breaker; and *8* foam liquid [113]

feed, the foam liquid and the residue liquid, respectively. In addition, the surface tension σ and foaminess Σ of the cultivation media were determined.

Hansenula polymorpha (CBS 4732) was cultivated in a synthetic nutrient medium [113] with glucose, ethanol and methanol as substrates, respectively, in batch and continuous operations. The flotation was performed in batch as well as in continuous mode. A comparison of the performances of batch flotation with continuous flotation indicated that, in the latter, the C_S^* values are higher than in the former. For example, at $C_P^* = 1.5\ g\ l^{-1}$, the cell concentration in the

foam liquid $C_S^* = 120\,g\,l^{-1}$ in continuous operation and $40\,g\,l^{-1}$ in batch operation mode. The enrichment E* and separation S* are higher in continuous operation as well.

In general C_S^* diminishes with increasing cell concentration. Factors which increase foaminess diminish C_S^* and thus E_S^* and S_R^* too. Systematic investigations dealt with the influence of (i) the cultivation conditions, and (ii) the flotation equipment, construction and operational parameters.

4.1.2 *Influence of Cultivation Conditions*

The medium feed rate ($10\,ml\,min^{-1}$), the gas feed rate ($1\,ml\,s^{-1)}$ of the flotation and the temperature (37 °C) and pH (5.0) of the cultivation were kept constant.

The investigations indicated that the cell separation factor S* is independent of:

- the growth phase (exponential, transient or stationary),
- the presence of low amounts of Ca^{2+} ions,
- pH value close to pH 5.0,
- cultivation temperature (close to the optimum),
- presence of a low amount of substrate, and
- growth limitation by O_2.

C_S is diminished with increasing age of the cells (after sampling) [113].

Typical flotation performances of *Hansenula polymorpha* cells from C-, N- and P-limited cultivations are shown in Table 6. The highest separation was obtained with cells cultivated under P-limitation (with $4 \times 25 \times 10^{-3}\,g\,P/g$ cell mass): S* = 442 and R* = 96.4 [116].

The cultivation medium composition and the proteins excreted by the yeast cells were determined and their influence on the flotation performance was investigated by Bahr et al. [115]. The sodium dodecyl sulfate polyacrylamide gel electrophoresis (SDS-PAAGE) and native PAAGE measurements indicated that during the cultivation various glycoproteins were excreted, which were distributed differently between the foam and the flotation residue liquid. A

Table 6. Typical flotation performances of the *Hansenula polymorpha* cells from C-, N- and P-limited cultures as well as C-limited cultures with amino acid supplement C(AS) in the dilution range 0.1 and 0.25 h^{-1} (1 Pirt unit = 0.0255 g P/g cell mass) [116]

Limitation	D (h^{-1})	$C_P^*(g\,l^{-1})$	$C_R^*(g\,l^{-1})$	$C_S^*(g\,l^{-1})$	R*(%)	S*
C	0.105	4.98	4.34	28.8	12.9	6.63
C(AS)	0.11	5.64	4.34	43.5	23.0	10.0
N	0.12	5.15	2.72	52.6	47.2	19.34
P (0.33 Pirt)	0.10	4.47	0.40	75.0	91.0	187.5
C	0.225	5.2	2.73	68.3	47.5	25.0
C(AS)	0.227	5.6	1.31	64.5	76.6	49.23
P (0.166 Pirt)	0.25	4.18	0.15	66.4	96.4	442.6

close relationship between the foaminess of the cultivation medium and the excreted proteins was observed. The foam stability increased in the sequence C-, N- and P-limited growth cultures.

In cultures with C- and N-growth limitation, the foaminess was influenced by the dilution rate. At low dilution rate, the foaminess was low, and the foam consisted of large foam lamellae that were unstable. This phenomenon was not caused by the change in the proteins, because the dilution rate did not influence the protein pattern, but by extracellular lipids that were excreted by the yeast at low dilution rates. The main proteins (75 kD) excreted at P-limitation had a significantly different electrophoretic behavior than those excreted during C- and N-limitation. They were quantitatively enriched in the foam. With increasing dilution rate the amount of excreted lipids diminished. The best cell recovery by flotation was obtained in cultures with P-limitation and just below the critical dilution rate where no lipids were excreted at all. The high molecular weight and strongly acidic glycoproteins enriched in the foam and the low molecular weight ones in the residue liquid. The proteins played a role as „foamer" and „collector" as defined by the flotation technique. Since *Hansenula polymorpha* has a hydrophilic surface (see below), its flotation is only possible with collectors. Exoproteins adsorb at the cell surface and act as collectors.

4.1.3
Influence of the Flotation Equipment, Construction and Operational Parameters

The column height and diameter, as well as the operational conditions, influence the performance of the flotation process [113]:

- S^* and C_S^* are improved by diminishing feed rate (reduction of water content)
- C_R^* is reduced, but C_S^* is not influenced, hence S^* is improved by increasing aeration rate
- C_S^* and C_R^* are reduced with diminishing bubble size, and S^* passes a slight maximum at 100–175 µm pore diameter (increasing water content in foam)
- temperature increase up to 50 °C slightly improves C_S^* but has no effect on C_R^*
- C_S^* and S^* have maxima at pH 5.0–5.5
- the dilution of cultivation medium increases C_S^* (diminution of the water content in foam) and C_R^* (due to the dilution)
- increase in the foam layer height up to 15 cm enlarges C_S^* and C_R^*, above that they are constant
- increasing height of the aerated liquid layer reduces C_S^* slightly, but C_R^* considerably, separation is improved
- enlargement of the foam column diameter improves C_S^* and S^* (reduction of wall effect)
- addition of structure-maker salts to the medium increases the foaminess and reduces C_S^*
- addition of structure-breaker salts to the medium decreases the foaminess and increases C_S^*, but does not influence C_R^*

At low dilution rates the foaminess and foam stability were low, because of extracellular lipids excreted by the cells. This caused low protein enrichment in the foam.

In synthetic medium and with a mean residence time of 6.5 h (dilution rate $D = 0.15\,h^{-1}$) and $10\,g\,l^{-1}$ glucose only $1.9\,g\,l^{-1}$ cell mass concentration was obtained. The flotation of this medium yielded a cell-free residue ($C_R^* = 0.0\,g\,l^{-1}$) and high cell mass concentration in the foam $C_S^* = 81\,g\,l^{-1}$. The separation factor S* was infinite. When the same medium was supplemented with a mixture of inositol, pantothenate and pyridoxine, $4.8\,g\,l^{-1}$ cell mass concentration was obtained. By flotation of this medium with a $3\,ml\,s^{-1}$ aeration rate $C_S^* = 65\,g\,l^{-1}$, $C_R^* = 80\,mg\,l^{-1}$ and S* = 812 were obtained.

4.1.4
Continuous Cultivation and Flotation in Pilot Equipment

All of the investigations with cell flotation presented in the cited literature were performed with small laboratory equipment. Gehle et al. [117] reported on the investigation on a pilot-scale apparatus consisting of a 300-l stirred tank reactor provided with a foam separator (Fundafoam; Chemap) and a flotation column, 3.6 m height, 10 cm internal diameter, which was directly connected to the reactor (Fig. 7).

Hansenula polymorpha and *Saccharomyces cerevisiae* were cultivated on synthetic medium with 1% glucose in fed-batch and continuous mode, respectively, in the absence of antifoam agents. For the nutrient preparation, sterilization and storage, 300-, 600-, 1000- and 5000-l stirred tank vessels were used. The nutrient salt medium was sterilized without glucose. The glucose solution was autoclaved separately and was added to the cold, sterilized nutrient medium. The flotation column was operated in continuous mode.

Hansenula polymorpha CBS 4732 was cultivated at pH 5 and 29 °C and 37 °C, respectively, relative aeration rates q_G [(vol min^{-1} gas)/(medium volume)] = 0.33 and 0.50 min^{-1}, impeller speed N = 200 – 300 rpm, dilution rates D = 0.1, 0.2 and 0.3 h^{-1} at C-limitation, O_2-limitation and at different phosphate concentrations, respectively. The highest separation and enrichment factors were obtained with $D = 0.1\,h^{-1}$, $0.106\,g\,l^{-1}$ phosphate, $q_G = 0.5\,min^{-1}$, at 29 °C under steady state operation in the reactor and flotation column: $C_P^* = 2.18\,g\,l^{-1}$, $C_R^* = 0.05\,g\,l^{-1}$, $C_S^* = 115\,g\,l^{-1}$, S* = 2311 and E* = 52.1, R* = 100 % with $90\,l\,h^{-1}$ gas flow rate in the flotation column.

Cultivations of *Saccharomyces cerevisiae* DSM 2155 were performed at pH 5.1, 29 °C, $q_G = 0.5\,min^{-1}$, N = 200 – 300 rpm and $D = 0.1\,h^{-1}$ at C-limitation under steady state operation in the reactor and flotation column: $C_P^* = 4.8\,g\,l^{-1}$, $C_R^* = 0.0\,g\,l^{-1}$, $C_S^* = 139.2\,g\,l^{-1}$, $S^* = \infty$, E* = 29.1, R* = 100 % with $180\,l\,h^{-1}$ gas flow rate in the flotation column.

The flotation performances in the pilot plant were better than those achieved on a laboratory scale, probably because of the reduced wall effect in the flotation column.

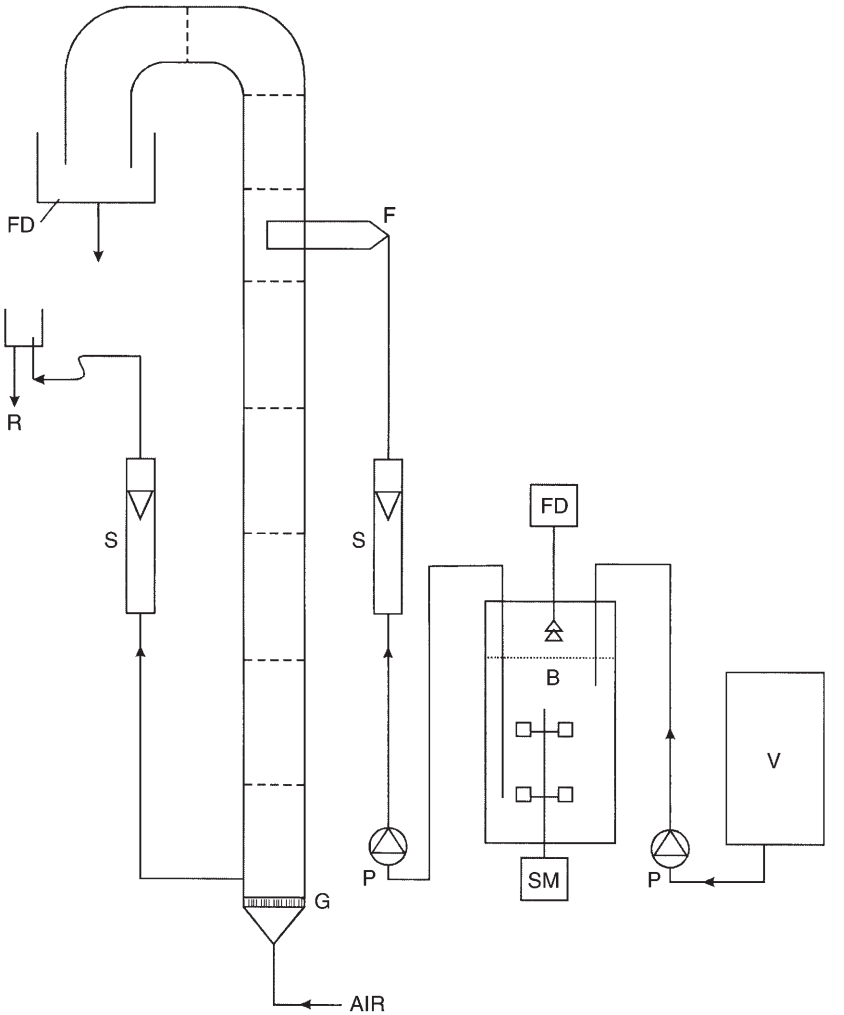

Fig. 7. Pilot plant equipment for continuous cell flotation with integrated bioreactor/cell flotator. *S* flow meter; *V* medium storage; *B* bioreactor; *F* feed; *FD* foam destroyer; *P* pump; *G* gas distributor; *SM* stirrer motor; and *R* residue [117]

4.2 Combination of Yeast Cells with Surfactants

Husband et al. [121] combined rehydrated *Saccharomyces cerevisiae* and a surfactant and used them as a model for flotation in a 100-cm high, 45-mm diameter laboratory column, which was provided with a stainless steel air sparger. The feed entered at half height into the column, the foam left the column at the top and the residual liquid at the bottom. No information was given on the control of the interface between the bubbling liquid layer and the foam layer. In some runs washing water was added to the foam layer at the top

of the column 2 cm below the foam exit. The operating conditions were: feed superficial velocity 0.21 cm s^{-1}, air superficial velocity 0.31 cm s^{-1}, bubble column height 60 cm, foam column height 40 cm, yeast concentration 2 g l^{-1}, surfactant concentration 40 mg l^{-1}, pH 5. Without surfactant the rehydrated yeast suspension formed only a very low amount of foam, or no foam at all. Therefore alkyl polyglycoside surfactant (APG 625CS; Henkel) was added to the suspension. The recovery of the surfactant amounted to R = 86 – 95 %, the yeast enrichment E* = 11 and recovery R* = 55 % The addition of sodium, potassium, magnesium and calcium chloride to the feed, respectively, increased E* and R*, and the use of wash water reduced them by an order of magnitude, because it removed the cells from the foam. The most effective salt levels for cell flotation were in the concentration range in which the electrophoretic mobility of the cells has a minimum. The proteins excreted by the yeast cells are obviously better „collectors“ than the surfactant APG 625CS.

4.3
Modeling of Microbial Cell Recovery by Foam Flotation

Only a few researchers have dealt with the modeling of cell separation by flotation [125, 126]. The model of Ramani [126] is based on the drainage model of Desai and Kumar [127] for semi-batch surfactant foams. By means of a material balance of films, horizontal and vertical Plateau borders, as well as film thinning rate, the drainage rate was evaluated. Variations in liquid holdups in films, horizontal and vertical Plateau borders were set up for the change in the drainage mechanism until the dimensions of either the films or the Plateau borders reached values close to that of agglomerate size. When an agglomerate is present in the liquid film, thinning occurs by a different mechanism. The final drainage expression with suitable initial and boundary conditions was solved using the method of characteristics [128]. For the separation factors, they obtained:

$$S^* = 1 + \frac{a_i C_i}{H a_c \varepsilon_t C_S} \left(1 - \frac{C_B R_{wd}}{\rho_{cell}} \right) \tag{17}$$

where a_i is the total interfacial area (m^2), a_c is the cross-sectional area of the column (m^2), C_i is the mass of dry cells on the interface per unit area (kg m^{-2}), C_B is the average concentration in the bulk (kg m^{-2}), H is the foam height (m), ε_t is the liquid holdup at time t, R_{wd} is the ratio of wet cell volume to dry cell volume, and ρ_{cell} is the density of cell culture (kg m^{-2}). The model has been verified against experimental results.

5
Characterization of Cells with Regard to Their Floatability

The degrees of floatability of microorganisms are very different (Table 7). Some of them can be recovered by foam flotation, others are not enriched in the foam at all [120]. To find out the basis of this phenomenon, two *Saccharomyces*

Table 7. Flotation performances of various microorganisms [120]

Microorganism	Medium operation	C_P^* (g l^{-1})	C_S^* (g l^{-1})	C_R^* (g l^{-1})	E*	S*
Clostridium acetobutylicum	complex	1.6	1.6	1.7	1.0	1.0
C. acetobutylicum	synthetic	0.65	4.0	0.5	6.12	16.0
Acetobacter peroxidans					0.85	0.83
Klebsiella pneumoniae					0.78	0.75
Escherichia coli	synthetic	3.0	22.5	2.25	7.5	10.0
Rhodococcus erythropolis	batch	2.5	25.5	0.06	10.2	396
R. erythropolis	continuous	4.4	27.0	0.91	6	29.5
Candida intermedia+s	O_2-limited, $t_F < 7$ h				11.9	13
C. intermedia	O_2-limited, $t_F < 7$ h	3.5	140	0.3	40	425
Hansenula polymorpha	synthetic	3.5	70	0.00	20	∞
H. polymorpha	synthetic	0.6	72	0.00	120	∞
Candida boidinii	synth. methanol	2.5	3.0	11.5	1.2	1.95
C. boidinii	synth. glucose	4.2	10.9	1.03	2.6	10.5
Saccharomyces cerevisiae	complex				10 – 20	350 – 545
S. cerevisiae	synthetic				26 – 45	∞

cerevisiae strains, LBG H620 and DSM 2155, with different floatabilities were investigated with regard to their properties [122, 123].

The yeast cells were cultivated in continuous operation mode under carbon (C)-limited, phosphorous (P)-limited and nitrogen (N)-limited growth conditions. Cell and protein concentrations in feed, foam and residue liquids as well as the enrichment E* and separation S* factors were evaluated at different dilution rates (D). The concentration of LBG H620 cells diminished and that of DSM 2155 cells enriched in the foam. The highest enrichment factors E* in DSM 2155 cells were obtained if they were cultivated under strong P-limitation at a low dilution rate. Fairly high E* values were attained under C-limitation, but under N-limitation the E* values were meager with low values of D. At the beginning of the continuous cultivations, all of the cells were recovered, but with advanced time the degree of recovery and cell concentration and enrichment factor diminished. The cellular properties of the yeasts were characterized by flow cytometry, measurement of surface properties, hydrophobicity, electrophoretic mobility, and chemical composition (using X-ray photoelectron spectroscopy, XPS).

The protein content in a medium of DSM 2155 yeast was always higher than that of the LBG yeast. There was no significant difference between the lipid contents of these two strains. The average size of the cells in the liquid residue was larger than the size of the cells in the foam. This can be explained by the ob-

servation that the cell wall of larger cells contains more polysaccharides and less proteins. Therefore, they are more hydrophilic. There was no difference in the fatty acid composition and amount of the cell wall of the two strains. DSM 2155 yeast cells differ in their morphology considerably. LGB H620 cells formed only single or budding cells, strain DSM 2155 formed chain-like cell aggregates with size depending on the cultivation conditions: in the presence of adequate substrate, concentration cell aggregates consisting of up to eight cells were formed, and during substrate limitation single cells dominated [123]. The difference of flotation between the two strains is related to their surface properties. The cells of the LBG strain are less hydrophobic (water contact angle 27°) and the cells of the DSM strain are very hydrophobic (water contact angle 70°). With prolonged cultivation time, the hydrophobicity of the cells diminished and, consequently, their flotation as well. The difference in surface hydrophobicity between the two strains originates from variations in their surface chemical composition. In batch-culture strain DSM 2155 had a lower oxygen and hydroxide content on its surface, and a higher proportion of hydrocarbon C, as compared with strain LBG H620. Another property that seems to be related to the behavior of the yeast is the surface charge. Strain LBG H620 is more negatively charged than DSM 2155 (electrophoretic mobility at pH 4.0 was $-1.85 \times 10^{-8}\,m^2\,V^{-1}$ and −1.35, respectively). The latter strain has a greater tendency to aggregate due to lower electrostatic repulsion and stronger hydrophobic interactions. According to Armory et al. [129] and Moses et al. [130] the hydrophobicity of the surface of yeasts and bacteria can be related to the O/C atomic ratio and the electrokinetic potential to the P/C atomic ratio. The P-limitation caused, as expected, a decrease in the surface P/C atomic ratio. The investigations by Tybussek et al. [122] indicate that the differences in the P/C atomic ratio correlate well with changes in the electrophoretic mobility for strain LBG H620, but not for strain DSM 2155, which does not change with the P/C ratio. More investigations are necessary to obtain quantitative relationships between physicochemical surface properties and floatability of yeast cells.

6 Conclusions

There have been many investigations on surfactant foams, foam films, Plateau border, foam drainage and their physical chemistry. The application of these results to protein foams is only partly possible. Proteins are macromolecules, their adsorption is coupled with a change in conformation at the gas/liquid interface which is a slow process. It takes 15 to 20 h to obtain the equilibrium surface tension. The residence time of the protein molecules in a flotation column is too short to attain the equilibrium surface tension during this time. Therefore, the transport of proteins to the interface and their adsorption at the interface are dynamical processes which are far from equilibrium. Surfactants have well-defined hydrophilic and hydrophobic domains. Thus it is relatively easy to calculate their interaction with the interface. Protein molecules have several hydrophilic and hydrophobic domains, and their interaction with the interface depends on the hydrophilic/hydrophobic character of their surface

which is a function of their conformation. Also the viscosity of the protein solutions which effects the film drainage depends on this conformation. In the case of cultivation media, the protein conformation, and therefore the foaminess and foam stability, is influenced by the medium composition as well, which is often not well defined and changes during the cultivation. In the case of microbial cell flotation, the process depends on the protein enrichment, i. e. on the interaction of the proteins with the gas/liquid interface, as well as on the reciprocal action of cells with the protein and gas/liquid interface.

Microorganisms have a complex cell envelope structure. Their surfaces charge and their hydrophobicity cannot be predicted, only experimentally determined [131]. Several microorganisms are not hydrophobic enough to be floated. They need collectors, similar to ore flotation. In cultivation media proteins which adsorb on the cell surface act as collectors. The interrelationship between cell envelope and proteins cannot be predicted, only experimentally evaluated. The accumulation of cells on the bubble surface depends not only on the properties of the interface, proteins and cells, but on the bubble size and velocity as well [132]. On account of this complex interrelationship between several parameters, prediction of flotation performance of microbial cells based on physicochemical fundamentals is not possible. Therefore, only empirical relationships are known which cannot be generalized. Based on the large amount of information collected in recent years, mathematical models have been developed for the calculation of the behavior of protein solutions and particular microbial cells. They hold true only for systems (e. g. BSA solutions and particular yeast strains) which are used for their evaluation. In spite of this, several recommendations for protein and microbial cell flotation can be made.

Flotation of proteins and microbial cells is especially efficient at low concentrations, which are well below the values common in microbial cultivations with complex media and high-performance strains used in industry. Therefore, they are only suited for the recovery of proteins and cells from synthetic media with low protein and cell concentrations. However, at low protein concentrations, the enzymes are deactivated. Dilution of the cultivation medium to enhance enrichment of the cells is uneconomical, because the improvement in the enrichment is fully compensated by the reduction in cell concentration in the feed. The final cell concentration in the foam liquid remains the same. The protein separation S can be increased by reducing the aeration rate and protein concentration in the feed and increasing the bubble size, the temperature, aerated liquid layer and foam layer heights, as long as the foam remains stable. The foaminess of several cultivation media can be predicted on the basis of the equilibrium surface tension.

Cell separation can be increased by reducing the feed rate, the aeration rate and increasing the aerated liquid layer and the foam layer height, as long as the foam remains stable. It is also increased with a larger column diameter. Modeling of microbial cell flotation is still in the early stages, because the model does not include microbial cell properties and therefore only holds true for e. g. a particular strain of *Saccharomyces carlsbergensis* with a strong hydrophobic cell envelope, which was used for the verification of the model.

Foam formation often impairs the cultivation of microorganisms and cells, and some recommendations can be made to control these foams using antifoaming agents (AFAs). Pure silicone and polymer AFAs are not suited for foam suppression in large reactors, because of their inadequate distribution in the medium. In addition, these AFAs quickly lose their effectiveness, because they are deposited on the reactor wall. Each emulsion has an optimal concentration at which they are very efficient. These optima are at very low concentrations. They have to be evaluated by tests using the original cultivation medium. At these low concentrations, the AFAs are not toxic for the microorganisms and they do not impair their growth and product formation. However, they often reduce the OTR and by that they can cause oxygen limitation. Some experience is necessary to find the optimum for foaminess control and maintenance of the required OTR. At high cell concentrations the enrichment of the cells in the foam is low, which is an advantage of high density cell cultivation.

References

1. Bikerman JJ (1973) Foams. Springer, Berlin Heidelberg New York
2. Prins A, van't Riet K (1987) TIBTECH 5:296
3. Cumper CWN, Alexander AE (1950) Trans Farad Soc 46:235
4. Cumper CWN (1953) Trans Farad Soc 49:1360
5. Kalischewsli K, Schügerl K (1979) Colloid Polym Sci 257:1099
6. Avrami M (1941) J Chem Phys 9:177
7. Kalischewski K, Bumbullis W, Schügerl K (1979) Eur J Appl Microbiol Biotechnol 7:21
8. Graham DE, Phillips MC (1976) Proc Symp on Foams, Brunel University. Akers RJ (ed) Academic Press, p 237
9. Tanford Ch, Buzzel JG (1955) J Am Chem Soc 77:6421
10. Kotsaridu M, Gehle R, Schügerl K (1983) Eur J Appl Microbiol Biotechnol 18:60
11. Hofmeister F (1888) Arch Exp Pathol Pharmakol 24:247
12. Luck W (1964) Fortschr Chem Forschung 4:653
13. Luck W (1976) Top Curr Chem 64:113
14. Bumbullis W, Kalischewski K, Schügerl K (1979) Eur J Appl Microbiol Biotechnol 7:147
15. Bumbullis W, Schügerl K (1979) Eur J Appl Microbiol Biotechnol 8:17
16. Mokrushin SG, Zhidkova LG (1959) Colloid J USSR 21:323
17. Bumbullis W, Schügerl K (1981) Eur J Appl Microbiol Biotechnol 11:106
18. Mann JA, Hansen RS (1963) J Colloid Sci 18:757, 805
19. Lucassen J, Tempel van den (1972) J Colloid Interface Sci 41:491
20. Gouda JH, Joos P (1975) Chem Eng Sci 30:521
21. Bumbullis W, Kalischewski K, Schügerl K (1981) Eur J Appl Microbiol Biotechnol 11:110
22. Wolfes H, Schügerl K (1983) Eur J Appl Microbiol Biotechnol 17:371
23. Gifford WA, Sciven LE (1971) Chem Eng Sci 26:287
24. Szarka L, Magyar K (1969) Biotechnol Bioeng 11:701
25. Buchholz H, Kalischewski K, Schügerl K (1979) Eur J Appl Microbiol Biotechnol 7:321
26. König B, Kalischewski K, Schügerl K (1979) Eur J Appl Microbiol Biotechnol 7:251
27. Kotsaridu M, Müller B, Pfanz V, Schügerl K (1983) Eur J Appl Microbiol Biotechnol 17:258
28. Angrick M (1980) Chemie in unserer Zeit 5:149
29. Vardar-Sukan F (1998) Biotechnol Adv 16:913
30. Noble J, Collins M, Porter N, Varley J (1994) Biotechnol Bioeng 44:801
31. Ghildyal NP, Lonsane BK, Karanth NG (1988) Adv Appl Microbiol 33:173
32. Chisti Y (1993) Bioproc Eng 9:191

33. Viesturs UE, Kristapsons MZ, Levitans ES (1982) Adv Biochem Eng 21:169
34. Solomon GL (1967) Proc Biochem 3:47
35. Schügerl K (1985) Process Biochem August, 122
36. Ross S (1950) The inhibition of foaming, Renessealer Polytechn Institut Bull 63
37. Robinson JV, Woods WWJ (1948) J Soc Chem Ind (London) 67:97
38. Evans JI, Hall J (1971) Proc Biochem 6:(4)
39. Adler I, Buchholz J, Voigt R, Wittler R, Schügerl K (1980) Eur J Appl Microbiol Biotechnol 9:249
40. Adler I, Diekmann J, Hartke W, Hecht V, Rohn F, Schügerl K (1980) Eur J Microbiol Biotechnol 10:171
41. Adler I, Eberhard U, Habermann WD, Schügerl K (1980) Eur J Microbiol Biotechnol 12:212
42. Sie TL, Schügerl K (1983) Eur J Appl Microbiol Biotechnol 17:221
43. Al-Masry WA (1999) Chem Eng Processing 38:197
44. Schügerl K, Lücke J, Lehmann J, Wagner F (1978) Adv Biochem Eng 8:63
45. Vardar F, Lilly MD (1982) Eur J Appl Microbiol Biotechnol 14:203
46. Nyiri L, Lengyel ZL (1965) Antibiot Advan Res Prod Clin Use Proc Congr Prague 729
47. Lengyel ZL, Nyiri L (1966) Biotechnol Bioeng 8:337
48. Bröring S, Fischer J, Korte T, Sollinger S, Lübbert A (1991) Can J Chem Eng 69:1227
49. Lübbert A (1992) J Biotechnol 25:145
50. Schügerl K (1996) Bubble column and airlift bioreactors. In: Bioreactor engineering. Course notes. EFB Bioreactor performance, p 22
51. Koch V, Rüffer H-M, Schügerl K, Innersberger E, Menzel H, Weis J (1995) Process Biochem 30:435
52. Berovic M, Cimerman A (1979) Eur J Appl Microbiol 7:313
53. Zhang S, Handa-Corrigan A, Spier RE (1992) J Biotechnol 25:289
54. van der Pol LA, Bonarius D, Wouw van de G, Tramper J (1993) Biotechnol Progr 9:504
55. Handa-Corrigan A, Emery AN, Spier RE (1989) Enzyme Microbiol Technol 11:230
56. Jöbses I, Martens D, Tramper J (1991) Biotechnol Bioeng 37:484
57. Wills BA (1985) Mineral processing technology. Pergamon Press, New York
58. Matis KA (1994) Flotation science and engineering. Marcel Dekker, New York
59. Schulze H-J (1984) Physicochemical elementary processes in flotation. Elsevier, Amsterdam
60. Loewenberg M, Davis RU (1994) Chem Eng Sci 49:3923
61. Rousseau RW (ed) (1987) Handbook of separation process technology. Wiley, New York
62. Verrall MS, Hudson MJ (eds) (1987) Separations for biotechnology. Ellis Horwood, Chichester
63. Pyle DL (ed) (1994) Separations for biotechnology 3. SCI, Cambridge
64. Li NN, Strathmann H (eds) (1987) Separation technology. A.I.Ch.E. New York
65. Lemlich R (ed) (1972) Adsorptive bubble separation technique. Academic Press, New York
66. Wilson DJ, Clark AN (1987) Bubble foam separation in waste treatment. In: Rousseau RW (ed) Handbook of separation process technology. Wiley, New York, chap 17
67. Schnepf RW, Gader EL (1959) J Biochem Microbiol Technol Eng 1:1
68. Ahmed SI (1975) Sep Sci 10:673
69. Ahmed SI (1975) Sep Sci 10:689
70. Gehle R, Schügerl K (1984) Appl Microbiol Biotechnol 20:133
71. Uraizee F, Narsimhan G (1990) Enzyme Microb Technol 12:315
72. Brown AK, Kaul A, Varley J (1999) Biotechnol Bioeng. 62:278
73. Brown AK, Kaul A, Varley J (1999) Biotechnol Bioeng 62:291
74. Bikermann JJ (1938) Trans Faraday Soc 34:634
75. Brown L, Narsimhan G, Wankat PC (1990) Biotechnol Bioeng 36:947
76. Ostermaier K, Dobiás B (1985) Colloids Surf 14:199
77. Liu Z-h, Liu Z, Shen Z, Ding F, Yuan N (1997) Bioseparation 6:353

78. Sarkar P, Bhattacharaya P, Mukherjea RN, Mukherjea M (1987) Biotechnol Bioeng 29:934
79. Miranda EA, Berglund KA (1993) Biotechnol Progr 9:41
80. Zheng L, Zhihong L, Wang D, Ding F, Yuan N (1998) Bioseparation 7:167
81. Varley J, Ball SK (1994) In: Pyle DL (ed) Separations for biotechnology 3. SCI, London, p 525
82. Graham DE, Phillips MC (1979) J Colloid Interface Sci 70:403
83. Graham DE, Phillips MC (1979) J Colloid Interface Sci 70:415
84. Miles GD, Shedlovski L, Ross J (1945) J Phys Chem 49:93
85. Jacobi WM, Woodcock KE, Grove CS (1956) Ind Eng Chem 48:2049
86. Steiner L, Hunkeler R, Hartland S (1977) Trans Inst Chem Eng 55:153
87. Desai D, Kumar R (1982) Chem Eng Sci 37:1361
88. Desai D, Kumar R (1983) Chem Eng Sci 38:1525
89. Desai D, Kumar R (1984) Chem Eng Sci 39:1559
90. Hartland S, Barber AD (1974) Trans Inst Chem Eng 52:43
91. Lemlich R (1978) Ind Eng Chem Fundamentals 17:89
92. Monsalve A, Schechter RS (1984) J Colloid Interface Sci 97:327
93. Callaghan IC, Lawrence FT, Melton PM (1986) Coll Polymer Sci 264:423
94. Krotov VV (1984) Colloid J (Russ) 48:913
95. Uraizee F, Narsimhan G (1995) Sep Sci Technol 30:847
96. Uraizee F, Narsimhan G (1996) Biotechnol Bioeng 51:384
97. Dognon A, Dumonte A (1941) CR Soc Biol 135:884
98. Dognon A (1942) Acta Scand Ind 932:157
99. Hopper SH, McGowen MC (1952) J Am Water Works Assoc 44:719
100. Grieves RB, Wang SL (1966) Biotechnol Bioeng 8:323
101. Bretz HW, Wang SL, Grieves RB (1966) Appl Microbiol 15:778
102. Rubin AJ, Cassel EA, Henderson O, Johnson JD, Lamb JC (1966) Biotechnol Bioeng 8:135
103. Levin GV, Clendenning JR, Gibor A, Bogar FD (1962) Appl Microbiol 10:169
104. Kalyuzhny MV, Petrushko GM, Novikova GP (1965) Microbiologica 34:918
105. Boyles WA, Lincoln RE (1958) Appl Microbiol 6:327
106. Desmaison GU, Schügerl K (1980) Chem Ing Techn 52:885
107. Gaudin AM, Mular AL, O'Connor RF (1960) Appl Microbiol 8:84, 91
108. Sadowski Z, Golab Z, Smith RW (1991) Biotechnol Bioeng 37:955
109. Matis KA, Zouboulis AI (1994) Biotechnol Bioeng 44:354
110. Ohmura N, Kitamura K, Saiki H (1993) Biotechnol Bioeng 41:671
111. Hashim MA, SenGupta B, Subramarian MB (1995) Bioseparation 5:167
112. Honeycutt SS, Wallis DA, Sebba F (1983) Biotechnol Bioeng 13:567
113. Viehweg H, Schügerl K (1983) Eur J Appl Microbiol Biotechnol 17:96
114. Bahr KH, Schügerl K (1988) In: Li NN, Strathmann H (eds) Separation technology. Engineering Foundation, New York, p 577
115. Bahr KH, Weisser H, Schügerl K (1991) Enzyme Microb Technol 13:747
116. Bahr KH, Schügerl K (1992) Chem Eng Sci 47:11
117. Gehle R, Sie TL, Kramer T, Schügerl K (1991) J Biotechnol 17:147
118. Hill GA, Robinson CW (1988) Biotechnol Lett 10:815
119. Parthasathy S, Das TR, Kumar R, Gopalakrishnan R (1988) Biotechnol Bioeng 32:174
120. Sie TW, Schügerl K (1989) Swiss Biotech 7:41
121. Husband DL, Masliyah JH, Gray MR (1994) Can J Chem Eng 72:840
122. Tybussek R, Linz F, Schügerl K, Moses N, Léonard AJ, Rouxhet PG (1994) Appl Microbiol Biotechnol 44:13
123. Wang S, Kretzmer G, Schügerl K (1994) Appl Microbiol Biotechnol 41:537
124. Buchholz H, Luttmann R, Zakrzewski W, Schügerl K (1981) Eur J Appl Microbiol Biotechnol 11:89
125. Parthasarathy S, Das TR, Kumar R (1988) Biotechnol Bioeng 32:174
126. Ramani MV, Kumar R, Gandi KS (1993) Chem Eng Sci 48:1819
127. Desai D, Kumar R (1983) Chem Eng Sci 38:1525

128. Aris R, Amundson NR (1973) Mathematical methods in chemical engineering. Prentice Hall, Engelwood Cliffs, NJ
129. Amory DE, Moses N, Hermesse MP, Leonard AJ, Rouxhet PG (1988) FEMS Microbiol Lett 49 : 197
130. Moses N, Leonard AJ, Rouxhet PG (1988) Biochim Biophys Acta 945 : 324
131. Arnold WN (1981) Physical aspects of the yeast cell envelope. In: Arnold WN (ed) Yeast cell envelopes: biochemistry, biophysics and ultrastructure, vol 1. CRC Press, p 25
132. Andrews GF, Fonta JP, Marrotta E, Stroeve P (1984) Chem Eng J 29 : B39

Received November 1999